A Thesis

Entitled

"Synthesis, Characterization and Applications of Transition Metal Complexes of Symmetric N_2O_2 Donor Schiff Bases Derived from 2-hydroxy-6-isopropyl-3-methyl benzaldehyde"

Submitted to

North Maharashtra University, Jalgaon.

For fulfillment of the requirements for the award of

Degree of Doctor of Philosophy (Ph. D.) in

Chemistry

Under the faculty of Science & Technology

By

Samina Karimkha Tadavi
**M. Sc, GATE**

(Registration No.: NMU/11/Ph.D./Chem./16/2013)

Under the Guidance of

Prof. (Mrs.) R. S. Bendre
M. Sc. Ph. D.

**School of Chemical Sciences,
North Maharashtra University,
Jalgaon- 425 001 (M. S.) India**

[FEBRUARY 2018]

DEDICATED TO
MY PARENTS AND
LATE GRAND FATHER

Urkund Analysis Result

Analysed Document: PhD. Thesis Miss Samina K. Tadavi for Urkund.pdf (D35580100)
Submitted: 2/13/2018 11:45:00 AM
Submitted By: bendrers@gmail.com
Significance: 10 %

Sources included in the report:

Doolesh G. Kokare - Thesis.pdf (D31275309)
MKK Thesis.pdf (D18468804)
Javeed Ahmad Ganaie, Correction complete thesis1.pdf (D30472015)
Asha-thesis plg.pdf (D19402750)
Javeed Ahmad Ganaie, corection file pdf.pdf (D29759042)
R_Jayalakshmi_Chemistry.pdf (D33662032)

Instances where selected sources appear:

75

CERTIFICATE

This is certify that the thesis entitled **"Synthesis, Characterization and Applications of Transition Metal Complexes of Symmetric N_2O_2 Donor Schiff Bases Derived from 2-hydroxy-6-isopropyl-3-methyl benzaldehyde",** which is being submitted herewith for the award of the Degree of Doctor of Philosophy in **Chemistry** under the faculty of **Science** of North Maharashtra University, Jalgaon is the result of the original research work completed by **Miss Samina Karimkha Tadavi**, under my supervision and guidance and to best of my knowledge and belief the work embodied in this thesis has not formed earlier the basis for the award of any Degree or similar title of this or any other University or examining body.

I give an undertaking that the material included in the thesis from other sources is duly acknowledged.

I have verified that, the research student has incorporated all the changes as suggested by the Pre-submission presentation Committee, if any.

Place: Jalgaon

Date:

Prof. (Mrs.) R. S. Bendre

Head, Dept. Pesticides and

Agrochemical,

School of Chemical Sciences,

North Maharashtra University,

Jalgaon

Forwarded through

D. H. More

(Director)

School of Chemical Sciences,

North Maharashtra University,

Jalgaon.

D E C L A R A T I O N

I hereby declare that the thesis entitled **"Synthesis, Characterization and Applications of Transition Metal Complexes of Symmetric N_2O_2 Donor Schiff Bases Derived from 2-hydroxy-6-isopropyl-3-methyl benzaldehyde"**, has been completed and written by me.

To best of my knowledge and belief the work embodied in this thesis has not formed earlier the basis for the award of any Degree or similar title of this or any other University or examining body.

I give an undertaking that the material included in the thesis from other sources is duly acknowledged.

Place: Jalgaon.

Date:

<div align="right">

Samina Karimkha. Tadavi

Research Student

School of Chemical Sciences,

North Maharashtra University,

Jalgaon.

</div>

Acknowledgements

I am very pleased to acknowledge my deep sense of gratitude to all who helped and supported me during the course of my research work.

I would like to express my sincere thanks to Prof.(Mrs.) R. S. Bendre, my supervising guide for her efficient guidance throughout the amazing route of research with great patience. Her constant valuable advice, encouragement and discussions at different stages were really a great motivation.

I am equally thankful to Prof. P. P. Patil, Hon'ble Vice-Chancellor, Prof A. B. Chaudhari, Officiating Registrar and Prof. P. P. Mahulikar,OSD, Research and Development, North Maharashtra University, Jalgaon, for giving me the opportunity to work at the University.

I'm also thankful to Prof. D. H. More, Director, School of Chemical Sciences, North Maharashtra University, Jalgaon, for giving me the prospects of work at the University school.

I'm thankful to Prof. A. U. Borase, Dr. V. V. Gite, Dr. D. S. Dalal, Mr. Amardip Patil for their help during my research.

I am thankful to our supporting non-teaching staff Dr. N. B. Patil, Mr. A. A. Shimpi, Mr.S. D. Mali, Rahul Badgujar and Veena Uddhage.

I gratefully thank SAIF IIT Bombay, SAIF Panjab University, Chandigarh, Dr. Babasaheb Ambedkar Marathwada University Auragabad and Savitribai Phule Pune University, School of Chemical Sciences and University Institute of Chemical Technology of North Maharashtra University Jalgaon for the analysis of research samples and equally thankful to Dr. T. N. Gururow and his group member Amar Hosamani IISc Bangalore and SAIF IIT Madras for solving majority of crystals structures.

My thanks are due to University Grants Commission, New Delhi, Government of India, for awarding the Rajiv Gandhi National Fellowship for the ST Candidates. (201314-RGNF-2013-14-ST-MAH-45781)

I wish to give my special thanks to seniors Dr. Jitendra Bhosale, Dr. Umesh Pete, Dr. Dipesh Mahajan, Dr. Chetan. Zade, Dr. Smita Patil, Dr Rakesh Sancheti,

Table of Contents

Sr.No.	Contents	Pg. no.
Chapter I		
Chapter II		

Chapter III

List of Figures

List of Tables

List of Abbreviations

Abbreviations	Description
Conc.	Concentration
Min	Minute
gm	Gram
wt	Weight
mm	Millimetre
ml	Millilitre
µl	Microlitre
µm	Micro meter
FTIR	Fourier transform infrared
NMR	Nuclear magnetic resonance
UV-vis	Ultra violet visible
LC-MS	Liquid chromatography mass spectroscopy
ESI-MS	Electro-Spray Mass Ionization Spectroscopy
M	Mole
mmol	milimole
No.	Number
%	Percentage
R.T.	Room temperature
MW	Molecular weight
TMS	Tetra methyl silane
DMF	N,N' -dimethylformamide
DMSO	Dimethyl sulphoxide
ppm	Parts per million
XRD	X-ray diffraction
ORTEP	Oak Ridge Thermal Ellipsoid Plot
Å	Angstrom
°C	Degree centigrade

i.e.	That is
ESR	Electron spin resonance
mT	megaTesla
K	Kelvin
MHz	Mega hertz
IC_{50}	Inhibitory concentration
EC_{50}	Effective concentration
MIC	Minimum inhibitory concentration
Fig. No.	Figure number
Tab No.	Table number

CHAPTER I

INTRODUCTION
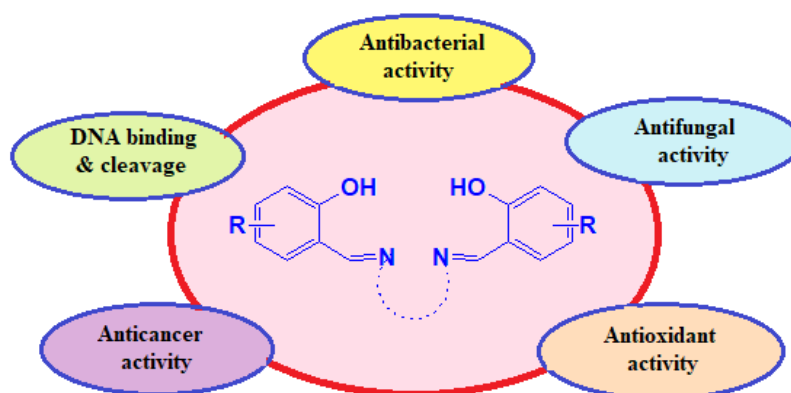
1.1 Introduction

During the past few decades the importance of the schiff bases and their metal complexes has been considerably increased bacause of multipurpose applications for the diverse fields including the biochemical, medicinal, pharmaceutical, catalytic and many more. A large number of schiff bases and their transition metal complexes have been dynamically investigated and further performed for their biological activities along with their interesting coordination chemistry. Largely schiff bases with multiple and different coordination environment and their metal complexes with metals in different oxidation states have been reported.

1.2 Short introduction of Schiff Bases (what is schiff bases ?)

Schiff bases were named after the German chemist Hugo schiff [1] and are produced by reacting aldehydes or ketones with primary amines under different conditions and in different solvents upon elimination of water molecule. The schiff base is synonymous with an azomethine and can be used as reactive intermediates for the synthesis of many natural products. Schiff bases of aliphatic aldehydes or ketones are relatively unstable and readily polymerisable, while those of aromatic aldehydes are more stable due to the presence of an effective conjugation. In general, aldehydes react faster than ketones in condensation reaction, leading to the formation of schiff bases, as the reaction center of aldehyde is sterically less hindered than that of ketone. Furthermore, the extra carbon of ketone donates electron density of the azomethine carbon and thus makes the ketone less electrophilic compared to aldehydes [3-4].

Presence of a lone pair of electrons in the sp^2 hybridized orbital of nitrogen atoms of the azomethine group is of significant chemical importance and offers good chelating ability to schiff bases especially when combined with one or more donor atoms close to the azomethine group [2]. The schiff bases possess different types of chelating abilities such as bidentate, tridentate, tetradentate, pentadentate or polydentate as shown in **Figure. 1.1**
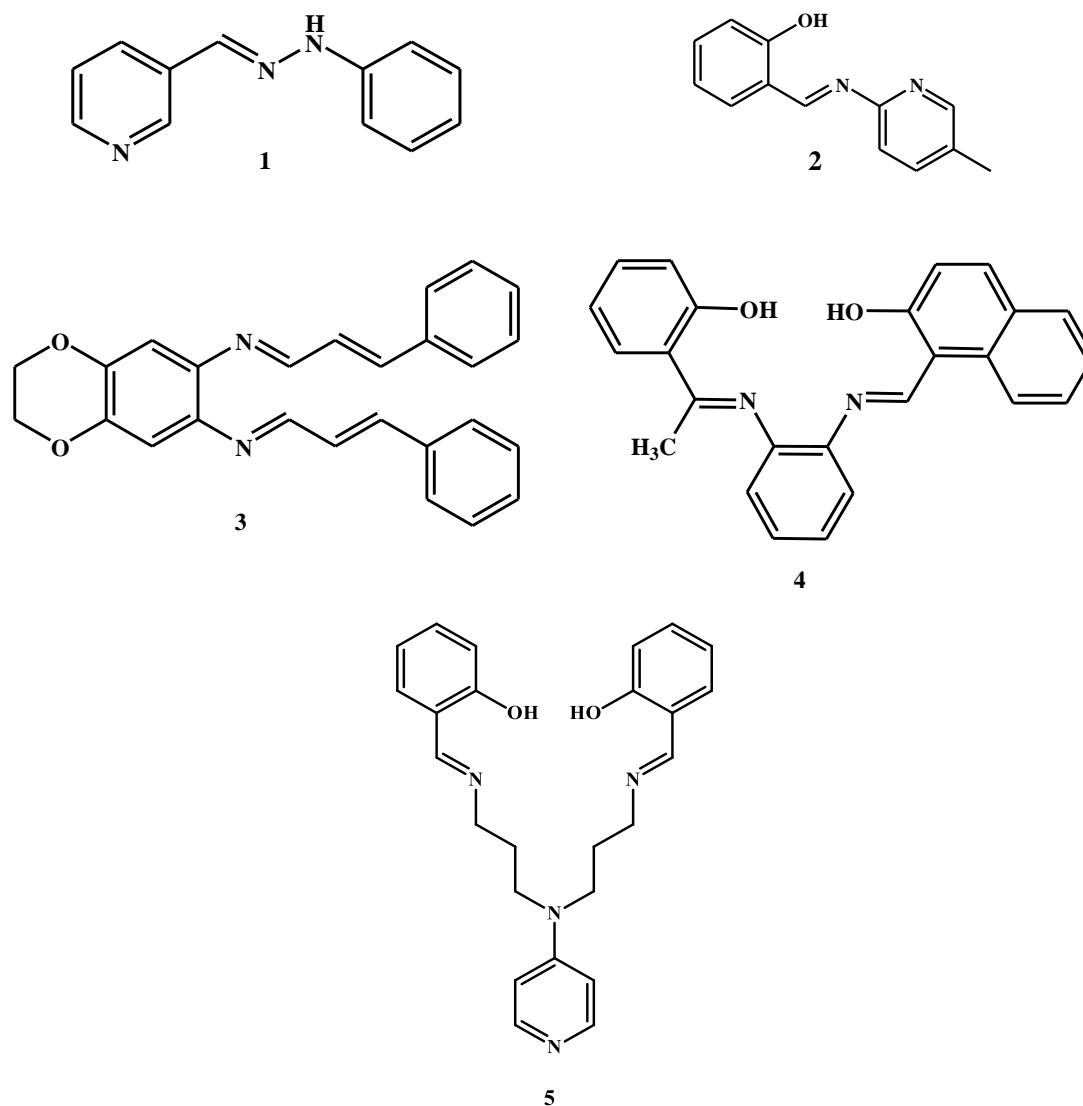
Figure 1.1: Schiff bases with different chelation modes (mono, bi etc)

During last few dacades, considerable efforts have been made for the development of metal free macrocyclic schiff bases, as macrocyclic schiff bases are also considered important in the supramolecular chemistry [5-6]. Some examples of the different types of macrocyclic schiff bases are shown in **Figure 1.2**.

6

7
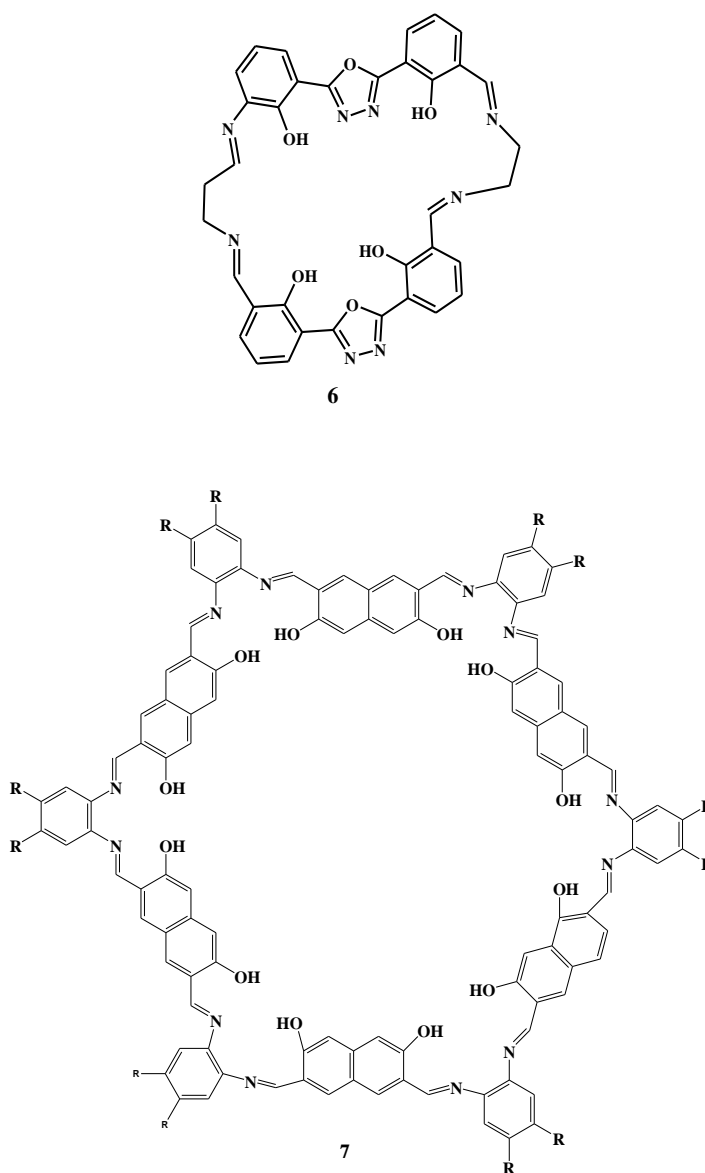
Figure 1.2: Macrocyclic schiff bases

Condensation of salicylaldehyde and ethylenediamine in 1:2 molar ratio produces an interesting N_2O_2 donor schiff base "Salen". The term "Salen" is an abriviation widely used to denote a family of bisimine compounds having oxygen and nitrogen containing structures derived from the N,N'-bis(salicylidine)ethylenediamine and are very much like porphyrins and, unlike the latter, can be easily prepared. Though the term salen was initially used only to describe the tetradentate N_2O_2 schiff bases derived from salicylaldehyde and ethylenediamine, now the term 'Salen-type' is used to describe the class of (O, N, N, O)

tetradentate bis-schiff ligands. salen and its analogues are versatile chelate ligands in inorganic and organometallic chemistry (R-Akine)

Stereogenic centers or other elements of chirality (planes, axes) can be introduced in the synthetic design of schiff bases (**Figure 1.3**) following are the representatives of the different types of salen type schiff bases.
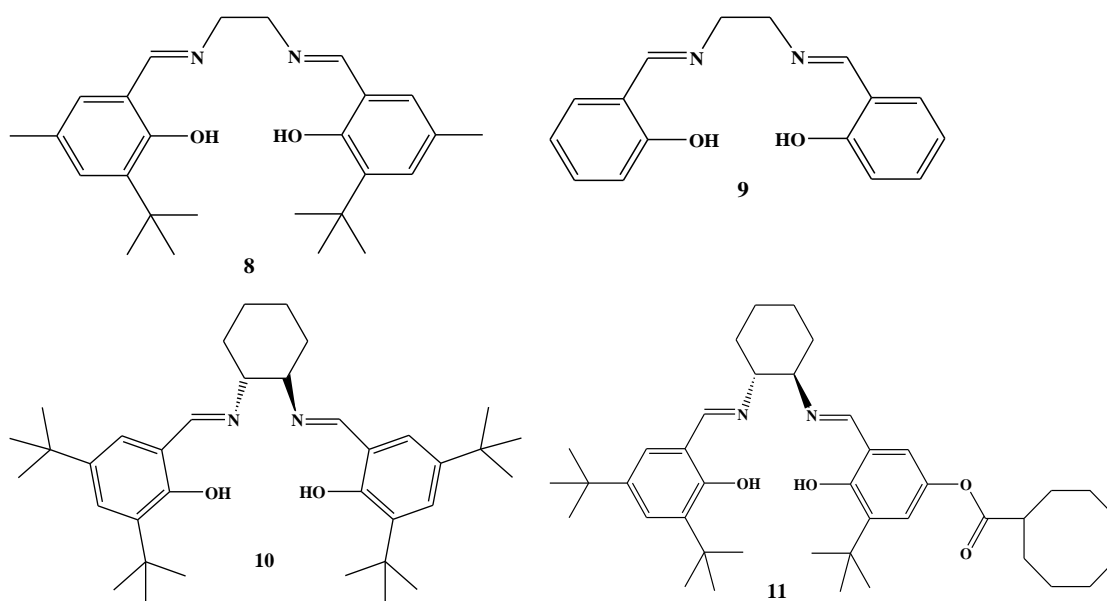
Figure 1.3: Various salen type ligands

1.3 Metal complexes of Schiff bases

Metal complexes of schiff bases have contributed widely to the inorganic chemistry of chelate systems. Stereochemical flexibility is well documented among schiff-base complexes which is arising from central metal, the source of the carbonyl function, the amine, as well as substituents on and steric bulkiness around the schiff base [7]. In view of that, metal-chelated schiff base complexes have continued to play the role of one of the most important stereochemical models in main group and transition-metal coordination chemistry due to their preparative accessibility, diversity and structural variability [8].The transition metal complexes having oxygen and nitrogen donor schiff bases possess unusual configurations and structural labiality and are sensitive to the molecular environment.

schiff base ligands and their complexes derived from the reaction of derivatives of salicylaldehyde with amines have been extensively studied in great details for their various crystallographic, structural and magnetic features [9-11]. Multidentate schiff bases generate stable complexes with most metallic ions and especially with transition ones and have the ability to stabilize them in various oxidation states. These systems can be acyclic or cyclic in nature as well as planar or tridimensional in their framework depending on the designed structure to which they give rise, the specific functions they must perform or the peculiar properties they must achieve [12].

There are new additions day by day and thousands of schiff bases have been reported till date. Since, the present research work is based on biological activities of metal complexes of four new N_2O_2 donor salen type ligands, the present review includes the literature on schiff bases containing oxygen and nitrogen as donor sites, "Salen type" schiff bases, their metal complexes and biological applications.

1.4 Different types of nitrogen and oxygen containing Schiff bases and their metal complexes:

A Variety of schiff bases and corresponding complexes have been reported. We are presenting here some schiff bases especially with N_2O_2 coordination environment and their metal complexes.

Mota and workmates have prepared schiff base N,N'-bis(salicylidene)-o-phenylenediamine by the condensation of salicylaldehyde with o-phenylenediamine. Density Functional Theory (DFT) was used to study the tautomerism of salophen. Presence of salophen **12** in solid state was confirmed through comparison of the stimulated and experimental structure [13].

12
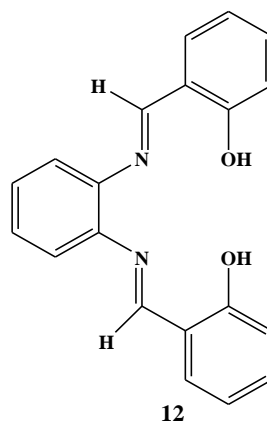
Salicylideneimine metal complexes **13** are often used as catalysts [14, 15] therfore Artus et al. prepared a new ligand by reacting 3,5-Di-tert-butylsalicylaldehyde and 1,3-diamino-2,2-dimethyl propane [16].

13
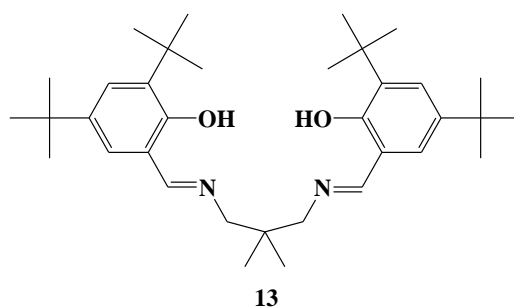
Pagadala and workers synthesized N,N'-bis(salicylaldehydo) ethylenediimine [HO(Ar)CH=N–(CH$_2$)$_2$–N=CH(Ar)OH] ligand **14** and its ML type Mn(II), Co(II), Ni(II), and Zn(II) complexes by classical and microwave technology [17].

14
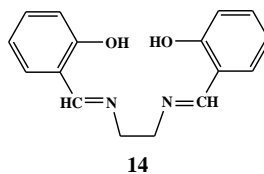
Di Bella and coworkers have presented a new synthetic strategy for obtaining thermally stable non centrosymmetric coordination complexes having sizable second-order NLO responses, tunable by the metal center and investigated comparative experimental/theoretical molecular second-order nonlinear optical (NLO) properties of a series of donor-acceptor bis(salicylaldiminato)nickel(II) Schiff base complexes **15** and **16** [18].

R= H
R= OMe

15

R= H, R_1= H
R= OMe R_1= H
R= H R_1= NO$_2$
R= OMe R_1= NO$_2$

16

Qian et al. prepared two new mononuclear cobalt(III) viz.[Co(MEA)(N$_3$)(DMF)] and manganese(III) viz.[Mn(EEA)(N$_3$)(OH$_2$)] complexes with bis-schiff base ligands bis(5-methoxysalicylidene)ethylenediamine (MEA) **17** and bis(6-ethoxysalicylidene) ethylenediamine (EEA) **18** and noted that small molecules such as DMF, azide, and water readily coordinate to the metal atoms at the axial positions [19].

MeO   **17**   OMe   OEt   **18**   EtO

Dioxomolybdenum(VI) complex **19** of N,N'-bis(5-methylsalicylidene)-1,3-diaminopropane, has been synthesized by Xue et al. and structure was determined by single-crystal X-ray. The Mo atom in the complex is coordinated by two phenolate O and two imine N atoms of the schiff base ligand, and by two oxo O atoms, resulting in an octahedral coordination [20].

19

Tella et al. reported series of five Ga(III) octahedral complexes **20** involving one bidentate acac ligand and one tetradentate schiff base N,N'-bis(salicylidene)propane-1,3-diamine (salpropH$_2$) or its substituted derivatives having electron-donating methyl groups or

electron withdrawing groups, such as Cl, Br and NO_2 at the fifth position of salicyalidene rings. Photoluminescence of free ligands and complexes was studied, which was found to be increased upon complex formation. Substitution of salpropH$_2$ ligand was found to alter the emission maxima [21]

R= H, Cl, Br, NO$_2$ and CH$_3$

20
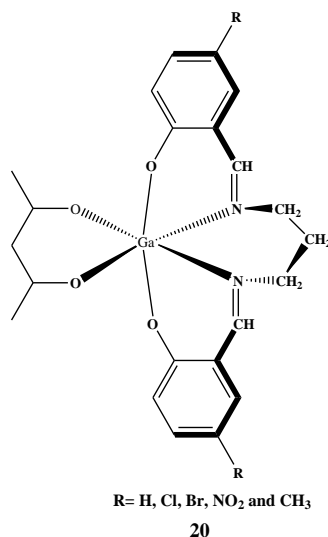
Popov and collegues have synthesized and and structurally characterized mononuclear copper(II) **21** and nickel(II) complexes of 1,3-bis(3,5-di-tert-butylsalicylideneamino)propan-2-ol schiff base ligand and observed that the presence of the tert-butyl groups prevents intermolecular hydrogen bonding in the crystals and their molecules are only linked by hydrophobic interactions [22].

21
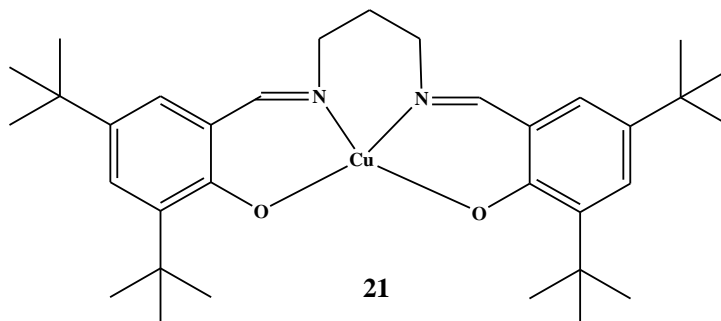
Two series of octahedral, pseudo-octahedral or pseudo-tetrahedral Fe(III) complexes of schiff-bases derived from two aldehydes, viz. 3-formyl-2-hydroxy acetophenone and 3,5-diformyl-4-hydroxyacetophenone condensed with 1,2-ethylenediamine or 1,3-propylenediamine respectively have been prepared by Saleh et al. and through ESR and

Mossbauer spectra they have studied the effect of varying the nature of the schiff-base ligands on the structure and properties of complexes [23]

In order to study the influence of the diverse nature of the anions such as poor coordinating perchlorates to more privileged carboxylates. Rodriguez et al. derived symmentrical tetradentate schiff base N,N'-(1,2-phenylene)-bis(3-hydroxysalicylidenimine) H_4L **22** by condensation of 2,3-dihydroxybenzaldehyde with 1,2-phenylenediamine in chloroform and its four novel manganese(III) complexes by employing different manganese(II) and manganese(III) starting salts (chloride, acetate, acetylacetonate and perchlorate). Although some of the starting salts were involving Mn(II) ions all the complexes formed were manganese(III) viz. $[Mn(H_2L)(H_2O)_2]Cl(H_2O)_3$, $[Mn(H_2L)(OAc)](H_2O)$, $[Mn(H_2L)(acac)](H_2O)_3$, and $[Mn(H_2L)(H_2O)(CH_3OH)](ClO_4)$, having anions belonging to the starting salts with different coordinating tendencies [24].

22

Akbari et al. synthesized the Pd(II) and Pt(II) complexes of N,N′-bis(salicylidene)-1,2-cyclohexanediamine quadridentate binegative chelate ligand. The square planar geometry of the complexes has been confirmed through the single crystal X-ray crystallographic structures of **23, 24** and to gain further insight into the spectral properties, results based on DFT calculations have been compared with experimental data [25, 26].

23   **24**

Abd-Elzaher et al. prepared three different ligands (SalophHz) **25**, (NophHz) **26** and (AophHz) formed by condensation of o-phenylenediamine with salicylaldehyde, 2-hydroxy-1-naphthaldehyde or o-hydroxyacetophenone in 1:2 molar ratio and their complexes with nickel, copper and zinc ions in 1: 1 molar ratio and studied them to observe structural changes occuring upon complexation [27].
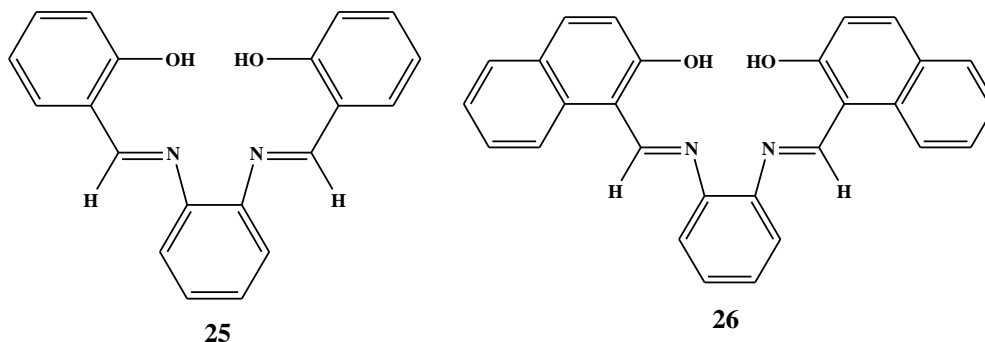
Pramanik et al. reported mesomorphic behaviour of square pyramidal iron(III) complexes [Fe(4-C$_{16}$H$_{33}$O)$_2$salcn)]Cl **27** and [Fe(4-C$_{16}$H$_{33}$O)$_2$salophen)]Cl **28** {salcn = N,N′-cyclohexanebis(salicylideneiminato) and salophen = N,N′-phenylenebis(salicylideneiminato)}, of 'Salen'-type ligands containing 4-substituted long alkoxy arms on the terminal aromatic ring and a central cyclohexane/phenylene spacer. Although free ligands were devoid of mesomorphism, induction of mesomorphic character occuring due to conformational change in the coordinated ligands and the mesophase was noted to be stable over wide range of temperature [28].
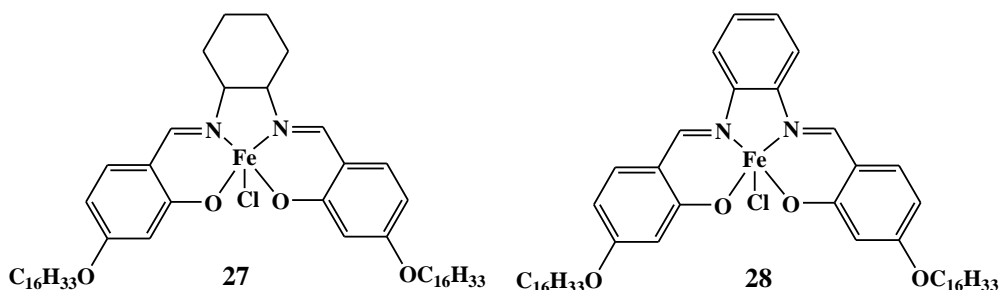
Liu et al. reported two tetradentate ligands, N,N'-bis[4-(benzeneazo) salicylaldehyde]-o-phenylenediamine **29** and N,N'-bis[4-(benzeneazo)salicylaldehyde] ethylenediamine **30** prepared by condensation of 4-(benzeneazo) salicylaldehyde with o-phenylenediamine or

ethylenediamine in 2:1 molar ratio and their Cu(II), Ni(II), Zn(II), Co(II), Mn(II) and Cd(II) complexes [29].

29

30
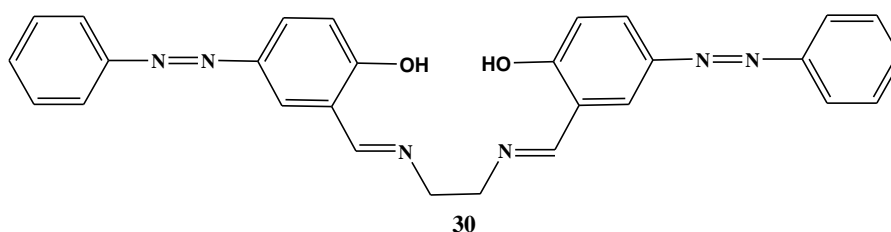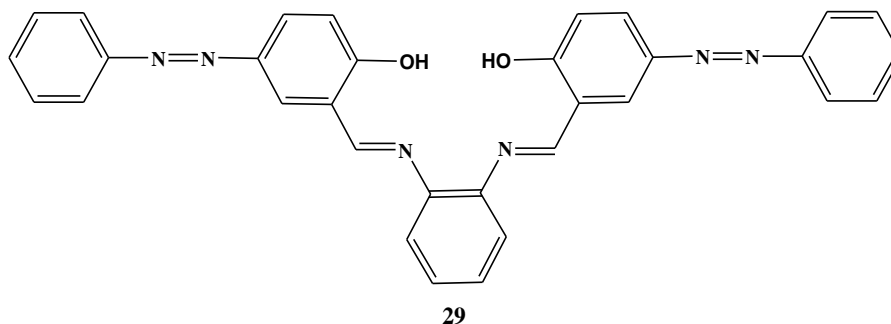
Deligonol et al. prepared Cu(II), Co(II), Ni(II), Fe(III) Ru(III) and VO(II) complexes with salen derivatives having different diamine bridges $H_2N (CH)_2 NH_2$ = ethylenediamine, 1,3-di-aminopropane and 1,4-di-aminobutane and 2,4-dihydroxy benzaldehyde moieties and reported C–C coupling, catalysis, electrochemical, thermal and spectroscopic properties of the transition metal complexes. Investigation of the keto-enol tautomeric forms of the ligands in polar and apolar solvents indicated that the ligands favor the keto-form [30].

Raisanen and workmates have studied structures of Cu(II) salen **31** complexes bearing long alkyl chains (C12 and C10) in the salicylidene moieties and reported important finding that an axially coordinated solvent can notably change the spatial orientation and packing of the complex while the spatial orientation and packing of the complexes are not affected by the alkyl chain length [31].

n= 12
n= 10

31

Bhattacharjee et al. reported aquated iron(III) schiff base complexes of the type $[Fe(Ln)(H_2O)_2]NO_3$, $[N_2O_2]$ donor tetradentate schiff bases prepared from condensation of 2-hydroxy-1-naphthaldehyde with o-phenylenediamine or ethylenediamine in 2:1 molar ratio **32, 33**. Ligand substitution of aquated cationic iron(III) complexes by neutral N-donor molecules (X) viz. imidazole, benzimidazole and pyridine led to substitution of weakly held axial aquo groups affording new mixed ligand complexes, $[FeLnX_2]NO_3$. The synthetic strategy adopted here has opened up new outlooks for a range of new mixed-ligand complexes [32].

32

33

Bayoumi. and coworker reported N_2O_2 dibasic schiff base ligand (N,N'-bis(5-(4-sulfanilamidophenylazo-salicylidene)-ethylenediamine) **34** and its 1:1 (M:L) complexes with Cu(II), Ni(II), Co(II) and Cr(III) ions and studied their spectroscopic, electrochemical behavior and thermal decomposition properties [33].

34

Tas et al. have prepared copper(II) and cobalt(II) **35, 36** complexes of newly developed schiff bases derived by condensation of 1,2-bis(p-aminophenoxy)ethane and 1,2-bis(m-aminophenoxy)ethane with 3,5-di-tert-butyl-2-hydroxybenzaldehyde [34].

35 **36**

M= Cu(II) and Co(II)   M= Cu(II) and Co(II)
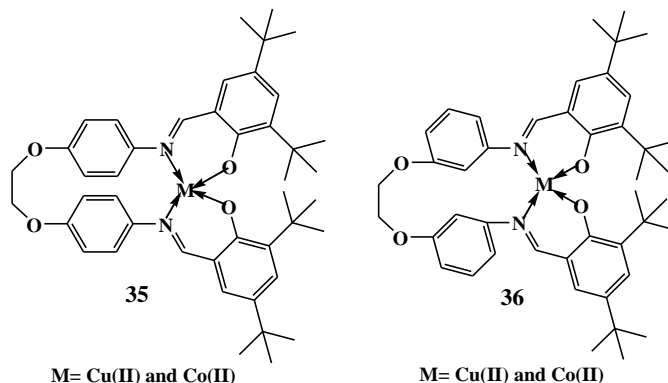
Grivani and workmates reported crystal structure of a new distorted square planar copper(II) Schiff base complex derived from asymmetrical schiff base ligand (L1 = salicylidene imino-ethylimino-pentan-2-one) with $Cu(OAC)_2$ **37** [35] and studied it theoretically at different levels of DFT and basis sets.

37
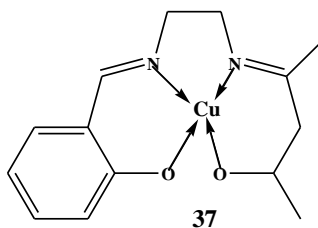
Tidjani et al. have synthesized Mn(II) and Cu(II) complexes in 1:1 molar ratio with symmetrical schiff bases **38** N,N'-bis(2-hydroxybenzy1)ethylenediimine (H_2L^1), N,N'-bis(2-hydroxyacetophenyl)ethylenediimine (H_2L^2) and N,N'-bis(2-hydroxypropiophenyl)ethylenediimine (H_2L^3) and 2:1 compound of H_2L^2 with manganese(II) and studied their electrochemical behavior [36].
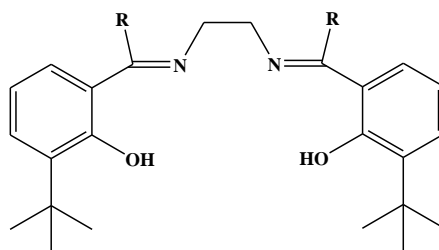
R= H: HL₁, R= CH₃: HL₂, R= C₂H₅: HL₃

38

Repo and workmates have reported X-ray crystal structure of titanium (IV) salen complex **39** of di-chloro{ 6, 6'-di-tert-butyl-2, 2'-[1,2-ethanediylbis(nitrilo- methylidyne-N)]-4,4'-dimethyldiphenolato- O, O'} [37].
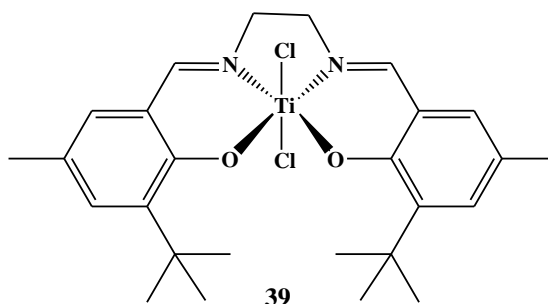
39

Chiral Ti(IV)-salen complexes are used as chiral Lewis acid catalysts for a variety of organic transformations.To discover new syntheses of symmetric and asymmetrically disubstituted titanium(IV)-salen complexes possessing oxygen-donor ligands Chen et al. have described reaction of in situ-generated Ti(OiPr)2(X)2 (X=OAr, OTf) with H2salen or H2salen* forming stable, well-characterized Ti(salen)X2 series of complexes. Ti(salen*)(OTf)2 could be obtained by reacting Ti(salen*)Cl2 with TMSOTf or AgOTf. The ditriflates could be converted back to the aryloxides upon reaction with 2 equiv of NaOAr.

Chen et al. have also demonstrated various routes of synthesis of six-coordinate Ti-salen complexes viz

- direct reaction of H2salen with several Ti(OiPr)2X2 and Ti(OiPr)3X functional equivalents,
- ligand substitution on preformed Ti(salen)X2 complexes,
- comproportionation reaction of two homobis-substituted Ti(salen)X2 complexes.

They noticed thr reactivity of symmetrically and unsymmetrically disubstituted complexes toward axial substitution mainly dominated by the acidity of the involved oxygen ligands [38].

Dogan synthesized the N,N'-bis(3,5-Di-t-Butylsalicylidene)Ethylenediamine and its Co(II), Ni(II) and Cu(II) complexes and studied their thermal decomposition kinetics [39]

Refat and coworker have reported the structural, spectral and thermal stability of charge-transfer (CT) complexes of schiff base; N,N'-disalicylidene-l,2-phenylenediamine (H_2dsp) **40** as a donor with chloranilic acid (CLA), p-chloranil (CHL), tetracyanoquinodimethane (TCNQ) or dichlorodicyanobenzoquinone (DDQ) as acceptors. The interaction between schiff base donor N,N'-disalicylidene-l,2-phenylenediamine and π acceptor has been discussed in the solid and solution form. The thermal behavior of complexes was also investigated by TG analysis which indicated that the formation of CT complexes was stable, exothermic and spontaneous [40].

40
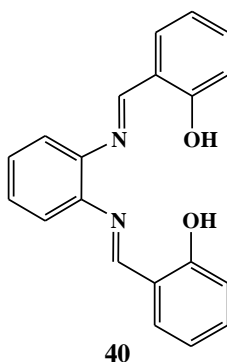
1.5 Biological applications of Schiff bases and their transition metal complexes

Vast applications of schiff bases and their metal complexes is the subject of many literature reviews due to a wide range of pharmacological activities including antibacterial, anti-fungal, anti-malarial and anti-viral as well as the anti-inflammatory, antioxidant and anticancer activities and all mentioned activities are recognized due to -C=N- functionality [41-44]. Several studies [45-47] showed that the presence of a lone pair of electrons in the sp^2 hybridized orbital of nitrogen atom of the azomethine group is of considerable chemical and biological importance. It was found that some drugs have higher activity when

administrated as metal complexes than as free ligands. As such the complexes containing O, N donor atoms are very important owing to their significant biological activities [48, 49]. Schiff bases are generally excellent chelating agents especially when a functional group such as -OH or -SH is present close to the azomethine group so as to form a five- or six-membered ring with the metal ion.

The variation in the effectiveness of different complexes against different organisms depends either on differences in the permeability of the cells of the microbes or on difference in ribosome's of the microbes [50, 51].

Mohie and El-Shishtawy have synthesised bis-hydroxybenzylidene-1,2-phenylene diamine schiff base and its Al(III), Ni(II) and Zn(II) complexes. The antibacterial activity data showed the complexes to be more potent than the parent schiff base ligand and among all, Al(III) complex was observed to be most effective [52].

Aziz and workmates have prepared and studied photoluminancence four novel mononuclear tetrahedral Zn(II) and square pyramidal Al(III) complexes of a salen derivative derived from N,N'bis(salicylaldehyde)4,5-dimethyl-1,2-phenylenediamine and N,N'bis(salicylaldehyde)4,5-dichloro-1,2-phenylenediamine **41,** the complexes exhibited intense fluorescence emission in the visible region upon UV-excitation, which is assigned to the strong coordination of the ligands to the small and the highly charged Zn(II) and Al(III) ions. Zn(II) complexes exhibited strong fluorescence at room temperature compared to Al(III) complexes; such strong coordination is thought to extend the π-conjugation of the complexes. The photoluminescent behavior of Zn(II) and Al(III) complexes is particularly important for their potential application as photoactive materials. Biological activity of the prepared complexes has been found to be comparable to standard antibiotics [53].

R= CH₃   H₂L¹

R= Cl   H₂L²
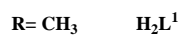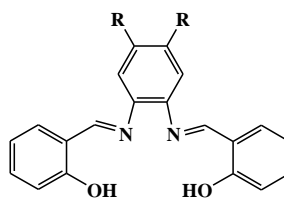
41

Singh et al. have specified the probable geometry and biological activity of the cobalt(II) and manganese(II) complexes of novel schiff base **42** derived from 4,5-dimethoxy-1,2-phenylenediamine and 5-substituted salicylaldehyde [54].

X= F, Cl, Br
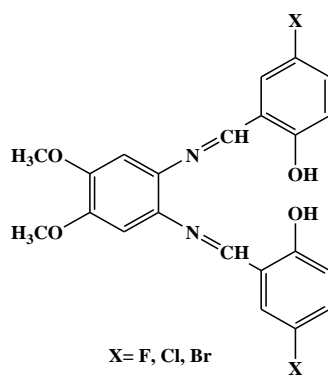
42

The direct electrochemical synthesis of metal complexes involving the anodic oxidation of a metal in a non-aqueous solution of the ligand precursor having significant advantages as the simplicity of the technique and high product yield was used for the preparation of the SalophH₂ (N,N'-bis(salicylidene)-o-phenylenediamine) complexes of titanium, iron, cadmium, tin, and lead by Liu and coworkers [55].

M= Ti(II), Fe(II), Cd(II), Sn(II) and Pb(II)
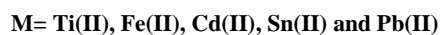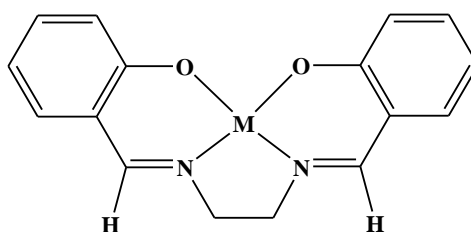
43

Pasini and Gullotti have synthesized oxovanadium(IV) complexes **44** with tetradentate schiff bases obtained by condensation of acetylacetone, trifluoroacetylacetone, salicylaldehyde and its 5-chloro and 5-nitro derivatives, with optically active 1,2-diamines, namely (+) propylenediamine, (+) and *meso* butanediamine, (+) and *meso* cyclohexanediamine, (-1) and *meso* stilbene diamine and studied infrared, circular dichroism and electronic spectra and the factors influencing the formation of hexa coordinate adducts with donor bases [56].

X= H, NO$_2$, Cl

44
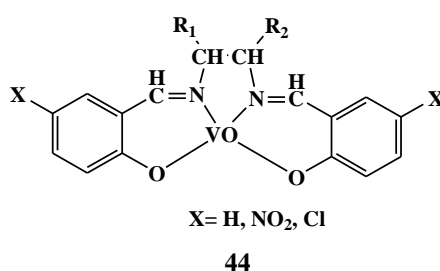
In order to study the reactivity of vanadium complexes in the oxygen-transfer catalysis of alkyl hydroperoxides to a wide range of substituted olefins, Haas and coworker have synthesized vanadium [VO(C$_{26}$H$_{34}$N$_2$O$_2$)] complex **45** having approximately square pyramidal geometry formed by an axial oxo ligand and a four-coordinate substituted schiff base ligand around vanadium center [57].

45
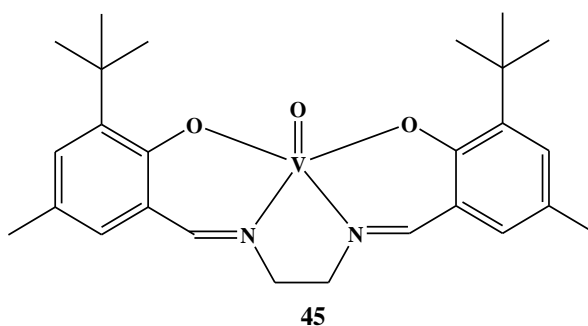
Chromium–salen complexes are well-known catalysts in heterogeneous and homogeneous systems Aranha et al. have prepared eight chromium(III) complexes of symmetrical tetradentate schiff bases containing the N$_2$O$_2$ donor set by condensing a substituted salicylaldehyde with ethylenediamine. The same synthetic process gives two series of

complexes **46, 47** depending on the amount and rate of addition of potassium carbonate used to deprotonate the schiff base [58].
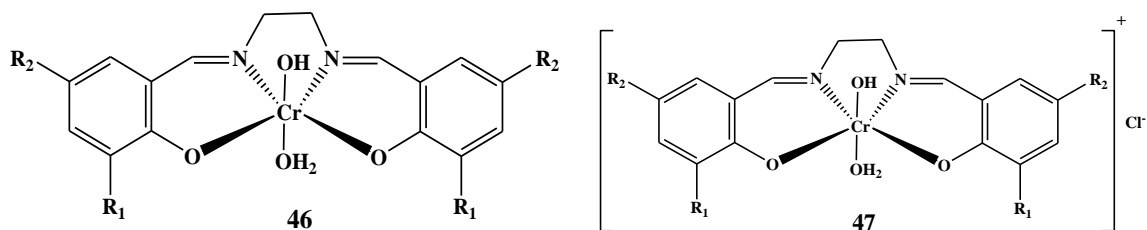
R¹	R²	L	Complexes
H	H	OH	[Cr(L^1)(OH)(H2O)]
H	Br	OH	[Cr(L^2)(OH)(H2O)]
H	Cl	OH	[Cr(L^3)(OH)(H2O)]
H	MeO	OH	[Cr(L^4)(OH)(H2O)]

R¹	R²	L	Complexes
H	NO$_2$	H$_2$O	[Cr(L^5)(H$_2$O)$_2$]Cl
Br	Br	H$_2$O	[Cr(L^6)(H$_2$O)$_2$]Cl
Cl	Cl	H$_2$O	[Cr(L^7)(H$_2$O)$_2$]Cl
I	I	H$_2$O	[Cr(L^8)(H$_2$O)$_2$]Cl

Kasumov et al. have described the synthesis, characterization and electrochemical behavior of nickel(II) complexes NiL **48** of a series of N,N'-polymethylenebis(3,5-Bu$_2^t$-salicylaldimine) ligands containing 2,4-di-Bu$_2^t$-phenol arms. cyclic voltammograms of NiLx (x = 1–4) complexes displayed two-step oxidation processes corresponding to the reversible one-electron oxidation process yielding Ni(III) species and ligand based oxidation generating a coordinated phenoxyl radical species [59].

H$_2$L$_x$	(CH$_2$)$_X$
H$_2$L$_1$	-(CH$_2$)$_2$-
H$_2$L$_2$	—C—C— H$_2$ / CH$_3$ H
H$_2$L$_3$	-(CH$_2$)$_3$-
H$_2$L$_4$	-(CH$_2$)$_4$-
H$_2$L$_5$	-(CH$_2$)$_5$-
H$_2$L$_6$	-(CH$_2$)$_6$-
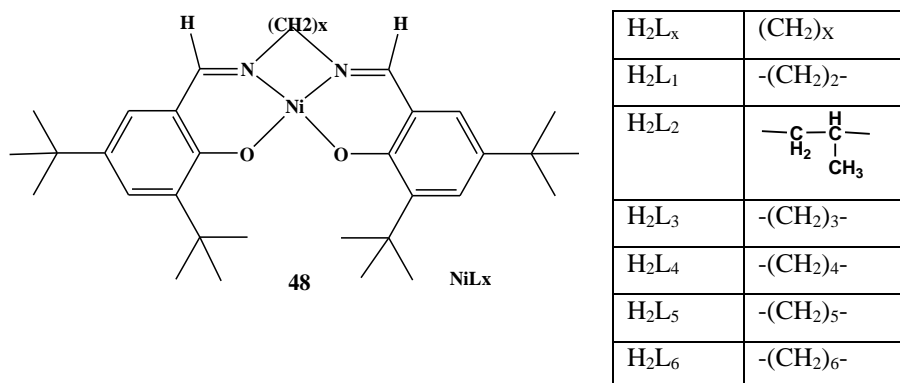
Khuhawar and Channar have synthesized four new Schift base polyemers poly 5,5'-methylenebis-salicylaldehyde-tetramethylethylenediimine (PMSATen), poly 5,5'-methylenebis-salicylaldehyde-meso-stilbene-diimine (meso-PMSAS), poly 5,5'-

methylenebis-salicylaldehyde-dl-stilbenediimine(dl-PMSAS) and poly 5,5'-methylenebis-salicylaldehyde 2,6-diiminopyridine(PMSAP) and their copper(II) and then nickel(II) chelates [60].

Zare and Ataeinia have reported schiff base ligand synthesized by condensation of 2,3-diaminopyridine and salicylaldehyde and its Fe, Cr and Co complexes having thiocyanate at fifth coordination site and studies on electrochemical behavior [61].

49

50

M= Fe, Cr and Co
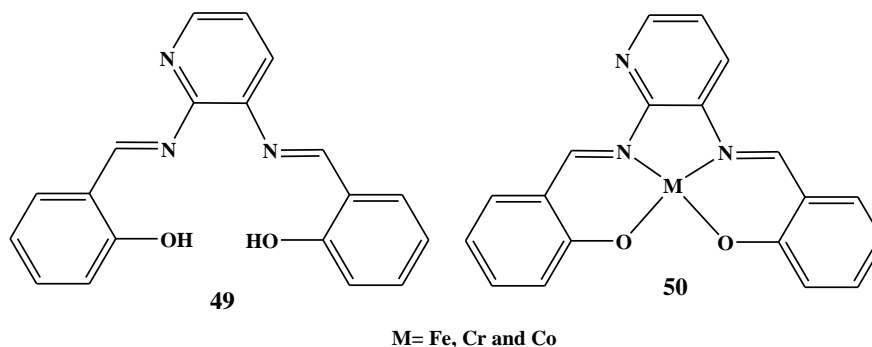
Sheng and workmates have synthesized square planar Ni(II) complexes **51, 52** of schiff bases N,N'-bis(3,5-dichlorosalicylidene)-1,3-pentanediamine and N,N'-bis(3-methylsalicylidene)-1,2-ethanediamine) [62].

51

52
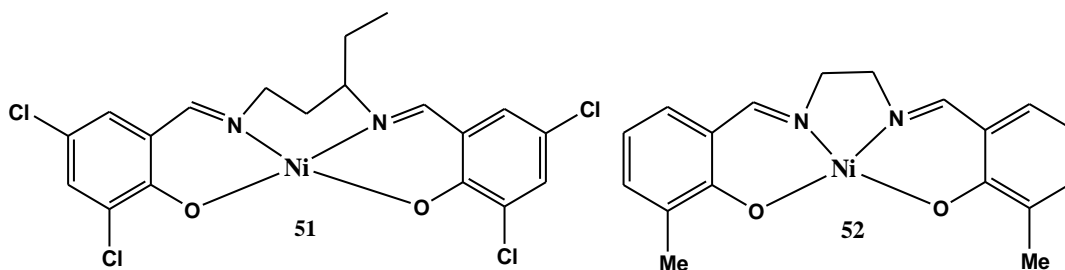
Klement et al. have reported spectroscopic (ESR) and an electrochemical investigation of substituted salen, tetra-hydrosalen, N,N'-dimethylated tetrahydrosalen, and corresponding salphen copper(II) CuL, Cu[H_4]L and Cu[H_2 Me$_2$]L complexes. Spectrophotometric titration with pyridine has been performed to determine the equilibrium constants for adduct formation.The influence of the methylation of the ethylenediamine bridge, N,N'-methylation of the tetrahydrosalen ligands and the effect of the phenylenediamine bridge on structural and magnetic properties of the complexes have been discussed [63].

Khanmohammadi et al. have reported mononuclear copper(II) complexes of a series of salen type ligands **53** viz H_2L^1 = N,N'bis(3,5-di-tert-butylsalicylidene)-2,2-dimethyle-1,3-diaminopropan, H_2L^2 = N,N'-bis(3,5-di-tert-butylsalicylidene)-1,2-diaminopropane, H_2L^3 = N,N'-bis(4-methoxysalicylidene)-2,2-dimethyle-1,3-diaminopropan; $H2L^4$ = N,N'-bis(4-methoxysalicylidene)-1,2-diaminopropane and $H_2[H_2L^1]$ = N,N'-bis(2-hydroxyl-3,5-di-tert-butylphenyl)-2,2-dimethyle-1,3-diaminopropan and $H_2[H_2L^2]$ = N,N'-bis(2-hydroxyl-3,5-di-tert-butylphenyl)-1,2-diaminopropane and studied their antibacterial and antifungal activities by the disc diffusion method. However the results were not notable [64].

H₂Lⁿ (n= 1-4)   H₂[H₂Ln] (n= 1,2)
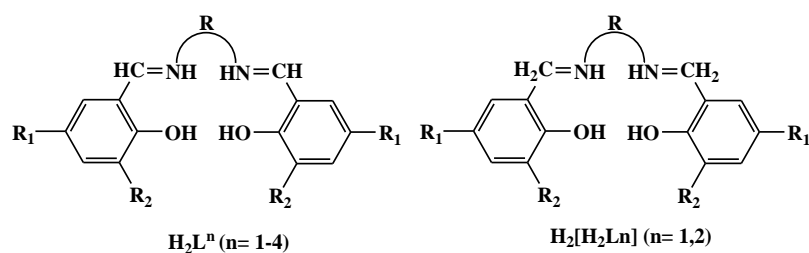
53

Ligands	R	R_1	R_2
H_2L^1	$-CH_2C(CH_3)CH_2-$	t-Bu	t-Bu
H_2L^2	$-CH_2(CH_3)HC-$	t-Bu	t-Bu
H_2L^3	$-CH_2C(CH_3)CH_2$	MeO	H
H_2L^4	$-CH_2(CH_3)HC-$	MeO	H
$H_2[H_2L^1]$	$-CH_2C(CH_3)_2CH_2-$	t-Bu	t-Bu
$H_2[H_2L^2]$	$-CH_2(CH_3)HC-$	t-Bu	t-Bu

Gaballa and workmates have synthesized four platinum(II) $[Pt(L)(H_2O)_2]Cl_2 \cdot nH_2O$ complexes of schiff bases derived from condensation of salicylaldehyde and 2-furaldehyde with o- and p-phenylenediamine **54** and screened for their antimicrobial activities and mode of action against the bacterial species: *E. coli*, *B. subtilis*, *P. aereuguinosa*, *S. aureus*; fungus *A. niger*, *A. fluvus*; and the yeasts *C. albican*, *S. cervisiea* and reported platinum (II) complexes to be more potent antimicrobials than the parent schiff base ligands against one or more microorganisms. The mode of action of the active complex is thought to involve the formation of hydrogen bonds with the active contents of the cell constituents through the nitrogen atom, resulting in interference with the normal cell processes [65].

55
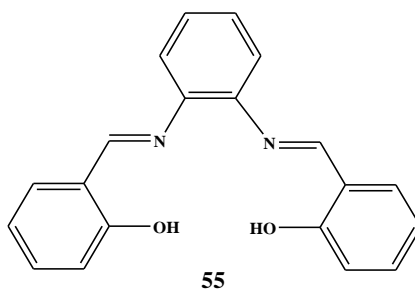
Pan and collegues have synthesized N,N'-3,4-methylphenylenebis(5-methylsalicylaldimine) (L1) and N,N'-bis(5-methylsalicylidene)-o-phenylenediamine (L$_2$) schiff bases ligands and their manganese(III) [Mn(L$_1$)(CH$_3$OH)(dca)] (dca = dicyanoamide) **55** and iron(III) [Fe(L$_2$)(CH$_3$OH)(NCS)] **56** complexes. Single-crystal X-ray crystallographic studies indicated the octahedral coordination of Mn and Fe atoms, with the equatorial donor atoms from the schiff base ligands, and the axial donor atoms from a methanol O atom and a pseudohalide N atom. Complexes have been reported to be effective against *Escherichia coli* and *Candida albicans* [66].

56

57
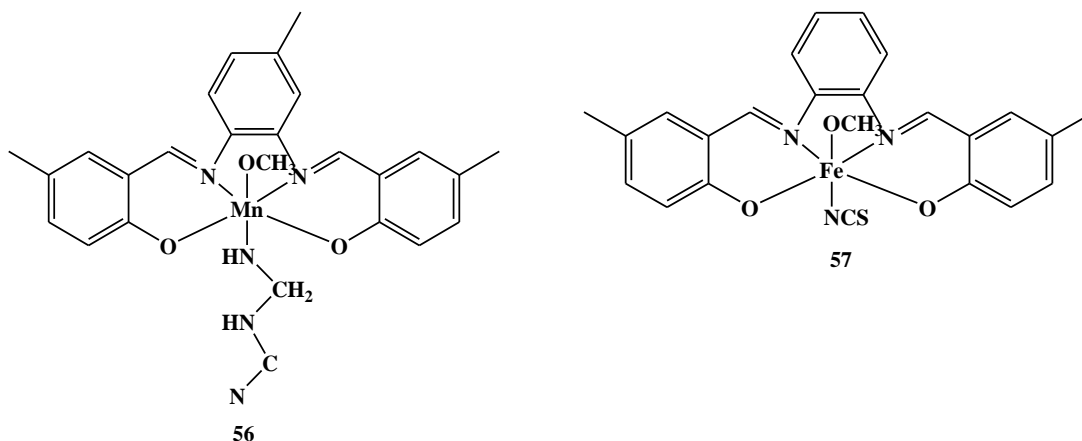
Ajlouni and coworker have reported biological activities and luminescent properties of lanthanide complexes [LnL(NO$_3$)$_2$2H$_2$O]NO$_3$, [Ln = La(III), Pr(III), Nd(III), Sm(III), Eu(III), Gd(III), Tb(III), Dy(III) and Er(III)] with L=N,N'-bis(2-hydroxy-1-naphthylidene)-1,6-hexadiimine **58**. The antimicrobial activities studied against a number of pathogenic bacteria revealed that the Ln(III) complexes possess good antibacterial activity and in most cases it was higher than that of the corresponding ligand [67].

58
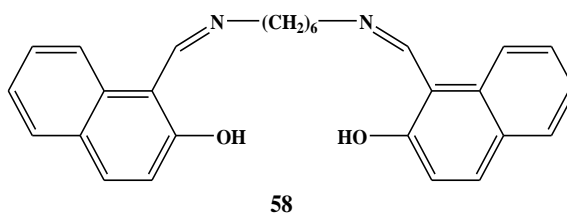
Shelke and collegues have prepared distorted octahedral La(III), Ce(III), Pr(III), Nd(III), Sm(III) and Gd(III) complexes of 4-hydroxy-3-(1-{2-(2-hydroxy-benzylidene)-aminophenylimino}-thyl)-6-methy-pyran-2-one **59** (H$_2$L) ligand derived from o-phenylenediamine, 3-acetyl-6-methyl-(2H)pyran,2,4(3H)-dione (dehydroacetic acid or DHA) and salicylic aldehyde; and characterized thoroughly by spectroscopic, magnetic and thermal analysis. From TGA/DTA data of the complexes kinetic parameters have been determined by Horowitz–Metzger and Coats–Redfern methods. Antibacterial activity of ligand and their metal complexes studied against *Staphylococcus aureus*, *Escherichia coli* and *Bacillus subtilis*. Fungicidal activity against *Aspergillus niger*, *Trichoderma* and *Fusarium oxysporum* indicated that the complexes have enhanced antimicrobial activities compared to free ligand [68].

59
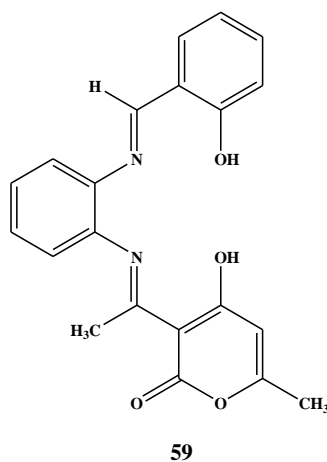
Aziz have performed reactions of Ru$_3$(CO)$_{12}$ with novel tetradentate schiff bases **60-65** in benzene under reduced pressure to form new Ru(II) octahedral complexes of the type [Ru(CO)$_2$(L$_{1-5}$)], where L = anion of N,N'-bis(salicylaldehyde)4,5-dimethyl-1,2-phenylenediamine (saldmophn), N,N'-bis(salicylaldehyde)4,5-dichloro-1,2-

phenylenediamine (saldcophn), N,N'-bis(salicylaldehyde) 2,3-diaminonaphthalene (saldnap), N,N'-bis(o-vanillin)4, 5-dimethy-l,2-phenylenediamine (ovaldmophn), and N,N'-bis(ovanillin) 4,5-dichloro-1,2-phenylenediamine (ovaldcophn), prepared by condensation of salicylaldehyde or o-vanillin with 4,5-dimethyl-1,2-phenylendiamine, 4,5-dichloro-1,2-phenylendiamine and 2,3-diaminonaphathalene. With respect to the biological activity, the moderate bactericidal activities of the ligands increased upon chelation with ruthenium. Further all the new complexes have been reported to be efficient catalysts for oxidation of primary and secondary alcohols into corresponding carbonyl compounds in presence of N-methylmorpholine-N-oxide (NMO) as the source of oxygen [69].

60-65
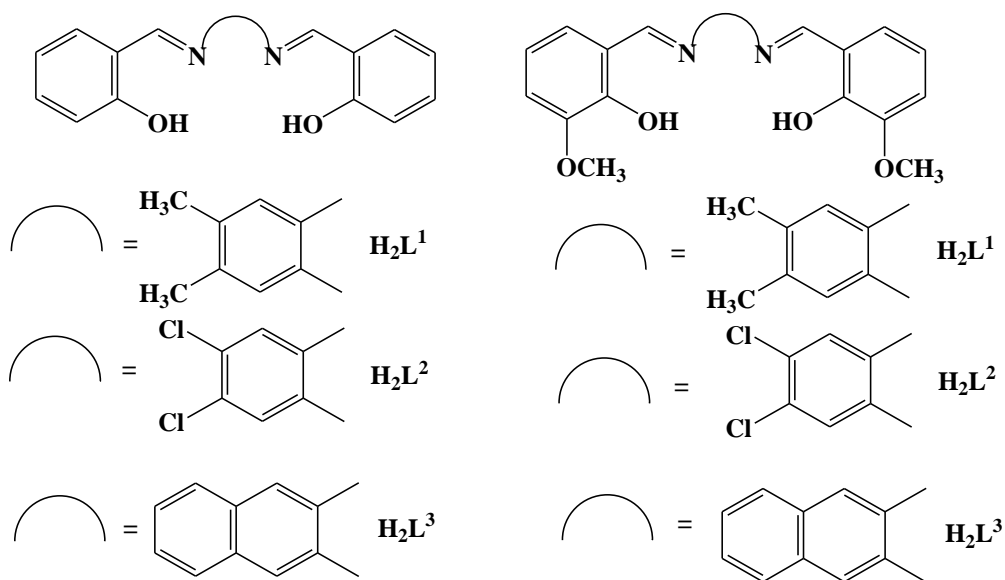
Damercheli and workmates have synthesised salen type Mn(III) complexes having general formula [MnClLx] with ligand derived from condensation of *meso*-1,2-diphenyl-1,2-ethylenediamine with parent and 3-OMe-, 5-Br- or 5-OMe, substituted salicylaldehydes **66**. The complexes showed considerable anticancer activity better than cisplatin and [Mn(salen)Cl] **67** by MTT and apoptosis assays against two human carcinoma cell lines viz. human breast (MCF-7) and liver (Hep G2) cancer cells. The steric factors were found

to be more important than the electronic factors of Mn(III). Docking simulations using AUTODOCK showed that all complexes fitted into the minor groove region of DNA [70].
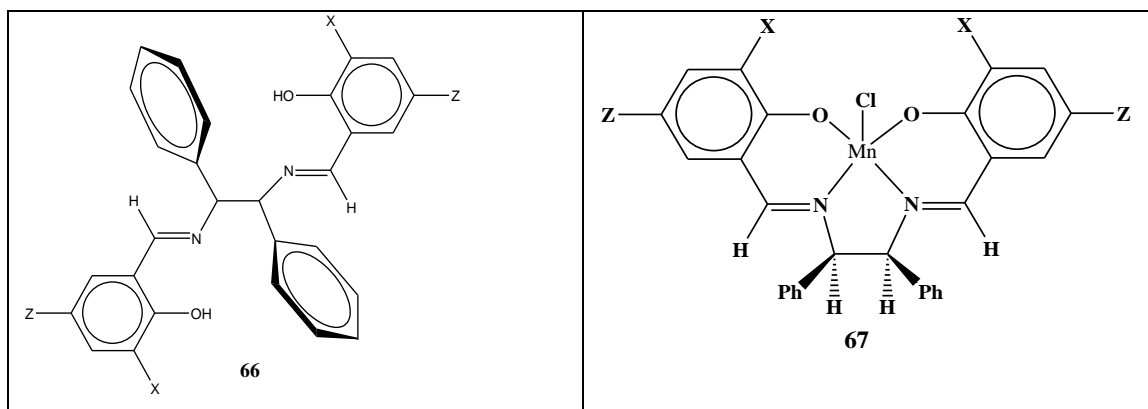
Ligands and Complexes		X	Z
H₂L¹	[MnClL¹] (1)	H	H
H₂L₂	[MnClL²] (2)	OCH₃	H
H₂L³	[MnClL³] (3)	H	Br
H₂L⁴	[MnClL⁴] (4)	H	OCH₃

DNA plays an important role in the life process since it includes genetic information for the cellular function and has been a long-standing target for the diagnosis and treatment of human diseases. The metal complexes suitable for binding and cleaving of DNA are of great interest in design and owing to different applications in nucleic acid chemistry as synthetic restriction enzymes, chemotherapeutic drugs and DNA foot printing agents. It is necessary to understand that the metal complexes interact with the double helix DNA in either a non covalent or a covalent way. The former way includes three binding modes; intercalation, groove binding and external static electronic effects [71-74].

Various research groups around the world have tried to develop small molecules as chemical nuclease.

Peng and collegues have synthesized planar schiff base platinum(II) complex of salphen ligand **68** derived from *o*-phenylenediamine and 5-chlorosalicylaldehyde and studied its crystal structure, in vitro antitumor activities and its influence on cell cycle, cell apoptosis

and colony formation, as well as its binding properties to potential target DNA. The complex exhibited potent in vitro cytotoxicities against six tested human tumor cell lines with IC_{50} values of ca. 11.61 µM and G1-phase arrest and apoptosis in A549 cells in a dose-dependent manner. The binding properties of the complex to DNA have been investigated by several methods which were found to be induced by complex during cell cycle analysis and demonstrated the most probable binding mode to be intercalation [75].

68
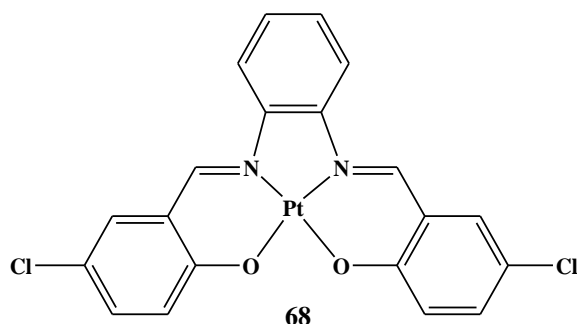
In particular, the schiff bases of o-phenylenediamine are reported to have variety of applications including biological and clinical [76]. The activity can be enhanced when the biologically active ligand is coordinated to a transition metal ion. Therefore, Sampath and Jayabalakrishnan reported four octahedral ruthenium (II) complexes of the type [Ru(CO)(EPh$_3$)L] (where E = P/As as co-ligands; L= dibasic tetradentate schiff base ligand) derived from condensation of 4-chloro-o-phenylenediamine with 3-ethoxysalicylaldehyde and 4-chloro-o-phenylenediamine with 2-hydroxy-1-naphthaldehyde **69**. The interactions of these compounds with CT-DNA studied by UV spectroscopy indicated that the ligands and ruthenium(II) complexes bind to DNA via intercalation. Investigation of antioxidative property showed that all the ruthenium (II) complexes can serve as potential antioxidants than the ligands against DPPH radical and from the results it has been concluded that the substitution of the naphthyl unit in the schiff base moiety with triphenylphosphine as coligand increases the activity of the complexes. [77].

69
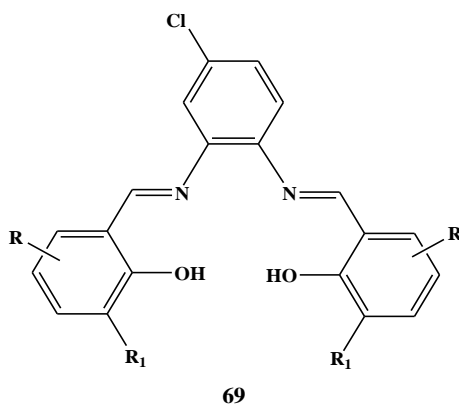
R	R1	Abbreviation
H	OC$_2$H$_5$	H$_2$L^1
C$_4$H$_4$	H	H$_2$L^2

Kulkarni et al. have synthesised La(III), Th(IV) and VO(IV) complexes with schiff bases derived from 8-formyl-7-hydroxy-4-methylcoumarin and o-phenylenediamine /ethylenediamine **70, 71**. Antimicrobial study revealed that, schiff bases and some metal complexes disply high antibacterial activity. The DNA cleavage studies showed that, the La(III) and VO(IV) complexes exhibit non-specific cleavage of DNA [78].

70

71
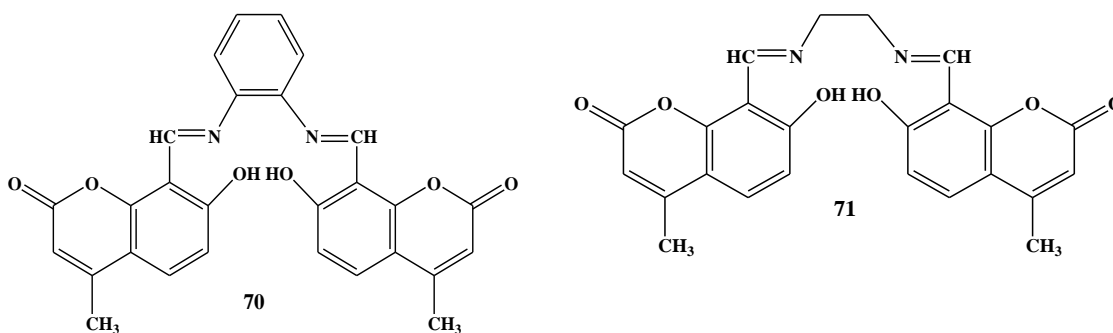
Chiririwa and Muzenda have reported three tetradentate schiff base ligands N,N'-bis (salicylaldehyde) ethylenediamine **72**, N,N'-bis (salicylaldehyde) o-phenylene diamine **73** and N,N'-bis (salicylaldehyde)-dimethylbenzene-1,2-diamine and their gold (III) complexes. The cytotoxic properties of the gold (III) complexes were also evaluated toward A2780 ovarian human cell line either sensitive (A2780/S) or resistant (A2780/R) to

cisplatin. The free ligands were found to be very active against some the cancer cell lines while the gold(III) complexes exhibited activity that is comparable to cisplatin and demonstrated potential towards development of new anticancer agents [79].

72   **73**
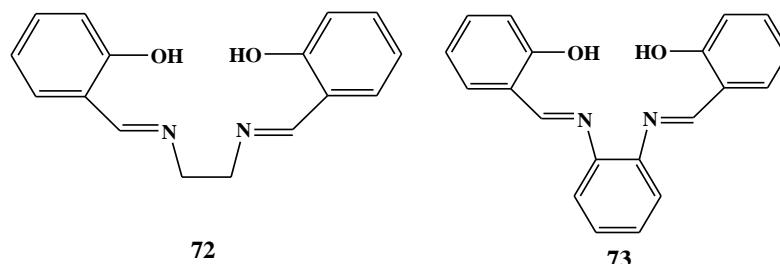
DNA is an important primary cellular target for most of the therapeutic drugs in clinical use [80, 81], hence considerable attention has been focused on the development of DNA targeted antimicrobials [82, 83]. It was also suggested that the reductive capability of reductants had a critical influence on DNA cleavage, hence several efficient DNA cleaving agents have been developed

Shahabadi et al. have investigated the binding interaction of a water soluble Co(II) complex **74** of a schiff base N,N'-bis{5-[(triphenylphosphonium chloride)-methyl] salicylidine}-o-phenylenediamine) with calf thymus DNA (CT-DNA). Intrinsic binding constant (Kb) indicated binding affinity of schiff base to be stronger than its Co(II) complex. The schiff base is found to intercalate between DNA base pairs while its Co(II) complex most likely interacts with DNA in an electrostatic binding mode [84].

74
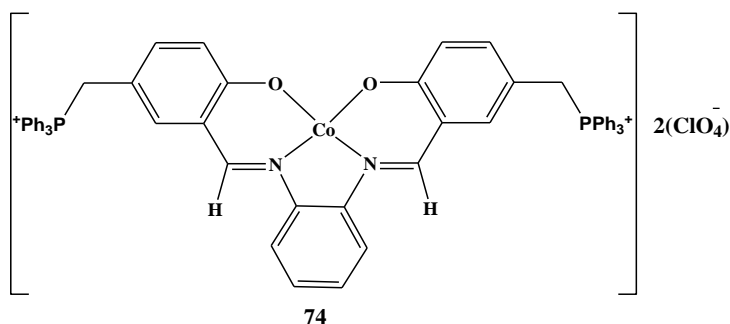
Jone and workmates have synthesized nickel salen complexes with sulfadiazine **75** and screened them for antimicrobial and cytotoxic activities. The in vitro anticancer study against human breast cancer cell line HeLa showed the IC_{50} value 116 µM [85].

75
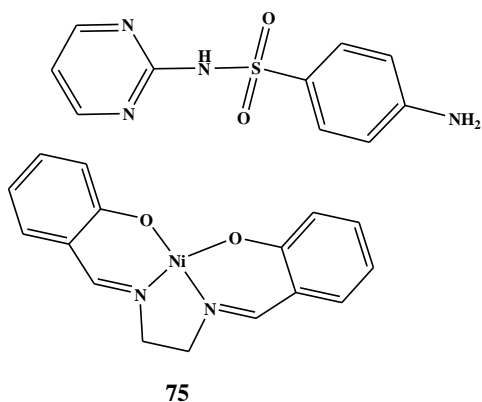
Usman et al. have synthesized Copper-based therapeutic drugs, viz. [Cu(dip)$_2$] **55** and [Cu(dimp)$_2$] **56** and characterized them throughly by single crystal X-ray diffraction and other spectroscopic techniques. Electrostatic mode of binding with partial intercalation in minor groove region has been revealed through *in vitro* DNA binding mode of the complexes. Verification of the trend of DNA binding site and affinity of the complexes performed through molecular docking studies have indicated that the complexes are having the ability to cleave DNA through an oxidative mechanism induced by reactive oxygen species (ROS).Further the anti-biofilm activity experiments have been carried out to validates the potency of the copper complexes as drugs so that they can be employed against bacterial biofilm infections [86].

76

77
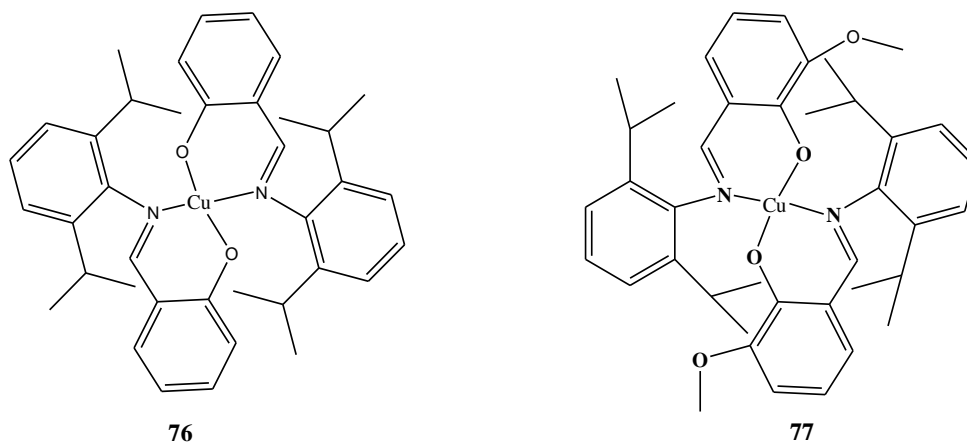
Salehi et al. have investigated spectroscopic and electrochemical properties of *trans*-[CoIII(L^1)(Py)$_2$]ClO$_4$ **78** and *trans*-[CoIII(L^2)(Py)$_2$]ClO$_4$ **79** complexes, where H$_2$L^1 is N,N'-bis(5-chloro-2-hydroxybenzylidene)-1,3-propylenediamine and H$_2$L^2 = N,N'-bis(5-bromo-2-hydroxybenzylidene) -1,3-propylenediamine and *in-vitro* antimicrobial activity of the schiff base ligands and their corresponding complexes against human pathogenic bacteria. Where cobalt(III) complexes showed lower antimicrobial activity than the free schiff base ligands [87].

78   79
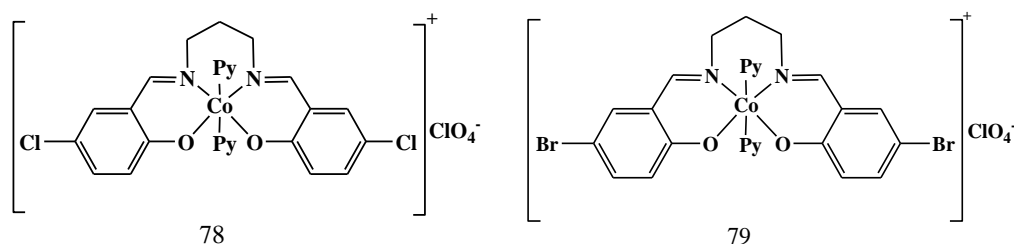
1.5.1 Unsymmetrical Schiff bases and their matal complexes

Although in the last few decades, less attention was focused on unsymmetrical tetradentate schiff bases derived from diamines with different aldehydes and ketones, recently studied on unsymmetrical schiff bases and their metal complexes have been attempted to investigate.

Asadi and workmates have described thermodynamic studies of 1:1 adduct formation of diorganotin(IV) dichlorides with Ni(II) Salophen-type [N,N'-bis(salicylaldehydo)-1,2-phenylenediimine] **1** N$_2$O$_2$ complexes and also investigated the electronic and the steric effect of the schiff type ligand of the Ni complexes and the organic groups of the tin dichlorides on the formation constant and free energy of the adducts formed **2**.[**88**].

80

(1-4) A, B, C= H(4); A=MeO and B,C= H (3)
B= MeO and A, B= H (2) and A, B= H (2); C= MeO
and A, C= H (1) and

81
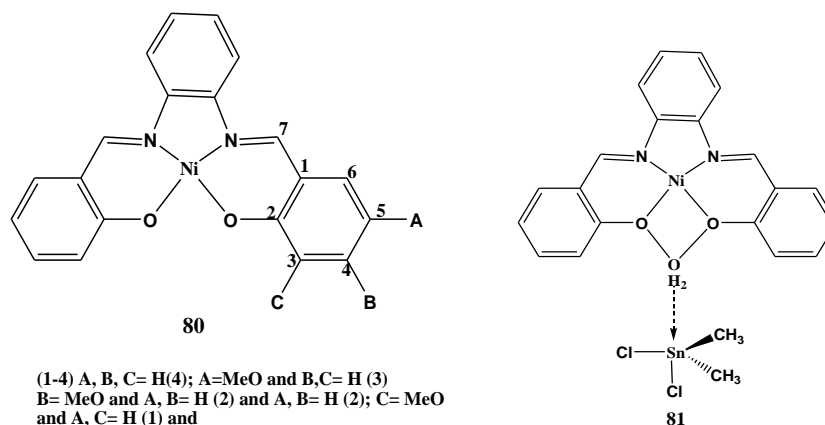
Kurt and Deniz have synthesized [Fe(L)Cl] **82**, [Ni(L)] **83**, and [Zn(L)C2H5OH] **84**
complexes of unsymmetrical N_2O_2 tetradentate N1,N4-diarylidene-S-methyl-
thiosemicarbazone ligand using 2-hydroxyacetophenone-S-methyl-thiosemicarbazone and
salicylaldehyde as starting compounds [89].

82

83

84
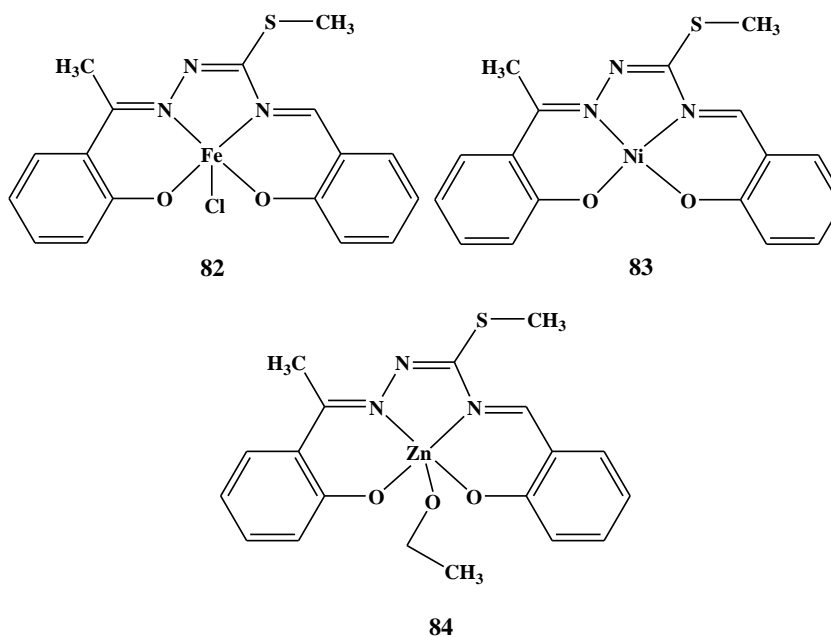
Lashanizadegan et al. have synthesized M(II)L (M= Ni, Cu, Co and Zn) complexes of non-
symmetrical tetradentate schiff-base **85** designed by the condensation of 2-
hydroxyacetonaphthone, phenylendiamine, with 2-hydroxy-1-naphthaldehyde and

reported single crystal X-ray structures of Ni and Cu complexes having slightly distorted square-planar coordination geometry [90].

85
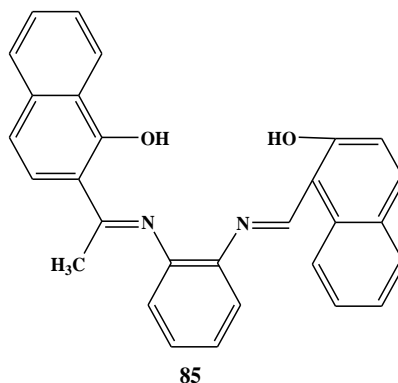
Akine and coworker have designed a series of salen-type chelate ligands that have two oxime bonds instead of imine bonds and compared their stability against exchange reaction of the C=N bonds, with the corresponding salen derivatives. Synthesis of unsymmetrical salen derivatives consisting of two different salicylideneimine moieties is difficult because of the C=N bond recombination; so the salamo ligands **86** were prepared by the reaction of 1,2-bis(aminooxy)ethane with 2 equivalents of salicylaldehyde derivatives under mild conditions. The crystal structure of ligand suggests that the oxime-OH form is more predominant than the keto-NH form. The metathesis of the C=N bonds of the salamo derivatives did not occur in H_2O/MeCN (5:95), hence, the salamo derivatives were reported to be at least 10^4 times more stable than salen derivatives. Therefore, symmetric and unsymmetrical salamo, as well as monooxime precursors, have been thought to be capable units for the construction of multidentate ligands having different kinds of C=N metal-chelate sites [91].

86
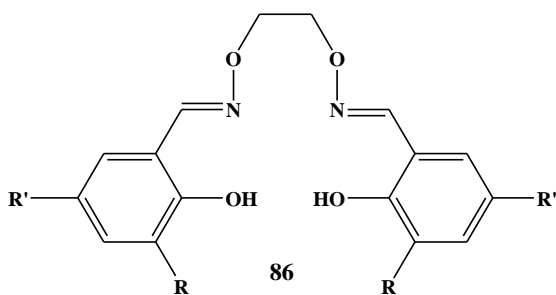
1a	R= R'= H
1b	R= OMe, R'= H
1c	R= R'= t-Bu
1d	R= SMe, R'= H
1e	R= H, R'= Br
1f	R= H, R'= OH
1g	R= OH, R'= H
1h	R= H, R'= NO$_2$

Cobalt(II) complexes of a new series of unsymmetrical schiff bases **87, 88** derived from 2-hydroxy-1-naphthaldehyde, o-phenylenediamine, and salicylaldehyde / substituted salicylaldehyde have been synthesized by Nejo et al. Minimum inhibitory concentration (MIC) of screening of the schiff bases and their complexes against 10 human pathogenic bacteria indicated that in a number of cases activities were comparable with or higher than, that of chloramphenicol against some strains of bacteria [92-96].

87   **88**
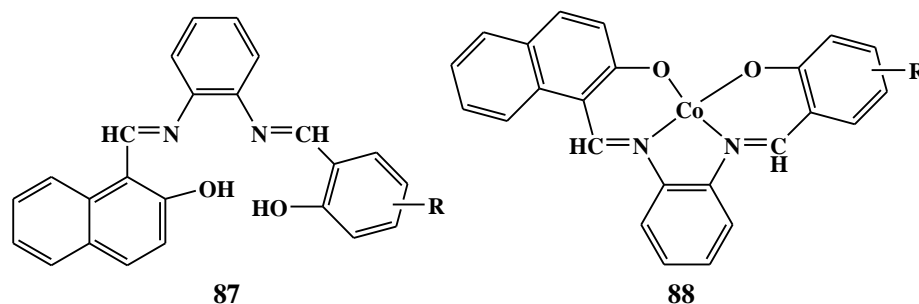
Ligands	R
H_2L^1	5-Cl
H_2L^2	5-NO$_2$
H_2L^3	3-OCH$_2$CH$_3$
H_2L^4	H

Hegazy and Gaafar have prepared new palladium (II) and platinum (IV) complexes of a series of unsymmetrical tetradentate schiff bases derived from aromatic 2-hydroxy aldehydes (salicylaldehyde/substituted salicylaldehyde, 2-hydroxy-1-naphthaldehyde) **89** and o-phenylenediamine. In vitro antibacterial results against 10 human pathogenic bacteria indicated that such complexes can be used as vital and effective antibiotics [97].

89

R= 5-Cl, H$_2$L^1, R= 5 -NO2, H$_2$L^2, R= 3 -OC$_2$H$_5$, H$_2$L^3, R= H, H$_2$L^4
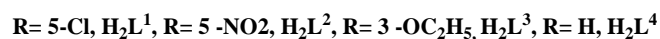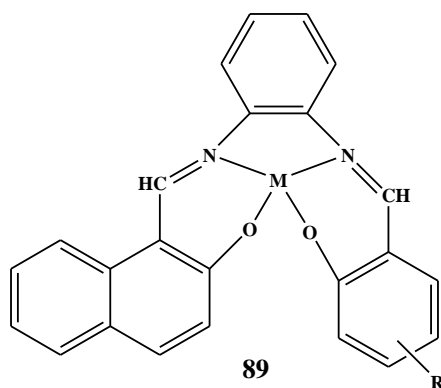
Meghdadi et al. have reported copper(II) and nickel(II) complexesof two new N$_2$O$_2$ unsymmetrical schiff bases prepared by condensation of the free amine group of the precursor tridentate ligand Hbacabza [3-(2-aminobenzylimino)-1-phenylbutan-1-ol], [98] with salicylaldehyde and 2-hydroxy-1-naphthaldehyde to form H$_2$L^1 = 3-[({o-[(E)-(o-hydroxyphenyl)methylideneamino]phenyl}methyl)imino]-1-phenyl-1-buten-1-ol **90- 93** and H$_2$L^2 = 3-[({o-[(E)-(2-hydroxy-1-naphthyl)methylideneamino] phenyl}methyl)imino]-1-phenyl-1-buten-1-ol respectively. Crystal structures of all these complexes determined by X-ray diffraction indicated distorted-puckered square geometry around Cu(II) and Ni(II) which has been thought due to the presence of the rigid –C$_{phenyl}$–C$_{phenyl}$–CH$_2$-spacer between the two nitrogens has been drawn through the detailed electrochemical studies have of these complexes have indicated a good correlation between the structural distortion and the redox potentials of the metal centers. The ligand and metal complexes showed in vitro antibacterial activity and particularly more against *B. cereus* [99].

90

91

92

M= Cu(II), Ni(II)

93

M= Cu(II), Ni(II)
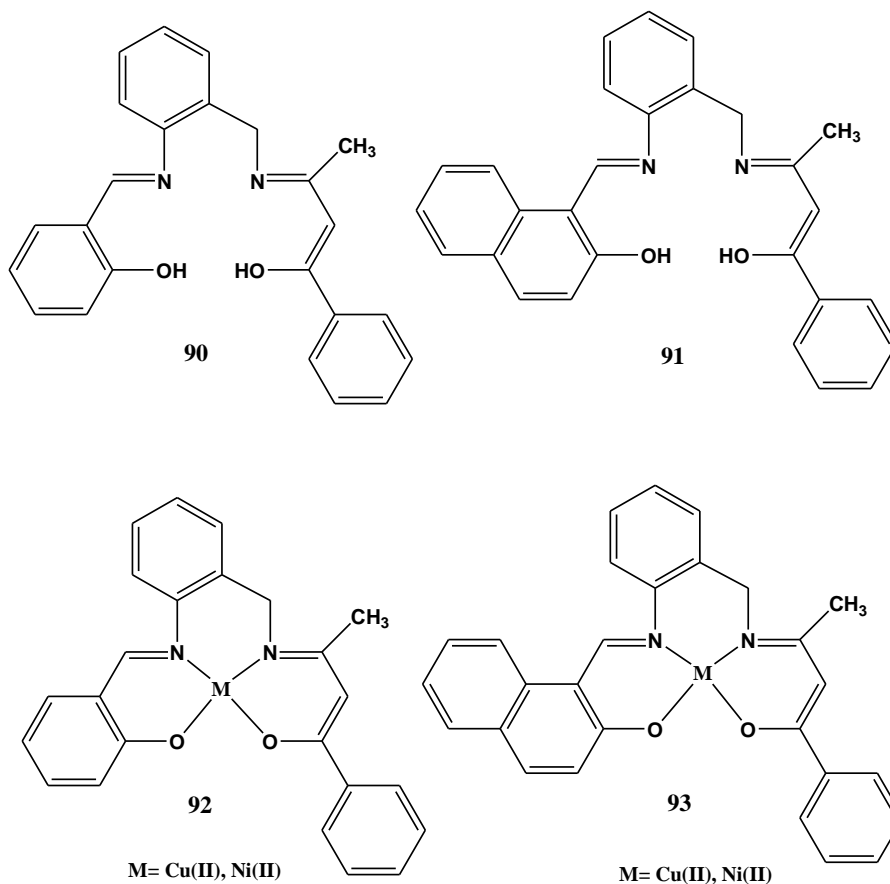
Gradinaru and coworkers have developed Ni(II), Cu(II), Zn(II), and VO(II) complexes of new unsymmetrical schiff base synthesized by template condensation of the tetradentate precursor 1-phenylbutane-1,3-dionemono-S-methylisothiosemicarbazone with o-hydroxybenzaldehyde or its 5-phenylazo derivative **94**. The crystal structures of five complexes **95- 99** have been comfirmed by X-ray diffraction. The compounds were found to have large thermal stability. The possible application of this class of compounds as second-order nonlinear optical (NLO) materials has been tested for the first time through a combined experimental (measurements of solution-phase direct current electricfield-induced second harmonic generation) and theoretical (time-dependent density functional theory (TDDFT) calculations) studies and the results found to be competitive with that of the best organic and metalorganic candidates of similar size [100].
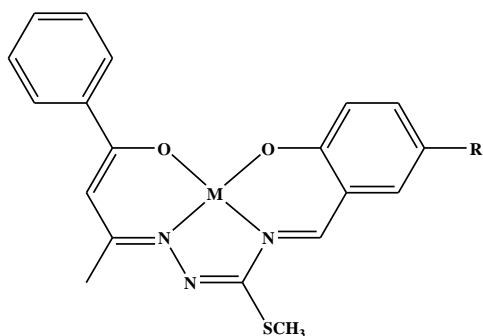
94

ML^1, R=H, M= Ni^{2+} (1), Cu^{2+} (2), Zn^{2+} (3), VO^{2+} (4)

ML^2, R=N$_2$Ph, M= Ni^{2+} (5), Cu^{2+} (6), Zn^{2+} (7), VO^{2+} (8)
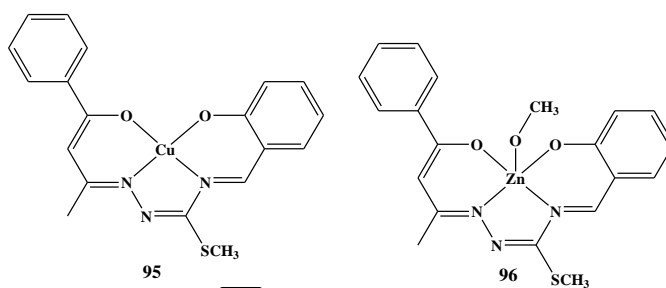
95

96
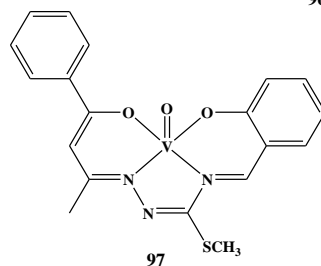
97
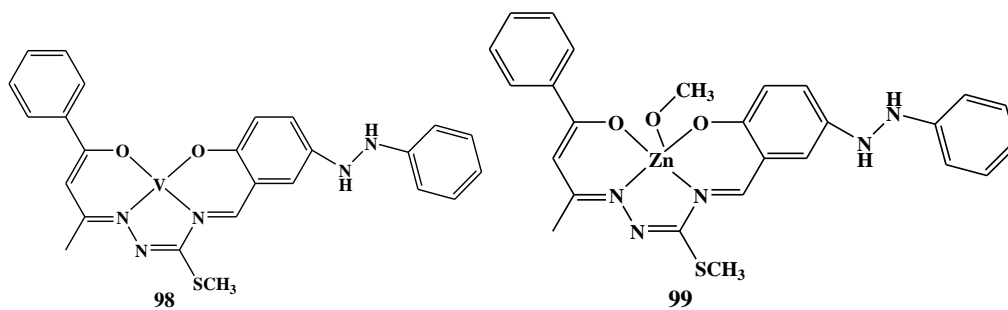
98

99

Huber and workmates prepared several unsymmetrically substituted salen-type cobalt(II) schiff-base CoL complexes and studied dioxygen affinity of the complexes in DMF at various temperatures to provide a finer tool for property tuning, to determine the corresponding equilibrium constants K_{O2}.

according to Equation (1), on the Lewis acidity of the cobalt center, as characterized by equilibrium constants K_{py} according to Equation (2), and on the oxidation potential, $E_{½}$, of complexes, according to the reaction $Co^{II}L \rightleftharpoons Co^{III}L^+ + e^-$ [101].

$$CoL + O_2 \xrightleftharpoons{K_{O_2}} CoL.O_2 \quad \text{------} \quad (1)$$

$$CoL + Py \xrightleftharpoons{K_{Py}} CoL.Py \quad \text{------} \quad (2)$$
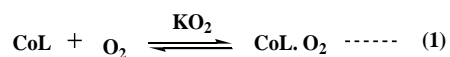
Rajasekar and collegues have discussed Ni(II) and Cu(II) complexes of unsymmetrical schiff-base ligands derived from salicylaldehyde/5-methylsalicylaldehyde and ethylenediamine or diaminomaleonitrile (DMN) **100-101**. The in vitro antimicrobial activity of the compounds was tested against human pathogenic bacterial microbes and antifungal activity was tested against *Candida albicans*. All the complexes exhibited antimicrobial activity and an electron-withdrawing group was found to enhance it [102].

M= Ni or Cu

100   **101**

.
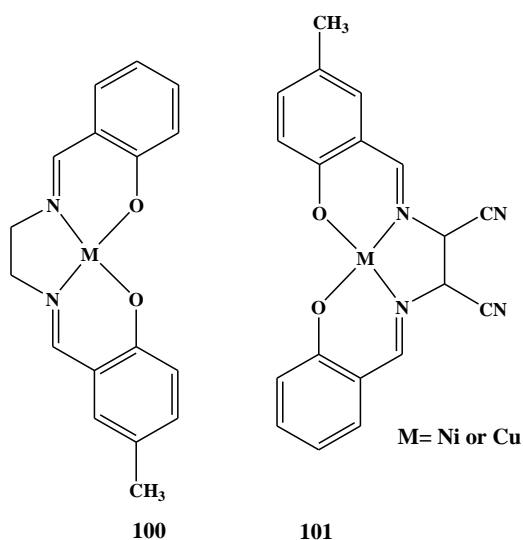
1.5.2 Binuclear Metal Complexes

A number of dinuclear complexes from various types of ligand systems have been prepared and examined for their oxygen uptake or redox processes of oxygen, their catalytic activity, and pharmacological activities [103-105]. Some examples of binuclear metal complexes involving N_2O_2 donor ligands are presented here.

Rabindra and Shilpa synthesized the dinuclear Cu(II) complexes of [Cu_2(salophen)$_2$] **102** and [Cu_2(salen)$_2$] **103** with schiff bases derived from salicylaldehyde and o-phenylenediamine (ophen) or ethylenediamine (en) and studied their DNA binding and cleavage abilities. Binding studies revealed that the complexes possess good binding propensities and good DNA-cleavage abilities were observed under oxidative and hydrolytic conditions with rate constants are 1.54 h^{-1} and 0.72 h^{-1} for **102** and **103**, respectively. The higher binding and cleavage activity of 1 is than that of 2 is explained on the basis of the presence of an extended aromatic phenyl ring in the former [106].

102   103
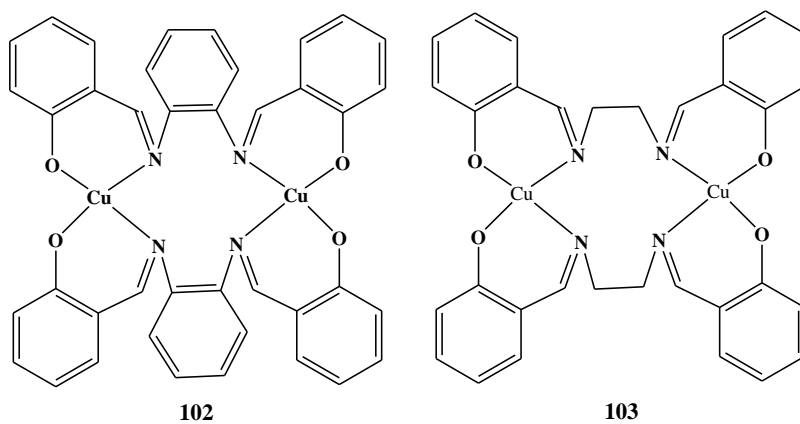
Akila et al. reported binucleating square planar Cu(II), Ni(II) and square pyramidal VO(II) complexes **104** derived from 1,5-diaminonapthalene and salicylaldehyde. The metal complexes have shown higher antibacterial activity than the free ligand according to the chelation theory [107].

M= Cu, Ni and VO

104
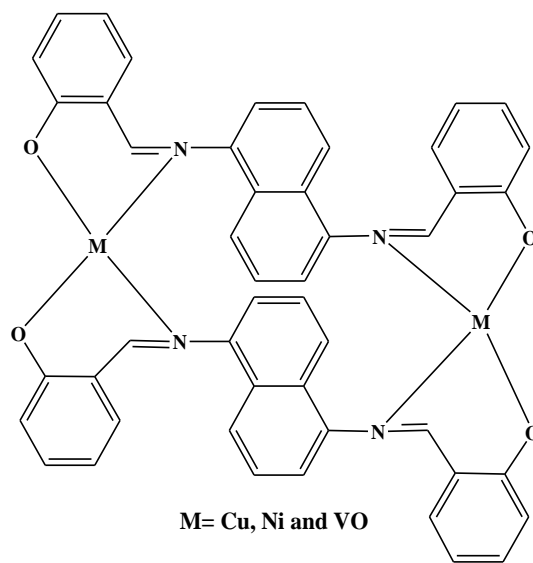
Cai and collegues have prepared dinuclear oxomolybdate **104** complex by the reaction of MoCl$_3$.3H$_2$O with N,N'-bis(salicylidene)-propane-1,3-diamine. The Single crystal X-ray diffraction analysis shows first example of nearly linear O-Mo-O-Mo-O arrangements [108].
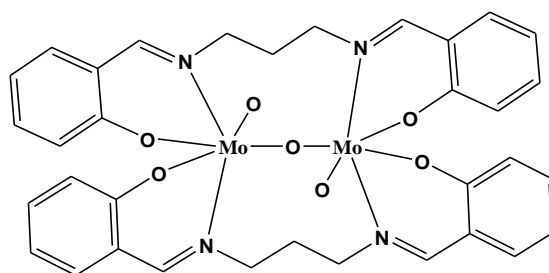
105

Kou and workmates have reported five binuclear copper(II) schiff base complexes [Cu$_2$(L)(OAc)]·3DMF, [Cu$_2$(L)(OAc)]2·3DMF, [Cu$_2$(L)(BNPP)]·3CH$_3$CN, [Cu$_2$(L)(Fa)]·2DMF and [Cu$_2$(L)(Pa)]·DMF from N,N'-bis(3,5-tert-butylsalicylidene-2-hydroxy)-1,3-propanediamine, OAc=acetic acid, BNPP= bis(4-nitrophenyl)phosphate, Fa=2-tetrahydrofuroic acid, Pa=benzoic acid) **106-110**.

All the complexes are reported to effectively promote cleavage of plasmid DNA without addition of any external agents and in the presence of hydrogen peroxide at pH = 7.2 and

37 °C. DNA cleavage mechanism studies have showed that the complexes might be capable of promoting DNA cleavage through an oxidative DNA damage pathway [109].
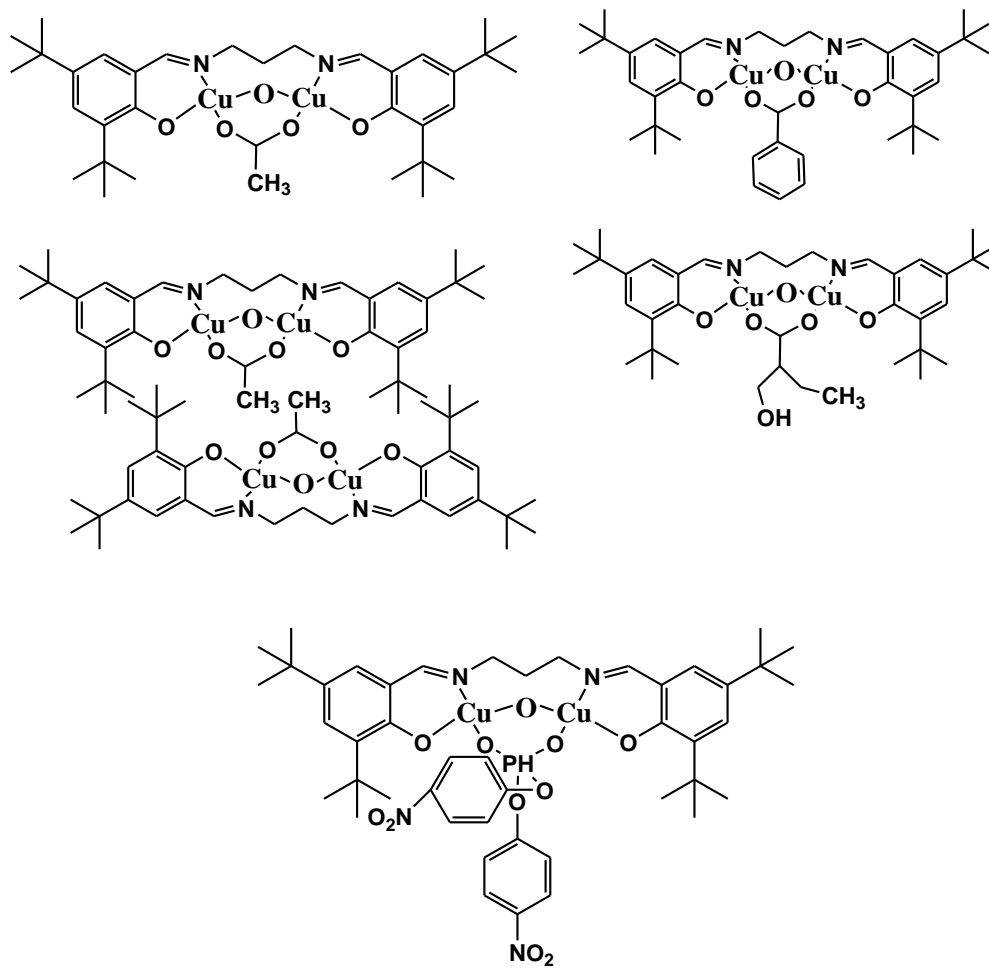
106- 110

Zhou and Peng synthesized two structurally similar centrosymmetric phenoxo-bridged dinuclear manganese(III) complexes, $[Mn_2(L^1)_2(N_3)_2]$ **111** and $[Mn_2(L^2)_2(NCS)_2]$ **112**, prepared from the tetradentate bis-schiff base ligands, N,N'-bis(salicylidene)propane-1,2-diamine (H_2L^1) and N,N'-bis(salicylidene)ethane-1,2-diamine (H_2L^2), in the presence of pseudohalides and studied their catalytic properties for the oxidation of various olefins to their corresponding epoxides [110].

111

112
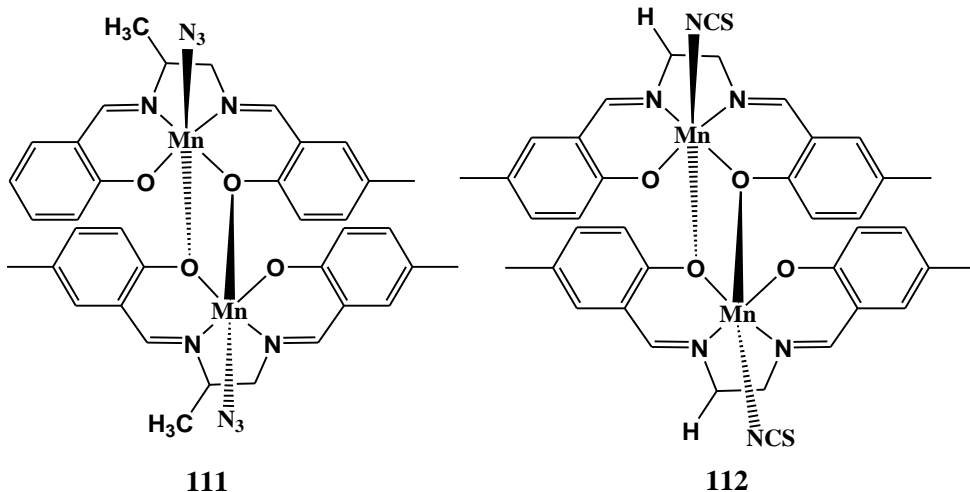
Sanzenbacher and colleges have prepared novel difluoro-bridged dinuclear chromium(III) complex by the reaction of trans-[Cr(py)₄F₂]ClO₄ in 2-methoxyethanol with a substituted tetrahydrosalen derivative N,N'-bis(2-hydroxy-3,5-di-tert-butylbenzyl)-1,2-ethanediamine) [111].

113
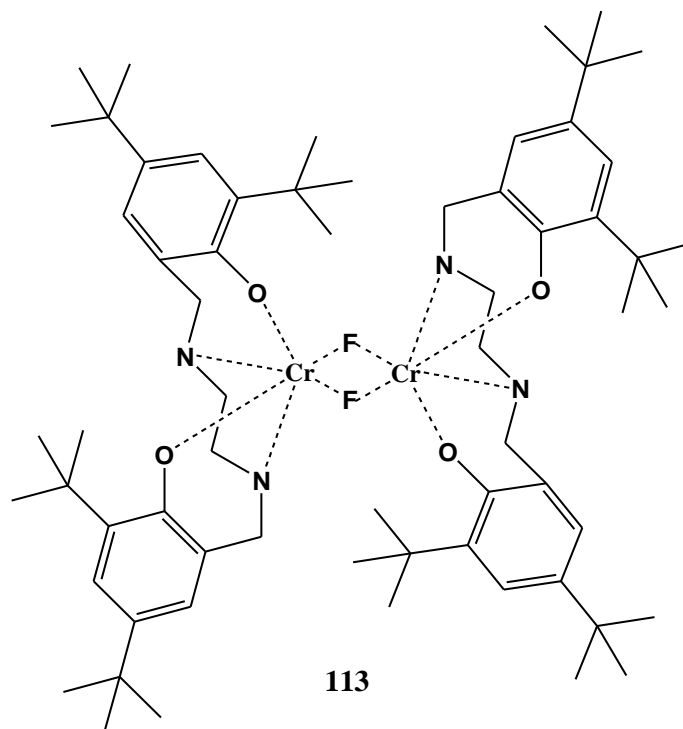
1.6 Scope of the present work

In the present research, substituted salicyaldehyde i.e. 2-hydroxy-6-isopropyl-3-methyl benzaldehyde has been condensed with different diamine linkages such as ethane-1,2 diamine, propane-1,2-diamine, benzene-1,2-diamine and propane-1,2-diamine to prepare four schiff bases EN, DP, PH and 1,2-DP as tetradentate N_2O_2 donor ligands. The manganese, cobalt, nickel and copper complexes of these four schiff bases have been prepared by reacting metal acetate/ chloride salts in the 1:1 molar ratios. The ligands were characterized through spectroscopic techniques, FT-IR, UV-Visible, ^{1}H and ^{13}C-NMR, elemental analysis, and finally with single crystal X-ray crystallography to solve structures of PH and 1,2-DP ligand. The characterization of all the metal complexes has been carried out by FT-IR, UV-visible, ESR spectroscopy and elemental, thermogravimetric and SEM analysis and conductivity and magnetic measurements, along with structures of ENMn(III), ENNi(II), DPNi(II), DPCu(II), PH, 1,2-DP, 1,2-DPNi(II) compounds solved through the single crystal X-ray crystallographic techniques. All the compounds have been studied for their biological applicability i.e. antibacterial, antifungal, antioxidant and DNA cleavage activities.

1.7 References:

1. Cozzi PG, Chemical Society Reviews, 33 (2004) 410-421.

2. Obasi LN, Kaior GU, Rhyman L, Alswaidan IA, Fun HK, Ramasami P, Journal of Molecular Structure,1120 (2016) 180-186.

3. Hine J, Yeh CY, Journal of the American Chemical Society, 89 (1967) 2669-2676.

4. Fessenden RJ, Fessenden JS, The Journal of Organic Chemistry, 32 (1967) 3535-3537.

5. Vigato PA, Tamburini S, Coordination Chemistry Reviews, 248 (2004) 1717-2128.

6. Borisova NE, Reshetova MD, Ustynyuk YA, Chemical reviews, 107 (2007) 46-79.

7. Kolawole GA, Osowole AA, Journal of Coordination Chemistry, 62 (2009) 1437-1448.

8. Sadeek SA, Refat MS, Teleb SM, Bulletin of the Chemical Society of Ethiopia. 2004;18(2).

9. Yıldız M, Kılıç Z, Hökelek T, Journal of molecular structure, 441 (1998) 1-10.

10. Sunatsuki Y, Motoda Y, Matsumoto N, Coordination chemistry reviews, 226 (2002) 199-209.

11. Rillema DP, Jones DS, Woods C, Levy HA, Inorganic Chemistry, 31 (1992) 2935-2938.

12. Alan I, Kriza A, Olar R, Stanica N, Badea M, Journal of thermal analysis and calorimetry, 111(2013) 1163-1171.

13. Mota VZ, de Carvalho GS, Corbi PP, Bergamini FR, Formiga AL, Diniz R, Freitas MC, da Silva AD, Cuin A, Spectrochimica Acta Part A: Molecular and Biomolecular Spectroscopy, 99 (2012) 110-115.

14. Zhang W, Loebach JL,Wilson SR, Jacobsen EN, J. Am. Chem. Soc, 112 (1990) 2801-2803.

15. Herrmann WA, Rauch MU, Artus GRJ, Inorg. Chem, 35 (1996) 1988-1991.

16. Artus GRJ, Rauch MU, Herrmann WA, Zeitschrift für Kristallographie - New Crystal Structures, 212 (1997) 227-228.

17. Pagadala R, Ali P, Meshram JS, Journal of Coordination Chemistry, 62 (2009) 4009-4017.

18. Di Bella S, Fragalà I, Ledoux I, Diaz-Garcia MA, Marks TJ, Journal of the American Chemical Society, 119 (1997) 9550-9557.

19. Qian SS, Cheng XS, You ZL, Zhu HL, Synthesis and Reactivity in Inorganic, Metal-Organic, and Nano-Metal Chemistry, 43 (2013) 1465-1470.

20. Xue LW, Li XW, Zhao GQ, Yang WC, Synthesis and Reactivity in Inorganic, Metal-Organic, and Nano-Metal Chemistry, 43 (2013) 1514-1517.

21. Tella S, Bekiari V, Kessler VG, Papaefstathiou GS, Polyhedron, 64 (2013) 77-83.

22. Popov LD, Levchenkov SI, Shcherbakov IN, Suponitskii KY, Tupolova YP, Lukov VV, Kogan VA, Russian Journal of Coordination Chemistry, 39 (2013) 689-693.

23. Saleh AA, Tawfik AM, Abu-El-wafa SM, Osman HF, Journal of Coordination Chemistry, 57 (2004) 1191-1204.

24. Rodríguez-Doutón MJ, Fernández MI, González-Noya AM, Maneiro M, Pedrido R, Romero MJ, Synthesis and Reactivity in Inorganic, Metal-Organic and Nano-Metal Chemistry, 36(2006) 655-662.

25. Akbari A, Ahmadi M, Takjoo R, Heinemann FW, Journal of Coordination chemistry, 66 (2013) 1866-1875.

26. Akbari A, Ahmadi M, Takjoo R, Heinemann FW, Journal of Coordination chemistry, 65 (2012) 4115-4124.

27. Abd-Elzaher MM, Sythesis and Reactivity in Inorganic and Metal-Organic Chemistry, 30 (2000) 1805-1816.

28. Pramanik HA, Chanda S, Bhattacharjee CR, Paul PC, Mondal P, Prasad SK, Shankar Rao DS, Liquid Crystals, 43 (2016) 1606-1615.

29. LIU J, Wu BW, Zhang B, Liu Y, Turkish Journal of Chemistry, 30 (2006) 41-48.

30. Deligönül N, Tümer M, Serin S, Transition metal chemistry, 31 (2006) 920-929.

31. Raisanan MT, Klinga M, Leskela M, Nieger M, Repo T, Journal of Coordination Chemistry, 63 (2010) 4280-4289.

32. Bhattacharjee CR, Goswami P, Mondal P, Inorganica Chimica Acta, 30 (2012) 86-92.

33. Bayoumi HA, Alaghaz AM, Aljahdali MS, Int. J. Electrochem Sci, 8 (2013) 9399-9413.

34. Tas E, Aslanoglu M, Ulusoy M, Temel H, Journal of Coordination Chemistry, 57 (2004) 677-84.

35. Grivani G, Baghan SH, Vakili M, Khalaji AD, Tahmasebi V, Eigner V, Dušek M, Journal of Molecular Structure, 1082 (2015) 91-96.

36. Tidjani-Rahmouni N, Djebbar-Sid S, Chenah N, Benali-Baitich O, Synthesis and reactivity in inorganic and metal-organic chemistry, 29 (1999) 979-994.

37. Repo T, Klinga M, Leskela M, Pietikainen P, Brunow GD, Acta Crystallographica Section C: Crystal Structure Communications, 52 (1996) 2742-2745.

38. Chen H, White PS, Gagné MR, Organometallics, 17 (1998) 5358-5366.

39. Dogan F, Ulusoy M, Ozturk OF, Kaya I, Salih B, Journal of thermal analysis and calorimetry, 96 (2009) 267-276.

40. Refat MS, El-Sayed MY, Adam AM, Canadian Chemical Transactions, 2 (2014) 149- 159.

41. Murtaza GH, Mumtaz AM, Khan FA, Ahmad SA, Azhar S, Najam-Ul-Haq MU, Atif M, Khan SA, Maalik A, Alam FI, Hussain I, Acta Pol. Pharm, 71 (2014) 531-535.

42. da Silva CM, da Silva DL, Modolo LV, Alves RB, de Resende MA, Martins CV, de Fátima Â, Journal of Advanced research, 2 (2011) 1-8..

43. Qin DD, Yang ZY, Wang BD, Spectrochimica Acta Part A: Molecular and Biomolecular Spectroscopy, 68 (2007) 912-917.

44. Shanker K, Rohini R, Ravinder V, Reddy PM, Ho YP, Spectrochimica Acta Part A: Molecular and Biomolecular Spectroscopy, 73 (2009) 205-211.

45. Singh P, Singh V, Goel R, Singh B, Journal of the Indian Chemical Society, 52 (1975) 958-959.

46. Perry BF, Beezer AE, Miles RJ, Smith BV, Miller J, Nascimento MD, Microbios. 1986.

47. Kabak M, Elmali A, Elerman Y, Journal of molecular structure, 477 (1999) 151-158.

48. Dhivya Priya D, Akila E, Usharani M, Rajavel R, International Journal Of Pharmacy &Technology, 4 (2012) 4067-4078.

49. Hamada Y, IEEE Transactions on electron devices, 44 (1997) 1208-1217.

50. Sari N, Arslan S, Logoglu E, Sakiyan I, GUJ Sci, 16 (2003) 283-288.

51. Jayabalakrishnan C, Natarajan K, Transition Metal Chemistry, 27 (2002) 75-79.

52. Mohie EM, El-Shishtawy RM, Asian Journal of Chemistry, 25 (2013) 2719.

53. Aziz AA, Badr IH, El-Sayed IS, Spectrochimica Acta Part A: Molecular and Biomolecular Spectroscopy, 97 (2012) 388-396.

54. Singh NP, Saini P, Kumar A, Asian Journal of Chemistry, 26 (2014) 7515.

55. Liu J, Zhang B, Wu B, Zhang K, Hu S, Turkish Journal of Chemistry, 31 (2007) 623-629.

56. Pasini A, Gullotti M, Journal of Coordination Chemistry, 3 (1974) 319-332.

57. Haas GE, Schimek GL, Pennington WT, Kolis JW, Acta Crystallographica Section C: Crystal Structure Communications, 54 (1998) 1263-1265.

58. Aranha PE, dos Santos MP, Romera S, Dockal ER, Polyhedron, 26 (2007) 1373-1382.

59. Kasumov VT, Özalp-Yaman Ş, Taş E, Spectrochimica Acta Part A: Molecular and Biomolecular Spectroscopy, 62 (2005) 716-720.

60. Khuhawar MY, Channar AH, Journal of Macromolecular Science, Part A, 32 (1995) 523-530.

61. Zare AJ, Ataeinia P, Life Science Journal, 9 (2012) 2396- 2405.

62. Sheng GH, Cheng XS, Wang X, Huang D, You ZL, Zhu HL, Synthesis and Reactivity in Inorganic, Metal-Organic, and Nano-Metal Chemistry, 44 (2014) 864-867.

63. Klement R, Stock F, Elias H, Paulus H, Pelikan P, Valko M, Mazur M, Polyhedron, 18 (1999) 3617-3628.

64. Khanmohammadi H, Salehifard M, Abnosi MH, Journal of the Iranian Chemical Society, 6 (2009) 300-309.

65. Gaballa AS, Asker MS, Barakat AS, Teleb SM, Spectrochimica Acta Part A: Molecular and Biomolecular Spectroscopy, 67 (2007) 114-121.

66. Pan ZH, Zhao GQ, Xue LW, Yang WC, Synthesis and Reactivity in Inorganic, Metal-Organic, and Nano-Metal Chemistry, 46 (2016) 1759-1764.

67. Ajlouni AM, Taha ZA, Al Momani W, Hijazi AK, Ebqa'ai M, Inorganica Chimica Acta, 388 (2012) 120-126.

68. Shelke VA, Jadhav SM, Patharkar VR, Shankarwar SG, Munde AS, Chondhekar TK, Arabian Journal of Chemistry, 5 (2012) 501-507.

69. Aziz AA, Synthesis and Reactivity in Inorganic, Metal-Organic, and Nano-Metal Chemistry, 41 (2011) 384-393.

70. Damercheli M, Dayyani D, Behzad M, Mehravi B, Shafiee Ardestani M, Journal of Coordination Chemistry, 68 (2015) 1500-1513.

71. David-Cordonnier MH, Hildebrand MP, Baldeyrou B, Lansiaux A, Keuser C, Benzschawel K, Lemster T, Pindur U, European journal of medicinal chemistry, 42 (2007) 752-771.

72. Elmroth SK, Lippard SJ, Journal of the American Chemical Society, 116 (1994) 3633-3634.

73. Shao D, Shi M, Zhao Q, Wen J, Geng Z, Wang Z, Zeitschrift für anorganische und allgemeine Chemie, 641 (2015) 454-459.

74. Li Y, Yang ZY, Journal of fluorescence, 20 (2010) 329-342.

75. Peng Y, Zhong H, Chen ZF, Liu YC, Zhang GH, Qin QP, Liang H, Chemical and Pharmaceutical Bulletin, 62 (2014) 221-228.

76. Mohindru A, Fisher JM, Rabinovitz M, Nature, 303 (1983) 64-65.

77. Sampath K, Jayabalakrishnan C, Synthesis and Reactivity in Inorganic, Metal-Organic, and Nano-Metal Chemistry, 45 (2015) 1145-1153.

78. Kulkarni A, Patil SA, Badami PS, European Journal of Medicinal Chemistry, 44 (2009) 2904-2912.

79. Chiririwa H, Muzenda E, InProceedings of the World Congress on Engineering and Computer Science, 2 (2014).

80. Lange RP, Locher HH, Wyss PC, Then RL, Current pharmaceutical design. 13 (2007) 3140-3154.

81. Zaki M, Arjmand F, Tabassum S, Inorganica Chimica Acta, 444 (2016) 1-22.

82. Bolhuis A, Aldrich-Wright JR, Bioorganic chemistry, 55 (2014) 51-59.

83. Boda SK, Pandit S, Garai A, Pal D, Basu B, RSC Advances, 6 (2016) 39245-39260.

84. Shahabadi N, Kashanian S, Darabi F, European journal of medicinal chemistry, 45 (2010) 4239- 4245

85. Jone Kirubavathy S, Velmurugan R, Tamilarasan B, Karvembu R, Bhuvanesh NS, Chitra S, Synthesis and Reactivity in Inorganic, Metal-Organic, and Nano-Metal Chemistry, 46 (2016) 1751-1758.

86. Usman M, Arjmand F, Ahmad M, Khan MS, Ahmad I, Tabassum S, Inorganica Chimica Acta, 453 (2016) 193-201.

87. Salehi M, Kubicki M, Dutkiewicz G, Rezaei A, Behzad M, Etminani S, Russian Journal of Coordination Chemistry, 39 (2013) 716-722.

88. Asadi M, Jamshid KA, Kyanfar AH, Transition Metal Chemistry, 32 (2007) 822-827.

89. Kurt Y, Deniz NG, Journal of Coordination Chemistry, 68 (2015) 4070-4081.

90. Lashanizadegan M, Boghaei DM, Shivapour Z, Seraj S, Synthesis and Reactivity in Inorganic, Metal-Organic, and Nano-Metal Chemistry, 40 (2010) 373-377.

91. Akine S, Taniguchi T, Dong W, Masubuchi S, Nabeshima T, The Journal of organic chemistry, 70 (2005) 1704-1711.

92. Nejo AA, Kolawole GA, Nejo AO, Journal of Coordination Chemistry, 63 (2010) 4398-4410.

93. Tan SF, Ang KP, Ng LH, Davies AG, Oprescu D, Transition metal chemistry, 15 (1990) 459-464.

94. Burke PJ, McMillin DR, Journal of the Chemical Society, Dalton Transactions. 9 (1980) 1794-1796.

95. Kolawole GA, Osowole AA, Journal of Coordination Chemistry, 62 (2009) 1437-1448.

96. Nejo AA, Kolawole GA, Opoku AR, Muller C, Wolowska J, Journal of Coordination Chemistry, 62 (2009) 3411-3424.

97. Hegazy WH, Gaafar M, American Chemical Science Journal, 2 (2012) 86.

98. Meghdadi S, Mereiter K, Langer V, Amiri A, Erami RS, Alshima'a AM, Amirnasr M, Inorganica Chimica Acta, 385 (2012) 31-38.

99. Meghdadi S, Amirnasr M, Mereiter K, Motaharipour S, Nasehi M, Bagheri M, Abbasi S, Journal of Coordination Chemistry, 68 (2015) 4055-4069.

100. Gradinaru J, Forni A, Druta V, Tessore F, Zecchin S, Quici S, Garbalau N, Inorganic chemistry, 46 (2007) 884-895.

101. Huber A, Muller L, Elias H, Klement R, Valko M, European journal of inorganic chemistry, (2005) 1459- 1467

102. Rajasekar M, Sreedaran S, Prabu R, Narayanan V, Jegadeesh R, Raaman N, Kalilur Rahiman A, Journal of Coordination Chemistry, 63 (2010) 136-146.

103. Abdulghani AJ, Khaleel AM, 2013 (2013).

104. Karaboecek N, Karaboecek S, Kormali F, Turkish Journal of Chemistry, 31 (2007) 271-277.

105. Hassan AM, Nassar AM, Ahmed YZ, Elkmash AN, International Journal of Pharmaceutical Sciences and Research, 3 (2012) 2243.

106. Rabindra Reddy P, Shilpa A, Chemistry & biodiversity, 8 (2011) 1245-1265.

107. Akila E, Usharani M, Rajavel R, International Journal of Chem Tech Research. 5 (2013) 1502-1511.

108. Cai LZ, Song LJ, Zeng HY, Dong ZC, Guo GC, Huang JS, Inorganica chimica acta. 344 (2003) 61-64.

109. Kou Y, Tian J, Li D, Gu W, Liu X, Yan S, Liao D, Cheng P, Dalton Transactions. (2009) 2374-2382.

110. Zhou Y, Peng JN, Journal of Coordination Chemistry, 66 (2013) 2597- 2604.

111. Sanzenbacher R, Bottcher A, Elias H, Huber M, Haase W, Glerup J, Jensen TB, Neuburger M, Zehnder M, Springborg J, Olsen CE, Inorganic Chemistry, 35 (1996) 7493-7499.

CHAPTER II

Synthesis, crystal structures and biological activities of transition metal complexes of 6,6'-((1E,1'E)-(ethane-1,2-iylbis(azanylylidene))bis (methanylylidene)) bis(5-isopropyl-2-methylphenol)

2.1 Introduction

DNA has been a long-term goal for the diagnosis and treatment of human diseases [1]. DNA plays an essential role in the life process since it covers all the genetic information for the cellular functions [2]. Metal complexes of Schiff bases particularly, derived from salicyaldehyde have been found to be effective in DNA cleavage and also observed to possess anticancer and antibacterial activities [3-7]. Interaction of metal complexes with DNA are important areas of chemical research because of their applications in nucleic acid and cancer research. DNA cleavage may lead to various pathological changes in living organisms and may develop the synthetic restriction enzymes, chemotherapeutic drugs and DNA foot printing agents [8-9]. In last decades, direct scission of DNA in the presence of oxidizing or hydrolytic agents is the subject of various review articles. Recently the transition metal complexes in the presence of oxidants O_2, H_2O_2 or peracid have been extensively studied for DNA cleavage reactions and existing efforts are on to design transition metal complexes as chemical nucleases suitable for nicking or in a direct strand scission [10-12]. Cobalt complexes with different oxidation states have been found to possess the DNA cleavage activity [13-14].

2.2 Experimental section

2.2.1 Chemicals and solvents

The chemicals used for the synthesis of ligands such as carvacrol, Ethane-1,2-diamine, Propane-1,3-diamine, Benzene-1,2-diamine, Propane-1,2-diamine, Ethidium bromide, Tris boric acid EDTA buffer (10X TBE buffer), loading dye mix, Agarose gel were purchase from sigma aldrich and sodium hydroxide, triethyl amine, chloroform, ethanol, methanol, hexane, ethyl acetate, acetonitrile, DMF, DMSO, EDTA, manganese acetate tetrahydrate, cobalt acetate tetrahydrate, nickel chloride hexahydrate and cupric acetate monohydrate were the loba chemie and Merck products. All the chemicals and solvents were used without further purification. The pBR322 DNA and DNA loading dye were purchased from Banglore Genei. L-histidine, DABCO, D-mannitol, 30 % H_2O_2 were purchased from sigma aldrich.

2.2.2 Analytical methods

A variety of physico-chemical methods have been used to characterize the structure of organic Schiff base ligands and their transition metal complexes. A detailed account of these methods is given below.

2.2.2.1 Electronic Spectra

The electronic spectra of Schiff base ligands and their metal complexes were recorded in DMF as a solvent on the UV 2400 Series spectrophotometer in the wavelength range of 200 to 800 nm at School of Chemical Sciences, North Maharashtra University, Jalgaon, Maharashtra, India.

2.2.2.2 Infrared Spectra

FT-IR spectra were collected as KBr pellet at room temparature on Shimadzu FT-IR- 8400 spectrometer at M. J. College, North Maharashtra University, Jalgaon, Maharashtra, India.

2.2.2.3 NMR Spectra

^{1}H and ^{13}C- NMR spectra of Schiff ligands were measured with a BRUKER ADVANCE III (400 MHz) spectrometer at SAIF, Panjab University, Chandigarh. The proton chemical shifts are recorded in ppm relative to Me_4Si as an internal standard using $CDCl_3$ as solvent.

2.2.2.4 LC-MS Spectra

The LC-MS spectra of ligands and its metal complexes have been recorded with Waters Micromass Q-Tof Micro instrument at SAIF, Panjab University, Chandigarh, India and some of the complexes were characterized at IIT- Bombay with the 410 Prostar Binary LC with 500 MS IT PDA Detectors instrument.

2.2.2.5 Elemental Analyses

The CHN analyses of the ligands and their metal complexes were carried out with a ThermoFinnigan elemental analyzer at SAIF, IIT Bombay, Maharashtra, India.

2.2.2.6 ESR Spectra

The X-band ESR spectra of copper complexes were recorded in the solid state at liquid nitrogen temperature 77 k in DMF as solvent using DPPH as standard on the JES- FA200 ESR Spectrometer with X band at SAIF, IIT- Bombay, Maharashtra, India.

2.2.2.7 Magnetic susceptibility measurements

The measurement of magnetic susceptibility of metal complexes was done by using Guoy balance method at Dr. Babasaheb Marathwada University, Aurangabad. Mercury(II) tetrathiocynate cobaltate $Hg[Co(NCS)_4]$ was used as a celibrant. The finely powdered metal complex was filled in the experimental tube up to reference mark. The precaution was taken to ensure tight and uniform packing without any air gap in the column of sample. The Teflon stopper was tightly fixed on the tube and the tube was suspended between the poles with the help of silver chain suspension from pan of the balance.

From the experimental data, the magnetic susceptibility (χ_g) of metal complexes were calculated from the following expression.

$$\chi_g = \frac{\beta \Delta \omega}{W}$$

Where,

χ_g = susceptibility per gram of the substance.

β = tube constant or characteristic of the tube.

$\Delta \omega$ = force exerted by W gm of substances.

W = weight of the substances.

The molar susceptibilities (χ_M) of the complexes were then calculated by the expression,

$$\chi_M = \chi_g * \text{molecular weight}$$

The magnetic moments (μ_{eff}) of the complexes were calculated from the values of χ_M by the equation.

$$\mu_{eff} = 2.84 \sqrt{\chi A * T}$$

Where,

μ_{eff} = Magnetic moment of the metal ion in Bohr magnetons (B.M.)

T = Temparature in Kelvin scale

$$\chi_A = \chi_{corr.} = \chi_M - \chi_{diamagnetic (L)}$$

Magnetic susceptibilies were obtained by substracting the diamagnetic susceptibilities of ligand molecule calculated by pascal's constants [15, 16].

$$\chi_{diamagnetic (L)} = \Sigma \chi_{(atomic\ correction)} + \Sigma \chi_{(multiple\ bonds)}$$

The reproducibility of magnetic susceptibility measurements of the complexes was within $\pm 2\ \%$.

2.2.2.8 Conductivity measurements

The molar conductivities of the complexes using 10^{-3} M solution in dimethylformamide (DMF) as solvent were recorded at room temperature on a Systronic conductivity bridge with dip type cell at School of Chemical Sciences, North Maharashtra University, Jalgaon, Maharashtra.

2.2.2.9 SEM analyses

SEM-EDS analysis were performed on SEM JEOL JSM 6360 and JEOL JSM 5400, Japan at the UICT, North Maharashtra University, Jalgaon, Maharashtra.

2.2.2.10 Thermogravimetric studies

TG-DTG analysis of all metal complexes were carried out under air and nitrogen at a heating rate of 20 ℃ min^{-1} using Shimadzu TGA 50, Japan at School of Chemical Sciences, North Maharashtra University, Jalgaon, Maharashtra.

2.3 Synthesis of 2-hydroxy-6-isopropyl-3-methyl benzaldehyde i.e. (Carvacrol Aldehyde)

In this procedure carvacrol was formulated selectively at position ortho to the hydroxyl group as shown in **Figure 2.1**. In a 250 ml round bottom flask (40 mmol, 6 gm) carvacrol, 150 ml acetonitrile, (150 mmol, 15.15 gm) triethylamine and (40 mmol, 3.80 gm) anhydrous MgCl$_2$ were charged and the solution was stirred for 20 min at room temperature. The (270 mmol, 8.10 gm) paraformaldehyde was then added, and the reaction mixture was refluxed for 3.5 hrs and the entire reaction was carried out under inert atmosphere. The solution was then allowed to cool to room temperature and acidified by

the addition of aqueous HCl (320 ml) followed by stirring for 30 min under inert atmosphere. The product was extracted by diethyl ether and the ether portion was collected and washed with aqueous saturated NaCl solution. The volatiles were removed under reduced pressure to yield the crude carvacrol aldehyde yellow liquid product and purified by coloum chromatography by using hexane and ethyl acetate solvents [17].
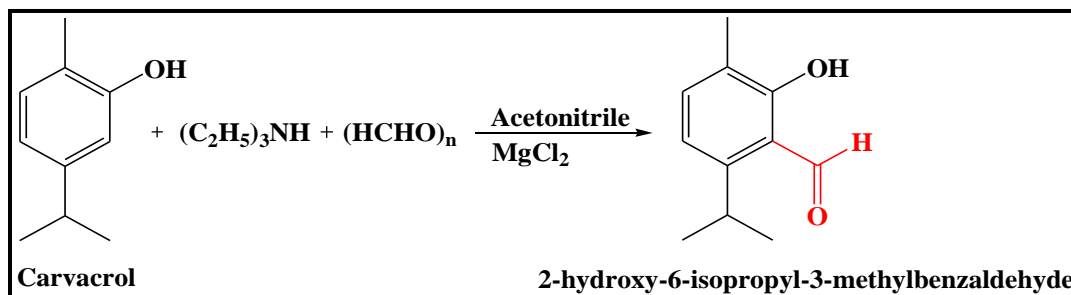
Figure 2.1: Reaction scheme for the synthesis of 2-hydroxy-6-isopropyl-3-methyl benzaldehyde

2.4 Synthesis of Schiff base ligand 6,6'-((1E,1'E)-(ethane-1,2-diylbis(azanylylidene)) bis(methanylylidene))bis(5-isopropyl-2-methylphenol) (EN) and its ENMn(III), ENCo(II), ENNi(II) and ENCu(II) complexes

The systematic synthesis route for Schiff base ligand 6,6'-((1E,1'E)-(ethane-1,2-diylbis(azanylylidene))bis(methanylylidene))bis(5-isopropyl-2-methylphenol) (EN) and its ENMn(III), ENCo(II), ENNi(II) and ENCu(II) complexes are shown in **Figure 2.2**.
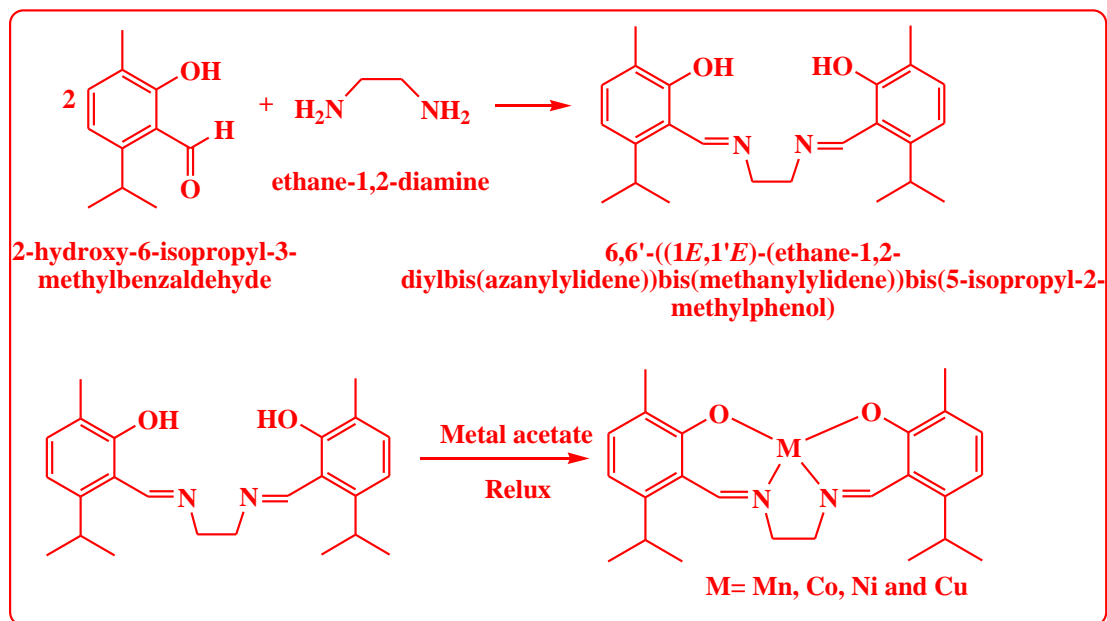
Figure 2.2: Synthesis of 6,6'-((1E,1'E)-(ethane-1,2-diylbis(azanylylidene))bis(methanylylidene))bis(5-isopropyl-2-methylphenol) (EN) ligand and its metal complexes

2.4.1 Synthesis of Schiff base ligand 6,6'-((1E,1'E)-(ethane-1,2-diylbis(azanylylidene))bis(methanylylidene))bis(5-isopropyl-2-methylphenol) (EN)

The EN schiff base ligand was prepared according to previously reported method [15], in which simple condensation of methanolic solutions 2-hydroxy-6-isopropyl-3-methyl benzaldehyde (2 mmol, 0.356 gm) with ethane-1,2-diamine (1 mmol, 0.060 gm) was carried out under refluxed condition for 2 hrs to give a yellow precipitate. This crude product was filtered and wash with cold methanol and then ether. The product recrystallized by ethanol and dried at room temperature [18].

Analytical and spectral data of EN ligand: Colour: Yellow Solid. Yield: 73%. ^{1}H-NMR (CDCl$_3$, 400 MHz) (δ, ppm): 14.60 (*brs,* 2H, OH), 8.72 (d, 2H, -HC=N), 7.09 (d, 2H, Ar-CH, *J*= 8 Hz), 6.61 (d, 2H, Ar-CH, *J*= 8 Hz), 3.95 (s, 4H, -CH$_2$), 3.28-3.21 (m, 2H, -CH of isopropyl group), 2.18 (s, 6H, 2(-CH$_3$)), 1.11 (d, 12H, *J*= 4Hz, 4(-CH$_3$)). ^{13}C-NMR (CDCl$_3$, 400 MHz) (δ, ppm): 164.59, 160.74, 147.26, 133.74, 123.52, 114.30, 114.10, 59.63, 27.78,

23.90, 15.52. UV-Vis (DMF) λ_{max} (nm): 273, 334. FT-IR (KBr pellet, cm^{-1}) ν_{max}: 3498 (-OH), 1609 (-C=N), 1462 (-C=C), 1259 (C-O). LC-MS (m/z): calcd 381.52, obsv 381.30. Anal. calcd for $C_{24}H_{32}N_2O_2$ (%): C 75.75, H 8.48, N 7.36, Found: C 75.59, H 9.19, N 7.58.

2.4.2 Synthesis of ENMn(III) complex

The dropwise addition of (1 mmol, 0.245 gm) methanolic solution of manganese acetate tetrahydrate to a stirred (1 mmol, 0.380 gm) methanolic solution of EN ligand under nitrogen atmosphere condition. The solution changed its coloured to shining reddish brown. The refluxed condition maintained for 6-8 hrs. After completion of reaction filter the resulting solution as product and then evaporate it collected the shining dark reddish brown coloured crystals and washed with hexane for several times then further proceed for single X-ray crystallographic studies. The metal complexes formulated as ML-OAC i.e. Mn(III) oxidation state as shown in the crystal structure.

Analytical and spectral data of ENMn(III) complex: Colour: Shining reddish brown, solid. Yield: 78%. UV-Vis (DMF) λ_{max} (nm): 275, 333, 417. FT-IR (KBr, pellet cm^{-1}) ν_{max}: 1585 (C=N), 1276 (C-O), 1379 (C=C), 518 (M-O), 452 (M-N). LC-MS (m/z): calcd 492.49, obsv 433.1 [M-OAC]. Anal. calcd for $C_{26}H_{33}MnN_2O_4$ (%): C 63.41, H 6.75, N 5.69, Found: C 63.61, H 6.71, N 5.76. μ_{eff}: 4.82 B.M.. Conductance ($\Lambda_{M,}$ Ω^{-1} cm^2 mol^{-1}) in DMF: 19.60.

2.4.3 Synthesis of ENCo(II) complex

The dropwise addition of (1 mmol, 0.249 gm) hot methanolic solution of cobalt acetate tetrahydrate to (1 mmol, 0.380 gm) methanolic EN ligand solution with constant stirring. The refluxed condition maintained for 6 hrs. After completion of reaction filter the resulting solution as product and then evaporate it collected product and washed with cold methanol.

Analytical and spectral data of ENCo(II) complex: Colour: Green, solid. Yield: 71 %. UV-Vis (DMF) λ_{max} (nm): 269, 410, 632. FT-IR (KBr pellet, cm^{-1}) ν_{max}: 1564 (C=N), 1234 (C-O), 1456 (C=C), 520 (M-O), 412 (M-N). LC-MS (m/z): calcd 437.44, obsv 437.2. Anal.

calcd for $C_{24}H_{30}CoN_2O_2$ (%): C 65.90 H 6.91, N 6.40, Found: C 65.09, H 7.30, N 6.90. μ_{eff}: 4.23 B.M.. Conductance (Λ_M, Ω^{-1} cm^2 mol^{-1}) in DMF: 14.35.

2.4.4 Synthesis of ENNi(II) complex

The dropwise addition of light green coloured (1 mmol, 0.237 gm) methanolic warm solution of nickel chloride hexahydrate to the (1 mmol, 0.380 gm) methanolic EN ligand solution with constant stirring. The solution changed its coloured to shining orange colour. The refluxed condition maintained for 4-5 hrs. The orange coloured precipitate obtained after completion of reaction and filtered it and washed with the cold ethanol and dried at room temperature. Attempted to grow the single crystal for nickel complex in chloroform at room temperature was successful.

Analytical and spectral data of ENNi(II) complex: Colour: Shining orange, solid. Yield: 79 %. UV-Vis (DMF) λ_{max} (nm): 268, 349, 352, 442, 552. FT-IR (KBr pellet, cm^{-1}) ν_{max}: 1560 (C=N), 1234 (C-O), 1452 (C=C), 474 (M-O), 432 (M-N). LC-MS (m/z): calcd 437.20, obsv 437. Anal. calcd for $C_{24}H_{30}N_2NiO_2$ (%): C 65.93, H 6.92, N 6.41, Found: C 65.60, H 6.72, N 6.51. Conductance (Λ_M, Ω^{-1} cm^2 mol^{-1}) in DMF: 15.64.

2.4.5 Synthesis of ENCu(II) complex

The dropwise addition of (1 mmol, 0.199 gm) methanolic hot solution of cupric acetate monohydrate to the (1 mmol, 0.380 gm) methanolic EN ligand solution with constant stirring. The refluxed condition maintained for 3-4 hrs. The Shining dark brown coloured precipitate obtained after completion of reaction and filtered it and washed with the cold ethanol and dried at room temperature. Attempted to grow the single crystal of the metal complexes was not successful.

Analytical and spectral data of ENCu(II) complex: Colour: Shining dark brown, solid. Yield: 72 %. UV-Vis: (DMF) λ_{max} (nm): 284, 379, 560, 572. FT-IR (KBr, cm^{-1}) ν_{max}: 1560 (C=N), 1240 (C-O), 1408 (C=C), 520 (M-O), 410 (M-N). LC-MS (m/z): calcd 442.05, obsv 442.05. Anal. calcd for $C_{25}H_{32}CuN_2O_2$(%): C 65.21, H 6.84, N 6.34, Found: C 65.62, H 6.97, N 6.64. μ_{eff}: 1.69. Conductance (Λ_M, Ω^{-1} cm^2 mol^{-1}): 12.67.

2.5 Characterization of EN ligand and its ENMn(III), ENCo(II), ENNi(II) and ENCu(II) complexes

All the synthesized compounds have been characterized by NMR, UV-Visible, FT-IR, LC-MS and ESR spectroscopic techniques, elemental analysis, Magenetic susceptibility, conductivity measurements, SEM analysis and finally the single crystal X- ray diffraction techniques are discussed below.

2.5.1 NMR Spectra

The ^{1}H & ^{13}C NMR spectra of Schiff base ligand (EN) are shown in **Figure 2.3 & Figure 2.4** while, the spectral data are summarized in **Table 2.1**. The peaks in the region are 6.61-7.09 δ are attributable to aromatic ring protons. A sharp singlet at 8.72 δ assignable to azomethine protons (-CH=N-) confirms the formation of the ligand as expected. Another singlet peak at 2.18 δ is observed for methyls protons. The broad peak of 14.60 δ value is assigned to broad phenolic OH group. The doublet peak and multiplet peaks at 1.13 δ and 3.2 δ indicate the isopropyls groups $(CH_3)_4$ and (-CH) protons respectively. The singlet peak appearing at 3.95 δ is for ethylene diamines protons.

Table 2.1: NMR spectral data of EN ligand

Compound	Assignment δ ppm
EN ligand	**^{1}H-NMR, CDCl$_3$, 400 MHz, δ ppm:** 14.60 (brs, 2H, -OH), 8.72 (s, 2H,-CH=N), 7.09 (d, 2H, ArCH, J=8Hz), 6.61 (d, 2H, J= 8Hz, Ar-CH), 3.95 (s, 4H, N-CH$_2$-CH$_2$-N), 3.28-3.21 (m, 2H, CH$_3$-CH-CH$_3$), 2.18 (s, 6H, (CH$_3$)$_2$), 1.11 (d, 12H, J= 4Hz, (CH$_3$)$_4$). **^{13}C- NMR, CDCl$_3$, 400 MHz, δ ppm:** 164.59, 160.74, 147.26, 133.24, 123.52, 114.30, 114.10, 59.63, 27.78, 23.90, 15.52.
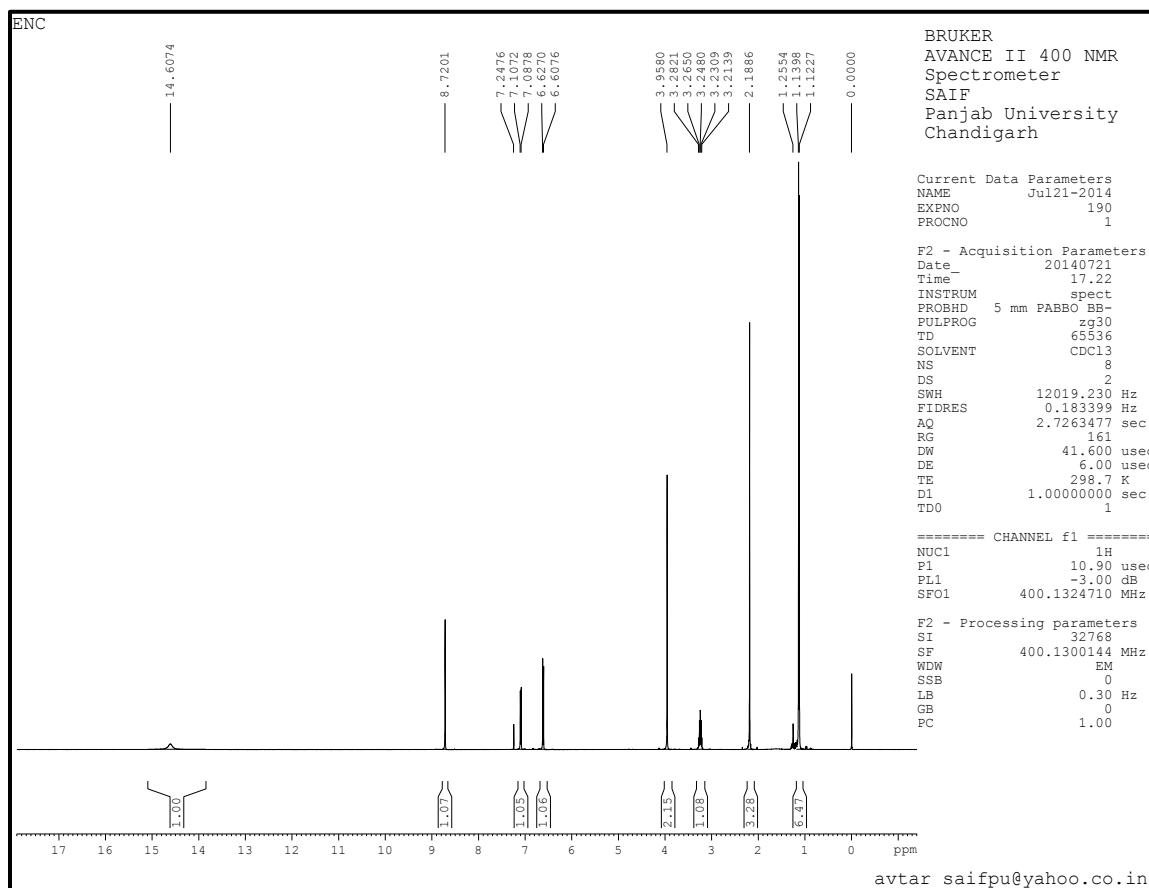
Figure 2.3:. ¹H-NMR spectrum of EN ligand
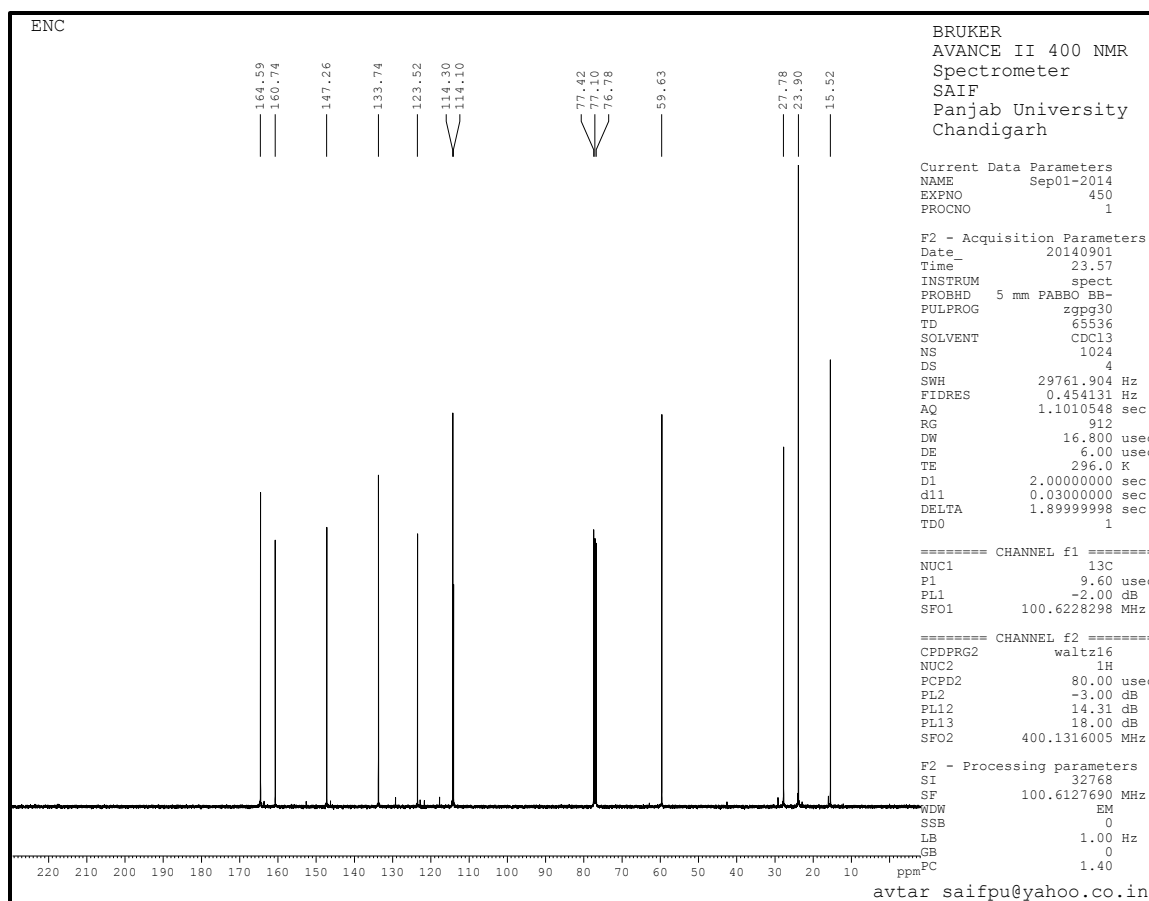
Figure 2.4:. ¹³C-NMR spectrum of EN ligand

2.5.2 UV-Visible spectra

The UV-Visible spectra of the EN ligand and its metal complexes are listed in the **(Table 2.2 and Figures 2.5- 2.9).** The UV-Visible stectrum of EN ligand shows two intense bands at 273 and 332 nm which could be assigned to the $\pi \rightarrow \pi^*$ transitions of the aromatic rings and imine's absorption, respectively [19]. These bands also appeared at similar positions in the UV-Visible spectra of the complexes. The new band at above 417 nm and weak absorbance at higher wavelengths in UV-Visible spectrum of ENMn(III) complex were assigned to metal-to-ligand charge transfer and d–d transitions respectively which are in accordance with the previously reported closely related manganese(III) complexes [20]. The absorption band at 632 nm indicated that the ENCo(II) complex possesses tetrahedral geometry. The UV-Visible spectrum shows an absorption band below 600 nm for the DPNi(II) complex. Lack of any electronic transition at longer wavelength indicates a large crystal-field splitting and this observation is consistent with the square planar geometry of

nickel(II) complexes. The spectrum of ENCu(II) complex in solution state shows a shoulder at 560 nm which is assigned to d-d transition of square planar geometry [21].

Table 2.2: UV-Visible spectral data of EN ligand its metal complexes

Compounds	λmax(nm)
EN Ligand	273, 332, 334
ENMn(III)	275, 333, 417
ENCo(II)	269, 410, 632
ENNi(II)	268, 349, 352, 442. 552
ENCu(II)	284, 379, 560, 572
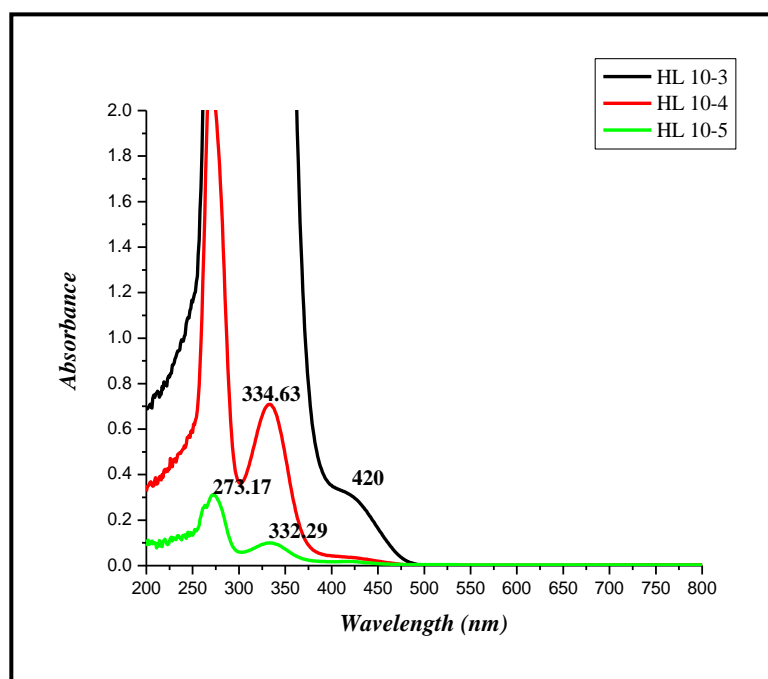
Figure 2.5: UV-Visible spectrum of EN ligand
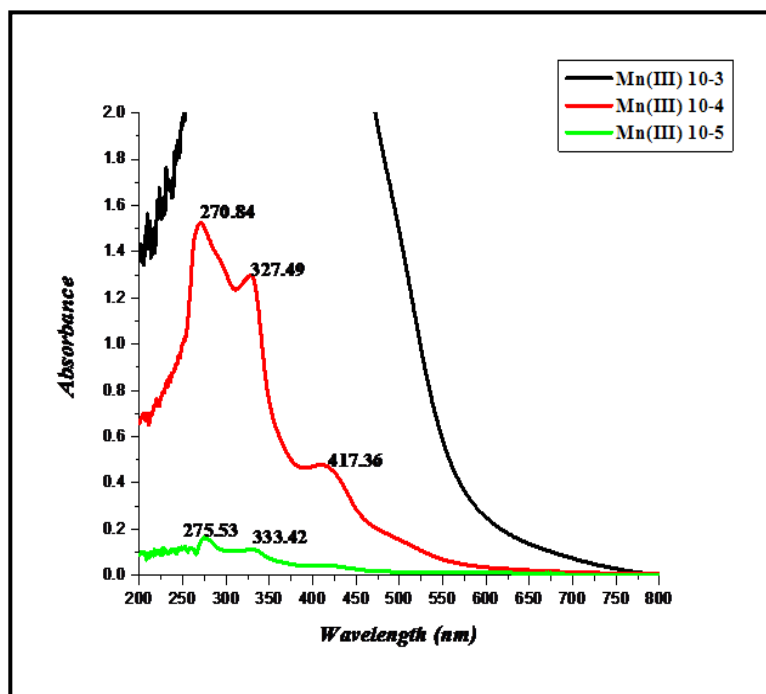
Figure 2.6: UV-Visible spectrum of ENMn(III) complex
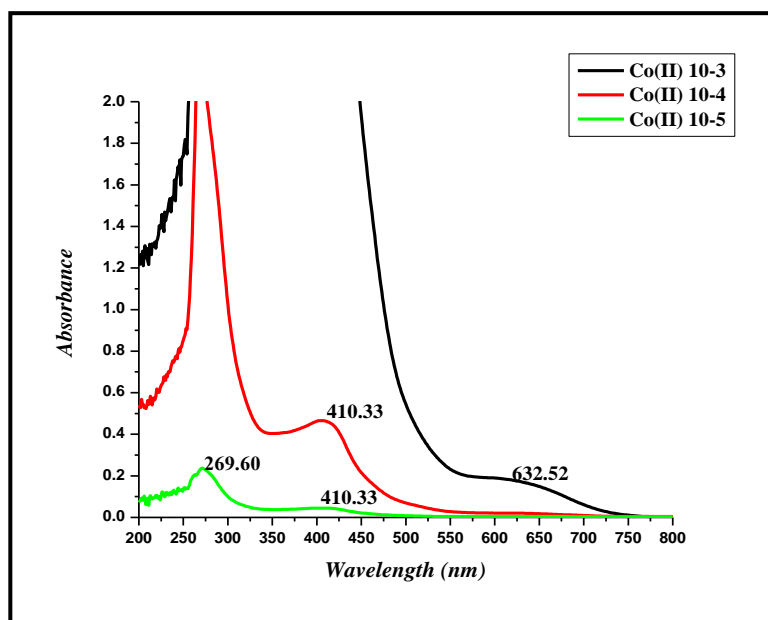
Figure 2.7: UV-Visible spectrum of ENCo(II) complex
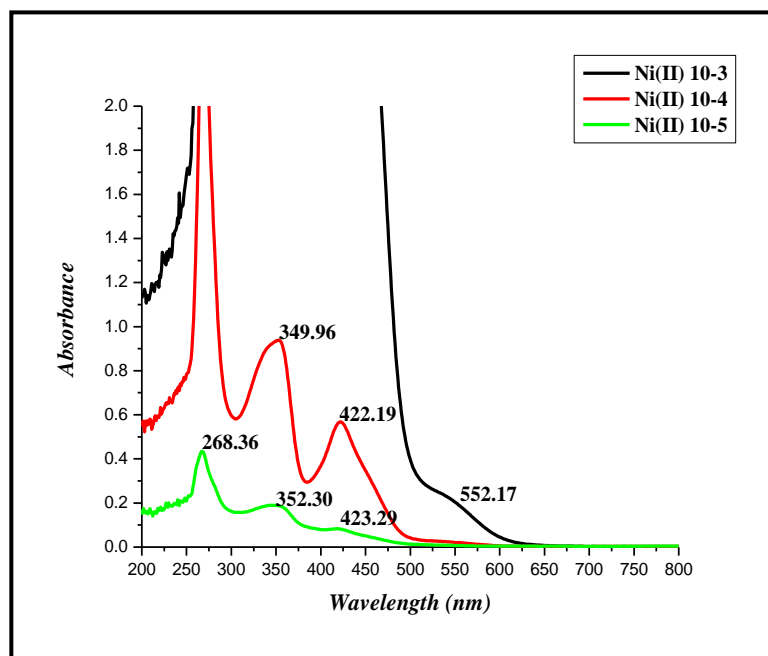
Figure 2.8: UV-Visible spectrum of ENNi(II) complex
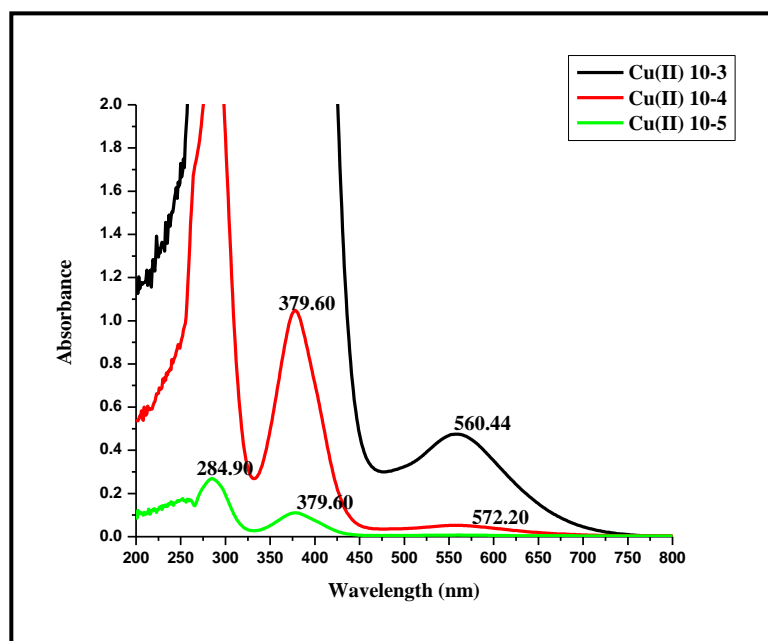
Figure 2.9: UV-Visible spectrum of ENCu(II) complex

2.5.3 FT-IR spectra

Table 2.3 lists the FT-IR spectral bands of EN ligand and its metal complexes and corresponding spectra are given in **Figures 2.10- 2.14.** FT-IR spectroscopy provides the information about the functional groups and the linkage of the ligands to the metal complexes. In the complexes, the four coordination sites of the metal ions are fullfilled by two donor nitrogen and two oxygen atoms. The (OH) vibrations at 3438 cm^{-1} in the IR spectrum of ligand is attributed to the phenolic OH groups assigned and this absorption band is found to disappear in the IR spectra of metal complexes. The absorption in the region 1609–1560 cm^{-1} appears due to the vibration of the azomethine groups (C=N) of the ligand and the position of absorption band is found to be altered upon complexation. The characteristic absorption bands for the C=C and C-O groups of the ligand were observed at 1462 cm^{-1} and 1259 cm^{-1} respectively [22-23].

There was a significant change in their positions of these bands in case of metal complexes as compared to ligands. The absorptions in the ranges 410–452 and 510–525 cm^{-1} can be assigned to the (M–N) and (M–O) stretching vibrations of the complexes [22-23].

Table 2.3: FT-IR sprectral data of EN ligand and its metal complexes

Compounds	Spectral bands cm^{-1}
EN Ligand	3438, 1609, 1462, 1259
ENMn(III)	1585, 1325, 1379, 1276, 738, 452, 518, 634
ENCo(II)	1618, 1564, 1849, 1454, 1390, 1319, 1228, 723, 655, 524, 475
ENNi(II)	1608, 1564, 1456, 1348, 1230, 1085, 648, 412, 520
ENCu(II)	1625, 1560, 1408, 1332, 600, 520, 510, 410
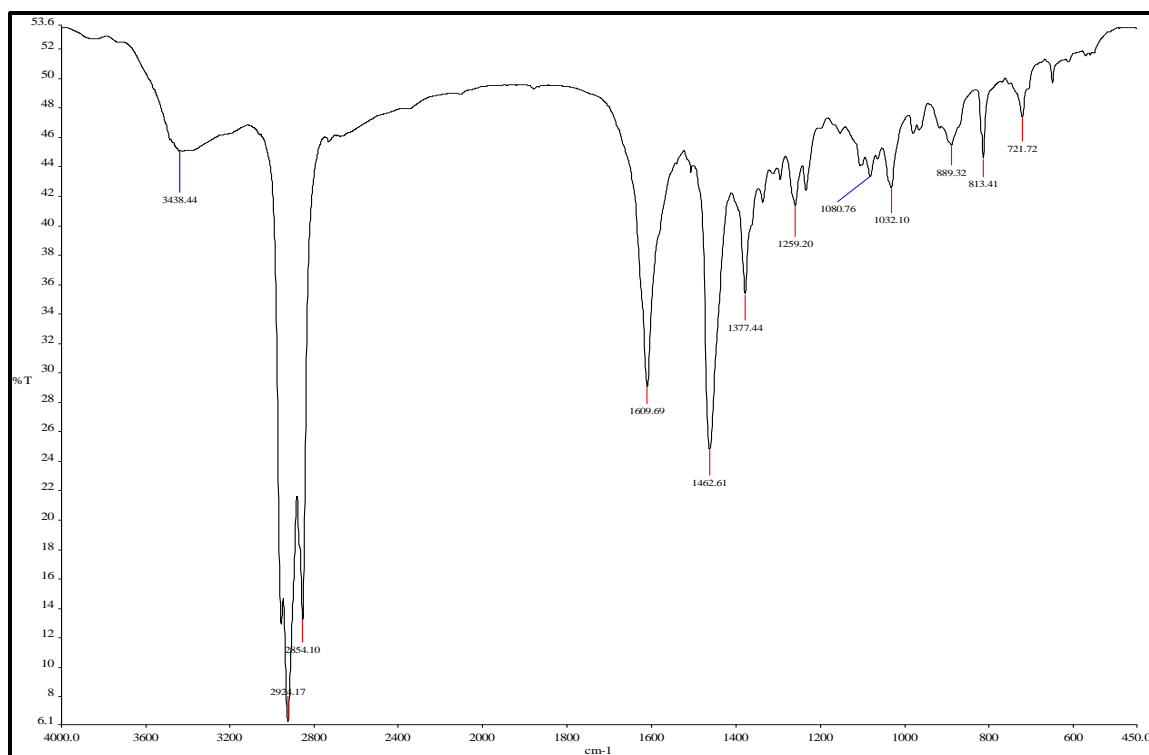
Figure 2.10: FT-IR spectrum of EN ligand
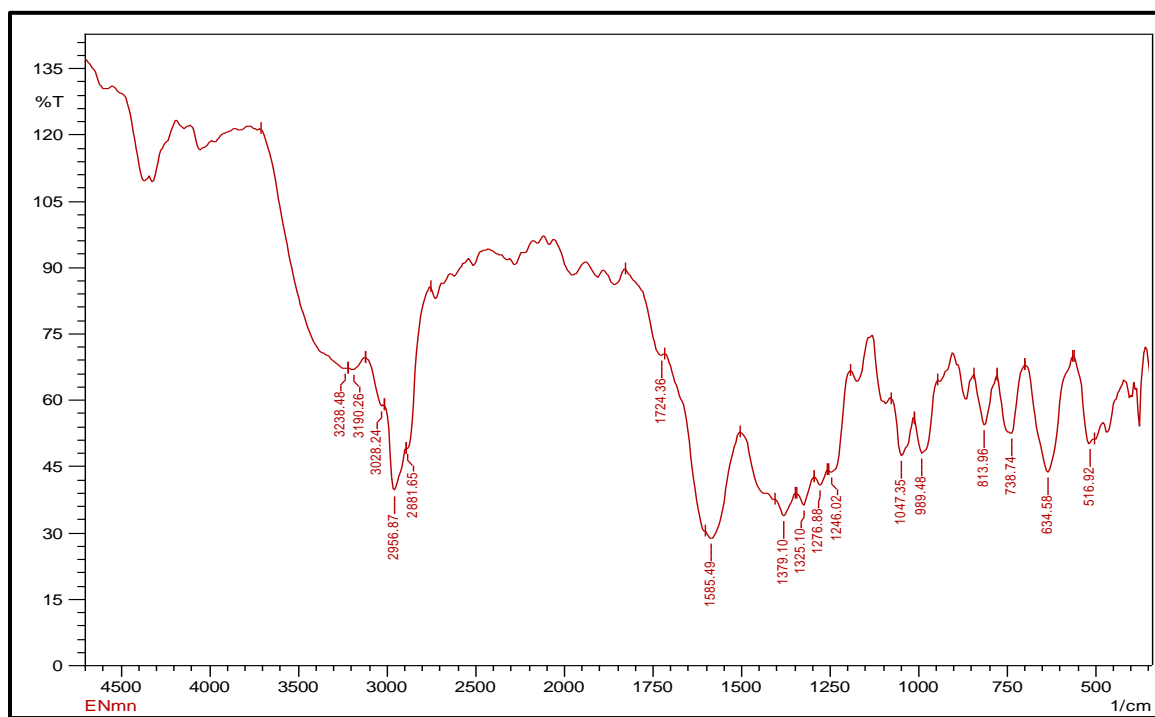
Figure 2.11: FT-IR spectrum ENMn(III) complex
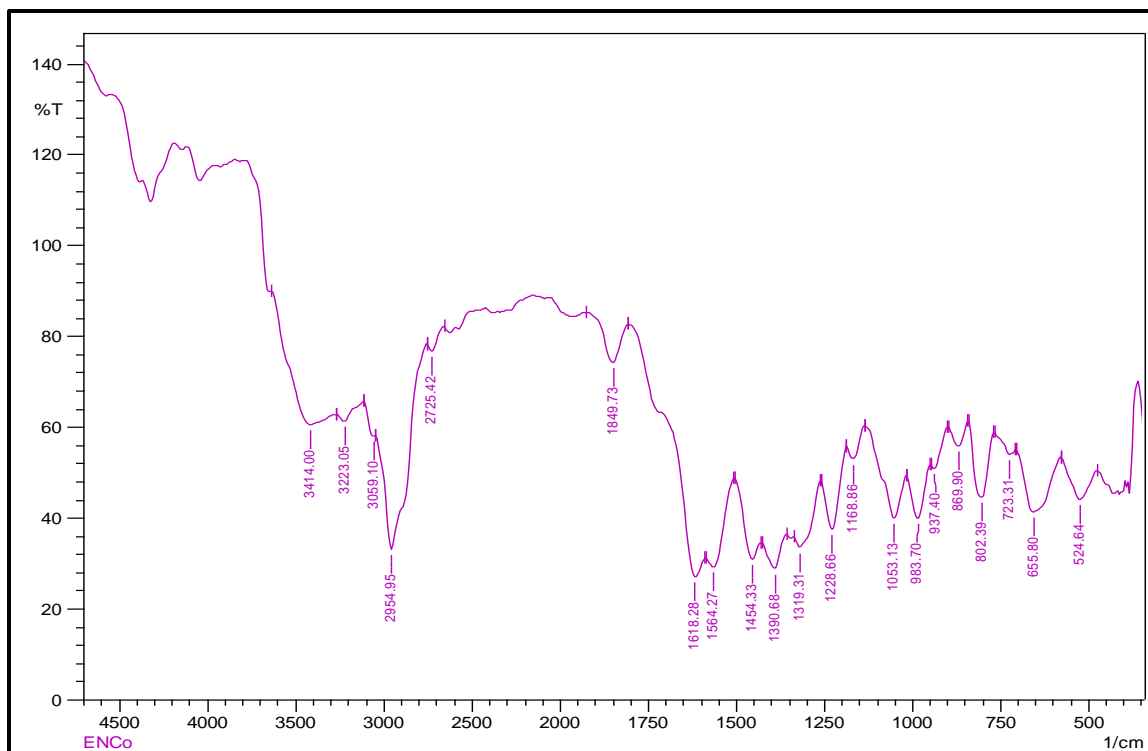
Figure 2.12: FT-IR spectral data of ENCo(II) complex
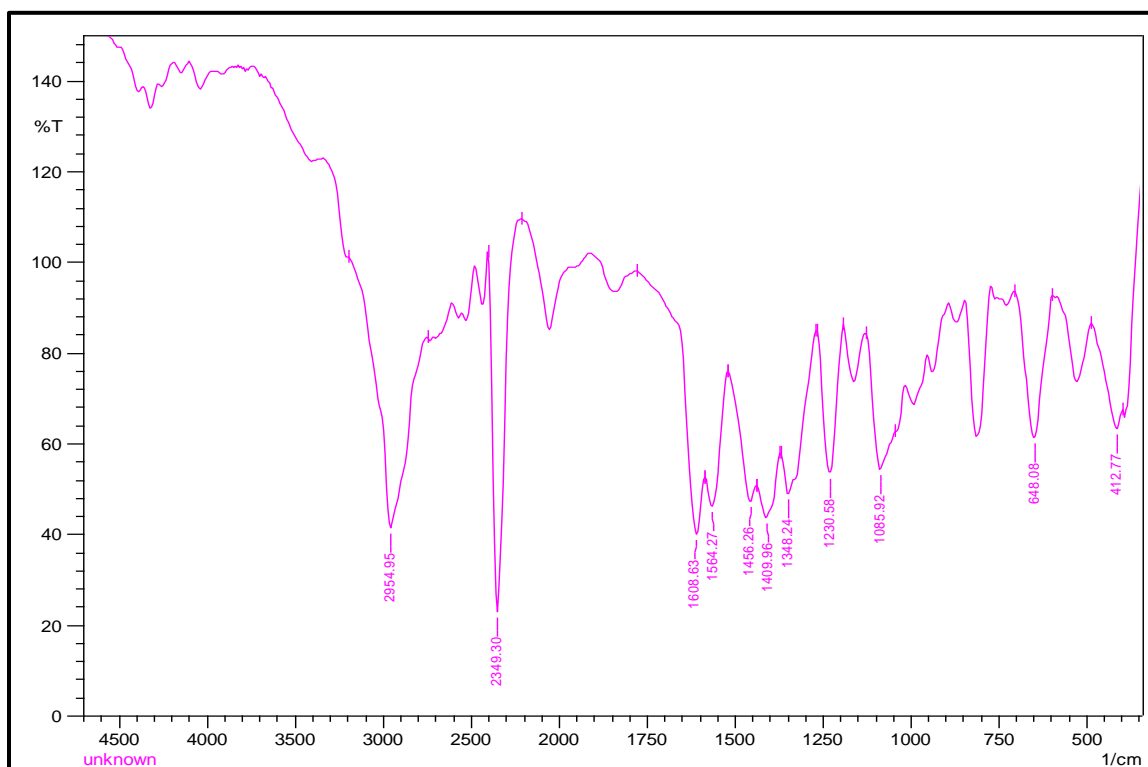
Figure 2.13:. FT-IR spectrum of ENNi(II) complex
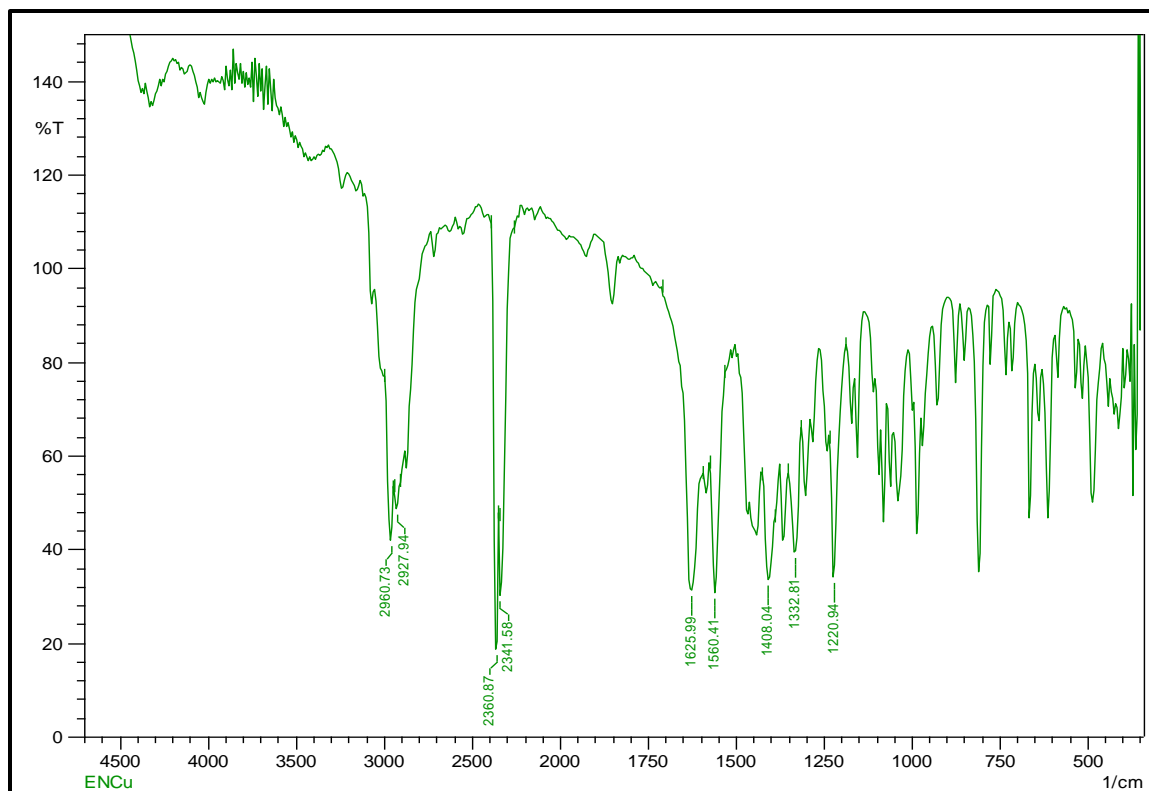
Figure 2.14: FT-IR spectrum of ENCu(II) complex

2.5.4. Mass Spectra

The LC-MS spectra of the EN ligand and its metal complexes as shown in **Figures 2.15-2.19.** The LC- MS spectrum of EN Ligand showed the molecular ion peak at m/z = 381.3 i.e. M^{+1} [Calcd. 380.52] confirming the empirical formula of the prepared schiff base ligand. LC-Mass spectra of ENMn(III), ENCo(II), ENNi(II) and ENCu(II) complexes showed the molecular ion peaks exactly equivalent with the empirical formulas of the corresponding metal complexes **(Table 2.4)**. The intensity of these peaks gave an idea about the stabilities of fragments.

Table 2.4: LC-MS Spectral data of EN ligand and its metal complexes

Comp. Name	Mol. Formula	Mol. Wt (Calcd)	Mol. Wt (Found)
EN Ligand	$C_{24}H_{32}N_2O_2$	$M^+= 380.52$	$M^{+1}= 381.3$
ENMn(III)	$C_{26}H_{33}MnN_2O_4$	$M^+= 433.45$	$M^+= 433.1$
ENCo(II)	$C_{24}H_{30}CoN_2O_2$	$M^+= 437.44$	$M^+= 437.2$
ENNi(II)	$C_{24}H_{30}N2NiO_2$	$M^+= 437.20$	$M^+= 437.0$
ENCu(II)	$C_{25}H_{32}CuN_2O_2$	$M^+= 442.05$	$M^+= 442.28$
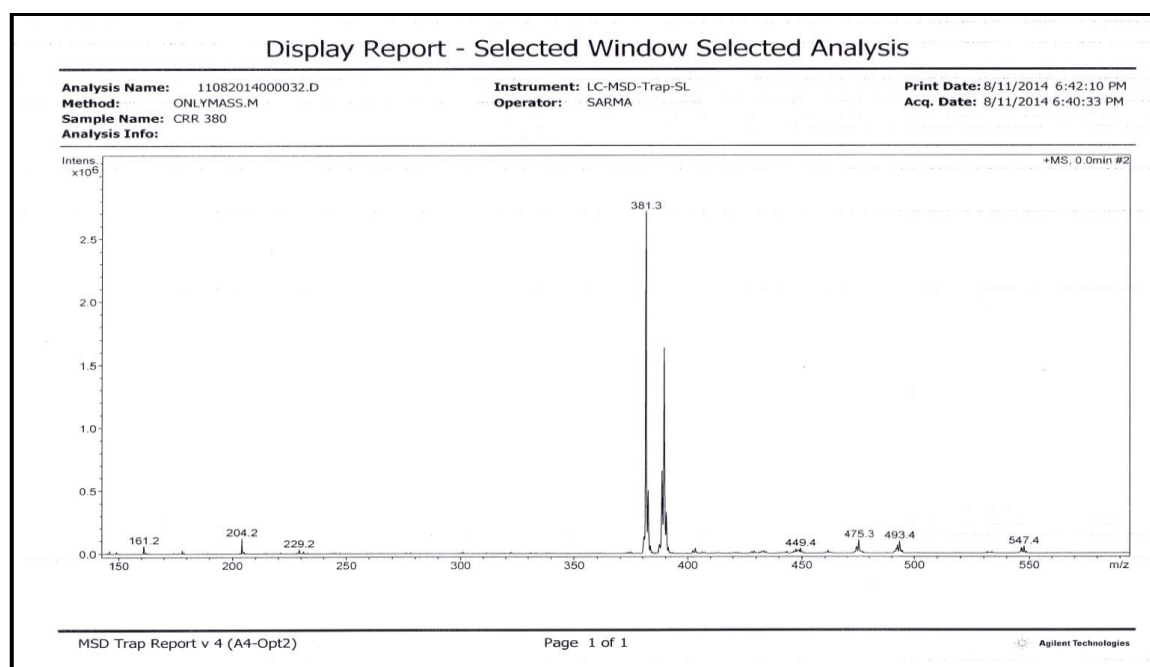
Figure 2.15: LC-MS spectrum of EN ligand
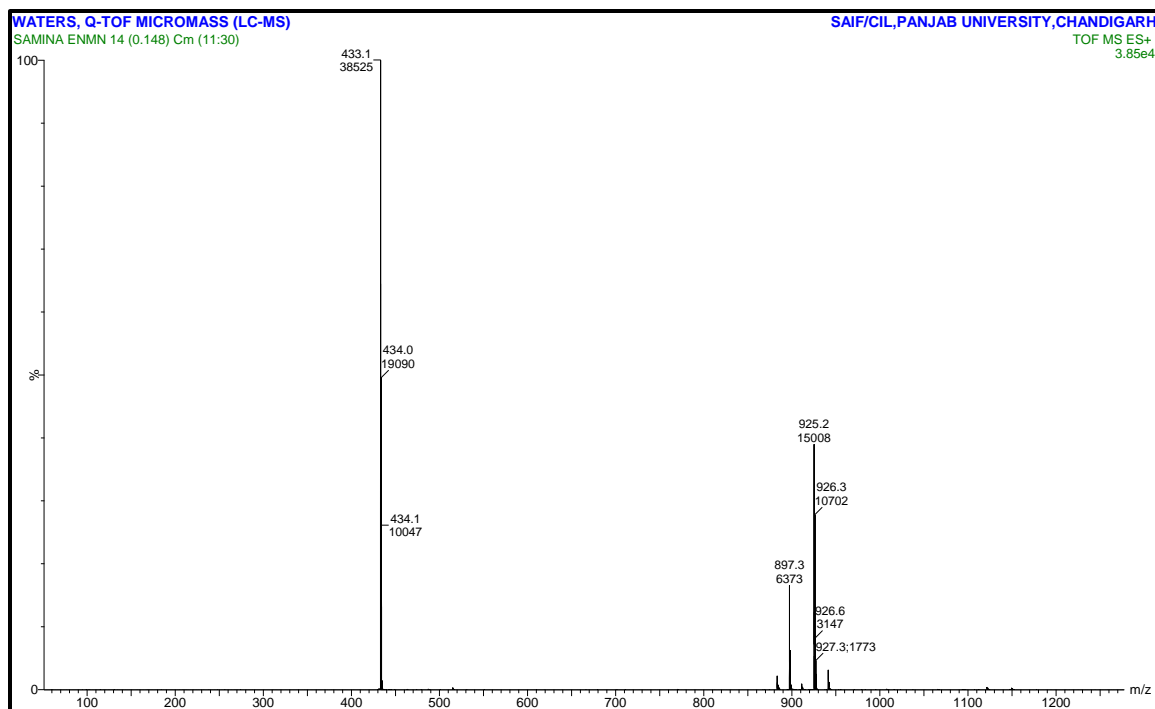
Figure 2.16: LC-MS spectrum of ENMn(III) complex
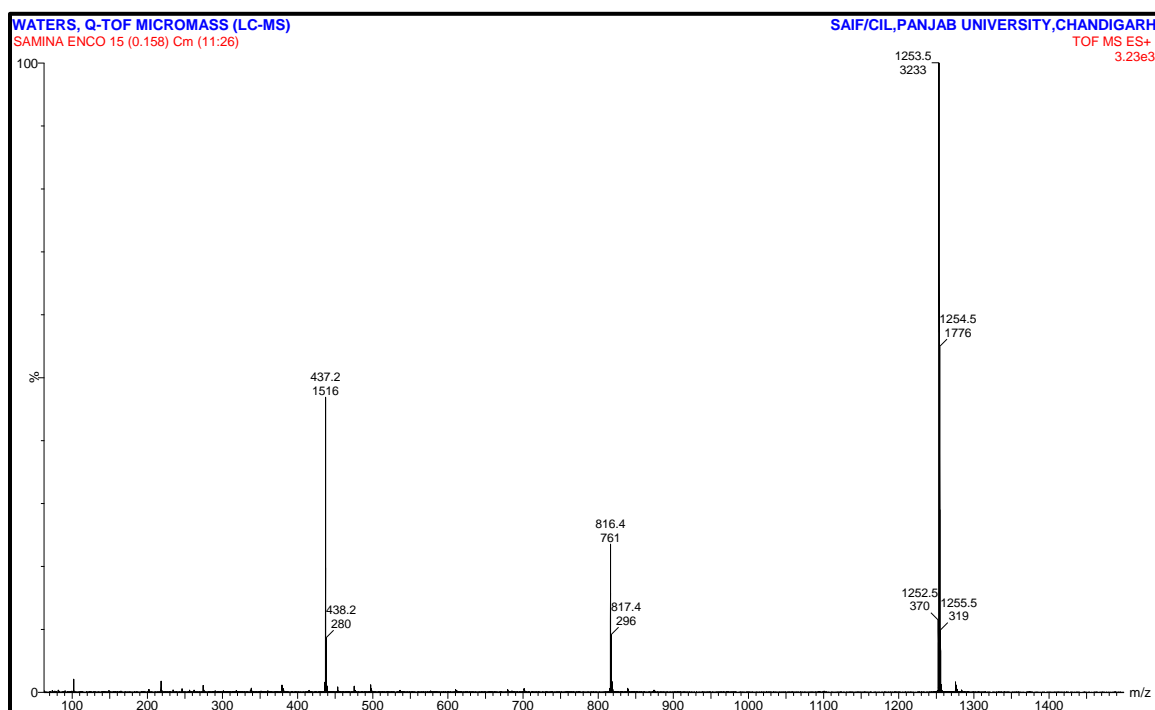
Figure 2.17: LC-MS spectrum of ENCo(II) complex
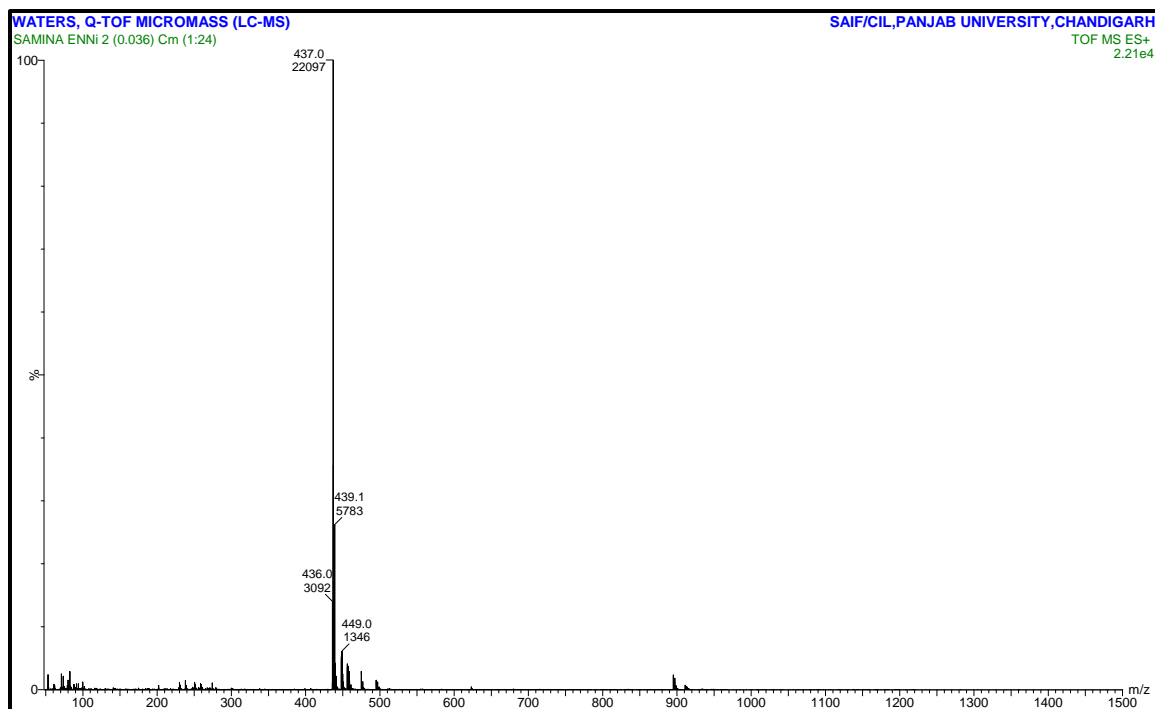
Figure 2.18: LC-MS spectrum of ENNi(II) complex
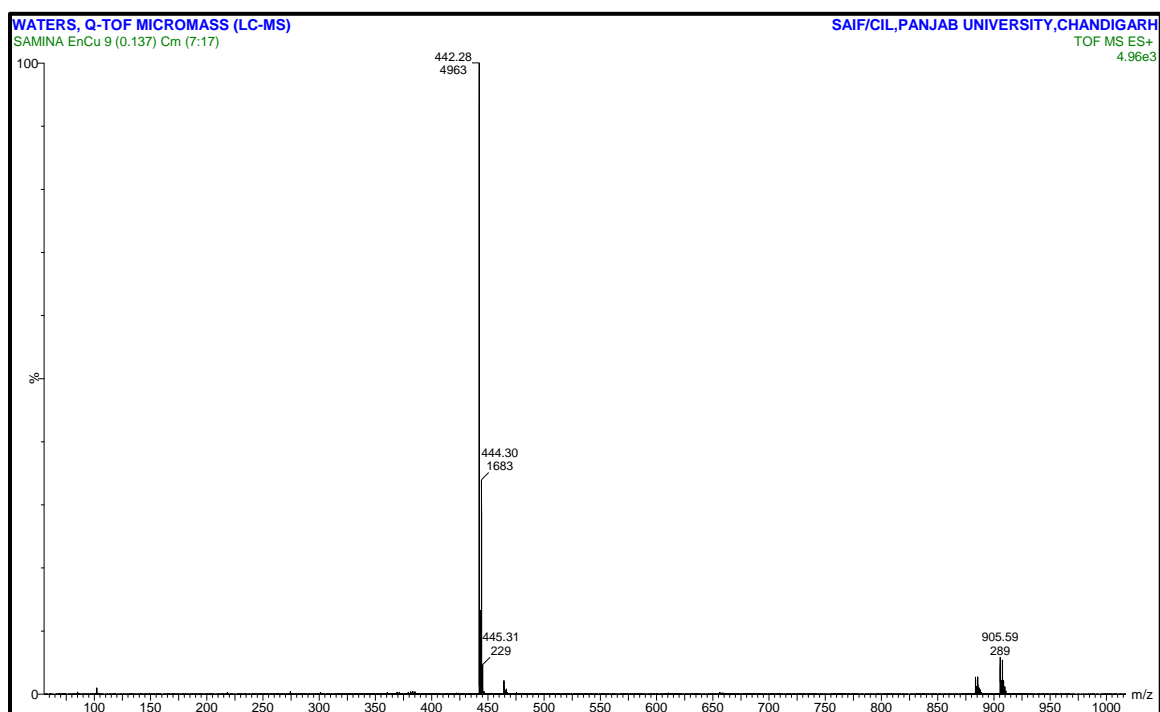
Figure 2.19: LC-MS spectrum of ENCu(II) complex

2.5.5 Elemental analysis:

The elemental analyses of the ligand 6,6'-((1E,1'E)-(ethane-1,2-diylbis(azanylylidene)) bis(methanylylidene))bis(5-isopropyl-2-methylphenol)) (EN) and its four complexes ENMn(III), ENCo(II), ENNi(II) and ENCu(II) are exactly matched with the corresponding the molecular formula **(Table 2.5).**

Table 2.5: Elemental analyses data of EN ligand its metal complexes (%):

Comp. Name	Molecular Formula	C (Cal) Found	H(Cal) Found	N(Cal) Found
EN Ligand	$C_{24}H_{32}N_2O_2$	(75.75) 75.59	(8.48) 9.19	(7.36) 7.58
ENMn(III)	$C_{26}H_{33}MnN_2O_4$	(63.41) 63.61	(6.75) 6.71	(5.69) 5.76
ENCo(II)	$C_{24}H_{30}CoN_2O_2$	(65.90) 65.09	(6.91) 7.30	(6.40) 6.90
ENNi(II)	$C_{24}H30N2NiO_2$	(65.93) 65.60	(6.92) 6.72	(6.41) 6.51
ENCu(II)	$C_{25}H_{32}CuN_2O_2$	(65.21) 65.62	(6.84) 6.97	(6.34) 6.64

2.5.6 Molar conductivity measurement

The molar conductivity of 10^{-3} M solutions of metal complexes in DMF was measured at room temperature. The observed molar conductance values were falling in the range 12.67 - 19.60 Ω^{-1} cm^2 mol^{-1} designated that all the complexes possess non-electrolytic nature are shown in **Table 2.6** [24].

2.5.7   Magnetic susceptibility measurement

The magnetic moment of ENMn(III), ENCo(II) and ENCu(II) were found to be 4.82, 4.23 1.69 B. M., respectively. The values confirmed square pyramidal geometry of ENMn(III), tetrahedral and square planar geometries of ENCo(II) and EnCu(II) complexes respectively [25-26]. The ENNi(II) complex was found to be diamagnetic and indicated square-planar

geometry which was also confirmed through the single crystal structure. The results are summarized in **Table 2.6**.

Table 2.6: Conductivity and Magnetic Susceptibilty measurements of metal complexes

Comp Name	Conductivity values (Λ_M, Ω^{-1} cm^2 mol^{-1})	Magnetic moment μeff (B.M.)
ENMn(III)	19.60	4.82
ENCo(II)	14.35	4.23
ENNi(II)	15.64	Diamagnetic
ENCu(II)	12.67	1.69

2.5.8   ESR spectrum

The EPR spectrum of the ENCu(II) complex at liquid nitrogen temperature 77 k was recorded in DMF solvent as presented in **Figure 2.20**. The g tensor values of copper complexes can be used to derive the ground state [27-28], hence from ESR spectrum of ENCu(II) complex the g values and other factors $g_∥ = 2.43$, $g_⊥ = 2.077$, G= 5.76, g_{avg}= 2.195, f= 136.01 were derived. It was observed that the $g∥ > g⊥ > ge$ and the f values are in the range 105–135 cm^{-1}. This type of pattern has been reported for the square planar complexes. Similarly the data indicates that the unpaired electron lies in the $d_{x2–y2}$ orbital giving ^2B1_g as the ground state [29]. Furthermore, $g_∥ = 2.34$ is near to 2.3–2.4 indicating the presence of mixed copper–nitrogen and copper–oxygen bonds in these chelates [30]. Geometric parameter, G = ($g∥$-2/$g⊥$-2), for axial spectra measures the exchange interaction between copper(II) centers in the polycrystalline state; if G > 4.0, the exchange interaction is negligible and if G < 4.0 considerable exchange interaction is indicated. In present complex G is 5.76 indicating negligible exchange interaction. [31].
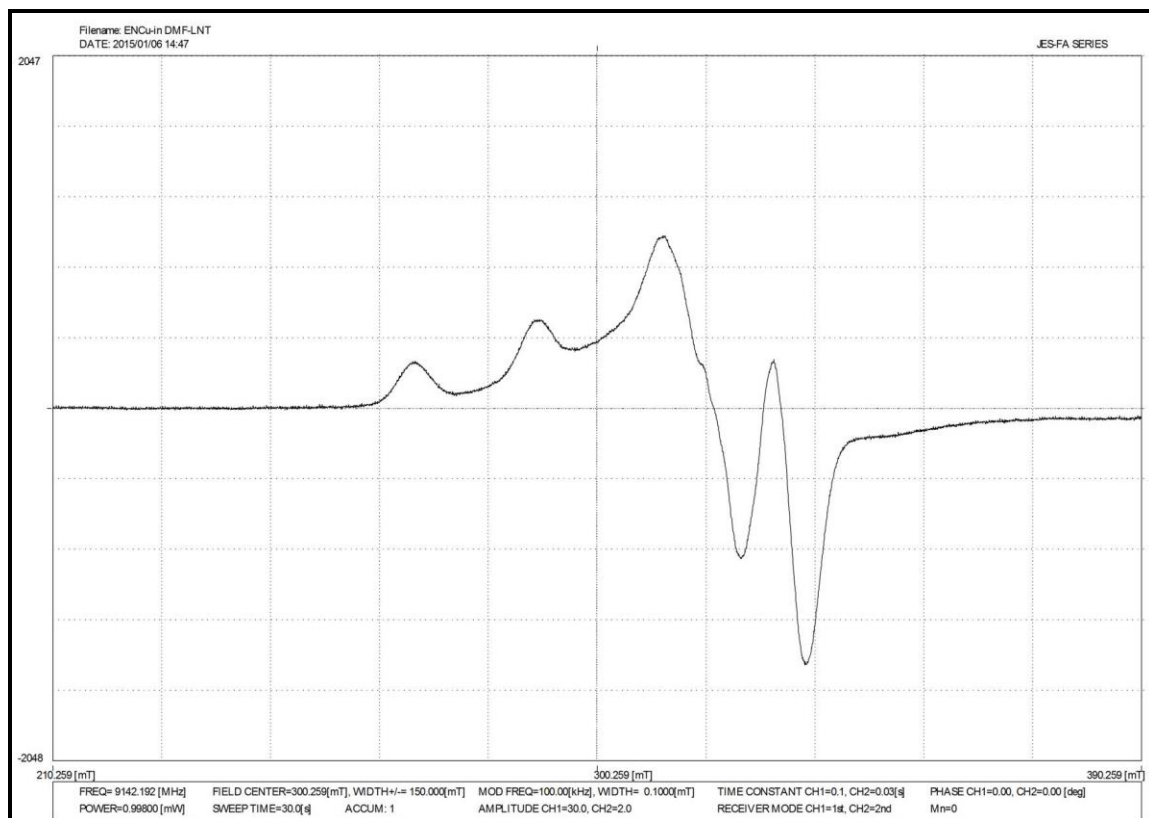
Figure 2.20: X-band ESR spectrum of ENCu(II) complex

2.5.9 Sem analysis

In field emission scanning electron microscopy (FE-SEM), images of a material are obtained by scanning the surface of that material with a focused beam of electron. The focused incident beam of electrons interacts with electrons of atoms in the compounds in the path and creates various signals which contain information about the material's surface topography and composition. Using this technique, image resolution better than 1 nanometer is reachable. Specimens can be observed in low vacuum, or in high vacuum or wet conditions in different pressure or environmental SEM and at a broad range of cryogenic or elevated temperatures with particular instruments [32].

FE-SEM images in **Figures 2.21- 2.24** show morphologies and structures of prepared ENMn(III), ENCo(II), ENNi(II) and ENCu(II) complexes respectively. All images clearly show the well crystalline nature of complexes. ENMn(III) and ENCo(II) possess flakes like Morphology and surface structure, while ENNi(II) and ENCu(II)

complexes are similar in morphology, they consist of irregular rectangular particles and show noticeable aggregation with average grain size 100 µm - 10 µm.
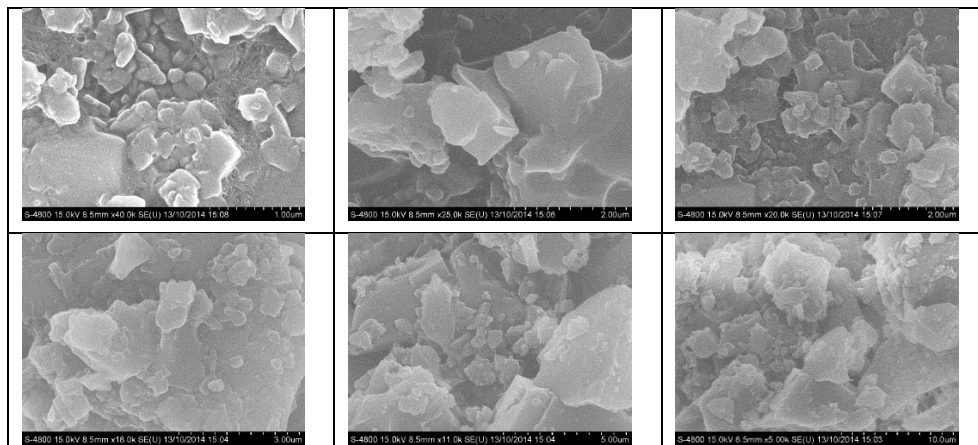
Figure 2.21(a): FE-SEM images of ENMn(III) complex at different magnifications


```
Spectrum:   2990

El  AN   Series   unn. C  norm. C Atom. C Error (1 Sigma)
                  [wt.%]   [wt.%]   [at.%]          [wt.%]
-----------------------------------------------------------
C   6   K-series   24.22    55.21    71.91            3.81
O   8   K-series   10.52    23.98    23.45            2.15
Mn  25  K-series    6.40    14.59     4.15            0.32
Au  79  M-series    2.73     6.22     0.49            0.17
-----------------------------------------------------------
        Total:     43.86   100.00   100.00
```
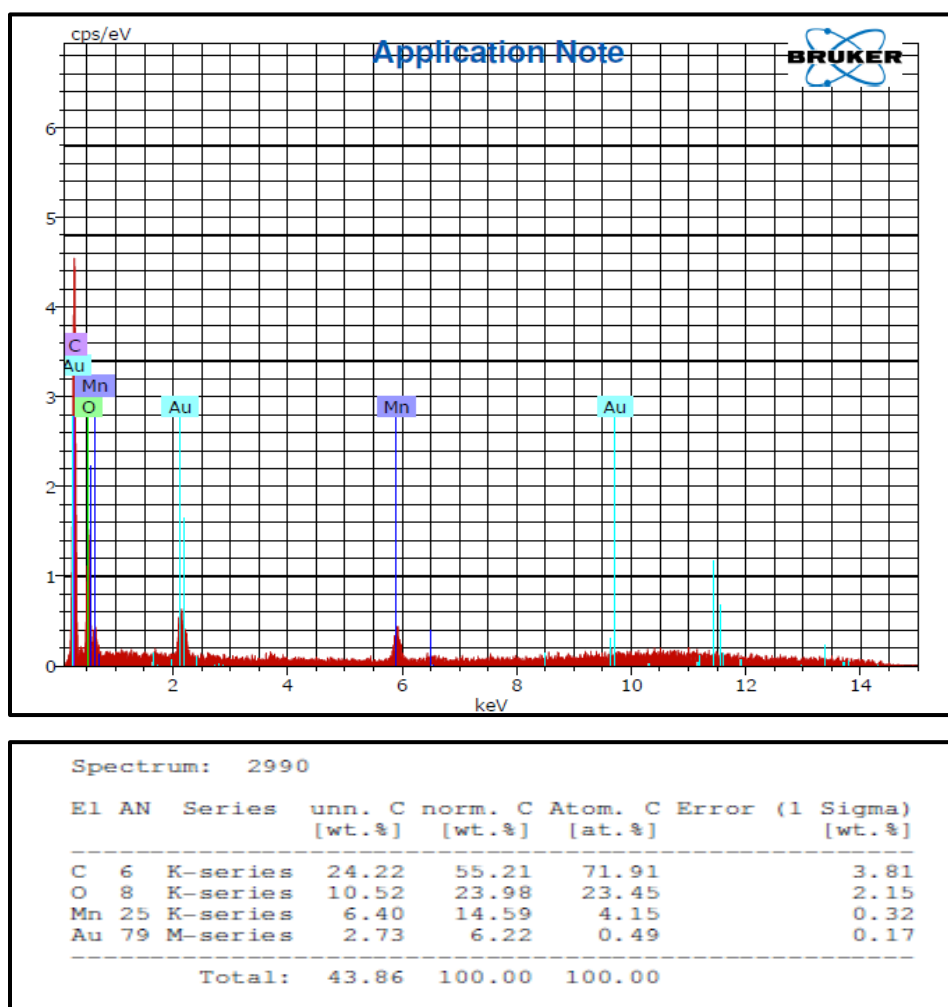
Figure 2.21(b): EDX analysis of ENMn(III) complex
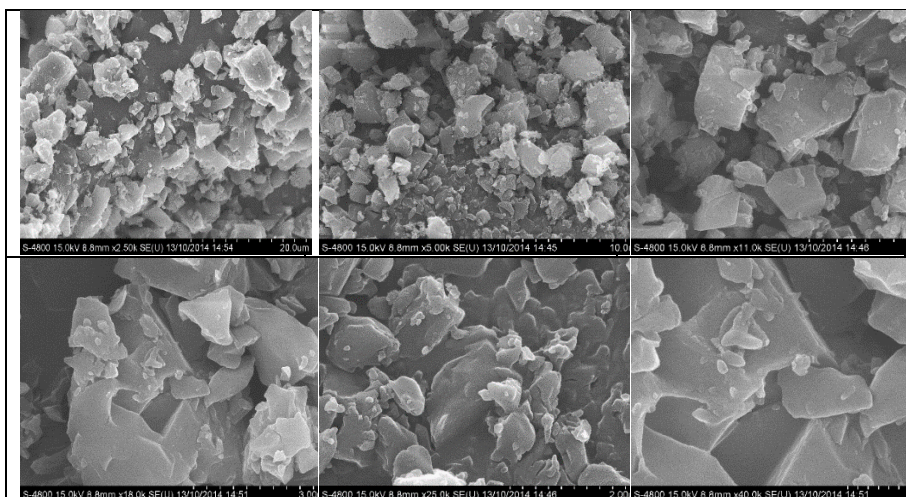
Figure 2.22(a): FE-SEM images of ENCo(II) complex at different magnifications


```
Spectrum:   2992

El AN   Series   unn. C norm. C Atom. C Error (1 Sigma)
                 [wt.%]   [wt.%]   [at.%]       [wt.%]
-----------------------------------------------------------
C   6  K-series   27.58    65.71    84.13        4.72
O   8  K-series    5.03    11.98    11.51        1.58
Co 27  K-series    6.00    14.30     3.73        0.45
Au 79  M-series    3.36     8.01     0.63        0.23
-----------------------------------------------------------
       Total:     41.98   100.00   100.00
```
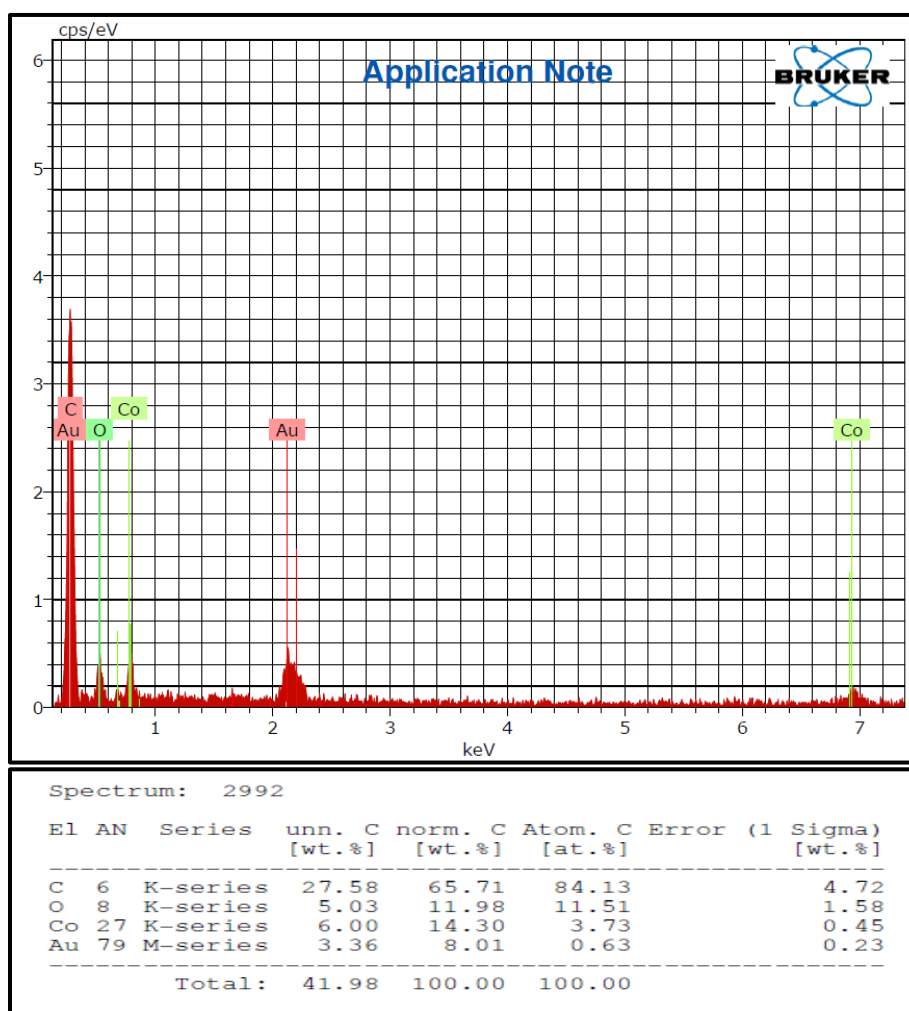
Figure 2.22(b): EDX analysis of ENCo(II) complex
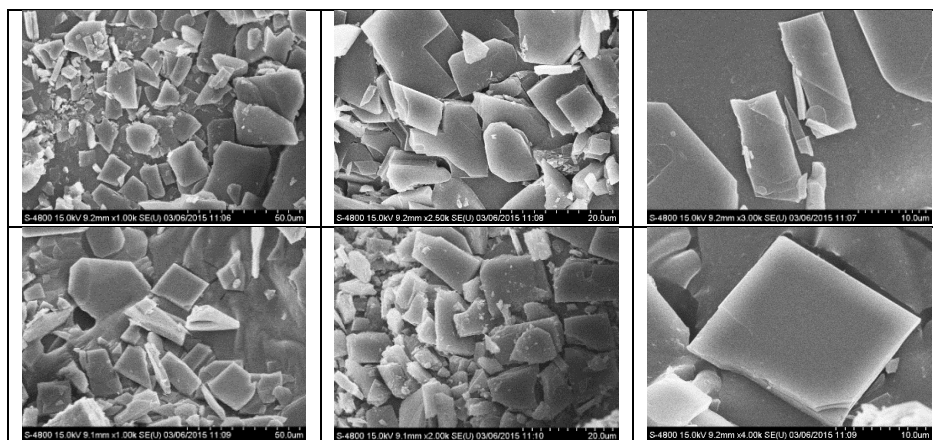
Figure 2.23(a): FE-SEM images of ENNi(II) complex at different magnifications

Spectrum: 4245

El	AN	Series	unn. C [wt.%]	norm. C [wt.%]	Atom. C [at.%]	Error (1 Sigma) [wt.%]
C	6	K-series	19.64	56.37	76.13	3.87
N	7	K-series	3.37	9.67	11.20	1.81
O	8	K-series	2.82	8.08	8.19	1.17
Cl	17	K-series	1.14	3.28	1.50	0.12
Ni	28	K-series	2.01	5.76	1.59	0.32
Au	79	M-series	5.87	16.84	1.39	0.36
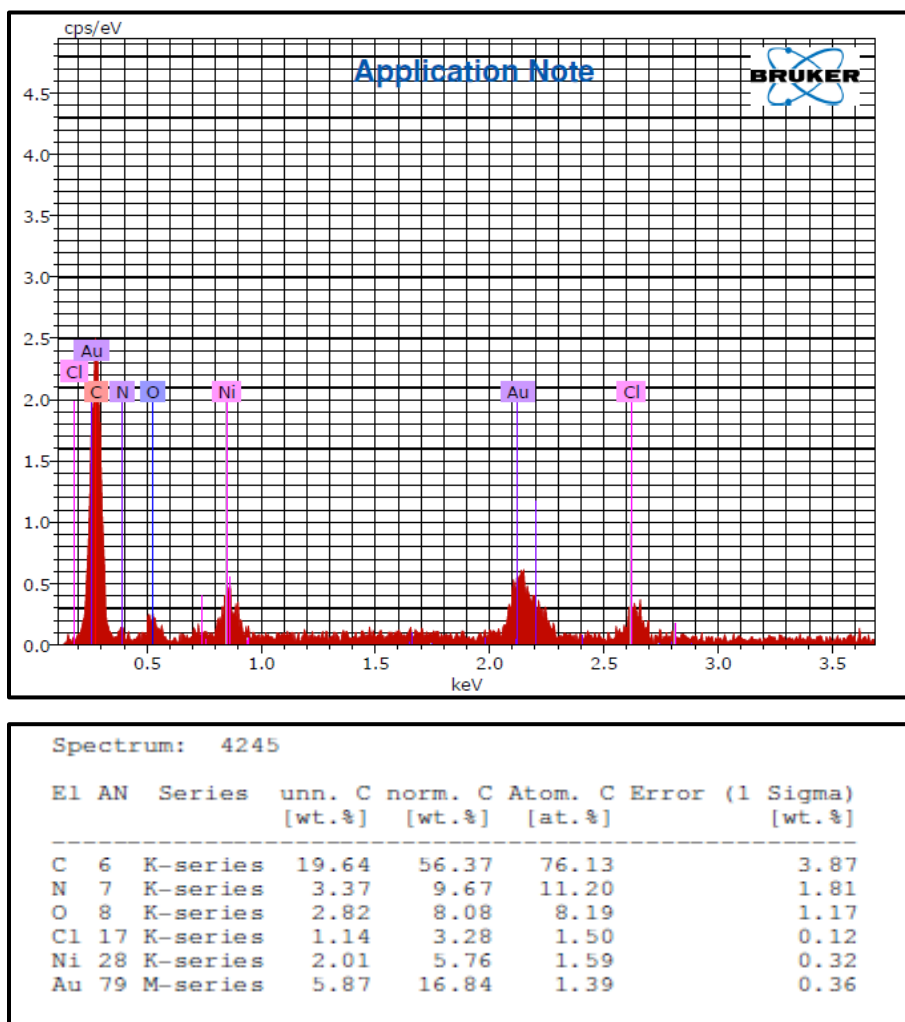
Figure 2.23(b): EDX analysis of ENNi(II) complex
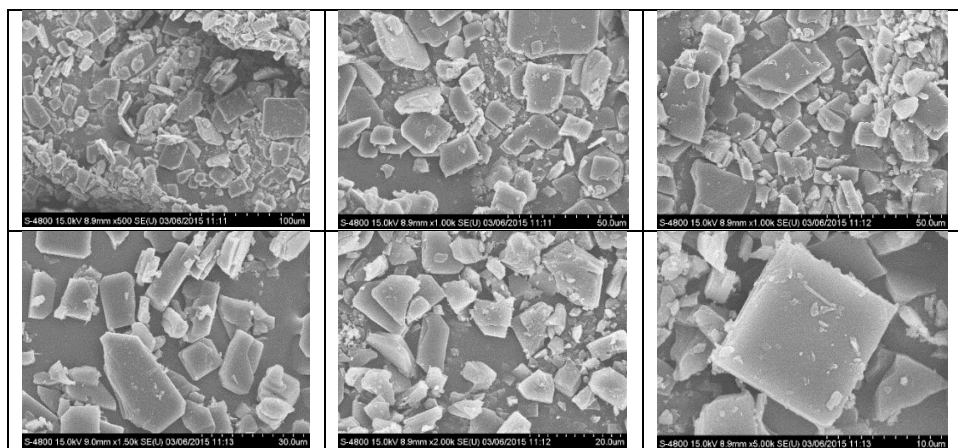
Figure 2.24(a): FE-SEM images of ENCu(II) complex at different magnifications

Spectrum: 4246

El	AN	Series	unn. C [wt.%]	norm. C [wt.%]	Atom. C [at.%]	Error (1 Sigma) [wt.%]
C	6	K-series	50.07	70.87	87.20	8.47
O	8	K-series	6.47	9.16	8.46	2.30
Cu	29	K-series	12.76	18.07	4.20	0.95
Au	79	M-series	1.35	1.91	0.14	0.14
		Total:	70.66	100.00	100.00	
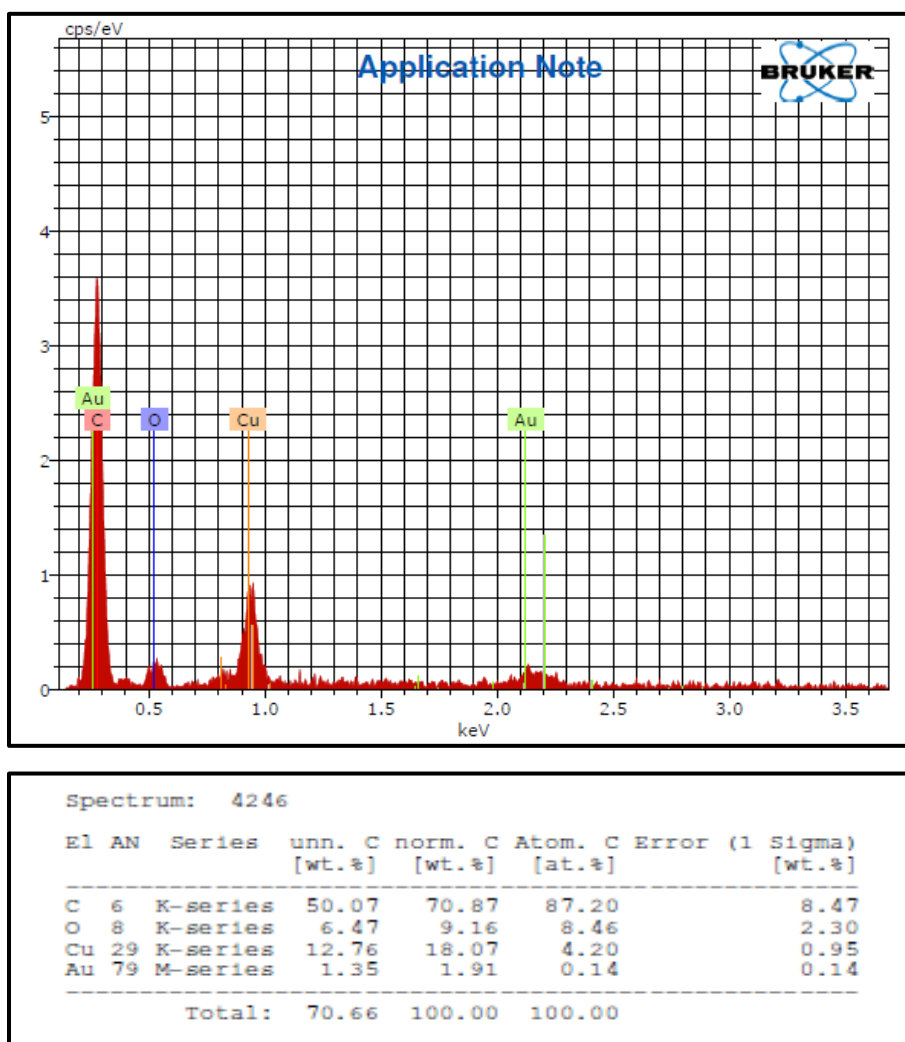
Figure 2.24(b): EDX analysis of ENCu(II) complex

2.5.10 X-ray crystallographic analysis

Single crystals ENMn(III) and ENNi(II) complexes suitable for X-ray analysis of were obtained by the slow evaporation of the methanolic and chloroform solutions of the respective complexes at room temperature. Shining reddish brown and shining orange coloured crystals of ENMn(III) and ENNi(II) were mounted on a APEX 2 (Brucker 2004). The cell refinement and data reduction were performed by using APEX2/SAINT (Bruker 2004) and SAINT/XPREP (Bruker 2004) respectively [33]. The structures were solved by using SIR92 [34] and the structures were refined by SHELXL-2014/7 [35]. The computing molecular graphics were investigated by using ORTEP 3.0 software [36] and Mercury [37]. **Figure 2.25 and Figure 2.26** show the ORTEP representations and packing diagram of Mn(III)OAC while **Figures 2.27- 2.28** shows ORTEP and packing diagram for ENNi(II) complex with the common atomic numbering scheme. The summary of the crystallographic data and structure refinement for ENMn(III) and ENNi(II) complexes has been collected in **Table 2.7**. The selected bond lengths and angles are mentioned in **Tables 2.8 & 2.9** respectively. X-ray studies of both the complexes reveal that each central metal is surrounded by one molecule of ligand through one five-membered and two six-membered rings. The ENMn(III) complex exhibits the irregular five-coordinate environment, maintained by a basal plane formed by N_2O_2 of the Schiff base ligand from its two deprotonated phenol oxygens and two imino nitrogens and an acetate (-$OCOCH_3$) group at the apical position. The ENMn(III) complex possesses square pyramidal geometry. The observed Mn–N, Mn–O and Mn–OAC bond lengths are in the range of previously reported manganese(III) complexes. Similarly, in ENNi(II) complex the Ni–O and Ni–N distances are within the limit ranges of 1.83–1.87 and 1.83–1.89 Å for Ni–O and Ni–N distances described for N_2O_2 square-planar nickel(II) complexes. In the present nickel's crystal structure the bond lengths of Ni-O and Ni-N are in the range of 1.831-1.832 Å and 1.829-1.825 Å respectively. The bond angles around the metal ion *viz*. N2-Ni-O2, O1-Ni-O2, N2-Ni-N1 and O1-Ni-N1 exhibit the values 93.95° (15), 87.47° (12), 85.7° (3) and 92.8° (3) respectively. The N(2)-Ni(1)-O(1) and N(1)-Ni(1)-O(2) bond angles have been found to be 178.99˚ (18) and 178.78˚ (18) respectively. From these trans values, it can be concluded that the complex has distorted square planar geometry. All these mentioned values are nearly close to related reported nickel complexes [38-40].
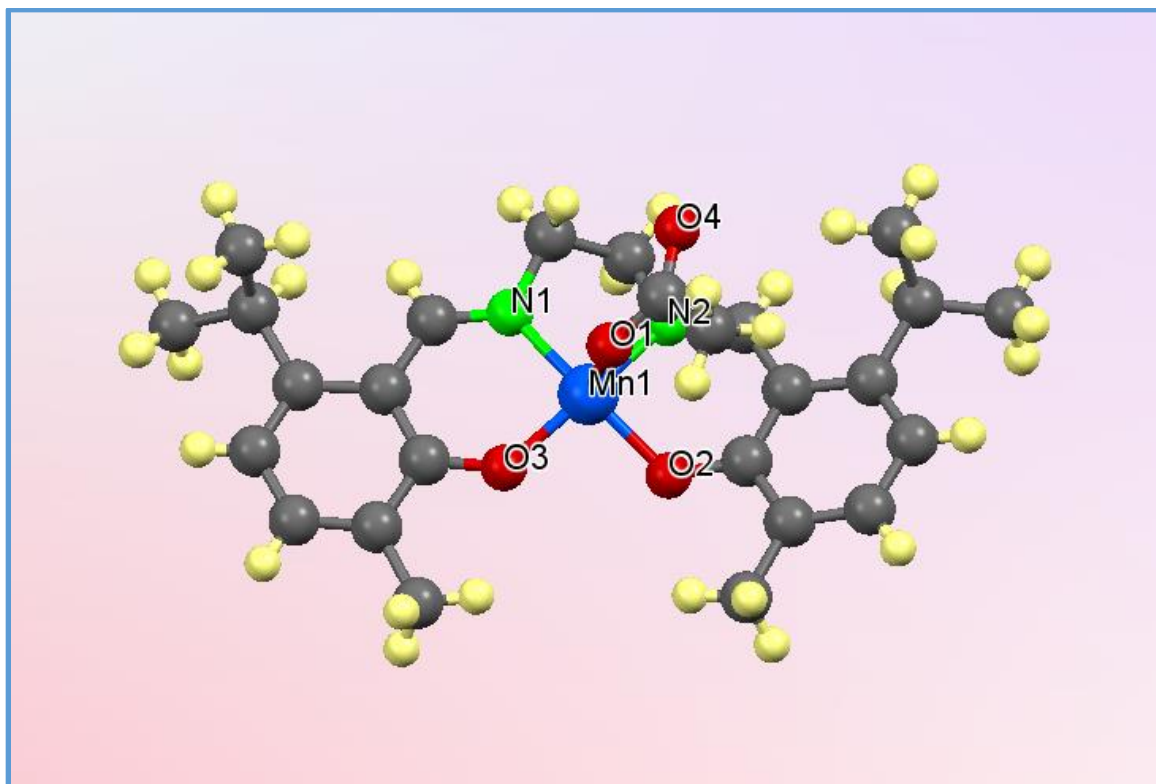
Figure 2.25: ORTEP diagram of ENMn(III) complex with atomic labeling.

The CCDC No. for ENMn(III) complex= 1554257
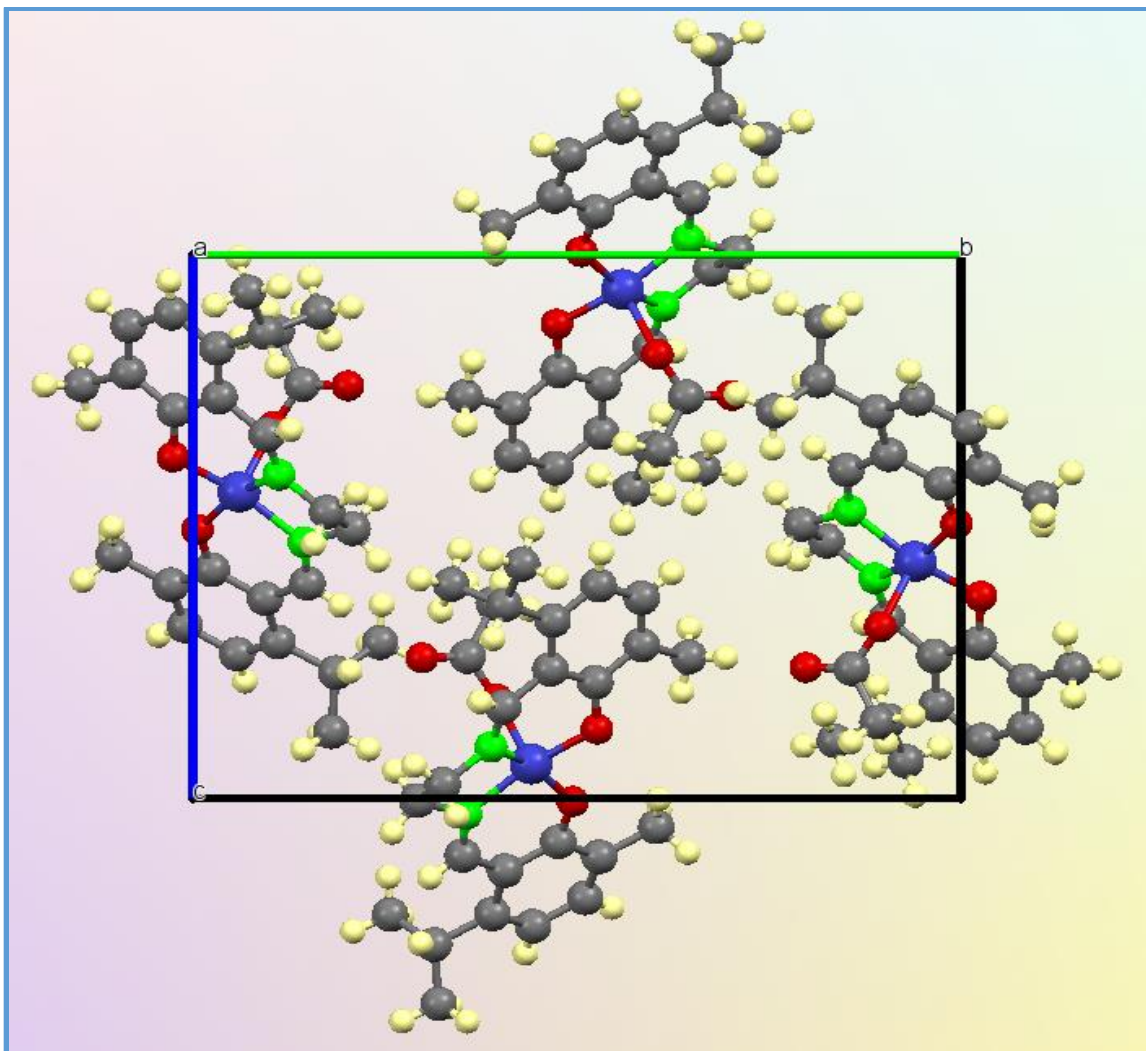
Figure 2.26: The molecular packing diagram ENMn(III) complex along a axis and all atomic labels have been omitted for the clarity
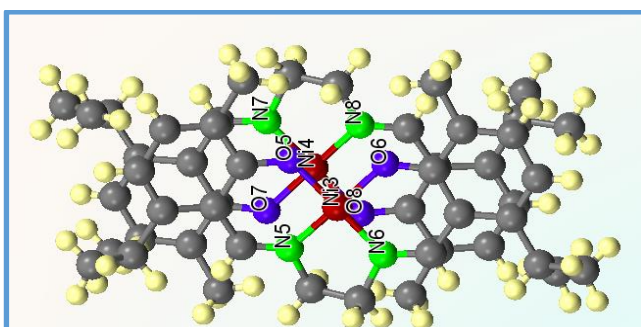
Figure 2.27: ORTEP diagram of ENNi(II) complex with atomic labeling.
The CCDC No. for ENNi(II) complex= 1544860
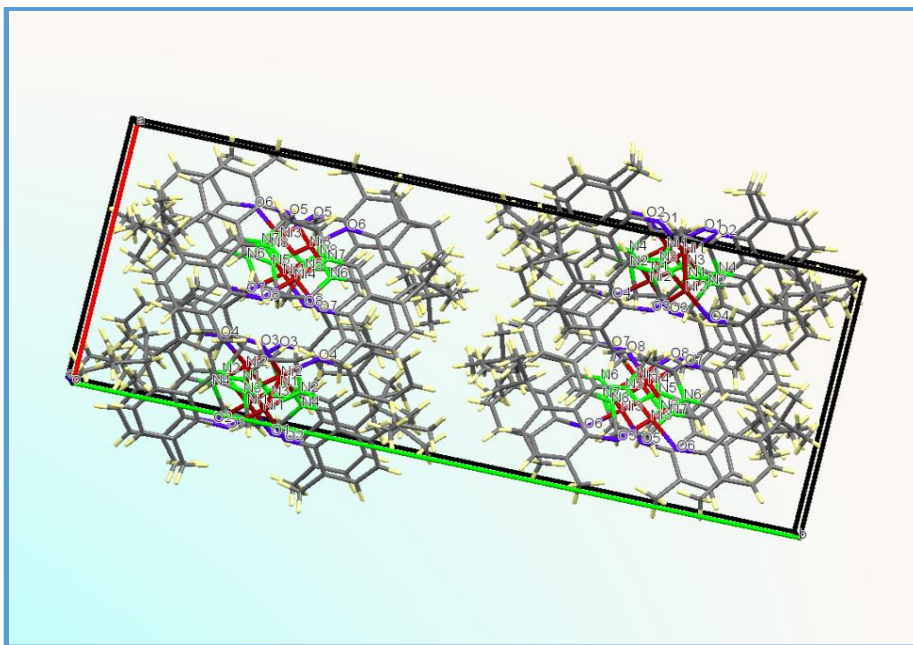
Figure 2.28: Molecular packing diagram of ENNi(II) complex along a axis and atomic labels have been omitted for the clarity

Table 2.7: Crystal data and structure refinement for ENMn(III) and ENNi(II) complexes

Compounds	ENMn(III) complex	ENNi(II) complex
Empirical formula	$C_{26}H_{33}MnN_2O_4$	$C_{24}H_{30}N_2NiO_2$
Formula weight	492.48	437.21
Temperature	298 K	296(2) K
Crystal system	Monoclinic	Monoclinic
Space group	$P112_1/b$	$P2_1/c$
Unit cell dimensions Å	a= 10.5058 (7) Å α= 90° b= 13.2920 (8) Å β= 90° c= 17.7194 (10) Å γ= 90°	a = 12.0742(7) Å α= 90° b=31.331(2)Å β=90.305(2)° c = 23.0947(12) Å γ= 90°
Volume	2474.4(3) Å³	8736.5(9) Å³
Z	4	16

Density (calculated)	1.322 g/cm^3	1.330 Mg/m^3
Absorption coefficient	0.567 mm^{-1}	0.910 mm^{-1}
F(000)	1040.0	3712
Crystal size	0.23 × 0.22 × 0.21 mm^3	0.300 x 0.250 x 0.200 mm^3
Theta range for data collection	3.84 to 54.98°	0.650 to 25.919°
Index ranges	-13 ≤ h ≤ 13, -17 ≤ k ≤ 17, -22 ≤ l ≤ 22	-14<=h<=14, -38<=k<=38, -27<=l<=28
Reflections collected	20688	154854
Independent reflections	4962 [R_{int} = 0.1267, R_{sigma} = 0.1324]	16936 [R(int) = 0.1000]
Data / restraints / parameters	4962/0/305	16936 / 3 / 1052
Goodness-of-fit on F^2	0.949	1.049
Final R indices [I>2sigma(I)]	R_1 = 0.0642, wR_2 = 0.1317	R1 = 0.0503, wR2 = 0.1191
Final R indexes [all data]	R_1 = 0.1489, wR_2 = 0.1610	R1 = 0.1063, wR2 = 0.1513
Largest diff. peak and hole	0.35/-0.48 e Å^{-3}	0.694 and -0.456 e Å^{-3}

Table 2.8: Selected bond lengths and bond angles for ENMn(III) complex

Bond Lengths/Å and Bond Angles/°			
C(25)-O(4)	1.226(5)	O(3)- Mn(1)	1854(2)
C(25)-O(1)	1.271(5)	O(3)-Mn(1)-O(2)	93.53(2)
N(1)-Mn(1)	1.955(3)	O(3)-Mn(1)-N(1)	90.23(11)
N(2)- Mn(1)	1.969(3)	O(2)-Mn(1)-N(1)	162.74(14)
O(1)- Mn(1)	2.042(3)	O(3)-Mn(1)-N(2)	161.29(12)
O(2)- Mn(1)	1.869(3)	O(2)-Mn(1)-N(2)	88.36(12)

Table 2.9: Selected bond lengths and bond angles for ENNi(II) complex

Bond Lengths/Å and Bond Angles/°			
N(1)-Ni(1)	1.829(4)	N(2)-Ni(1)-O(1)	178.99(18)
N(2)-Ni(1)	1.825(4)	N(1)-Ni(1)-O(1)	93.64(16)
Ni(1)-O(1)	1.831(3)	N(2)-Ni(1)-O(2)	93.28(16)
Ni(1)-O(2)	1.832(3)	N(1)-Ni(1)-O(2)	178.78(18)
N(2)-Ni(1)-N(1)	87.08(18)	O(1)-Ni(1)-O(2)	86.02(15)

2.6 Biological activities

2.6.1. Protocol for antibacterial activity

The antibacterial activities of the compounds were assayed by the colony count method, using the selected test organisms *Bacillus subtilis* (NCIM- 2063), *Staphylococcus aureus* (NCIM- 2901) and *Pseudomonas aeruginosa* (NCIM- 2036). In this procedure, cells of the test organisms were grown in nutrient broth until mid-log phase and used as inoculums for performing antibacterial tests. Approximately 1×10^6 cells/ml of the test organisms were each inoculated with 0–500 µg/ml concentrations of the test compounds and incubated for 16–18 h at 37 °C. After incubation, the number of viable cells was assayed by spreading an aliquot from the broth on Muller–Hilton agar and counting the number of colony forming units per milliliter (CFU/ml). DMSO was used as negative control. Minimum inhibitory concentration (MIC) was determined. Ciprofloxacin, ampicillin and

streptomycin were used as positive controls for the comparison of antibacterial activity [41].

2.6.2 Results of antibacterial activity

The EN ligand and its metal complexes have been tested for the antibacterial activity against *B. subtilis* and *S. aureus* as Gram +ve bacterial species and *P. aeruginosa* as Gram –ve bacteria and results are presented as their MIC values along with that for ciprofloxacin, ampicillin and streptomycin as standard drugs are outlined in **Table 2.10**. Comparison of the results indicated that the ligand possesses activity against *B. subtilis* and *S. aureus* which is comparable to the standard ampicillin. In case of complexes the results indicated that some metal complexes possess superior activity than the ligand as well as the standard ampicillin. The ENMn(III) complex shows excellent activities with MIC values 85, 87 and 70 µg/ ml against *B. subtilis*, *S. aureus* and *P. aeruginosa* bacterial strains which are comparable to standard ampicillin. The ENCo(II) complex shows better activity against *B. subtilis* and *S. aureus* as compared to reference drug ampicillin. The ENNi(II) complex also shows better activity against *S. aureus* as compared to standard ampicillin while, the ENCu(II) complex exhibited best activity against the *B. subtilis* and *S. aureus* as compared to standard ampicillin. However, all the compounds displayed poor activity as compared to ciprofloxacin and streptomycin drugs. These results suggest that antibacterial activities of the complexes are effected by ligand as well as metal ions. The increased lipophilic character of these complexes seems to be the reason of their enhanced potent antibacterial activity. The other factors which may influence the activity are solubility, conductivity and bond lengths between the metal and the ligand is shown in **Figure 2.29** [42].

Table 2.10: Antibacterial activity of EN ligand and its metal complexes

Compounds Name	(MIC µg/ml)		
	B. subtilis	*S. aureus*	*P. aeruginosa*
EN Ligand	240	143	225
ENMn(III)	85	87.5	70
ENCo(II)	250	140.5	159.5
ENNi(II)	276	175	250
ENCu(II)	152	114	172
Ciprofloxacin	50	50	25
Ampicillin	250	250	100
Streptomycin	25	25	12.5
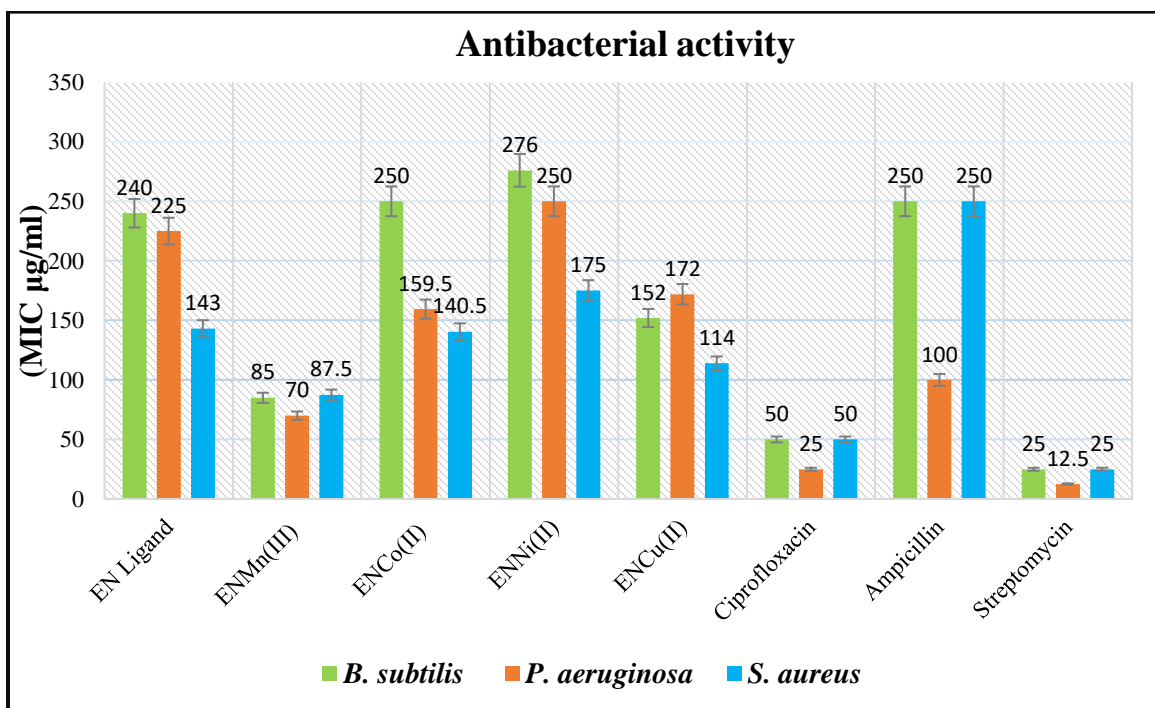
Figure 2.29: Graphical representation of antibacterial activity

2.6.3. Protocol for antifungal activity

The antifungal activity was evaluated against four different fungal strains such as *Candida albicans* (NCIM-3471), *Fusarium oxysporum* (NCIM-1332), *Aspergillus flavus* (NCIM-1196) and *Aspergillus niger.* Minimum inhibitory concentration (MIC) values were determined using standard agar method and the MIC values were determined as per CLSI guidelines [43]. The standards used in the study were dissolved in a suitable solvent. The primary solutions were further diluted to the final strength using test medium

Medium:

The medium yeast nitrogen base (Himedia, India) was dissolved in Phosphate buffer pH 7 and it was autoclaved at 110 °C for 10 minutes. The suitable concentration of the standards was incorporated in the medium. With each set a growth control without the antifungal agent and solvent control DMSO were included.

Preparation of standard inoculum:

The fungal strains were freshly subcultered on to Sabouraud dextrose agar (SDA) and incubated at 25 °C for 72 h. The fungal cells were suspended in sterile distilled water and diluted to get n 10^5 cells/mL. Ten microlitre of standardized suspension was inoculated onto the control plates and the media incorporated with the antifungal agents. The inoculated plates were incubated at 25 °C for 48 h. The readings were taken at the end of 48 hours and 72 h.

Measurement of MIC:

The MIC was the lowest concentration of drug preventing growth of macroscopically visible colonies on drug containing plates when there was visible growth on the drug free control plates.

2.6.4 Results of antifungal activity

The minimum inhibitory concentration (MIC) values of the screened compounds are outlined in **Table 2.11**. Representative graph of antifungal activities is shown in **Figure 2.30**. The EN ligand and its metal complexes are also investigated for the antifugal activity. The chosen fungal strains are *C. albicans, F. oxysporum, A. flavus* and *A. niger* and

Miconazole and Fluconazole have been used as standard drugs, but uncertainly we found the negative antifungal activity for all the compouds

Table 2.11: Antifungal activity of EN ligand and its metal complexes

Compounds Name	(MIC µg/ml)			
	C. albicans	*F. oxysporum*	*A. flavus*	*A. niger*
EN ligand	*	*	*	*
ENMn(III)	*	*	*	*
ENCo(II)	*	*	*	*
ENNi(II)	*	*	*	*
ENCu(II)	*	*	*	*
Miconazole	25	25	12.5	12.5
Fluconazole	5	5	5	10

* No activity reported up to 300 µg/ml
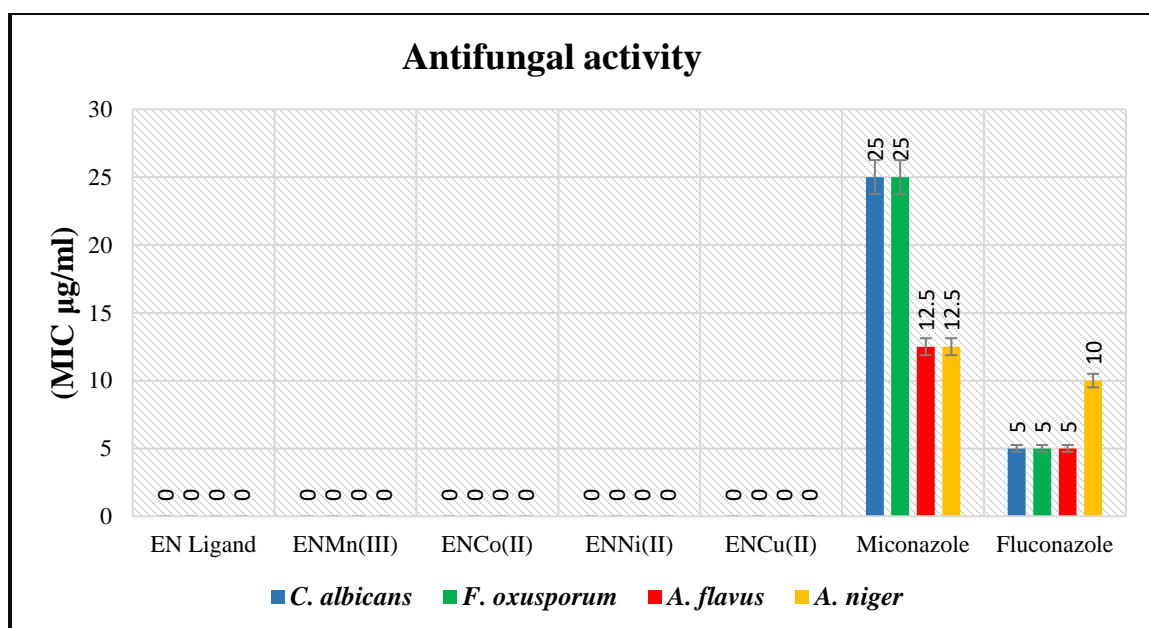
Figure 2.30: Graphical representation of antifungal activity

2.6.5. Protocol for DPPH radical scavenging activity

The hydrogen atom or electron donation ability of the compounds was measured from the bleaching of the purple colored methanol solution of 1,1-diphenyl-1-picrylhydrazyl (DPPH) radical scavenging activity [44]. The spectrophotometric assay uses the stable radical DPPH as a reagent to 4 ml of 0.004 % (w/v) methanol solution of DPPH, 1 ml of various concentrations of the test compound (5, 10, 25, 50 and 100 µg/mL) in methanol was added. After 30 min incubation period at room temperature, the absorbance was measured against blank at 517 nm. The percent inhibition (I %) of free radical production from DPPH was calculated by the following equation.

% of scavenging = [(A control - A sample)/A blank] ×100

Where 'A control' is the absorbance of the control reaction (containing all reagents except the test compound) and 'A sample' is the absorbance of the test compound. Tests were carried in triplicate.

2.6.6 Results of antioxidant activity

An antioxidant is defined as 'any substance that when present at low concentrations, compared with those of the oxidisable substrate significantly delays or inhibits oxidation of that substrate [45]. The DPPH radical absorbs at 517 nm and in a second substrate-free system, antioxidant activity can be determined by monitoring the decrease in this absorbance upon acceptance of an electron or hydrogen radical and get converted to a stable, diamagnetic molecule. Results are reported as the IC_{50} is shown in **Table 2.12**.

All the title compounds were subjected to antioxidant activity and the results were compared with standard drugs, butylated hydroxyl toluene (BHT), ascorbic acid and α-tocopherol. The results as indicated in **Figure 2.31** show that, the free ligand has poor antioxidant activity however, after complexation with metal ions, the activity was found to differ significantly. The ENNi(II) and ENCu(II) complexes showed the excellent activity better than BHT and near about comparable activity to ascorbic acid and α- tocopherol. The ENCo(II) complex also exhibited IC_{50} value very close to that of BHT. Among all the complexes ENMn(III) complex exhibited poor activity as compared to all the standard references.

Table 2.12: Antioxidant activity of EN ligand and its metal complexes

Compounds	IC$_{50}$
EN Ligand	49.55
ENMn(III)	55.36
ENCo(II)	18.25
ENNi(II)	14.21
ENCu(II)	15.29
BHT	16.50
Ascorbic acid	12.80
α-Tocopherol	12.20
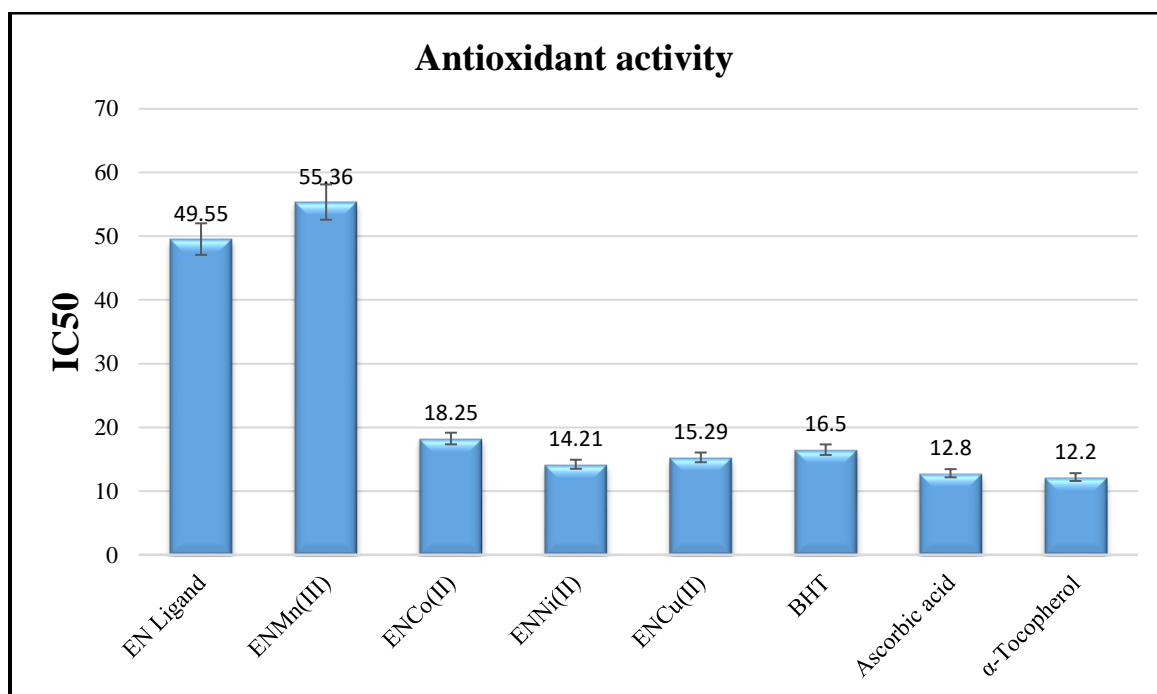
Figure 2.31: Graphical representation of antioxidant activity

2.6.7. DNA cleavage experiment

DNA cleavage potential of the ligand and its metal complexes has been studied by gel electrophoresis on a total sample volume 10 µl in 0.5 ml transparent Eppendorf microcentrifuge tubes containing pBR322 DNA (200 ng). For the gel-electrophoresis experiments, supercoiled pBR322 DNA was treated with the compounds (10, 20, 50, 100, 150 and 200 µM concentrations) and the mixtures were incubated in the dark for 30 min at 37 °C. The reaction was quenched by adding 2 µl DNA loading dye (two dye mixture containing bromophenol blue and xylene cyanol) and the samples were loaded in the wells prepared by 1% agarose gel electrophoresis (Tris-boric acid-EDTA (TBE) buffer, pH=8.2) for 3 h at 40 V. The pBR322 DNA bands were stained by Ethidium bromide and then the level of cleavage of pBR322 DNA was determined by measuring the intensities of the bands using a UVITECH Gel Documentation System. For mechanistic investigations, initially, experiments were carried out in the presence of oxidizing agent H_2O_2 at different concentrations of samples [46].

2.6.8 DNA cleavage study

The pBR322 DNA has been used for the study of agarose gel electrophoresis, DNA cleavage is controlled by relaxation of super coiled circular form of DNA into nicked circular and linear forms **(Figures 2.32- 2.37).** When circular DNA is introduced for electrophoresis study, the fastest migration will be observed for the super coiled form (Form I). If one strand is cleaved, the super coils will convert to produce a slower-moving open circular form (Form II) and if both the strands are cleaved, a linear form (Form III) will be generated; this migrates in between Form I and Form II. It was observed that EN ligand and its respective ENMn(III), ENNi(II) and ENCu(II) complexes at different concentrations do not have any effect on DNA in the presence or absence of hydrogen peroxide suggesting that the oxidative cleavage are not involved in DNA cleavage except for ENCo(II) complex. The ENCo(II) complex possesses the DNA cleavage activity at higher concentration, 200 µM in the presence of oxidant H_2O_2, as evident (Lane 7) from **Figure 2.34**, where the conversion of super coiled DNA to nicked DNA occurs.
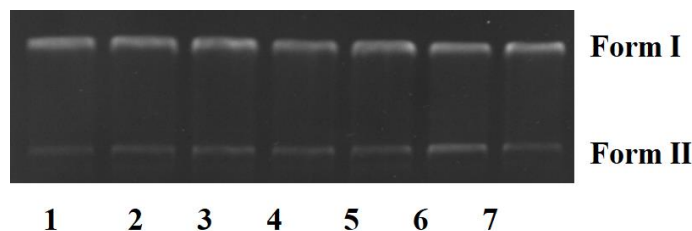
Figure 2.32: Changes in the agarose gel electrophoretic pattern of pBR322 DNA induced by H_2O_2 and EN ligand. Lane 1-DNA+ H_2O_2; Lane 2- DNA + 10 μM sample + H_2O_2; Lane 3-DNA + 20 μM sample + H_2O_2; Lane 4-DNA + 50 μM sample + H_2O_2; Lane 5-DNA + 100 μM sample + H_2O_2; Lane 6-DNA+ 150 μM sample + H_2O_2; Lane 7-DNA + 200 μM sample + H_2O_2.
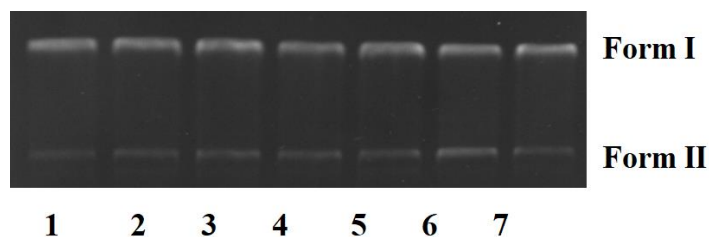
Figure 2.33: Changes in the agarose gel electrophoretic pattern of pBR322 DNA induced by H_2O_2 and ENMn(III) complex. Lane 1-DNA+ H_2O_2; Lane 2- DNA + 10 μM sample + H_2O_2; Lane 3-DNA + 20 μM sample + H_2O_2; Lane 4-DNA + 50 μM sample + H_2O_2; Lane 5-DNA + 100 μM sample + H_2O_2; Lane 6-DNA+ 150 μM sample + H_2O_2; Lane 7-DNA + 200 μM sample + H_2O_2.
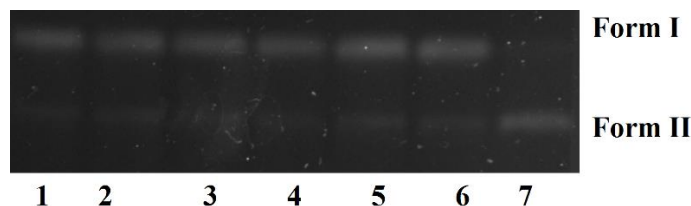
Figure 2.34: Changes in the agarose gel electrophoretic pattern of pBR322 DNA induced by H_2O_2 and ENCo(II) complex. Lane 1-DNA+ H_2O_2; Lane 2- DNA + 10 μM sample + H_2O_2; Lane 3-DNA + 20 μM sample + H_2O_2; Lane 4-DNA + 50 μM sample + H_2O_2; Lane 5-DNA + 100 μM sample + H_2O_2; Lane 6-DNA+ 150 μM sample + H_2O_2; Lane 7-DNA + 200 μM sample + H_2O_2.
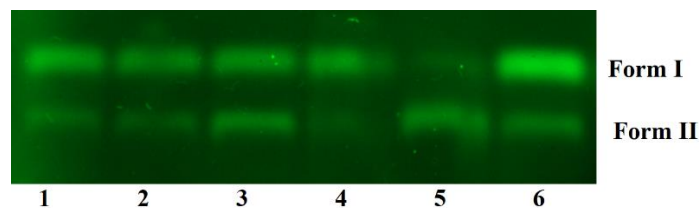
Figure 2.35: **Changes in the agarose gel electrophoretic pattern of pBR 322 DNA. Induced by H₂O₂ and ENCo(II) complex. Lane 1, DNA+ 200 µM sample; lane 2, DNA+ 200 µM sample + d-mannitol; lane 3, DNA + 220 µM sample + DMSO; lane 4, DNA + 200 µM sample +DABCO; lane 5, DNA + 200 µM sample + H₂O₂; lane 6, DNA + 200 µM sample + l-histidine.**
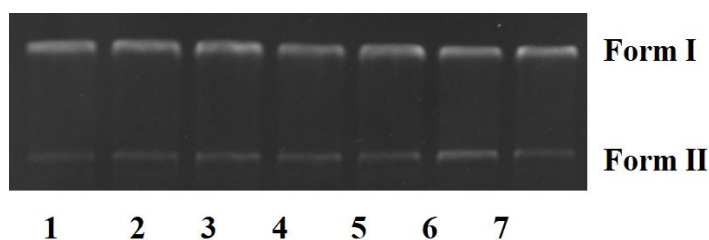
Figure 2.36: Changes in the agarose gel electrophoretic pattern of pBR322 DNA induced by H₂O₂ and ENNi(II) complex. Lane 1-DNA+ H₂O₂; Lane 2- DNA + 10 µM sample + H₂O₂; Lane 3-DNA + 20 µM sample + H₂O₂; Lane 4-DNA + 50 µM sample + H₂O₂; Lane 5-DNA + 100 µM sample + H₂O₂; Lane 6-DNA+ 150 µM sample + H₂O₂; Lane 7-DNA + 200 µM sample + H₂O₂.
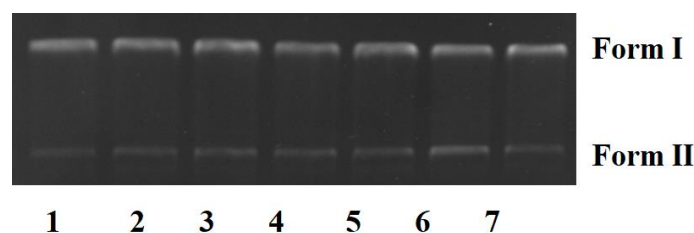
Figure 2.37: Changes in the agarose gel electrophoretic pattern of pBR322 DNA induced by H₂O₂ and ENCu(II) complex. Lane 1-DNA+ H₂O₂; Lane 2- DNA + 10 µM sample + H₂O₂; Lane 3-DNA + 20 µM sample + H₂O₂; Lane 4-DNA + 50 µM sample + H₂O₂; Lane 5-DNA + 100 µM sample + H₂O₂; Lane 6-DNA+ 150 µM sample + H₂O₂; Lane 7-DNA + 200 µM sample + H₂O₂.

Thereafter, we carried out experiments with the ENCo(II) complex at a constant concentration (200 μM) **Figure 2.35** in the presence of different radical scavengers, namely D-mannitol, DMSO DABCO, H_2O_2 and L-histidine. In the presence of H_2O_2, the Form I DNA was to Form II, while partial conversion occurred in the presence of DABCO **Figure 2.35 (Lane 4)** and there was no effect of D-Mannitol, DMSO and L-histidine on Form I DNA. This suggests that oxidative DNA cleavage is mediated by hydroxyl radicals in the presence of the complex. The mechanism of DNA cleavage in similar systems has been described in the literature, and mechanistic studies are in progres [47-49].

2.7 Conclusion

The four transition metal complexes manganese(III), cobalt(II), nickel(II) and copper(II) complexes with N_2O_2 donor Schiff base ligand 6,6'-((1E,1'E)-(ethane-1,2-diylbis(azanylylidene)) bis(methanylylidene))bis(5-isopropyl-2-methylphenol) were synthesized and studied by physico-chemical properties through NMR, UV-Visible, IR, LC-MS, elemental analysis, ESR spectroscopic techniques and further by magnetic susceptibility and molar conductance measurements. Finally, square pyramidal and distorted square planar geometries were confirmed through single crystal x- ray crystallographic techniques. Manganese and copper complexes were found to possess super antibacterial activities against the *B. subtilis*, *S. aureus* and *P. aeruginosa* as compared to standard ampicillin. However, all the compounds showed negative antifungal activity. Nickel, copper and cobalt complexes exhibited excellent antioxidant activity as compared to standard BHT compound and near about comparable antioxidant activity with ascorbic acid and α-Tocopherol. The cobalt complex was found to cleave pBR322 DNA in the presence of oxidant H_2O_2.

2.8 References

1. Zhang HZ, He SC, Peng YJ, Zhang HJ, Gopala L, Tangadanchu VK, Gan LL, Zhou CH, European Journal of Medicinal Chemistry, 136 (2017)165-183.

2. Rizzotto M. complexes as antimicrobial agents, In A Search for Antibacterial Agents 2012. InTech.

3. Peng YL, Liu XL, Wang XH, Zhao ZG, Chemical Papers, 68 (2014) 401-408.

4. Alekshun MN, Levy SB, Molecular mechanisms of antibacterial multidrug resistance Cell, 128 (2007) 1037-50.

5. Rama I, Selvameena, International Journal of Pharmaceutical, Chemical & Biological Sciences, 4 (2014) 416-423.

6. Shrivastava HY, Devaraj SN, Nair BU, Journal of inorganic biochemistry, 98 (2004) 387-392.

7. Renehan MF, Schanz HJ, McGarrigle EM, Dalton CT, Daly AM, Gilheany DG Journal of Molecular Catalysis A: Chemical, 231(2005) 205-220.

8. Da Silva CM, da Silva DL, Modolo LV, Alves RB, de Resende MA, Martins CV, de Fátima Â, Journal of Advanced research, 2 (2011) 1-8.

9. Peng Y, Zhong H, Chen ZF, Liu YC, Zhang GH, Qin QP, Liang H, Chemical and Pharmaceutical Bulletin, 62 (2014) 221-228.

10. Chakravarty AR, Anreddy PA, Santra BK, Thomas AM, Journal of Chemical Sciences, 114 (2002) 391-401.

11. Ghosh K, Kumar P, Mohan V, Singh UP, Kasiri S, Mandal SS Inorganic chemistry, 51(2012) 3343-3345.

12. Pogozelski WK, Tullius TD, Chemical reviews, 98 (1998) 1089-1108.

13. Wang XY, Zhang J, Li K, Jiang N, Chen SY, Lin HH, Huang Y, Ma LJ, Yu XQ Bioorganic & medicinal chemistry, 14 (2006) 6745-6751.

14. Vaidyanathan VG, Nair BU, Journal of inorganic biochemistry, 94 (2003) 121-126.

15. Rajbhoj S. W. and Chondekar T. K., "Systematic Experimental Physical Chemistry" Anjali Publication Aurangabad. 2nd Eds. (2000) 304-315.

16. Wang B, Jiang S, Wang X, Gao S, Science in China Series B: Chemistry, 52 (2009) 1739-1758.

17. Fei C, Zhilong S, Neoh KG, Kang ET, Kang Biotechnology and Bioengineering, 104 (2009) 30-39.

18. Kuwar AS, Fegade UA, Tayade KC, Patil UD, Puschmann H, Gite VV, Dalal DS, Bendre RS, A Novel Cation Sensor. Journal of fluorescence, 23(2013) 859-864.

19. Ghaffari A, Behzad M, Dutkiewicz G, Kubicki M, Salehi M, Journal of Coordination Chemistry, 65 (2012) 840-855.

20. Damercheli M, Dayyani D, Behzad M, Mehravi B, Shafiee A M, Journal of Coordination Chemistry, 68 (2015)1500-1513.

21. Chattopadhyay S, Ray MS, Chaudhuri S, Mukhopadhyay G, Bocelli G, Cantoni A, Ghosh A. Inorganica chimica acta, 35 (2006) 1367-1375.

22. İkiz M, İspir E, Aytar E, Ulusoy M, Karabuğa Ş, Aslantaş M, Çelik Ö, New Journal of Chemistry, 39 (2015).8204-8204.

23. Alan I, Kriza A, Badea M, Stanica N, Olar R, Journal of thermal analysis and calorimetry, 111 (2013) 483-490.

24. Abdallah SM, Mohamed GG, Zayed MA, El-Ela MS, Spectrochimica Acta Part A: Molecular and Biomolecular Spectroscopy, 73(2009) 833-840.

25. Temel H, Şekerci M, Synthesis and Reactivity in Inorganic and Metal-Organic Chemistry, 31 (2001) 849-857.

26. Satpathy KC, Mishra HP, Mishra R, Journal of Inorganic and Nuclear Chemistry, 43 (1981) 2765-2769.

27. Ballhausen CJ, Ligand field theory, McGraw-Hill, New York, 256 (1962).

28. Srinivasan S, Athappan P, Rajagopal G, Transition Metal Chemistry, 26 (2001) 588-593.

29. Raj BB, Kurup MP, Suresh E, Spectrochimica Acta Part A: Molecular and Biomolecular Spectroscopy, 71 (2008) 1253-1260.

30. Raman N, Raja Y.P, Kulandaisamy A, In Proceedings-Indian Academoy f Sciences (Chemical Sciences), 113 (2001) 183-190.

31. Hathaway B, Billing DE, Coordination Chemistry Reviews, 5 (1970) 143-207.

32. Stokes D, John Wiley & Sons, (2008)

33. Bruker A.X.S., Inc (2004): APEX2 (Version 1.08), SAINT (Version 7.03), and SADABS (Version 2.11), Bruker advanced X-ray solutions, Madison, Wisconsin, USA.

34. Altomare A, Cascarano G, Giacovazzo C, Guagliardi A, Completion and refinement of crystal structures with SIR92, Journal of Applied Crystallography, 26 (1993) 343-350.

35. Sheldrick GM, 2014, SHELXL-2014/7: Program for the Solution of Crystal Structures, University of Gottingen, Gottingen, Germany.

36. Farrugia LJ, ORTEP-3 for Windows-a version of ORTEP-III with a Graphical User Interface (GUI), J. Appl. Crystallogr, 30 (2002) 565.

37. Bruno IJ, Cole JC, Edgington PR, Kessler M, Macre CF, McCabe P, Pearson J, Taylor R, Acta Crystallogr, B 58 (2002) 389–397.

38. Sreeja PB, Kurup MP, Kishore A, Jasmin, C, Polyhedron, 23(2004) 575-581.

39. Hulme C, Pritchard R, McAuliffe C, Bermejo M, Journal of the Chemical Society, Dalton Transactions, 11 (1997) 1805-1814.

40. Ghosh M, Fleck M, Mahanti B, Ghosh A, Pilet G, Bandyopadhyay D, Journal of Coordination Chemistry, 65 (2012) 3884-3894.

41. Greenwood D, Slack R.C.B., Peutherer JF, Medical Microbiology, vol. 1, 14th edn. (ELBS, London, 1992)

42. Wissner A, Berger DM, Boschelli DH, Floyd MB, Greenberger LM, Gruber BC, Johnson BD, Mamuya N, Nilkantan R, Reich MF, Shen R, Journal of Medicinal Chemistry, 43 (2000) 3244-3256.

43. Saundane AR, Rudresh K, Satyanarayan ND, Hiremath SP, Indian journal of pharmaceutical sciences, 60 (1998) 379.

44. Burits M, Bucar F, Phytotherapy research, 14 (200) 323-328.

45. Antolovich M, Prenzler PD, Patsalides E, McDonald S, Robards K, Methods for testing antioxidant activity, Analyst, 127 (2002) 183-198.

46. Bhat SS, Kumbhar AA, Heptullah H, Khan AA, Gobre VV, Gejji SP, Puranik VG, Inorganic chemistry, 50 (2010) 545-558.

47. Kavitha P, Reddy KL, Arebian Journal of Chemistry, 9 (2016) 640-648.

48. Jayaseelan P, Prasad S, Vedanayaki S, Rajavel R, Arebian Journal of Chemistry, 9 (2016) 668-677.

49. Arish D, Nair MS, Spectrochimica Acta Part A: Molecular and Biomolecular Spectroscopy, 82 (2011) 191-199.

CHAPTER III

Synthesis of some salen-based transition metal complexes of 6,6'-((1E,1'E)-(propane-1,3-diyl bis(azanylylidene))bis(methanylylidene))bis(5-isopropyl-2-methylphenol): characterization, crystal structures and biological activities

3.1. Introduction

During the past few decades, considerable attention has been paid to the chemistry of metal complexes of schiff bases containing nitrogen and oxygen as donor atoms, which have been found to occupy an important role in the development of the chemistry of chelate systems [1, 2]. Schiff bases have been reported to possess antimicrobial, antiviral, anticancer and anti-inflammatory activities [3]. The salen type schiff base ligands feature two covalent and two coordinate covalent sites situated in a planar array. This makes the ligands ideal for the equatorial coordination of transition metals, leaving the two axial sites open for ancillary ligands [4]. The salen type ligands thus closely resemble to metallo-proteins [5]. A good quality of work has been reported on the synthesis and structural investigation of different types of schiff bases and their complexes [6]. These N_2O_2 donor schiff bases coordinate to d-block transition metals in a tetradentate fashion to afford stable mononuclear complexes [7]. The field of salen complexes is fast growing because of the wide variety of possible structures for the ligands, depending on the type of aldehyde and amine used. Transition metal salen complexes have been studied as catalysts in olefin epoxidations [8], reversible oxygen transport agents, potent antiviral and antitumor agents, in enantioselective and asymmetric catalysis and as models for vitamin B12 [9], for interaction with DNA [10-12], several metal complexes have been used as chemosensor [13-15], metalloproteins involved in important biological electron transfer reactions, as well as in redox processing of molecular oxygen [16].

3.2 Experimental section

3.2.1 Chemicals and Solvents:

Chemicals and solvents are same as described in Chapter 2, section 2.2.1

3.2.2 Analytical methods

Analytical methods are same as described in Chapter 2, section 2.2.2

3.3 Synthesis of schiff base ligand 6,6´-((1E,1´E)-(propane-1,3-iylbis(azanylylidene))bis(methanylylidene))bis(5-isopropyl-2-methylphenol) (DP) and its four mononuclear transition metal complexes.

Preparation of ligand 6,6´-((1E,1´E)-(propane-1,3-iylbis(azanylylidene))bis (methanylylidene)) bis(5-isopropyl-2-methylphenol) (DP) and its metal complexes were carried according to scheme presented in **Figure 3.1** by the procedures of **section 3.3.1 to 3.3.5.**

3.3.1 Synthesis of ligand 6,6´-((1E,1´E)-(propane-1,3-iylbis(azanylylidene))bis(methanylylidene))bis(5-isopropyl-2-methylphenol) (DP):

The DP ligand was prepared by dropwise addition of solution of propane-1,3-diamine (1 mmol, 0.074 gm) in ethanol to constantly stirring solution of 2-hydroxy-6-isopropyl-3-methyl benzaldehyde (2 mmol, 0.356 gm) in ethanol. The reflux condition was maintained till formation of solid product. The product was filtered, washed with cold ethanol and recrystallized from ethanol and dried over sodium sulphate.

Analytical and spectral data of DP ligand: Colour: Yellow, solid. Yield: 67 %. ^{1}H- NMR (CDCl$_3$, 400 MHz) (δ, ppm): 14.87 (brs, 2H, -OH), 8.85 (s, 2H, HC=N), 7.14 (d, 2H, Ar-H, J = 8Hz), 6.68 (d, 2H, Ar-H, J = 8 Hz), 3.77-3.74 (m, 4H, CH$_2$), 3.39-3.32 (m, 1H, CH), 2.23-2.20 (m, 6H, 2(CH$_3$)), 2.17-2.10 (m, 2H, CH$_2$), 1.27-1.63 (m, 12H, 4(CH$_3$)). ^{13}C-NMR (CDCl$_3$, 400 MHz) (δ, ppm): 163.06, 160.95, 147.02, 133.68, 123.70, 114.26, 56.81, 31.81, 27.84, 24.10, 15.59. UV-Vis (DMF) λ$_{max}$(nm): 273, 330, FT-IR (KBr pellet, cm^{-1}) ν$_{max}$: 3221 (OH), 1610 (C=N), 1463 (C=C), 1259 (C-O). MS (m/z): calcd 394.55, obsv 395.3, Anal. calcd for C$_{25}$H$_{34}$N$_2$O$_2$(%): C, 76.10, H, 8.69, N, 7.10, Found: C, 77.77, H, 9.07, N, 6.85.

3.3.2 Synthesis of DPMn(III) complex

The DPMn(III) complex was prepared by dropwise addition of (1 mmol, 0.245 gm) ethanolic solution of manganese acetate tetrahydrate to stirring (1 mmol, 0.394 gm) solution of ligand in ethanol in basic condition under nitrogen atmosphere. The color of solution changed instantly. The reaction mixture was refluxed, and after completion of

reaction, the solution obtained, was evaporated and product was collected, washed with cold ethanol and then with diethyl ether.

Analytical and spectral data of DPMn(III) complex: Colour: Reddish brown, solid. Yield: 65%. UV-Vis (DMF) λ_{max} (nm): 266, 327. FT-IR (KBr, cm^{-1}) ν_{max}: 1560 (C=N), 1247 (C-O), 1409 (C=C), 520 (M-O), 439 (M-N). LC-MS (m/z): calcd 447.47, obsv 447.3. Anal. calcd for $C_{27}H_{35}MnN_2O_4$ (%): C 64.02, H 6.96, N 5.53, Found: C 64.98, H 6.00, N 5.51. μeff: 4.65 B.M.. Conductance (Λ_M, Ω^{-1} cm^2 mol^{-1}) in DMF: 9.60.

3.3.3 Synthesis of DPCo(II) complex

The DPCo(II) complex was prepared by dropwise addition of (1 mmol, 0.249 gm) of cobalt acetate tetrahydrate dissolved in ethanol to stirred solution of ligand (1 mmol, 0.394 gm) in ethanol. The reaction mixture was refluxed, and after completion of reaction, the solution obtained, was evaporated and collected product was washed with cold ethanol and then with diethyl ether.

Analytical and spectral data of DPCo(II) complex: Colour: Reddish brown, solid. Yield: 70 %. UV-Vis (DMF) λmax(nm): 269, 401, 622. FT-IR (KBr, cm^{-1}) ν_{max}: 1562 (C=N), 1230 (C-O), 1454 (C=C), 542 (M-O), 439 (M-N). LC-MS (m/z): calcd 451.47, obsv 451.4. Anal. calcd for $C_{25}H_{32}CoN_2O_2$(%): C 66.51, H 7.14, N 6.20, Found: C 68.06, H 6.57, N 5.90. μeff: 3.48 B.M.. Conductance (Λ_M, Ω^{-1} cm^2 mol^{-1}) in DMF: 11.68.

3.3.4. Synthesis of DPNi(II) complex

The DPNi(II) complex was prepared by dropwise addition of (1 mmol, 0.237 gm) ethanolic solution of nickel chloride hexahydrate to the stirred solution of ligand (1 mmol, 0.394 gm) in ethanol. Few drops of triethylamine were added to the solution and the color of solution changed instantly. The reaction mixture was refluxed, and after completion of reaction, precipitate obtained was collected, washed with cold ethanol and then with diethyl ether. The dark green single crystal of DPNi(II) suitable for X-ray crystallography were obtained by slow evaporation of ethanolic solution. The crystals were isolated and washed with hexane.

Analytical and spectral data of DPNi(II) complex: Colour: Dark green, solid. Yield: 68 %. UV-Vis (DMF) λmax (nm): 271, 354, 418, 579. FT-IR (KBr, cm^{-1}) ν_{max}: 1560 (C=N), 1234 (C-O), 1452 (C=C), 474 (M-O), 432 (M-N). LC-MS (m/z): calcd 451.23, obsv 451.0. Anal. calcd for $C_{25}H_{32}N_2NiO_2$ (%): C, 66.54, H, 7.15, N, 6.21, Found: C, 64.35, H, 6.94, N, 6.10. Conductance (Λ_M, Ω^{-1} cm^2 mol^{-1}) in DMF: 12.72.

3.3.5 Synthesis of DPCu(II) complex

The DPCu(II) complex was prepared by dropwise addition of (1 mmol, 0.199 gm) of cupric acetate monohydrate dissolved in ethanol to the stirred solution of ligand (1 mmol, 0.394 gm) in ethanol. Triethylamine was added as 2-3 drops, the color of solution changed instantly. The reaction mixture was refluxed and after completion of reaction, shining dark green crystals were collected by filtration and washed with cold ethanol and then diethyl ether.

Analytical and spectral data of DPCu(II) complex: Colour: Shining dark green, solid, Yield: 78 %. UV-Vis: (DMF) λmax (nm): 284, 379, 598. FT-IR (KBr, cm-1) ν_{max}: 1556 (C=N), 1224 (C-O), 1446 (C=C), 520 (M-O), 422 (M-N). LC-MS (m/z): calcd 456.08, obsv 456.30; Anal. calcd for $C_{25}H_{32}CuN_2O_2$ (%): C, 65.84, H, 7.07, N, 6.14, Found: C, 68.04, H, 7.20, N, 6.43. μeff: 1.85 B.M.. Conductance (Λ_M Ω^{-1} cm^2 mol^{-1}): 12.67; g$\parallel$= 2.2317, g$\perp$= 2.0472.
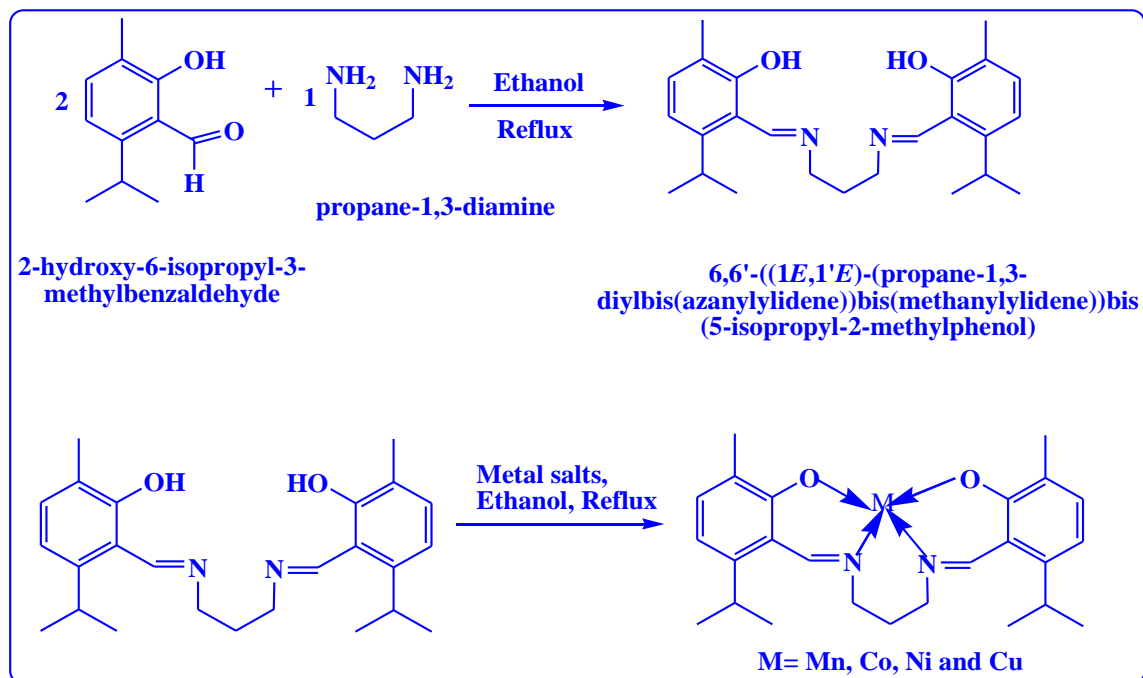
Figure 3.1: Synthesis of 6,6ʹ-((1E,1ʹE)-(propane-1,3-iylbis(azanylylidene)) bis(methanylylidene))bis(5-isopropyl-2-methylphenol) (DP) and its metal complexes

3.4 Characterization of DP ligand and its DPMn(III), DPCo(II), DPNi(II) and DPCu(II) metal complexes.

All the synthesized compounds have been characterized by sophisticated techniques such as, NMR, UV-Visible, FT-IR, LC-MS, ESR spectroscopy, Elemental analysis Magenetic susceptibility, Conductivity measurements, SEM analysis and finally the Single crystal X- ray diffraction techniques.

3.4.1 NMR Spectra

The ^{1}H & ^{13}C NMR spectra of schiff base ligand DP are shown in Figures 3.2- 3.3 and the δ values are given in **Table 3.1**. In the ^{1}H-NMR spectrum of schiff base DP the broad peak at δ 14.87 corresponds to the phenolic OH group. The singlet peak appearing at δ 8.85 for 2H is for (HC=N). The peak values in the range δ 6.68- 7.14 refer to aromatic protons. The multiplet signals for 4H and 2H of CH_2 appeared at 3.77-3.74 and 2.17-2.10 respectively. Another multiplet exhibited at 3.39-3.32 and 1.27-1.63 is for the isopropyl's group of -CH and 4(CH_3). The signal for the methyl protons appear at 2.23-2.20.

Table 3.1: NMR spectral data of DP ligand

Compounds	Assignments of peaks δ ppm
¹H-NMR (400 MHz, CDCl₃) (δ, ppm):	14.87 (brs, 2H, OH), 8.85 (s, 2H, HC=N), 7.14 (d, 2H, Ar-CH, J= 8Hz), 6.68 (d, 2H, Ar-CH, J=8 Hz), 3.77-3.74 (m, 4H, CH₂), 3.39-3.32 (m, 1H, CH), 2.23-2.20 (m, 6H, 2(CH3)), 2.17-2.10 (m, 2H, CH2), 1.27-1.63 (m, 12H, 4(CH3)).
¹³C-NMR (400 MHz, CDCl₃) (δ, ppm):	163.06, 160.95, 147.02, 133.68, 123.70, 114.26, 56.81, 31.81, 27.84, 24.10, 15.59.
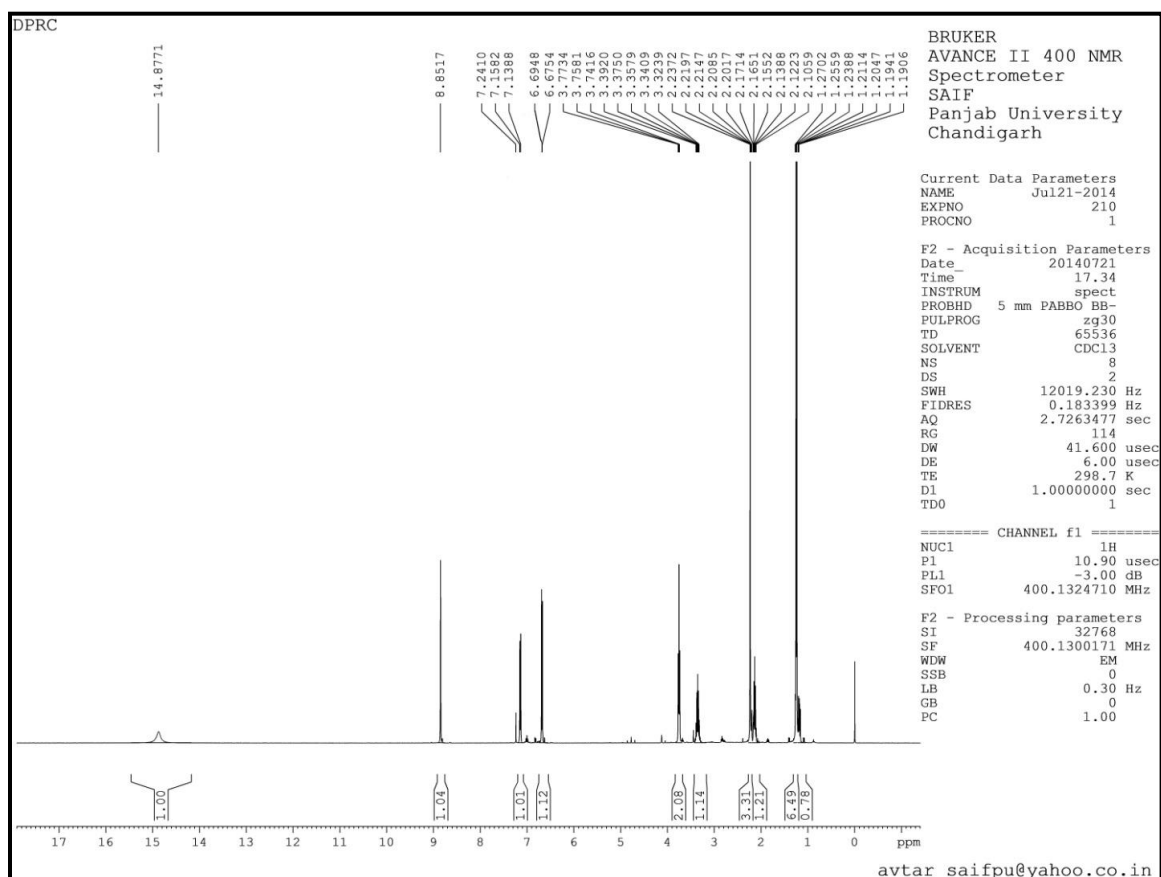
Figure 3.2: ¹H-NMR spectrum of DP ligand
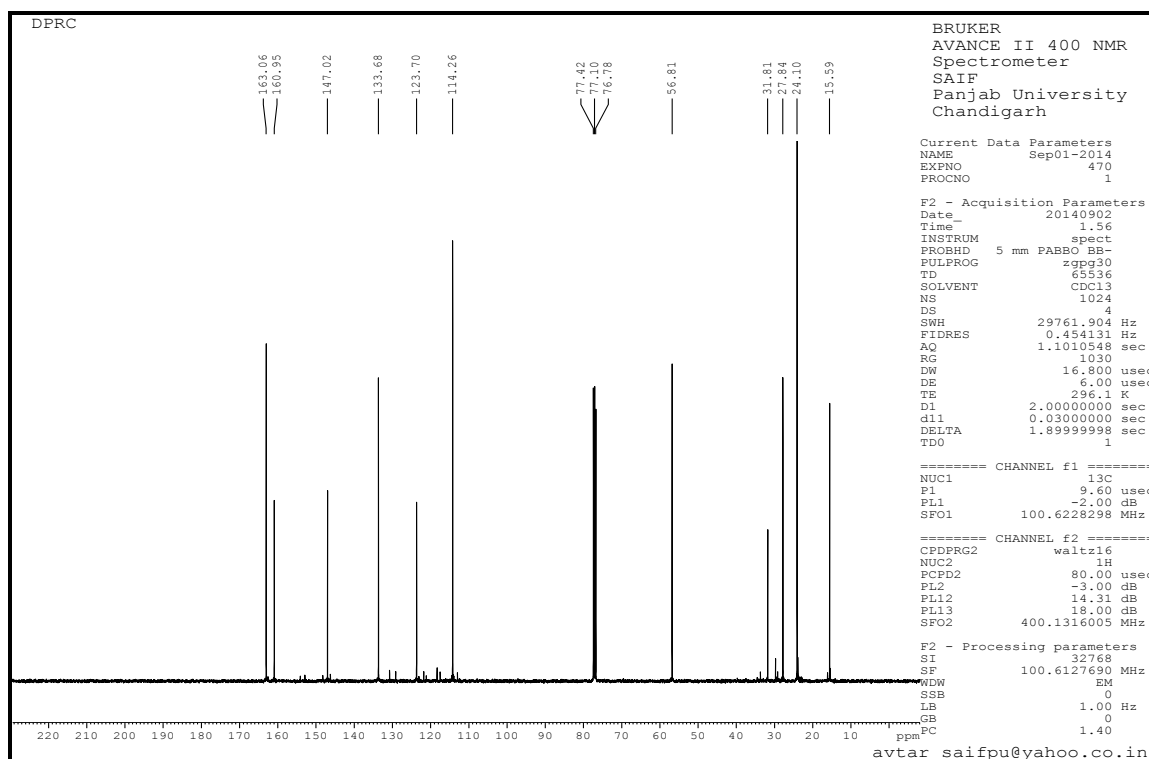
Figure 3.3:.^{13}C-NMR spectrum of DP ligand

3.4.2 UV-Visible spectra

The UV-Visible spectra of the synthesized DP ligand and its metal complexes were recorded in DMSO solution at different concentrations in the range 200- 800 nm are presented in the **Table 3.2**. The spectral data of the schiff base ligand DP shows two bands at 267 nm and 333 nm due to $\pi \rightarrow \pi^*$ and $n \rightarrow \pi^*$ transitions **(Figures 3.4- 3.8)** [17]. The UV-Visible spectra of manganese(III) complex shows absorption bands having λ_{max} 266 nm assigned to the $\pi \rightarrow \pi^*$ transitions of aromatic ring and 327 nm assigned to $n \rightarrow \pi^*$ transition of –C=N-. The cobalt(II) complex shows absorption bands having λ_{max} 269 nm assigned $\pi \rightarrow \pi^*$ of aromatic ring, 401 nm band assigned to ligand to metal ion charge transfer and d-d transition at 622 nm assigned as $^1A_{1g} \rightarrow {}^1B_{1g}$ transition of square planar complex [5]. The UV-Visible spectra of nickel(II) complex shows absorption bands having λ_{max} 271 nm assigned to the $\pi \rightarrow \pi^*$ of aromatic ring and 354 nm assigned to $n \rightarrow \pi^*$ transition of –C=N-, 418 nm band assigned to ligand to metal ion charge transfer and d-d transition at 579 nm of the complex indicating square planar geometry [18-20]. The electronic spectra of copper(II) complex shows absorption band having λ_{max} 284 nm

assignable to $\pi\to\pi^*$ of aromatic ring and band around 379 nm due to the ligand to metal charge transfer and 598 nm band assigned to $^2B_{1g}\to\,^2A_{1g}$ transition showing the square planar geometry [21-22].

Table 3.2: UV-Visible spectral data of DP ligand its metal complexes

Compounds	Wavelength (nm)
DP Ligand	273, 330
DPMn(III)	266, 327
DPCo(II)	273, 401, 622
DPNi(II)	271, 354, 418, 579
DPCu(II)	284, 379,598
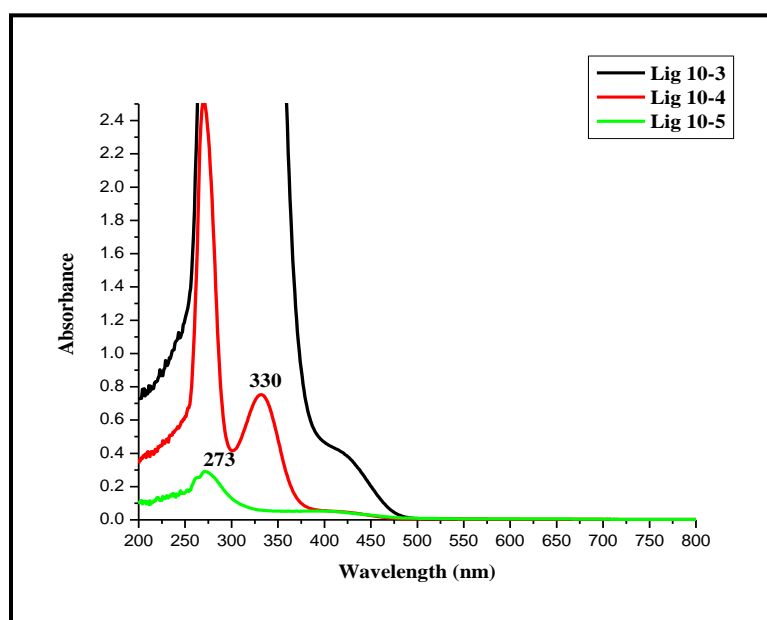
Figure 3.4: UV- Visible spectrum of DP ligand
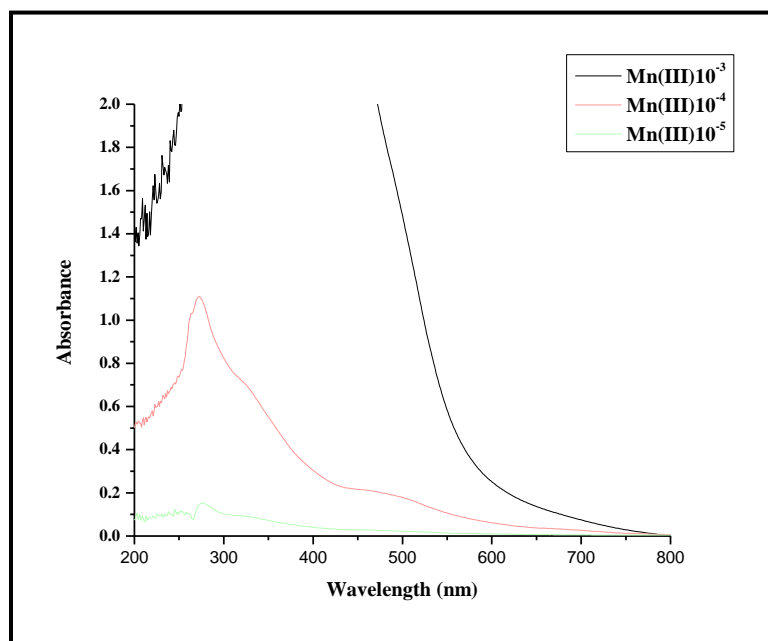
Figure 3.5: UV-Visible spectrum of DPMn(III) complex
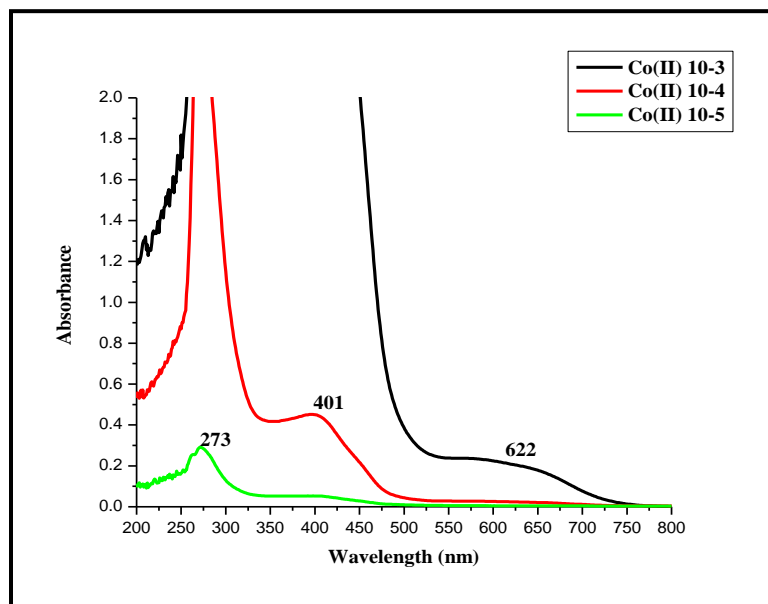
Figure 3.6: UV-Visible spectrum of DPCo(II) complex
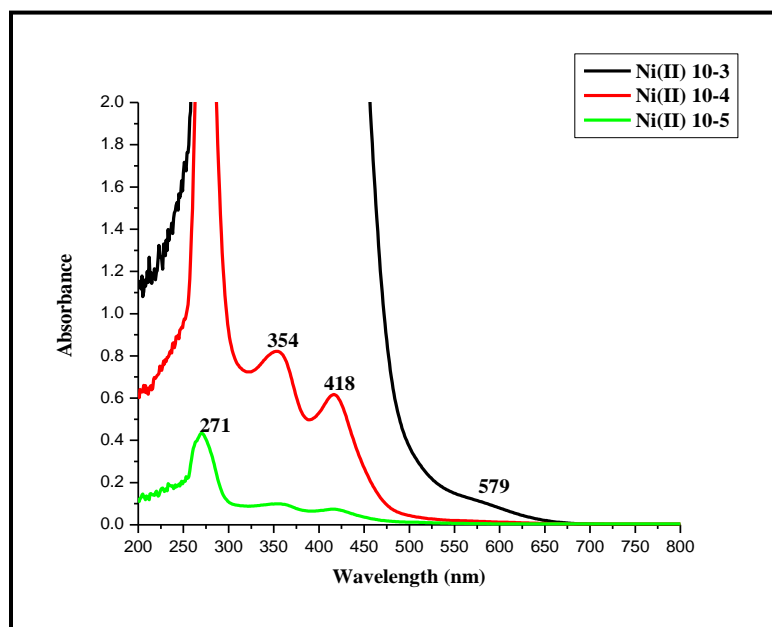
Figure 3.7: UV-Visible spectrum of DPNi(II) complex
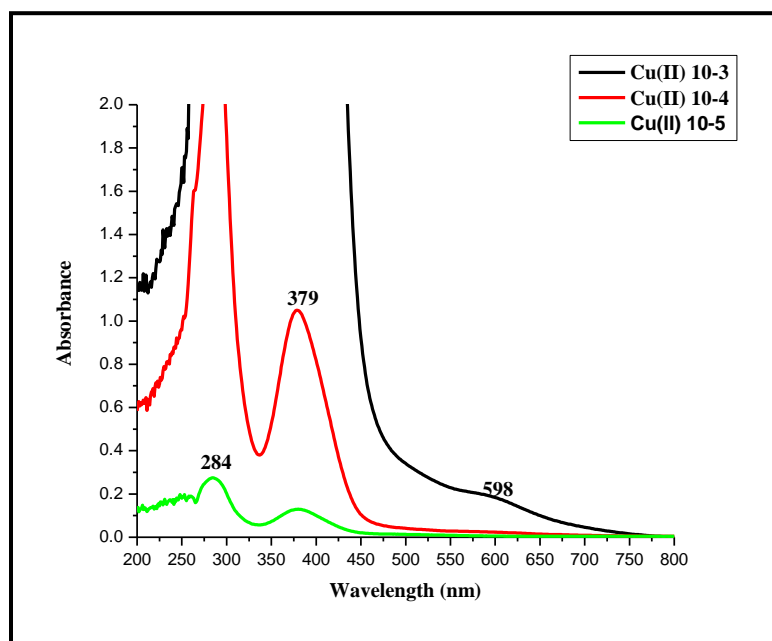
Figure 3.8: UV-Visible spectrum of DPCu(II) complex

3.4.3 FT-IR spectra

The FT-IR spectroscopy is an important tool to probe various structural ordering phenomena and this procedure provides the information about the position of ions in the crystal and about the interatomic vibration modes. The absorption of specific wavelength IR radiation depends on the natural frequency of vibration of the functional group/moiety [23]. The IR spectra of the ligand and complexes are represented in **Figures 3.9- 3.13** while IR spectral assignments are listed in **Table 3.3** and compared to confirm the coordination of ligand. The band at 1610 cm^{-1} attributed to the -C=N- in the schiff base DP ligand was observed to shift to lower frequency region, 1610-1556 cm^{-1} in all the complexes, illustrated participation of the azomethine nitrogen atom in coordination.

The peak at 3221 cm^{-1} appears for the phenolic –OH group. The peak appearing in the ligand at 1259 cm^{-1} due to C-O was found to shift to 1247-1340 cm^{-1} upon complexation. The weak and low frequency bands appearing in the range 400-600 cm^{-1} correspond to M-O and M-N in coordination with metal respectively [20].

Table 3.3: FT-IR sprectral data of DP ligand and its metal complexes

Compounds	Spectral bands (cm^{-1})
DP Ligand	3334, 3221, 1610, 1433, 1259, 1092
DPMn(III)	3456, 3340, 3230, 2958, 2096, 1870, 1560, 1409, 1247, 1128, 1012, 962, 806, 729, 661, 524, 439
DPCo(II)	2960, 2873 1616, 1562, 1454, 1398, 1332, 1230, 969, 808, 667, 542, 418, 366
DPNi(II)	2958, 2877, 1604, 1560, 1452, 1425, 1348, 1296, 1234, 1114, 1020, 806, 659, 634, 557, 474, 432
DPCu(II)	1608, 1556, 1446, 1417, 1340, 1224, 1022, 964, 810, 613, 520, 422
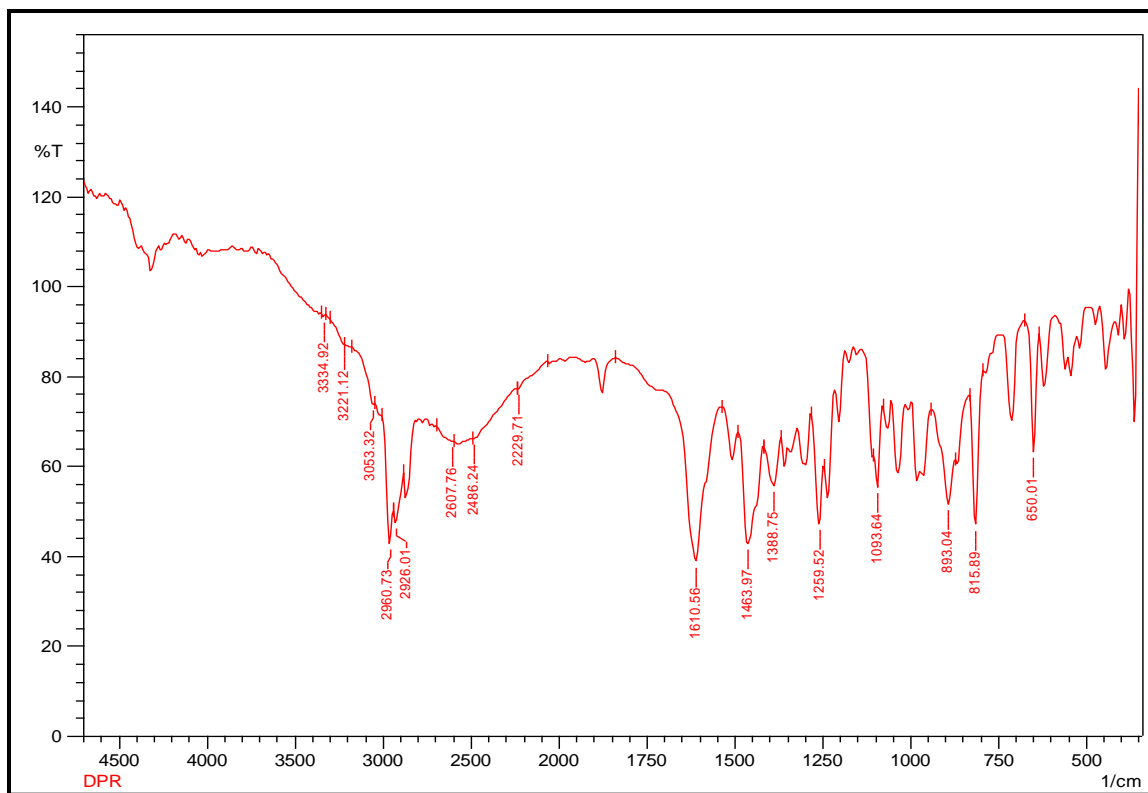
Figure 3.9: FT-IR spectrum of DP ligand
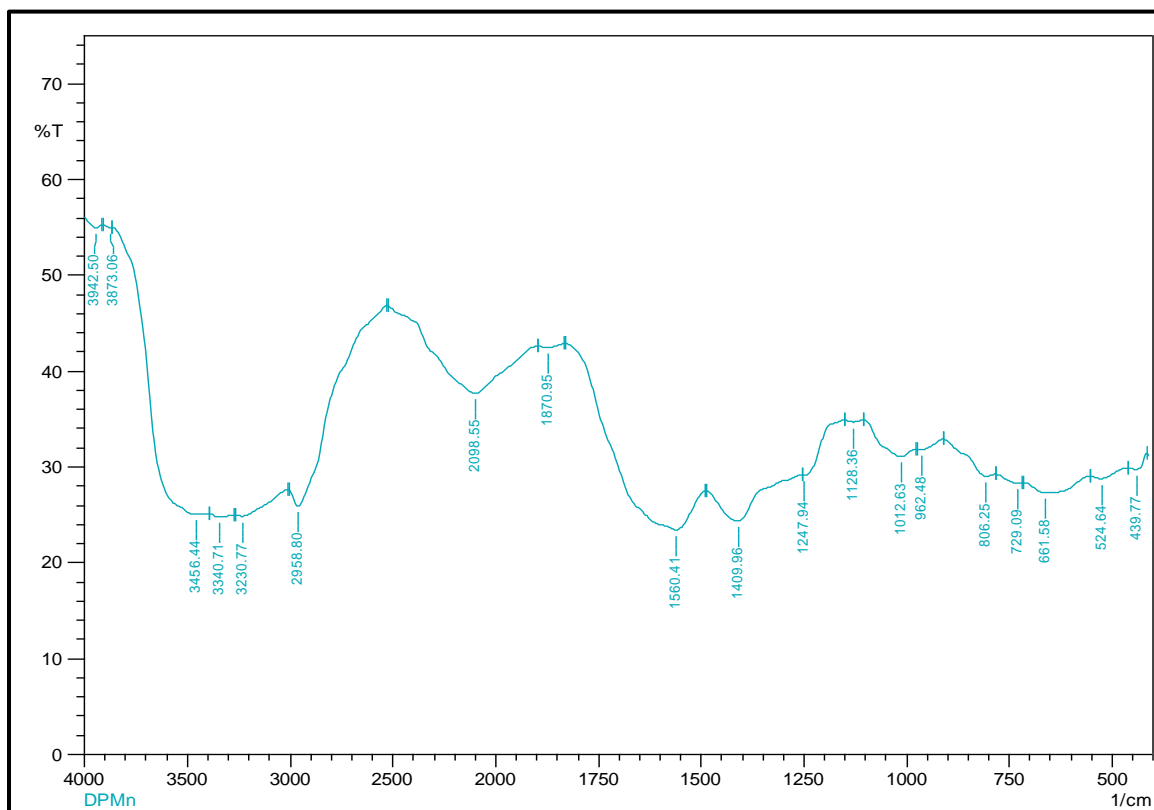
Figure 3.10: FT-IR spectrum of DPMn(III) complex
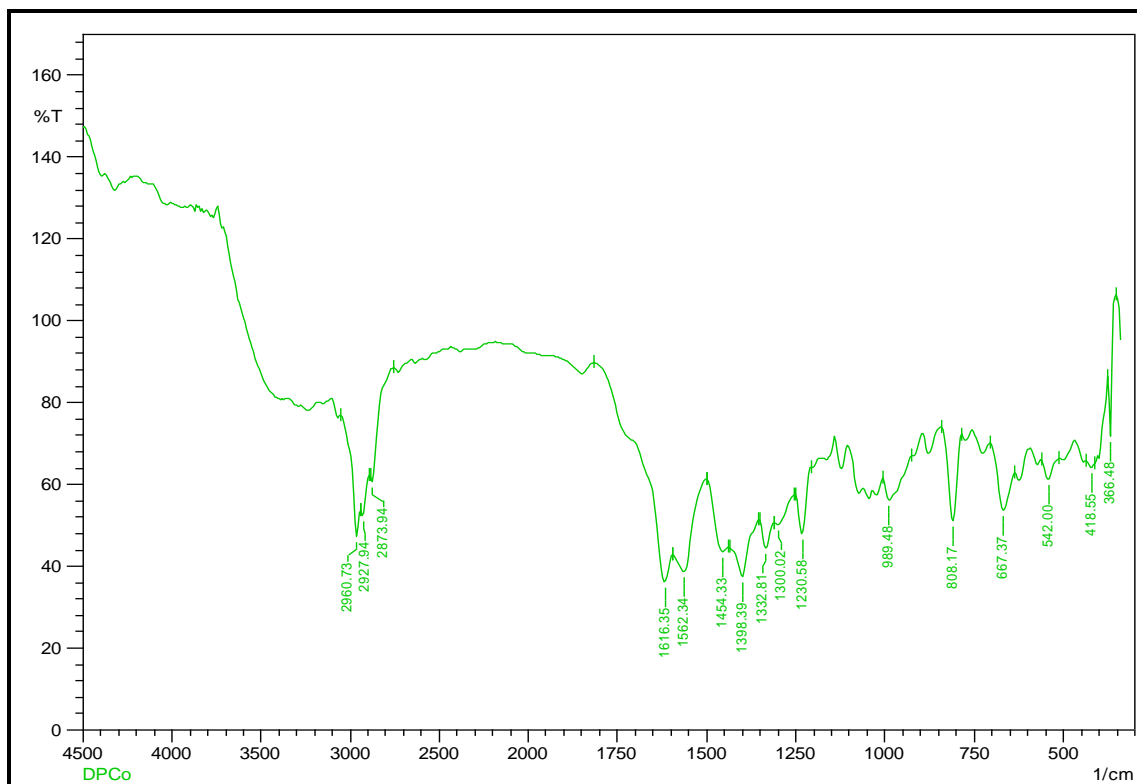
Figure 3.11: FT-IR spectrum of DPCo(II) complex
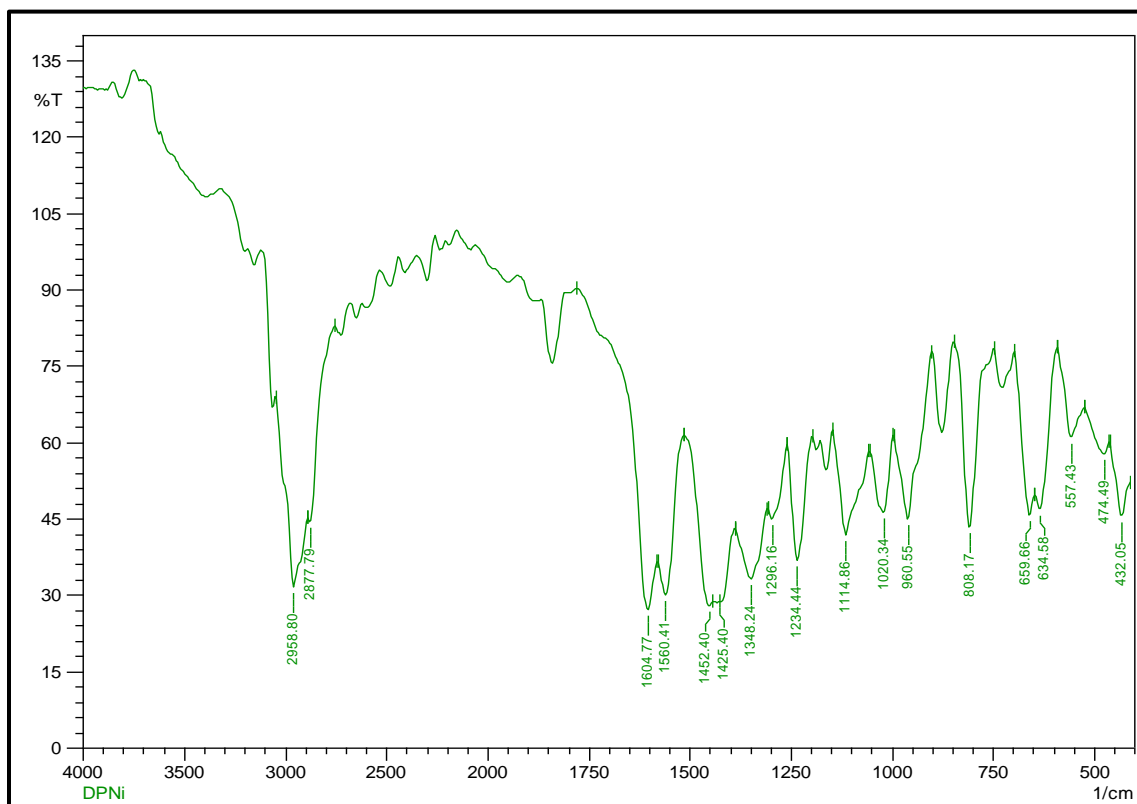
Figure 3.12: FT-IR spectrum of DPNi(II) complex
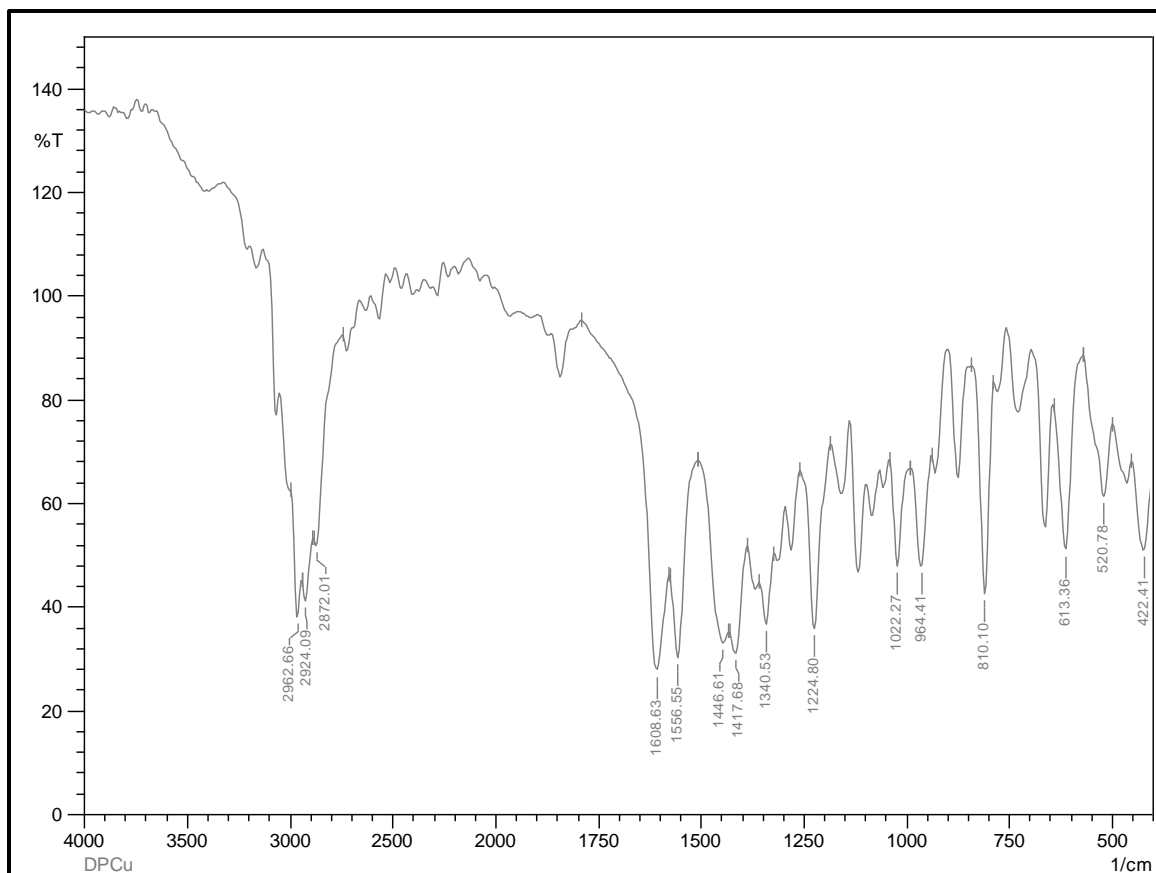
Figure. 3.13: FT-IR spectrum of DPCu(II) complex

3.4.4 Mass spectroscopy

The mass spectra of the DP ligand and its four mononuclear transition metal complexes are shown as **Figures. 3.14-3.18** and the data is compiled in the **Table 3.4**. The calculated molecular weights of the synthesized compounds are found to exactly match with the expected values.

Table 3.4: LC-MS Spectral data of DP ligand and its metal complexes

Comp. Name	Mol. Formula	Mol. Wt (Calcd)	Mol. Wt (Found)
DP ligand	$C_{25}H_{34}N_2O_2$	$M^+ = 394.55$	$M^{+1} = 395.3$
DPMn(III)	$C_{27}H_{35}N_2O_4$	$M^+ = 506.52$	$M^+ = 447.3$
DPCo(II)	$C_{25}H_{32}CoN_2O_2$	$M^+ = 451.47$	$M^+ = 451.4$
DPNi(II)	$C_{25}H_{32}N_2NiO_2$	$M^+ = 451.23$	$M^+ = 451.0$

DPCu(II)	$C_{25}H_{32}CuN_2O_2$	$M^+= 456.08$	$M^+ = 456.30$
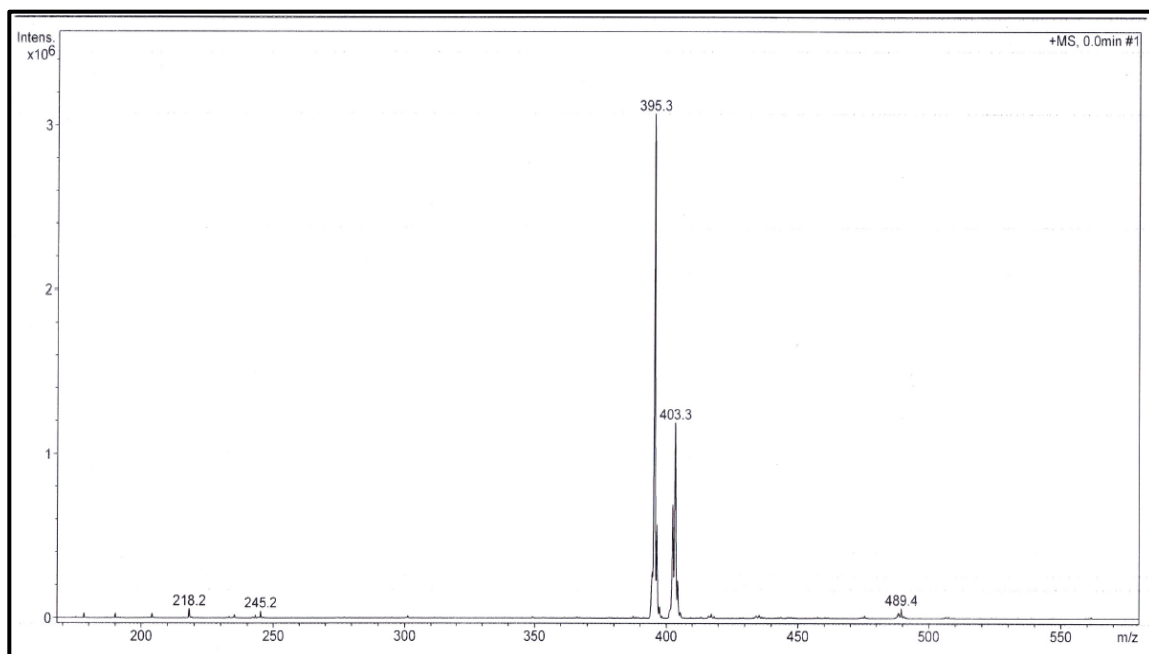
Figure 3.14: LC-MS spectrum of DP ligand
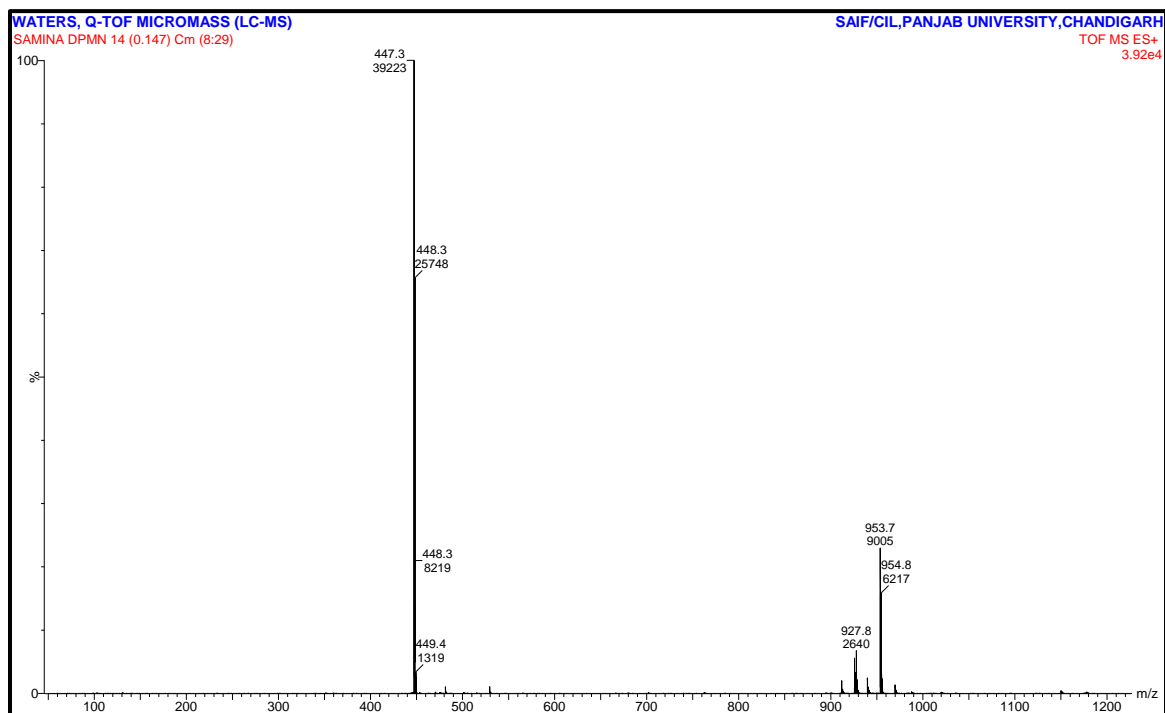
Figure 3.15: LC-MS spectrum of DPMn(III) complex
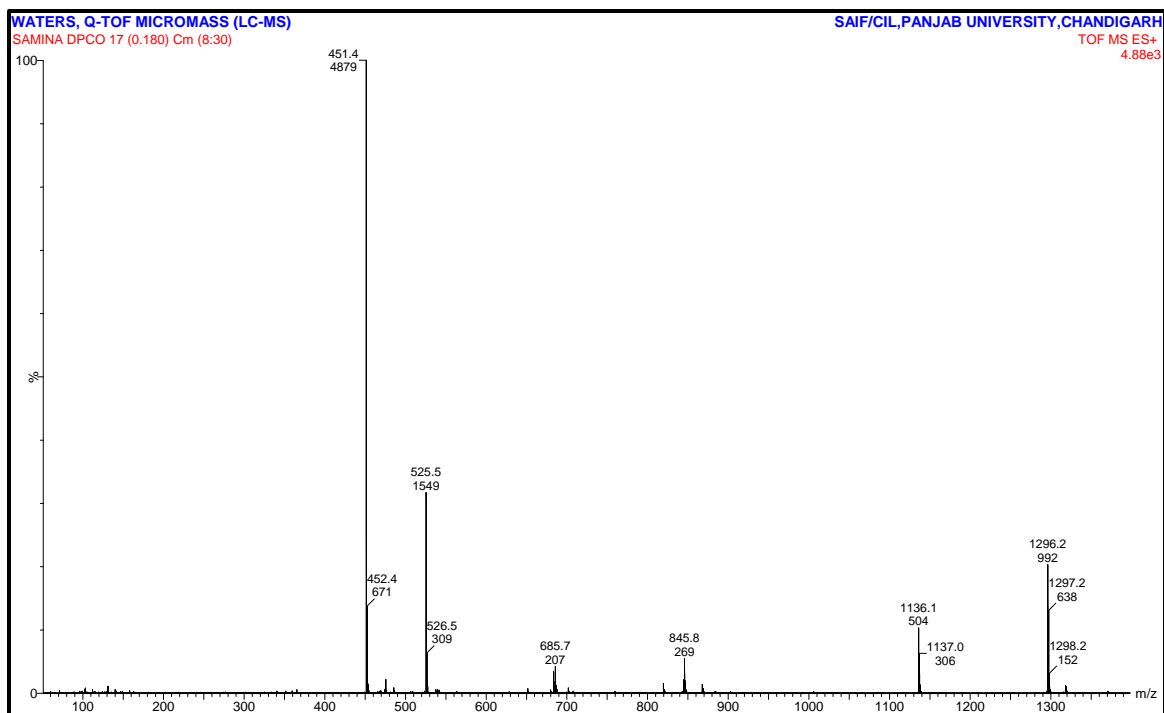
Figure 3.16: LC-MS spectrum of DPCo(II) complex
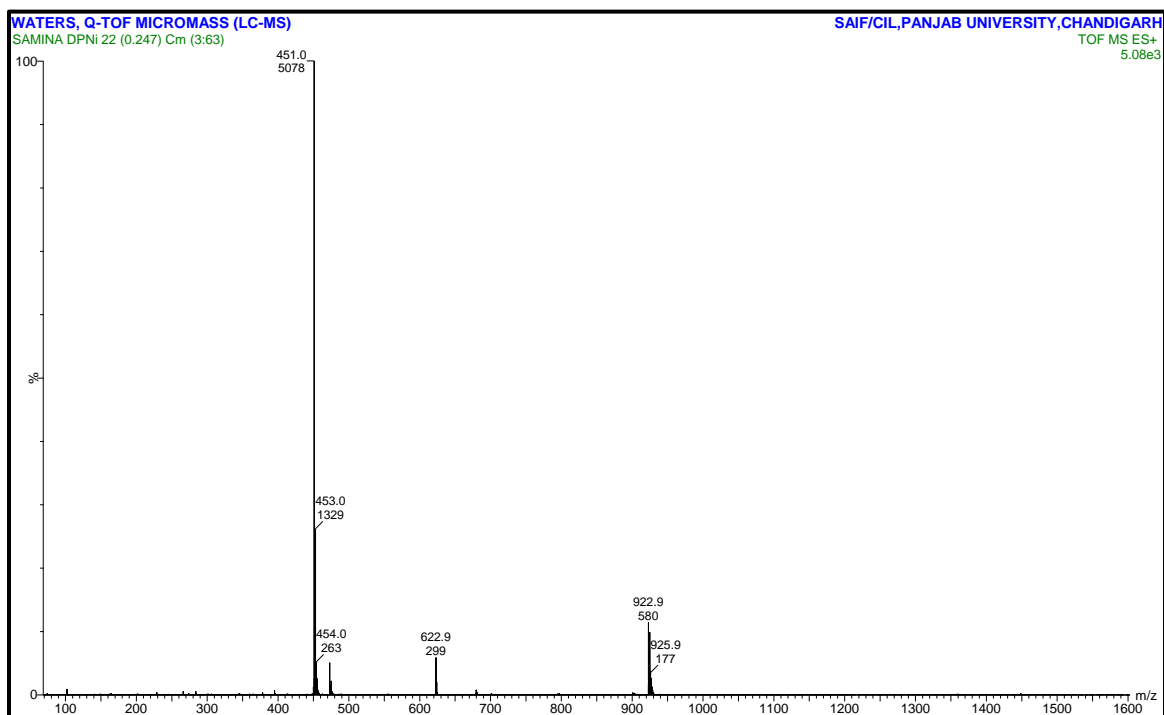
Figure 3.17: LC-MS spectrum of DPNi(II) complex
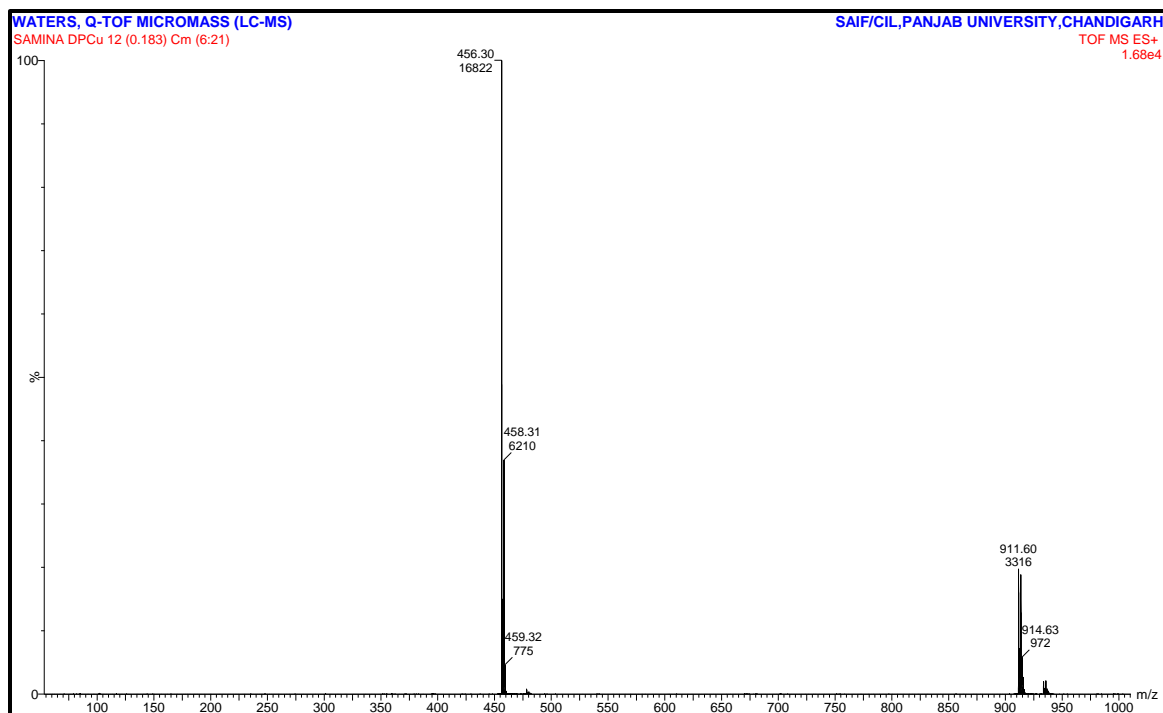
Figure 3.18: LC-MS spectrum of DPCu(II) complex

3.4.5 Elemental analysis

The elemental analyses of the 6,6'-((1E,1'E)-(propane-1,3-diylbis(azanylylidene))bis (methanylylidene)) bis(5-isopropyl-2-methylphenol) (DP) ligand and its four mononuclear transition metal complexes are given in the **Table 3.5**. The results are in good conformity with molecular formula, and confirm DPM(II) formula for Cobalt, Nickel and Copper complexes and [DPM(OAC)] for manganese(III) complex.

Table 3.5: Elemental analyses data of DP ligand its metal complexes (%):

Comp. Name	Molecular Formula	C (Cal) Found	H(Cal) Found	N(Cal) Found
DP ligand	$C_{25}H_{32}N_2O_2$	(76.10) 77.77	(8.69) 9.07	(7.10) 6.85
DPMn(III)	$C_{27}H_{35}MnN_2O_4$	(64.02) 64.98	(6.96) 6.00	(5.53) 5.51

DPCo(II)	$C_{25}H_{32}CoN_2O_2$	(66.51)	(7.14)	(6.20)
		68.06	6.57	5.90
DPNi(II)	$C_{25}H_{32}N_2NiO_2$	(66.54)	(7.14)	(6.21)
		64.35	6.94	6.10
DPCu(II)	$C_{25}H_{32}CuN_2O_2$	(65.84)	(7.07)	(6.14)
		68.04	7.20	6.43

3.4.6 Molar conductivity measurement

The molar conductivities Λ_M of the metal complexes as 10^{-3} Mol DMF solutions were found to be in the range 8-15 (Ω^{-1} cm^2 mol^{-1}). These low values **(Table 3.6)** pointout that all these complexes are non-electrolyte in nature due to the absence of any counter ions in their structures [24].

3.4.7 Magnetic susceptibility measurement

The manganese complex shows the magnetic moment 4.65 B.M. which is lower than expected value 5.92 B.M. of Mn(II) d^5 configuration which may be attributed to the oxidation to Mn(III). Formation of the DPMn(III) complex by coordination of acetate group is confirmed through the elemental analysis indicating [Mn^{III} DP(OAC)] formula of the complex. The DPCo(II) complex exhibited magnetic moment 3.48 B.M. indicating the square planar configuration [19-23, 25]. In general Ni(II) complexes are square planar and diamagnetic, while tetrahedral complexes have magnetic moment in the range 3.20- 4.10 B.M. [26]. In the present investigation DPNi(II) complex represented diamagnetic nature and represented square planar geometry around Ni(II) which is further confirmed from the crystal structure. The DPCu(II) complex has magnetic moment in the range 1.85 representing square planar geometry showing one unpaired electron [24, 27], which has been confirmed through single crystal structure of the DPCu(II) complex. The magnetic moment of the complexes as shown in the **Table 3.6.**

Table 3.6: Magnetic susceptibility and molar conductivity measurements of DP ligand and its four mononuclear transition metal complexes

Compunds	Magnetic susceptibility (μeff) (B. M.)	Molar conductivity (Ω^{-1} cm^2 mol, RT)
DP	---	---
DPMn(III)	4.65	9.60
DPCo(II)	3.48	11.68
DPNi(II)	Diamagnetic	12.72
DPCu(II)	1.85	12.67

3.4.8 ESR Spectroscopy

The X-band ESR spectrum of DPCu(II) complex at liquid nitrogen temperature (77 K) was recorded in DMF is represented in **Figure 3.19.** The ESR spectrum of the complex gives information about hyperfine and super hyperfine structures. The data is important in the study of the metal ion coordination in the complexes i.e., shape, the nature of the coordination sites of the ligand and the degree of covalency of the metal- ligand bond. From spectrum the observed values are $g\| = 2.2317$, $g\perp = 2.0472$ and $g = 2.0023$ which indicated that they follow the trend $g\| > g\perp > g$ indicating the square planar geometry [21] and also supporting that the unpaired electron lies in the $d_{x^2-y^2}$ orbital of the Cu(II) ion having $^2B_{1g}$ as ground state. The present EPR result shows that $g\|$ is less than 2.3 suggesting that the copper complex has covalent nature; it also shows $g_\|$ in the range 2.24-2.29, which is in conformity with the presence of mixed copper-nitrogen and copper-oxygen bonds in these chelates [28-31]. The empirical factor f = 135.23 is close to the range of 105-135 cm^{-1} for square planar complex [32, 33]. The geometric parameter G is a measure of the exchange interaction coupling constant by the expression $G = (g\|-2.0023)/(g\perp/2.0023)$ for axial spectra. If G > 4, exchange interaction is negligible and if G < 4, considerable exchange interaction is indicated in the solid complex. G value is 5.10 which is (in range 1.68-5.14) consistent with a $d_{x^2-y^2}$ ground state in square planar geometry [34, 35]. The value of in plane sigma banding parameter α^2 was estimated from following expression, α^2 = -(A\| / 0.036) + (g\| - 2.0023) +3/7(g⊥ - 2.0023) + 0.04

The value of $\alpha^2 = 0.5$, indicates complete covalent bonding, while the value of $\alpha^2 = 1.0$ suggests complete ionic bonding. The observed value of α^2 (0.77) is less than 1, which indicated that the complex has some covalent character in the ligand environment [36].
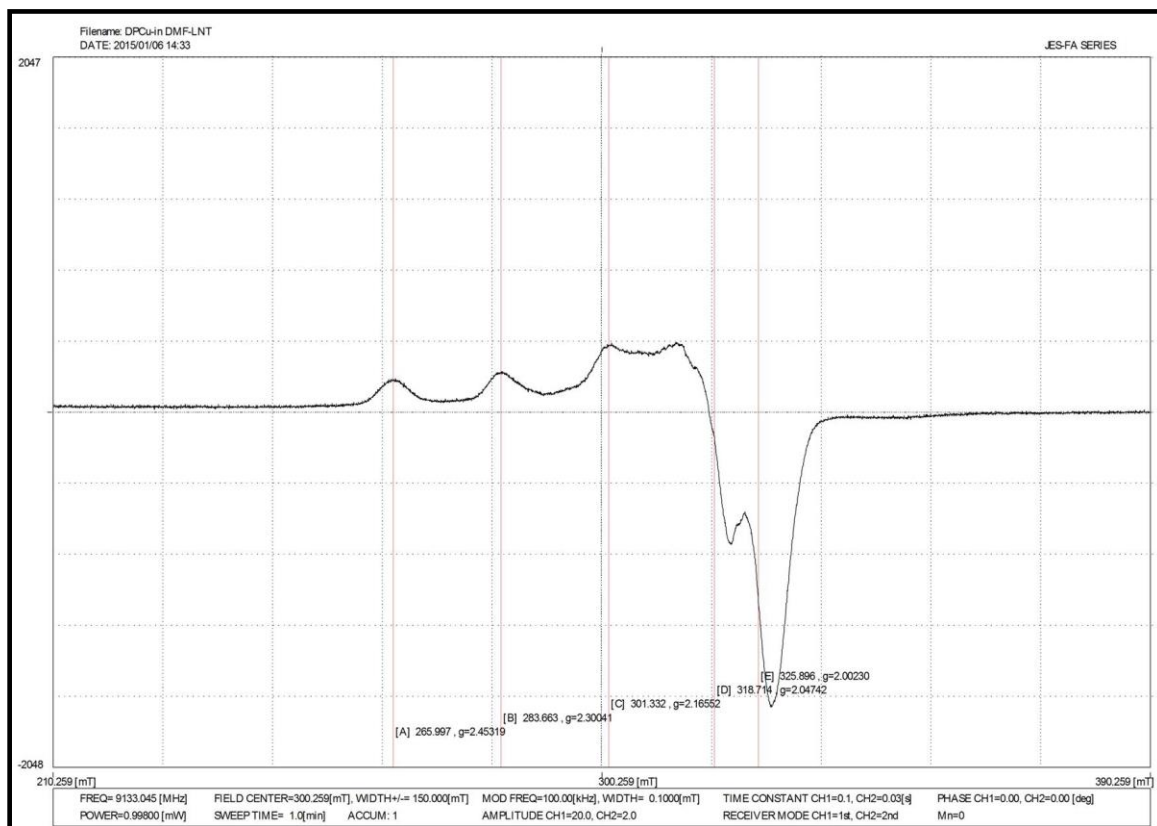
Figure 3.19: X-band ESR spectrum of DPCu(II) complex

3.4.9 SEM analysis

Scanning electron microscope has been used to evaluate morphology and particle size of the synthesized DPMn(III), DPNi(II) and DPCu(II) schiff base metal complexes and the SEM photographs are shown in **Figures 3.20- 3.22**.From SEM images we noted that there is a uniform matrix of the synthesized complexes, which leads to dealing with homogeneous phase material. All the complexes are having particles take agglomerisation and average grain size is found in between 50 nm to 10 μm with different morphology. Single phase formation of DPMn(III), DPNi(II) and DPCu(II) complexes having morphologies with particle size 1 μm to 10 μm.
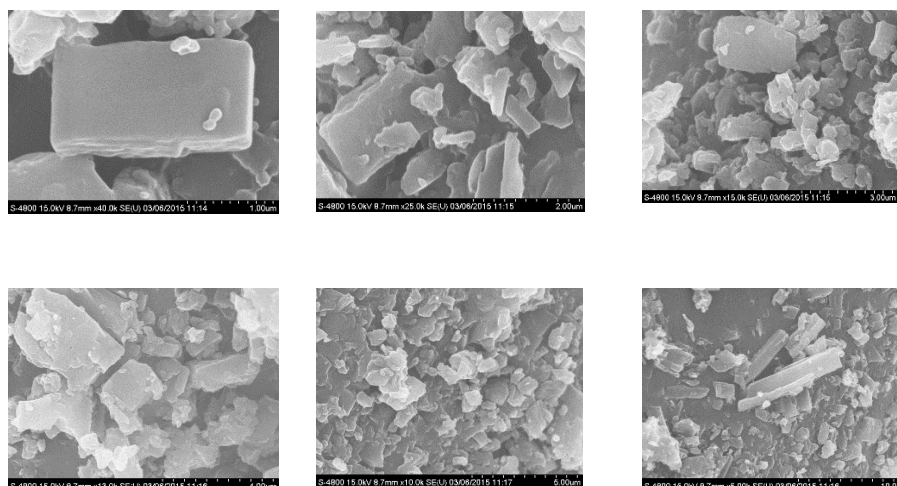
Figure 3.20(a): FE-SEM images of DPMn(III) complex at different magnifications
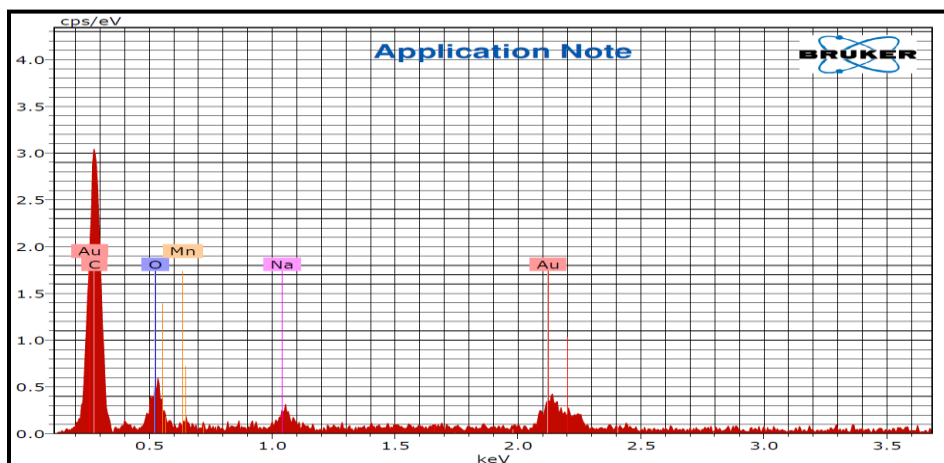
El	AN	Series	unn. C [wt.%]	norm. C [wt.%]	Atom. C [at.%]	Error (1 Sigma) [wt.%]
C	6	K-series	24.19	62.78	79.69	4.32
O	8	K-series	6.43	16.68	15.90	1.89
Na	11	K-series	1.02	2.64	1.75	0.15
Mn	25	K-series	2.46	6.39	1.77	0.21
Au	79	M-series	4.43	11.50	0.89	0.30
		Total:	38.53	100.00	100.00	

Figure 3.20(b): EDX analysis of DPMn(III) complex
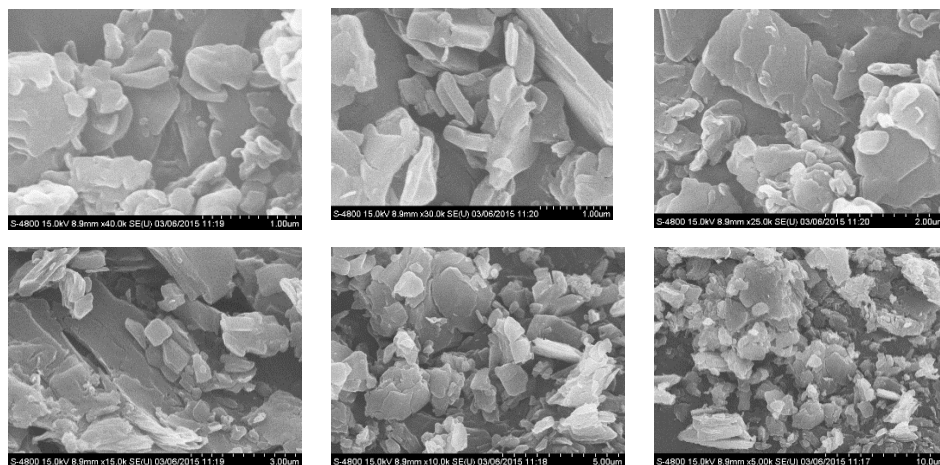
Figure 3.21(a): FE-SEM images of DPNi(II) complex at different magnifications

El	AN	Series	unn. C [wt.%]	norm. C [wt.%]	Atom. C [at.%]	Error (1 Sigma) [wt.%]
C	6	K-series	31.67	69.77	86.82	5.14
O	8	K-series	5.23	11.52	10.76	1.60
Ni	28	K-series	2.53	5.57	1.42	0.22
Au	79	M-series	5.96	13.13	1.00	0.39
		Total:	45.39	100.00	100.00	
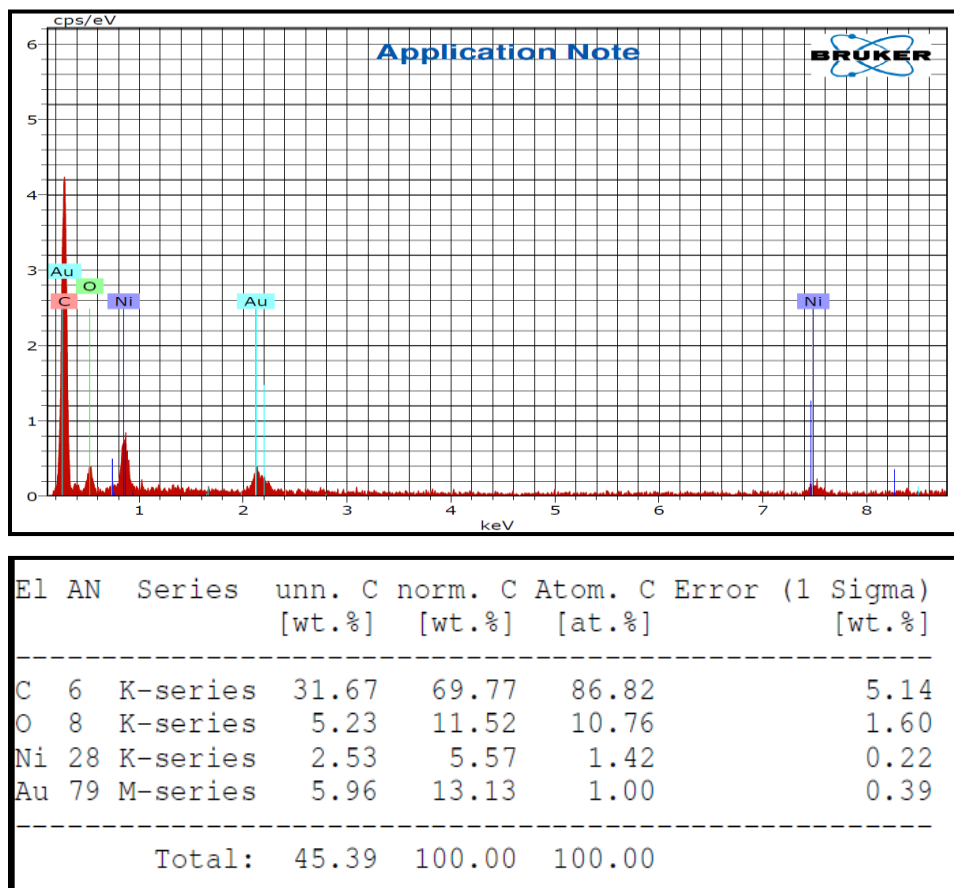
Figure 3.21(b): EDX analysis of DPNi(II) complex
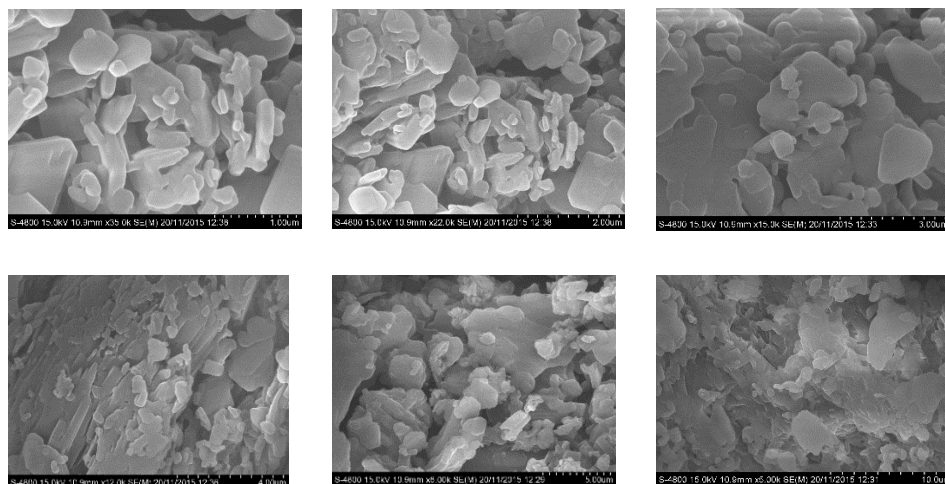
Figure 3.22(a): FE-SEM images of DPCu(II) complex at different magnifications


```
El AN   Series   unn. C norm. C Atom. C Error (1 Sigma)
                 [wt.%]  [wt.%]  [at.%]          [wt.%]
-------------------------------------------------------
C   6  K-series  44.11   61.28   78.69            6.44
N   7  K-series   5.86    8.14    8.97            2.13
O   8  K-series   5.62    7.81    7.53            1.52
Cu 29  K-series  13.28   18.45    4.48            0.73
Au 79  M-series   3.10    4.31    0.34            0.19
-------------------------------------------------------
         Total:  71.98  100.00  100.00
```
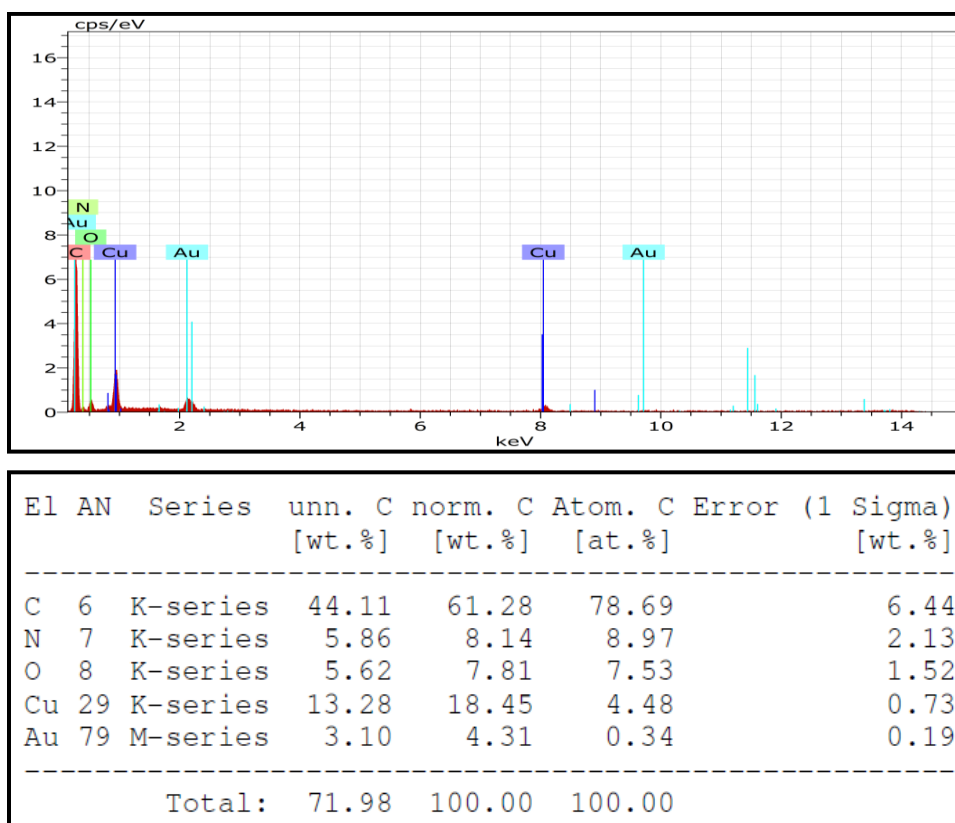
Figure 3.22(b): EDX analysis of DPCu(II) complex

3.4.10 Thermogravimetric Analysis

Thermogravimetric analyses are very useful for investigating the thermal decomposition of solid substances involving simple metal salts as well as complex compounds [37]. Thermogravimetric analyses also give information about the presence of water molecules inside or outside the inner coordination sphere of the central metal ion [38]. Thermogravimetric studies were performed for DPMn(III), DPCo(II), DPNi(II) and DPCu(II) complexes, and the thermograms are shown in **Figures 3.23- 3.26**. The DPMn(III) complex showed decomposition in two stages, the first shows the decomposition of uncoordinated water molecule below 100 $^{\circ}$C, and second decomposition of ligand with acetate group from 498 $^{\circ}$C resulting in formation of manganese oxide. In case of DPCo(II), DPNi(II) and DPCu(II) complexes thermograms showed only major single decomposition for the loss of ligand moiety and formation of corresponding oxides above 600 $^{\circ}$C [39].
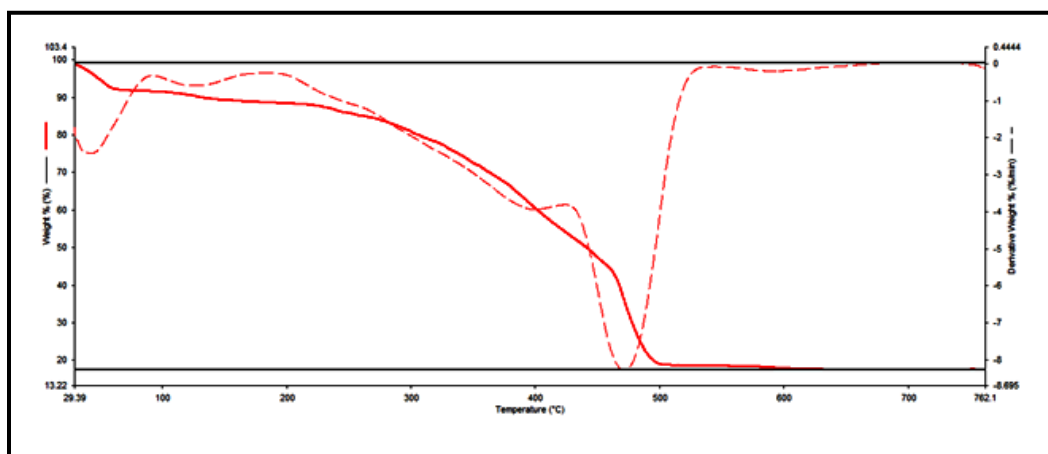
Figure.3. 23: TGA curve of DPMn(III) complex
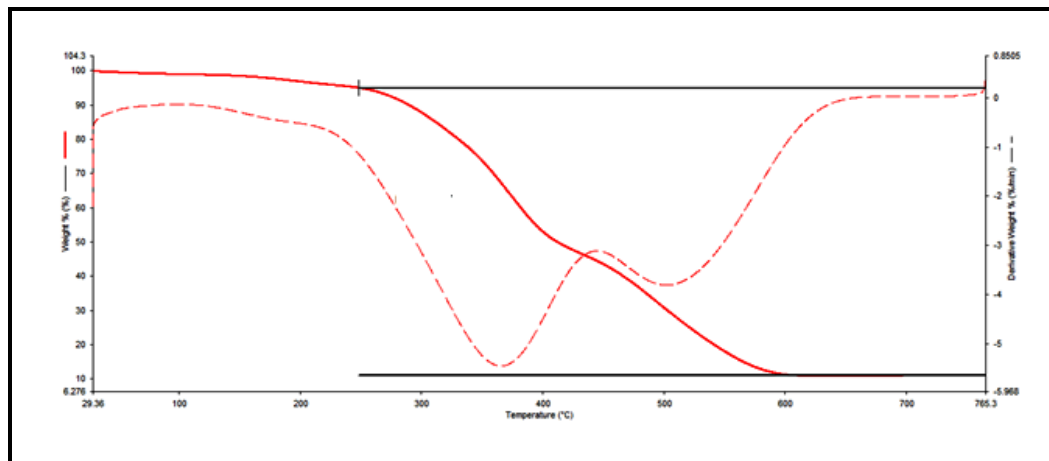
Figure 3.24: TGA curve of DPCo(II) complex
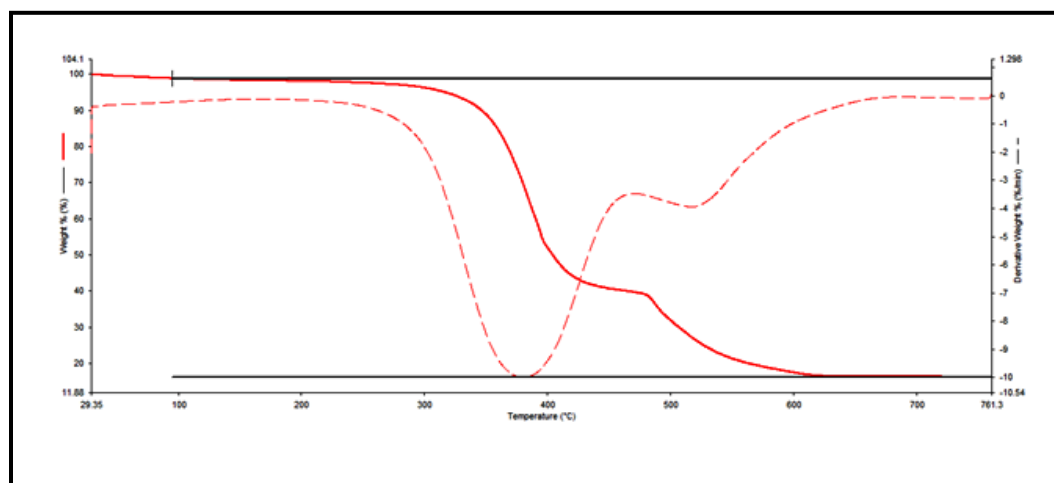
Figure 3.25: TGA curve of DPNi(II) complex
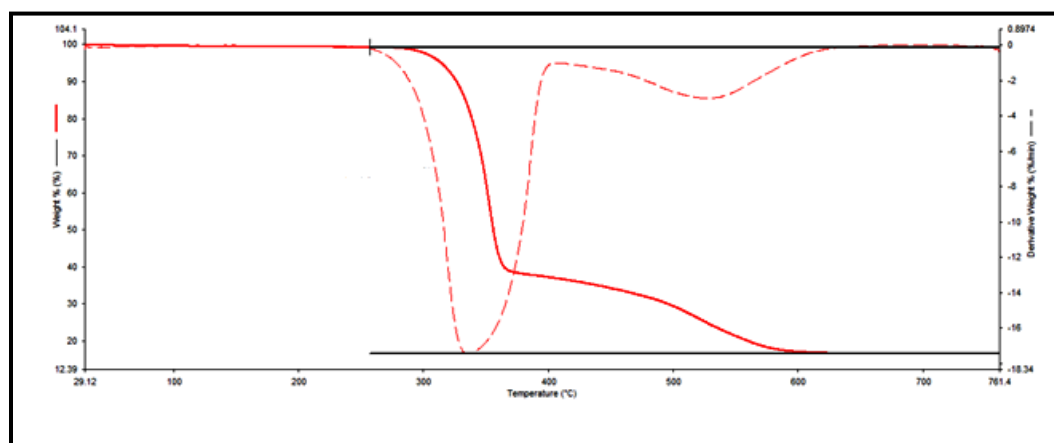
Figure 3.26: TGA curve of DPCu(II) complex

3.4.11 Electrochemical properties

The electrochemical behavior of ligand and metal complexes was examined in DMF and TBAP as supporting electrolyte. **Figure 3.27** shows the electrochemical cyclic voltammograms of curves of ligand, DPMn(III), DPCo(II), DPNi(II) and DPCu(II) complexes in DMF at the 10^{-3} M concentration of complexes in DMF containing 0.1 M tetrabutyl ammonium perchlorate (TBAP) as electrolyte with Ag/AgCl as reference electrode at scan rate 100 mVs^{-1}. The electrochemical data is summarized in **Table 3.7.**
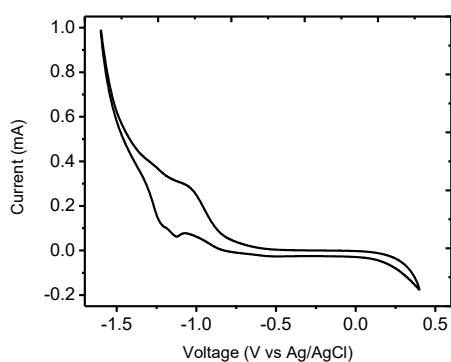
(a) DP ligand
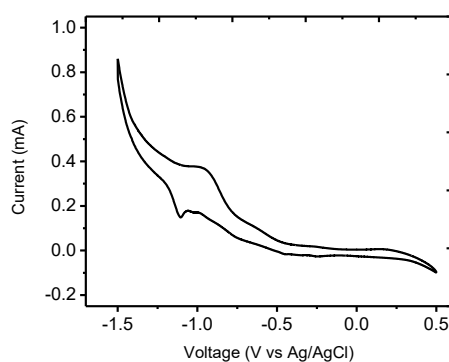
(b) DPMn(III)
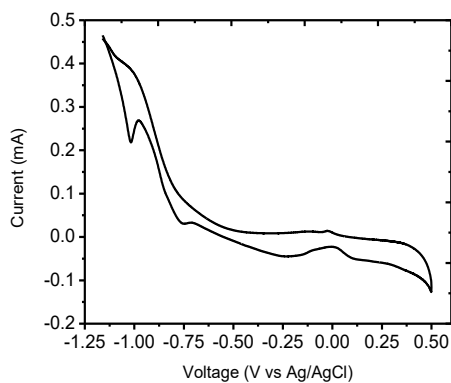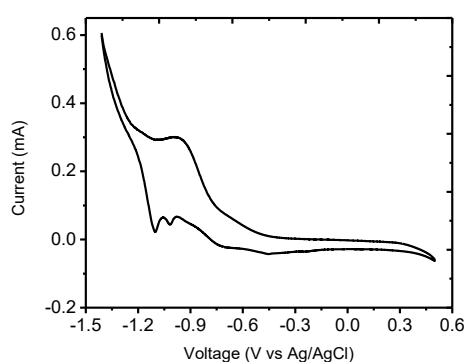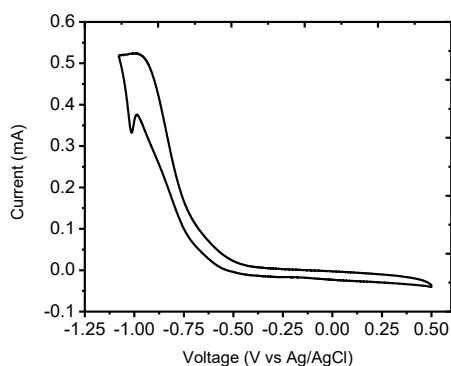
(c) DPCo(II)

(d) DPNi(II)

(e) DPCu(II)

Figure 3.27 Cyclic voltammograms of (a) DP ligand; (b) DPMn(III); (c) DPCo(II); (d) DPNi(II); and (e) DPCu(II) complexes at room temperature in DMF solution containing 0.1 M TBAP as electrolyte at scan rate of 100 mVs⁻¹.

Table 3.7 Electrochemical cyclic voltammetry data of metal complexes in DMF solution.

Compounds	Epa (II→I) (V)	Epc (I→II) (V)	ΔE (V)
DPMn(III)	-1.200	-0.944	0.256
DPCo(II)	-1.030	-0.956	0.074
DPNi(II)	-1.116	-0.929	0.187
DPCu(II)	-1.019	-0.971	0.048

In case of the DP ligand, a cyclic sweep in the range -1.5 to +0.50 V shows a cathodic peak at -1.03 V and an anodic peak at -1.146 V. Electrochemical properties of manganese complex show the one-electron reduction peak (Epc), corresponding to the Mn (III/II) occurs at –0.944 V and during the reverse scan the reoxidation peak (Epa) is observed at -1.200 V. The electrochemical data of DPCo(II) and DPNi(II) complexes have similar reduction peaks (Epc) in the potential range given in **Table 3.7**, attributed to the Co (II/I) and Ni (II/I), the sweep potential shows the reoxidation peak (Epa) for both complexes the potential value -1.030 V and -1.116 V respectively while the copper complex shows the

one-electron reduction peak (Epc) corresponding to the Cu (II/I), at -0.971 V and in the reverse scan the reoxidation peak (Epa) is observed at -1.019 V [40].

3.4.12 Single crystal X-ray crystallography studies

Single crystals suitable for X-ray analysis of DPNi(II) complex were obtained by the slow evaporation of the ethanolic solution of the DPNi(II) complex at room temperature. A dark green-coloured crystal of suitable size $0.400 \times 0.200 \times 0.100$ mm^3 was mounted on a Bruker axs kappa apex2 CCD Diffractometer equipped with Mo-Ka radiation at the wavelength 0.71073 Å. The cell refinement and data reduction were performed by using an APEX2/SAINT (Bruker 2004) and a SAINT/XPREP (Bruker 2004), respectively [41]. The multi-scan absorption corrections were applied to the data using the SADABS (Bruker) program [42]. The structure was solved by using SIR92 [43] and the structure was refined by full-matrix least squares refinement on F2. The molecular structure, Packing diagrams and hydrogen bonding were generated by using ORTEP 3.0 software [44, 45].

Crystals suitable for X-ray analysis of DPCu(II) complex were obtained by slow evaporation of a chloroform–ethanol (1:1 v/v) at room temperature. A suitable crystal size $0.26 \times 0.25 \times 0.24$ mm^3 was selected on a Xcalibur, Eos, Nova diffractometer. The crystal was kept at 298 K during data collection. Using Olex2 [46], the structure was solved with the ShelXT [47] structure solution program using Direct Methods and refined with the ShelXT [48] refinement package using Least Squares minimization. The pertinent details of the crystallographic parameters, data collection and refinement for both the DPNi(II) and DPCu(II) complexes are given in **Table 3.8**. Additional details regarding the data collections, structure solution and refinement are included in the supporting data. The CCDC No. for DPNi(II) complex is **1451939** and for the DPCu(II) complex is **1443333**. The ORTEP diagram and molecular packing diagrams of DPNi(II) complex are shown in the **Figures 3.28** and **3.29** respectively. The crystal structure and molecular packing diagram of DPCu(II) complex are presented in **Figures. 3.30** & **3.31** respectively. The presented structures illustrate that DPNi(II) and DPCu(II) complexes are formed by the deprotonation of a symmetrical tetradentate ligand. The crystal structures indicate that two nitrogen and two oxygen atoms are coordinated to the central metal ion. Both the complexes show a square planar structure. The Cu–O and Cu–N distances are in the ranges

of 1.87–1.91 and 1.92–1.95 Å reported for Cu–O and Cu–N distances, respectively, and normally observed in N_2O_2 donor square-planar Cu(II) complexes [49-51]. Similarly, the Ni–O and Ni–N distances are within the limit ranges of 1.83–1.87 and 1.83–1.89 Å for Ni–O and Ni–N distances reported for N_2O_2 square-planar Ni(II) complexes [52, 53] Selected bond lengths and bond angles for the DPNi(II) and DPCu(II) crystal structures are listed in **Table 3.9.**

Table 3.8: Crystallographic parameters, data collection and refinement for DPNi(II) and DPCu(II) complexes.

Compound	DPNi(II)	DPCu(II)
Empirical formula	$C_{25}H_{32}N_2NiO_2$	$C_{50}H_{62}Cu_2N_4O_4$
Formula weight	451.23	912.13
Temperature	296(2) K	298 K
Crystal system	Triclinic	Triclinic
Space group	P-1	P-1
a/Å	11.9382(12)	11.8984(6)
b/Å	12.5436(11)	12.6574(5)
c/Å	16.1220(18)	16.2719(8)
α/°	81.889(6)	81.947(4)
β/°	75.740(6)	75.567(4)
γ/°	89.998(6)	89.970(3)
Volume/Å^3	2314.9(4)	2348.34(19)
Z	4	2
Density	1.295 Mg/m^3	1.290 g/cm^3
Absorption coefficient/mm^{-1}	0.861	0.952
F(000)	960.0	964.0
Crystal size/mm^3	$0.400 \times 0.200 \times 0.100$	$0.26 \times 0.25 \times 0.24$
Radiation		MoKα ($\lambda = 0.71073$)
2Θ range for data collection/°	1.949 to 24.999	4.862 to 49.998

Index ranges	-13<=h<=14, -14<=k<=14, -19<=1<=19	-11 ≤ h ≤ 14, -13 ≤ k ≤ 15, -15 ≤ l ≤ 19
Reflections collected	35956	17083
Independent reflections	7723[R(int) = 0.0815]	8251 [R_{int} = 0.0538, R_{sigma} = 0.0611]
Data/restraints/parameters	7723/85/583	8251/0/553
Goodness-of-fit on F^2	1.040	1.101
Final R indexes [I>=2σ (I)]	R_1 = 0.0572, wR_2 = 0.1236	R_1 = 0.0531, wR_2 = 0.1442
Final R indexes [all data]	R_1 = 0.1349, wR_2 = 0.1764	R_1 = 0.0671, wR_2 = 0.1604
Largest diff. peak/hole / e Å^{-3}	0.760 and -0.653	0.72/-0.57
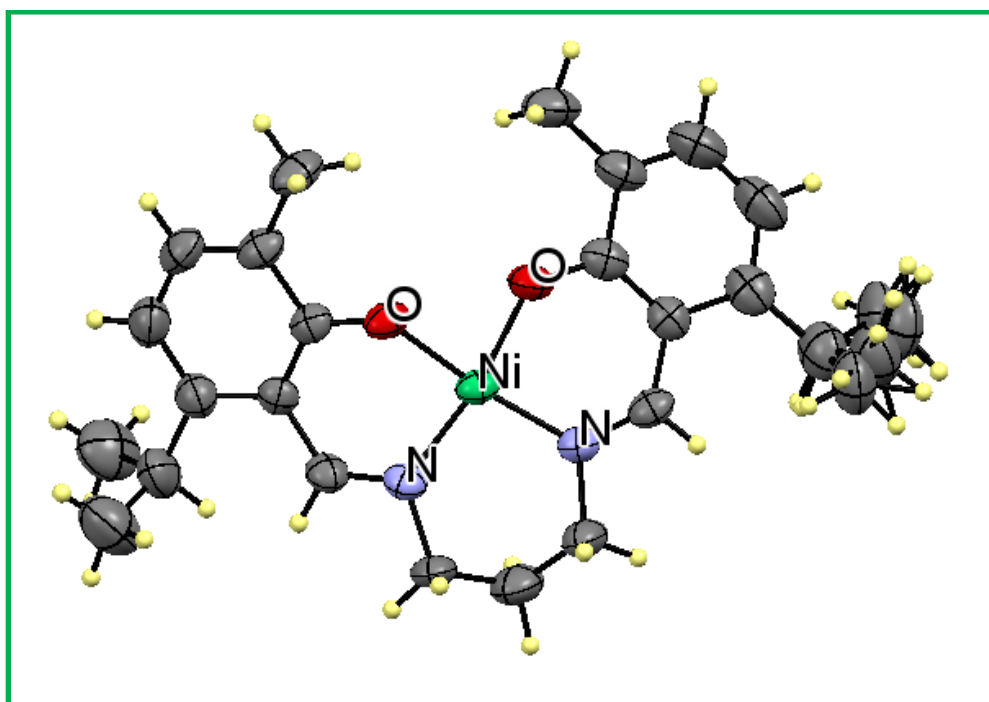
Figure 3.28: ORTEP diagram of DPNi(II) complex with atomic labeling

The CCDC No. for DPNi(II) complex= 1451939
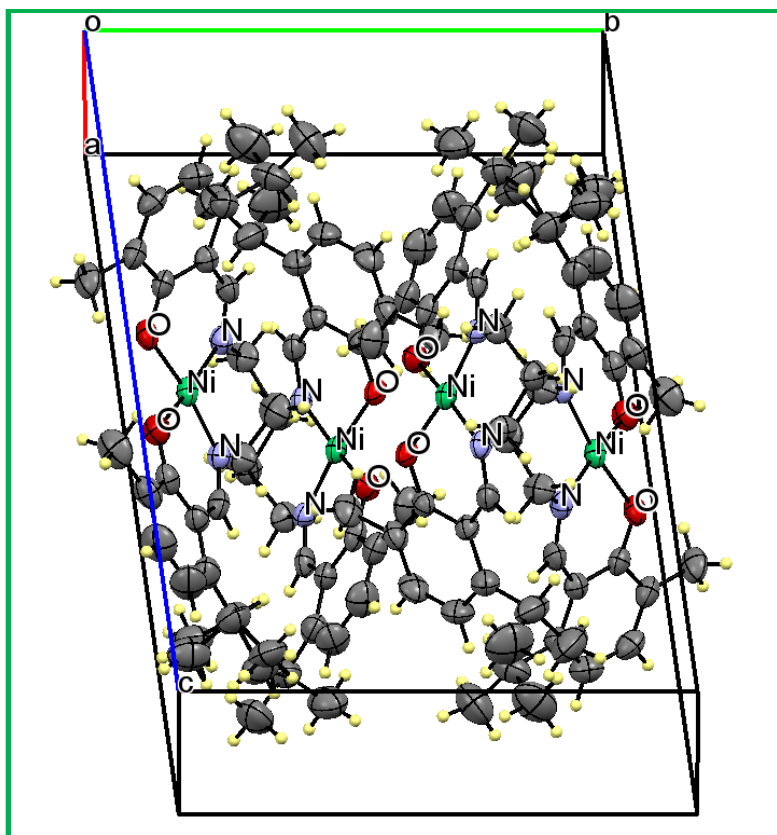
Figure 3.29: The molecular packing diagram of DPNi(II) complex along a axis
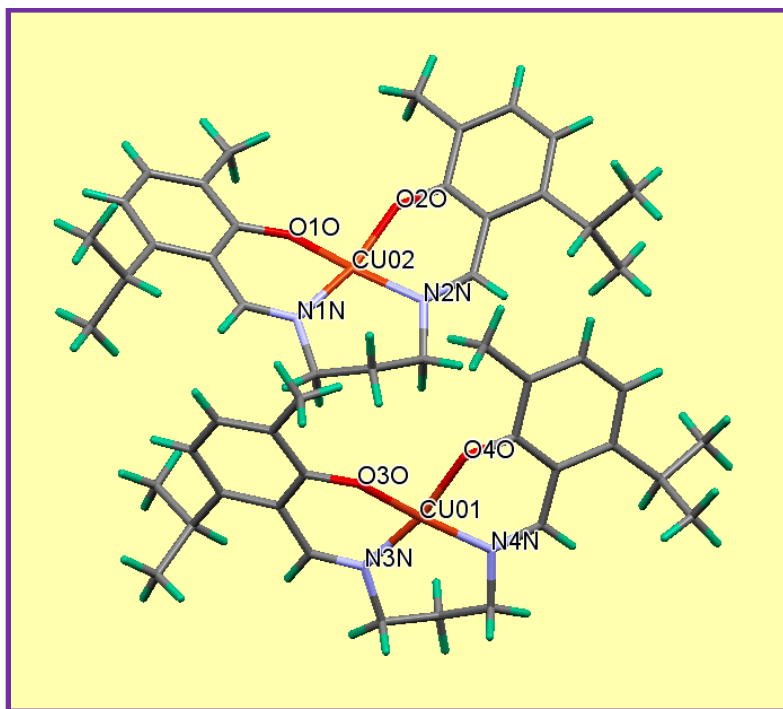
Figure 3.30: Crystal structure diagram of DPCu(II) complex

The CCDC No. for DPCu(II) complex= 1443333.
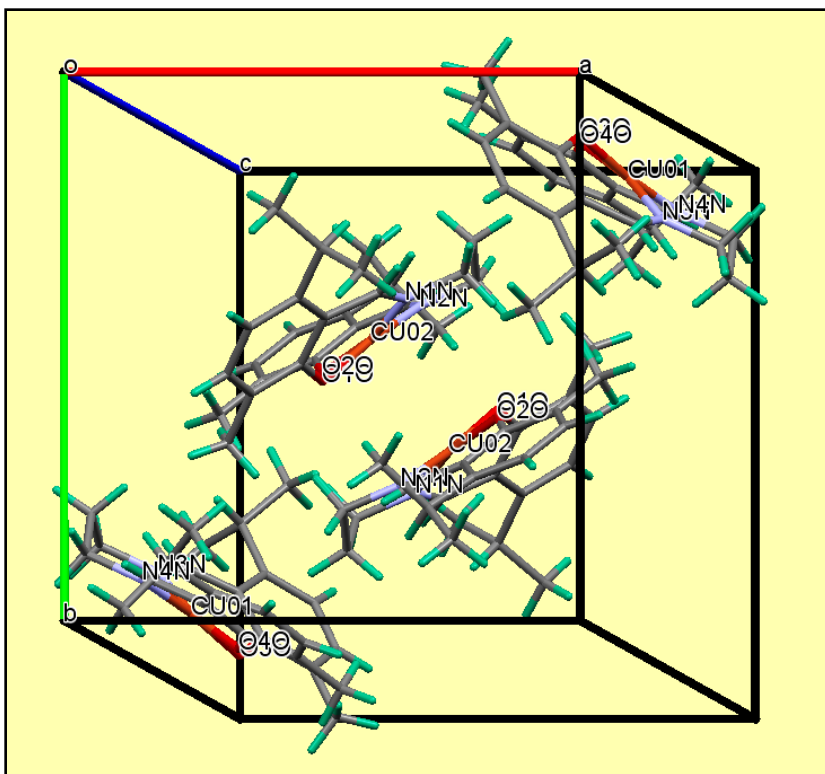
Figure 3.31: The molecular packing diagram of DPCu(II) complex

Table 3.9: Selected bond lengths/(Å) and bond angles/(°) for DPNi(II) and DPCu(II) complexes

Bond lengths/(Å)			
Ni1-N1	1.878(5)	Cu01-O3O	1.905(2)
Ni1-N2	1.872(5)	Cu01-O4O	1.896(2)
Ni1-O1	1.843(4)	Cu01-N3N	1.969(3)
Ni1-O2	1.822(4)	Cu01-N4N	1.967(3)

Bond Angles/(°)			
O1-Ni-N2	90.19(19)	O3O-Cu01-N3N	88.93(10)
O1-Ni-N1	172.09(18)	O3O-Cu01-N4N	172.01(10)
O2-Ni-N2	168.5(2)	O4O-Cu01-O3O	83.47(10)
O2-Ni-O1	81.64(18)	O4O-Cu01-N3N	168.15(11)
O2-Ni-N1	92.6(2)	O4O-Cu01-N4N	90.27(11)
N2-Ni-N1	96.3(2)	N4N-Cu01-N3N	98.02(11)

3.5 Biological activities

3.5.1 Protocol for antibacterial activity

Protocol for antibacterial activity are same as described in chapter 2 and section 2.5.1

3.5.2 . Results of antibacterial activity

The ligand DP and their four mononuclear metal complexes are subjected to *in vitro* antibacterial activity on the selected species such as *Bacillus subtilis*, *Pseudomonas aeruginosa* and *Staphylococcus aureus* by using Ciprofloxacin, Ampicillin and Streptomycin as standards for the comparison. The results of the antibacterial activity are presented in **Table 3.10** and graphical represented in **Figure 3.32**.

Table 3.10: Representation of Antibacterial activity of DP ligand and its metal complexes

Compounds Name	(MIC μg/ml)		
	B. subtilis	*P. aeruginosa*	*S. aureus*
DP ligand	130	117.5	127
DPMn(III)	220	206	246
DPCo(II)	136	195	210
DPNi(II)	55	49	42
DPCu(II)	275	255	294
Ciprofloxacin	50	25	50

Ampicillin	250	100	250
Streptomycin	25	12.5	25
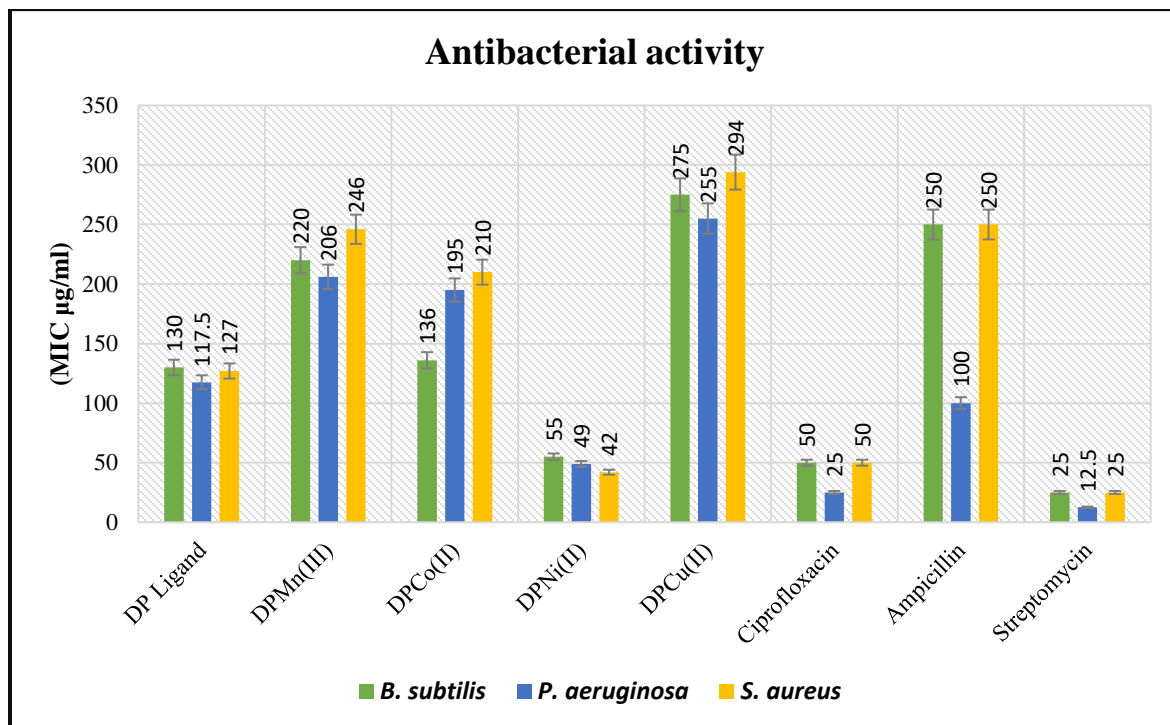
Figure 3.32: Graphical representation of antibacterial activity

The schiff base exhibits the better activity as campared to ampicillin drug. DPMn(III) and DPCo(II) complexes possesses better activity against the *Bacillus subtilis* and *Staphylococcus aureus* as campared to ampicillin standard drug. The DPNi(II)complex shows the superior antibacterial activity against all the bacterial strains *Bacillus subtilis*, *Pseudomonas aeruginosa* and *Staphylococcus aureus* as compared to Ciprofloxacin and Ampicillin standard drugs. DPCu(II)complex shows the moderate to poor activity against all the bacterial strains as compared to all the standards. The increased activity of the metal chelates can be explained by Overtone's concept and Tweedy's theory [54, 55].

3.5.3 Protocol for antifungal activity

Protocol for antifungal activity are same as described in **chapter 2 and section 2.5.3**

3.5.4 Results of antifungal activity

The antifungal activity was evaluated against different fungal strains such as *Candida albicans, Fusarium oxysporum*, *Aspergillus flavus* and *Aspergillus niger* using Miconazole and Fluconazole as standard drugs and results are presented in **Table 3.11**.

Table 3.11: Representation of antifungal activity of DP ligand and its mononuclear transition metal complexes

Compounds	(MIC µg/ml)			
	C. albicans	*F. oxysporum*	*A. flavus*	*A. niger*
DP Ligand	*	*	*	*
DPMn(III)	*	*	*	*
DPCo(II)	*	*	*	*
DPNi(II)	*	*	*	*
DPCu(II)	*	*	*	*
Miconazole	25	25	12.5	12.5
Fluconazole	5	5	5	10

* No activity reported upto 300 µM
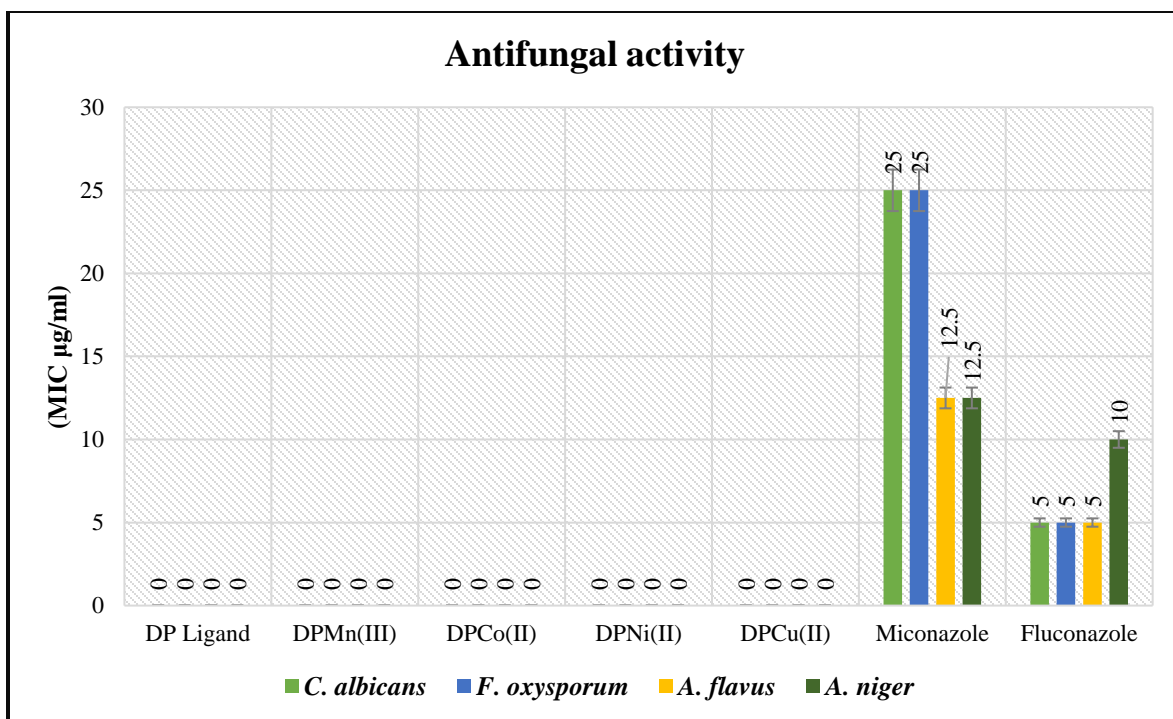
Figure 3.33: Graphical representation of antifungal activity

The antifungal activity of DP ligand and its four mononuclear transition metal complexes doesn't show fungal activity. The graphical representation of antifungal activity are shown in **Figure 3.33**.

3.5.5 Protocol for antioxidant activity (DPPH radical scavenging activity)

Protocol for antioxidant activity are same as described in Chapter 2, section 2.5.5

3.5.6 Results of antioxidant activity

All the title compounds are also subjected to antioxidant activity and the results are compared with the standard drugs, butylated hydroxyl toluene (BHT), ascorbic acid and α-Tocopherol. The results of the antioxidant activity are summarized in **Table 3.12** and presented in **Figure 3.33**. The results indicated that free ligand showed moderate activity, however upon complexation with metal ions the activity were found to vary from better to poor results significantly. The DPCo(II) complex shows the good antioxidant activity as compared to the butylated hydroxyl toluene (BHT) standard drug.

Table 3.12: Representation Antioxidant activity of DP ligand and its mononuclear transition metal complexes

Compounds	IC_{50}
DP	25.08
DPMn	77.16
DPCo	18.91
DPNi	86.33
DPCu	34.16
BHT	16.50
Ascorbic acid	12.80
α- Tocopherol	12.20
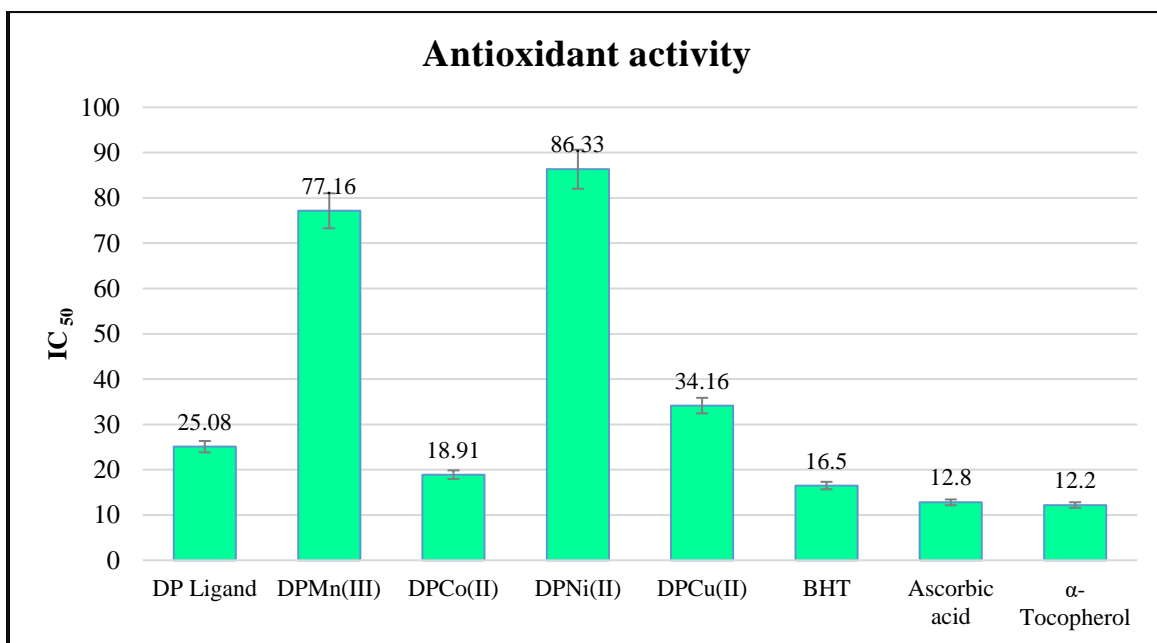
Figure 3.34: Graphical representation of antioxidant activity

3.5.7 DNA cleavage experiment

DNA cleavage experiment are same as described in chapter 2, section 2.5.7

3.5.8 Results of DNA cleavage activity

The DNA cleavage ability of the DP ligand and its DPMn(III), DPCo(II), DPNi(II) and DPCu(II) complexes were monitored by gel electrophoresis in presence of H_2O_2 as an oxidant at different concentrations **(Figures 3.34- 3.38)**. The DP ligand and its metal complexes except DPCo(II) (Lane 1) do not show any apparent cleavage comparable to control. From **Figure 3.36** it is illustrated that at higher concentration (200 µM) DPCo(II) complex has ability to cleave pBR322 DNA in to the linear form (form III) that migrates between form I and form II is generated.
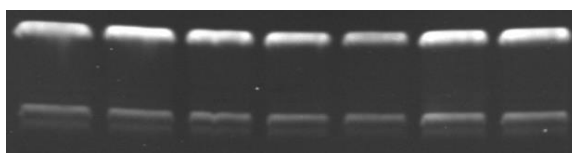
Figure 3.35: From left to right agarose gel electrophoretic pattern of pBR322 DNA induced by DP ligand and H_2O_2. Lane 1-DNA+ H_2O_2 alone; Lane 2- DNA + 10 µM sample + H_2O_2; Lane 3-DNA + 20 µM sample + H_2O_2; Lane 4-DNA + 50 µM sample + H_2O_2; Lane 5-DNA + 100 µM sample + H_2O_2; Lane 6-DNA+ 150 µM sample + H_2O_2; Lane 7-DNA + 200 µM sample + H_2O_2.·

Figure 3.36: From left to right agarose gel electrophoretic pattern of pBR322 DNA induced by DPMn(III) complex and H_2O_2. Lane 1-DNA+ H_2O_2 alone; Lane 2- DNA + 10 µM sample + H_2O_2; Lane 3-DNA + 20 µM sample + H_2O_2; Lane 4-DNA + 50 µM sample + H_2O_2; Lane 5-DNA + 100 µM sample + H_2O_2; Lane 6-DNA+ 150 µM sample + H_2O_2; Lane 7-DNA + 200 µM sample + H_2O_2.
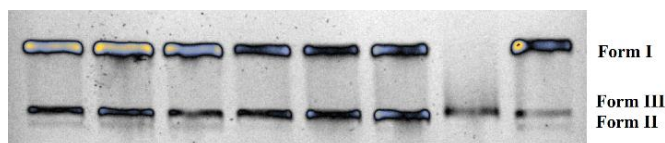
Figure 3.37: From left to right agarose gel electrophoretic pattern of pBR322 DNA induced by DPCo(II) complex and H₂O₂. Lane 1-DNA+ H₂O₂ alone; Lane 2- DNA + 10 µM sample + H₂O₂; Lane 3-DNA + 20 µM sample + H₂O₂; Lane 4-DNA + 50 µM sample + H₂O₂; Lane 5-DNA + 100 µM sample + H₂O₂; Lane 6-DNA+ 150 µM sample + H₂O₂; Lane 7-DNA + 200 µM sample + H₂O₂.
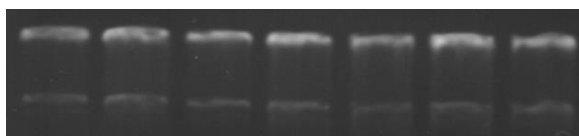
Figure 3.38: From left to right agarose gel electrophoretic pattern of pBR322 DNA induced by DPNi(II) complex and H₂O₂. Lane 1-DNA+ H₂O₂ alone; Lane 2- DNA + 10 µM sample + H₂O₂; Lane 3-DNA + 20 µM sample + H₂O₂; Lane 4-DNA + 50 µM sample + H₂O₂; Lane 5-DNA + 100 µM sample + H₂O₂; Lane 6-DNA+ 150 µM sample + H₂O₂; Lane 7-DNA + 200 µM sample + H₂O₂.
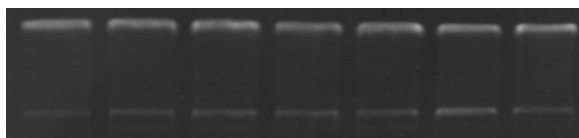
Figure 3.39: From left to right agarose gel electrophoretic pattern of pBR322 DNA induced by DPCu(II) complex and H₂O₂. Lane 1-DNA+ H₂O₂ alone; Lane 2- DNA + 10 µM sample + H₂O₂; Lane 3-DNA + 20 µM sample + H₂O₂; Lane 4-DNA + 50 µM sample + H₂O₂; Lane 5-DNA + 100 µM sample + H₂O₂; Lane 6-DNA+ 150 µM sample + H₂O₂; Lane 7-DNA + 200 µM sample + H₂O₂.

3.6 Conclusion

In this investigation, we are reporting the synthesis and characterization of a symmetrical salen-based schiff base DP ligand and the DPMn(III), DPCo(II), DPNi(II) and DPCu(II) complexes. The single crystal structures of DPNi(II) and DPCu(II) have been solved by X-ray crystallography which indicated square planar geometry around the metal centers. The ligand and metal complexes were screened for their biological activities such as in vitro antibacterial, antifungal anti-oxidant and DNA cleavage activities. The results indicated that the DPNi(II) complex has the superior antibacterial activity against all the bacterial

strains *Bacillus subtilis*, *Pseudomonas aeruginosa* and *Staphylococcus aureus* as compared to standard ampicilin. The complexes DPCo(II) and DPMn(II) exhibited the higher antibacterial activity against *Bacillus subtilis* and *Staphylococcus aureus* as compared to the standard drug ampicillin, while the ligand presented better activity against *Bacillus subtilis*, *Pseudomonas aeruginosa* and *Staphylococcus aureus* as compared to ampicillin. All the compounds could not show antifungal activity against fungal strains *C. albicans*, *F. oxysporum*, *A. flavus* and *A. niger*. The DPCo(II) complex shows good anti-oxidant activity which is close to the standard drug BHT as well as pBR322 DNA cleavage activity using gel electrophoresis experiment in the presence of H_2O_2 as oxidant.

3.7 References

1. Djebbar SS, Benali BO, Deloume JP, Polyhedron, 16 (1997) 2175–2182.

2. He L, Gou S, Shi Q, Qian M, Duan C, J. Chem. Crystallogr, 29 (1999) 207–210.

3. Sobola A.O, Watkins GM, J. Chem. Pharm. Res, 5 (2013) 147–154.

4. Atwood DA, Harvey MJ, Chem. Rev, 101 (2001) 37–52.

5. Raman N, Thangaraja C, Johnsonraja S, Open Chem, 3 (2005) 537–555.

6. Liu J, Zhang B, Wu B, Zhang K, Hu S, Turk. J. Chem, 31 (2007) 623–629.

7. Akine S, Dong W, Nabeshima T, Inorg. Chem, 45 (2006) 4677–4684.

8. Patel SA, Sinha S, Mishra AN, Kamath BV, Ram RN, J. Mol. Catal. A Chem. 192 (2003) 53–61.

9. Salehi M, Kubicki M, Dutkiewicz G, Rezaei A, Behzad M, Etminani S, Rus. J. Coord. Chem, 39 (2013) 716–722.

10. Routier S, Bernier JL, Waring MJ, Colson P, Houssier C, Bailly C, J. Org. Chem, 61 (1996) 2326–2331.

11. Lin S, Kang TS, Lu L, Wang W, Ma DL, Leung CH, Biosensors and Bioelectronics, 86 (2016) 849-857.

12. Lu L, Zhong HJ, He B, Leung CH, Ma DL, Scientific reports, 6 (2016) 19368.

13. Mao Z, Liu J, Kang TS, Wang W, Han QB, Wang CM, Leung CH, Ma DL, Science and Technology of advanced MaTerials, 17 (2016) 109-114.

14. Wang W, Mao Z, Wang M, Liu LJ, Kwong DW, Leung CH, Ma DL, Chemical Communications, 52 (2016) 3611-3614.

15. Chatterjee N, Mahaling B, Sivakumar S, Bharadwaj PK, Journal of Photochemistry and Photobiology A: Chemistry, 330 (2016) 110-116.

16. Schatz M, Becker M, Thaler F, Hampel F, Schindler S, Jacobson RR, Tyeklar Z, Murthy NN, Ghosh P, Chen Q, Zubieta J, Inorg. Chem, 40 (2001) 2312–2322.

17. Hammud HH, Ghannoum A, Masoud MS, Spectrochim. Acta Part A, 63 (2006) 255–265.

18. Alex PM, Aravindakshan KK, Synth. React. Inorg. Met. Org. Nano Met. Chem, 39 (2009) 718–733.

19. Raman N, Muthuraj V, Ravichandran S, Kulandaisamy A, J. Chem. Sci, 115 (2003) 161–167.

20. Raman N, Raja YP, Kulandaisamy A, J. Chem. Sci, 113 (2001) 183–189.

21. Chattopadhyay S, Ray MS, Chaudhuri S, Mukhopadhyay G, Bocelli G, Cantoni A, Ghosh A, Inorg. Chim. Acta, 359 (2006) 1367–1375.

22. Ray MS, Bhattacharya R, Chaudhuri S, Righi L, Bocelli G, Mukhopadhyay G, Ghosh A, Polyhedron, 22 (2003) 617–624.

23. Angadi VJ, Anupama AV, Kumar R, Matteppanavar S, Rudraswamy B, Sahoo B, Journal of Alloys and Compounds, 682 (2016) 263-274.

24. Youssef NS, NEl-Zahany EA, Barsoum BN, El-Seidy A M, Transit. Met. Chem, 34 (2009) 905–914.

25. Dutta RL, Syamal A, Elements of Magnetochemistry, 2nd edn. (Elsevier, New Delhi, 1992).

26. Osowole AA, Kolawole GA, Fagade OE, J. Coord. Chem, 61 (2008) 1046–1055.

27. Nair MS, Joseyphus RS, Spectrochim. Acta Part A, 70 (2008) 749–753.

28. Neelakantan MA, Rusalraj F, Dharmaraja J, Johnsonraja S, Jeyakumar T, Pillai MS, Spectrochim. Acta Part A, 71 (2008) 1599–1609.

29. Kandil SS, Ali GY, El-Dissouky A, Transit. Met. Chem, 27 (2002) 398–406.

30. You ZL, Zhu HL, Liu WS, Zeitschriftfu ̈ranorganische und allgemeine Chemie 630 (2004) 1617–1622.

31. You ZL, Zhu HL, Zeitschriftfu ̈ranorganische und allgemeine Chemie, 630 (2004) 2754–2760.

32. Raj BB, Kurup MP, Suresh E, Spectrochim. Acta Part A, 71 (2008) 1253–1260.

33. Pogni R, Baratto MC, Diaz A, Basosi R, J. Inorg. Biochem, 79 (2000) 333–337.

34. Manoj E, Kurup MP, Punnoose A, Spectrochim. Acta Part A, 72 (2009) 474–483.

35. Hathaway B, Billing DE, Coord. Chem. Rev, 5 (1970) 143–207.

36. Raman N, Ravichandran S, Thangaraja SC, J. Chem. Sci, 116 (2004) 215–219.

37. AbdelLatif SA, Issa YM, Natural Science, 2 (2010) 1035.

38. Mohamed GG, Omar MM, Hindy AM, Turk. J. Chem, 30 (2006) 361–382,

39. Mohamed GG, Omar MM, Hindy AM, Spectrochim. Acta Part A. 62(4), 1140–1150 (2005)

40. Tas E, Aslanoglu M, Ulusoy M, Temel H, J. Coord. Chem, 57 (2004) 677–684.

41. Bruker AP, SAINT (Version 7.03), SADABS (Version 2.11), SHELXTL (Version 6.12) (Bruker AXS, Madison, 2004)

42. S.A.I.N.T. Bruker, Blok Version 6.02 includes XPREP and SADABS (Bruker AXS, Madison, 1999)

43. Altomare A, Cascarano G, Giacovazzo C, Guagliardi A, Completion and refinement of crystal structures with SIR92. J. Appl. Crystallogr, 26 (1993) 343–350.

44. Farrugia LJ ORTEP-3 for Windows-a version of ORTEP-III with a Graphical User Interface (GUI), J. Appl. Crystallogr, 30 (2002) 565.

45. Bruno IJ, Cole JC, Edgington PR, Kessler M, Macre CF, McCabe P, Pearson J, Taylor R, Acta Crystallogr B, 58 (2002) 389–397.

46. Dolomanov OV, Bourhis LJ, Gildea RJ, Howard JA, Puschmann H, J. Appl. Crystallogr, 42 (2009) 339–341.

47. Sheldrick GM, SHELXT–Integrated Space-Group and Crystal-Structure Determination, Acta Crystallogr. Sect. A, 71 (2015) 3–8.

48. Sheldrick GM, A short history of SHELX. Acta Crystallogr, A 64 (2008) 112–122.

49. Lashanizadegan M, Seraj S, Turk. J. Chem, 34 (2010) 263–268.

50. Matsumoto N, Akui T, Murakami H, Kanesaka J, Ohyoshi A, kawa H. O, J. Chem. Soc. Dalton Trans, 4 (1988) 1021–1035.

51. Meghdadi S, Amirnasr M, Bagheri M, Najafabadi FA, Mereiter K, Schenk KJ, Ziaee F, J. Iran. Chem. Soc, 11 (2014) 985–991.

52. Lashanizadegan M, Boghaei DM, Inorg. Met. Org. Chem, 32 (2002) 345–355.

53. Mederos A, Medina A, Medina E, Manrique FG, Nunez P, Rodriguez ML, Journal of Coord. Chem, 15 (1987) 393–404.

54. Dharmaraj N, Viswanathamurthi P, Natarajan K, Transit. Met. Chem, 26 (2001) 105–109.

55. Tweedy BG, Plant extracts with metal ions as potential antimicrobial agents. Phytopathology, 55(1964) 910–914.

CHAPTER IV

Crystal structure, spectral characterization and biologically studies of mononuclear transition metal complexes derived from o-phenylenediamine and substituted salicyaldehyde type of ligand

4.1 Introduction

The salphen ligands are prepared by the simple combination of two equivalents of a (substituted) salicylaldehyde with one equivalent of 1,2-phenylenediamine. The scope for producing salphen ligands with various substitutions is wide given that many differently substituted salicylaldehydes and 1,2-phenylenediamines are readily available and they act as tetra-dentate N_2O_2 donor schiff bases and widely studied in solid state [1, 2]. Schiff base ligands with N_2O_2 donor atoms are well known to coordinate with a variety of metal ions. They have attracted much interest in recent years, due to their ease of synthesis, stability under a variety of oxidative and reductive conditions and their structural versatility associated with various applications. These compounds have various applications in industries as dyes, drug synthesis [3] bioinorganic chemistry [4] electrochemistry [5] and for dioxygen uptake and catalysis [6-10]. Previous work has shown that some drugs showed increased activity when administered as metal chelates rather than as organic compounds [11-13]. Hence in this chapter we discuss synthesis of a novel salphen ligand prepared by condensation of 2-hydroxy-6-isopropyl-3-methyl benzaldehyde & 1,2-phenylenediamine and its metal complexes.

4.2 Experimental section

4.2.1 Chemicals and Solvents

Chemicals and solvents are same as described in Chapter 2, section 2.2.1

4.2.2 Analytical methods

Analytical methods are same as described in Chapter 2, section 2.2.2

4.3. Synthesis of ligand 6,6'-((1E,1'E)-(1,2-phenylenebis(azanylylidene)) bis(methanylylidene))bis(5-isopropyl-2-methylphenol (PH)

The synthesis of ligand 6,6'-((1E,1'E)-(1,2-henylenebis(azanylylidene))bis (methanylylidene)) bis(5-isopropyl-2-methylphenol) (PH) was carried out according to scheme represented in **Figure 4.1** the procedure described below.
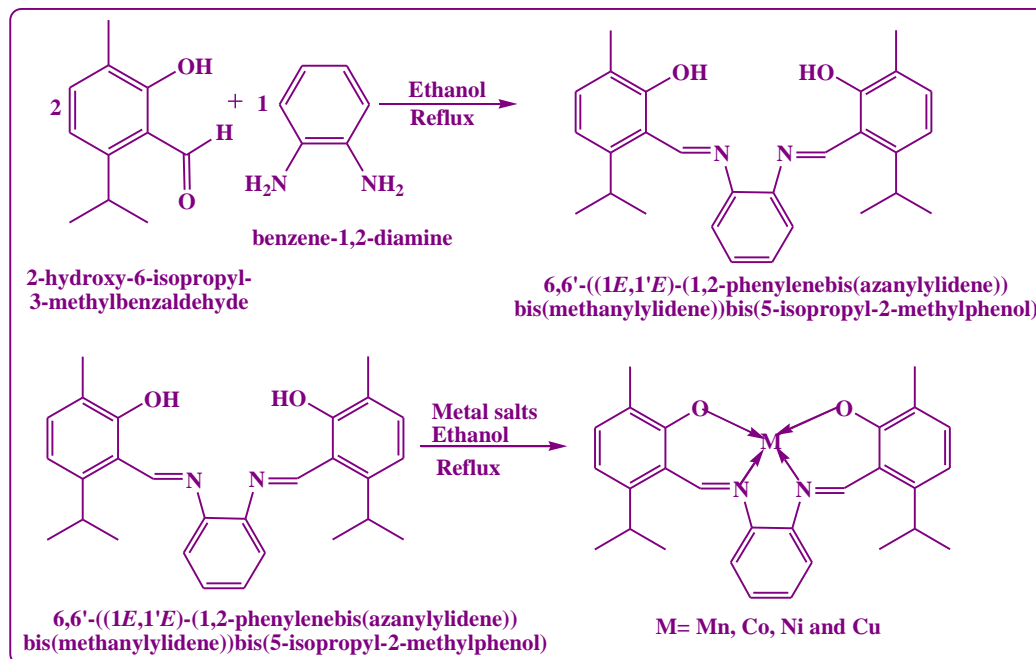
Figure 4.1: Synthesis of ligand 6,6'-((1E,1'E)-(1,2-phenylenebis(azanylylidene))bis(methanylylidene))bis(5-isopropyl-2-methylphenol (PH) and its metal complexes

The PH ligand was prepared by dropwise addition of a warm ethanolic solution of o-phenylenediamine (1mmol, 0.106 gm) to constantly stirring warm solution of 2-hydroxy-6-isopropyl-3-methyl benzaldehyde (2 mmol, 0.356 gm) in ethanol. The resulting solution was refluxed for 3h, till formation of orange precipitate. The obtained product was filtered, washed with cold ethanol and recrystallized from ethanol and dried at room temperature.

Analytical and spectral data of PH ligand

Colour: Orange, solid. Yield: 77 %. ^{1}H- NMR (CDCl$_3$, 400MHz) (δ, ppm): 14.16 (s, 2H, -OH), 7.39-7.37 (m, 2H, Ar), 7.32-7.30 (m, 2H, Ar), 7.20 (d, 2H, J= 8Hz), 6.74 (d, 2H, Ar), 3.48-3.45 (m, 2H, -2(CH$_3$)), 2.17 (s, 6H, 2(CH$_3$)), 1.19-1.24 (m, 12H, 4(CH$_3$)). ^{13}C- NMR (CDCl$_3$, 400 MHz) (δ, ppm): 162.31, 160.88, 147.99, 142.74, 134.72, 127.34, 124.05, 121.16, 114.95, 28.09, 24.07, 15.60. UV-Vis (DMF) λ_{max} (nm): 268, 341. FT-IR (KBr pellet, cm^{-1}) ν_{max}: 3412 (OH), 1601 (C=N), 1460 (C=C), 1253 (C-O). MS (m/z): calcd 428.57; obsv 429.4. Anal. calcd for C$_{28}$H$_{32}$N$_2$O$_2$(%): C 78.47, H 7.53, N 6.54; Found: C 78.31, H 8.16, N 6.61.

4.4 General procedure for synthesis of metal complexes

General procedure for the synthesis of mononuclear metal complexes is carried out as per scheme presented in **Figure 4.1**

The complexes were prepared by dropwise addition of (1 mmol, 0.428 gm) warm ethanolic solution of PH ligand to the ethanolic solution of corresponding suitable metal acetate or chloride salt (2 mmol) in basic condition under nitogen atmosphere. The reaction mixture was refluxed till completion of reaction, the precipitate was obtained and collected product was washed with cold ethanol and then diethyl ether.

4.4.1 Analytical and spectral data of PHMn(III)

Yield: 71%. Colour: Reddish brown, solid. UV-Vis (DMF) λ_{max} (nm): 268, 342, 471. FT-IR (KBr, pellet cm^{-1}) ν_{max}: 1591 (C=N), 1276 (C-O), 1382 (C=C), 530 (M-O), 480 (M-N). LC-MS (m/z): calcd 540.53; obsv 481.3. Anal. calcd for $C_{30}H_{33}MnN_2O_4$ (%): C 66.66, H 6.15, N, 5.18; Found: C 66.11, H 6.49, N 5.50. μ_{eff}: 4.82 B.M.. Conductance (Λ_M, Ω^{-1} cm^2 mol^{-1}) in DMF: 9.60.

4.4.2 Analytical and spectral data of PHCo(II)

Colour: Brown, solid. Yield: 65 %. UV-Vis (DMF) λ_{max} (nm): 264, 506, 620. FT-IR (KBr pellet, cm^{-1}) ν_{max}: 1541 (C=N), 1205 (C-O), 1382 (C=C), 530 (M-O), 480 (M-N). LC-MS (m/z): calcd 485.48; obsv 485.3. Anal. calcd for $C_{28}H_{30}CoN_2O_2$ (%): C 69.27 H 6.23, N 5.77, Found: C 68.29, H 5.14, N 5.58. μ_{eff}: 3.80 B.M. Conductance (Λ_M, Ω^{-1} cm^2 mol^{-1}) in DMF: 14.35.

4.4.3 Analytical and spectral data of PHNi(II)

Colour: Reddish orange, solid. Yield: 80 %. UV-Vis (DMF) λ_{max} (nm): 267, 307, 386, 490, 547. FT-IR (KBr pellet, cm^{-1}) ν_{max}: 1560 (C=N), 1234 (C-O), 1452 (C=C), 474 (M-O), 432 (M-N). LC-MS (m/z): calcd 485.23; obsv 485.41. Anal. calcd for $C_{28}H_{30}N_2NiO_2$ (%): C 69.31, H 6.23, N 5.77, Found: C 70.34, H 6.03, N 6.35. Conductance (Λ_M, Ω^{-1} cm^2 mol^{-1}) in DMF: 15.64

4.4.4 Analytical and spectral data of PHCu(II)

Colour: Shining dark green, solid. Yield: 78 %. UV-Vis: (DMF) λ_{max} (nm): 264, 444, 632. FT-IR (KBr, cm-1) ν_{max}: 1600 (C=N), 1240 (C-O), 1404 (C=C), 550 (M-O), 455 (M-N). LC-MS (m/z): calcd 490.10; obsv 490.40. Anal. calcd for $C_{28}H_{30}CuN_2O_2$(%): C 68.62, H 6.17, N 5.72, Found: C 66.79, H 5.18, N 5.67. μ_{eff}: 1.75 B.M. Conductance (Λ_M, Ω^{-1} cm^2 mol^{-1}): 12.67. $g_{\parallel}$= 2.2317, $g_{\perp}$= 2.0472.

4.5 Characterization of PH ligand and its PHMn(III), PHCo(II), PHNi(II) and PHCu(II) metal complexes

All the synthesized compounds have been characterized through NMR, UV-Visible, FT-IR, LC-MS, ESR spectroscopic techniques, elemental analyses, magnetic susceptibility, conductivity measurements, SEM analysis and single crystal X- ray diffraction techniques and the results discussed below.

4.5.1 NMR Spectra

The ^{1}H and ^{13}C NMR spectra of the PH ligand recorded in DMSO are shown in **Figure 4.2 & Figure 4.3** and the NMR spectral data are summarized in **Table 3.1.**

In the ^{1}H- NMR spectrum, the 14.16 δ singlet is assigned to the phenolic –OH group and the peaks at 7.39-7.37, 7.32-7.30, 7.20, 6.74 δ are assigned to the aromatic protons, the multiplets at 3.48-3.45 δ and 1.19-1.24 δ are assigned to 2(-CH) and four methyl groups of isopropyl groups respectively. While the singlet peak at 2.17 δ is assigned for methyl protons.

Table 4.1: NMR spectral data of DP ligand

Compounds	Assignments of peaks δ ppm
^{1}**H-NMR (400 MHz, CDCl$_3$)** **(δ, ppm):**	14.16 (s, 2H, OH), 7.39- 7.37 (m, 2H, Ar) 7.39-7.37 (m, 2H, Ar), 7.32-7.30 (m, 2H,Ar), 7.20 (d, 2H, J= 8Hz, Ar), 6.74 (d, 2H, J= 8Hz, Ar), 3.48-3.45(m, 2H, -2(CH$_3$)), 2.17 (s, 6H, 2CH$_3$), 1.30-1.24 (m, 12H, 4(CH$_3$)).

^{13}C-NMR (400 MHz, CDCl$_3$) (δ, ppm):	162.31, 160.88, 147.99, 142.74, 134.72, 127.34, 124.05, 121.16, 114.05, 121.16, 114.95, 114.69, 28.09, 24.07, 15.60.
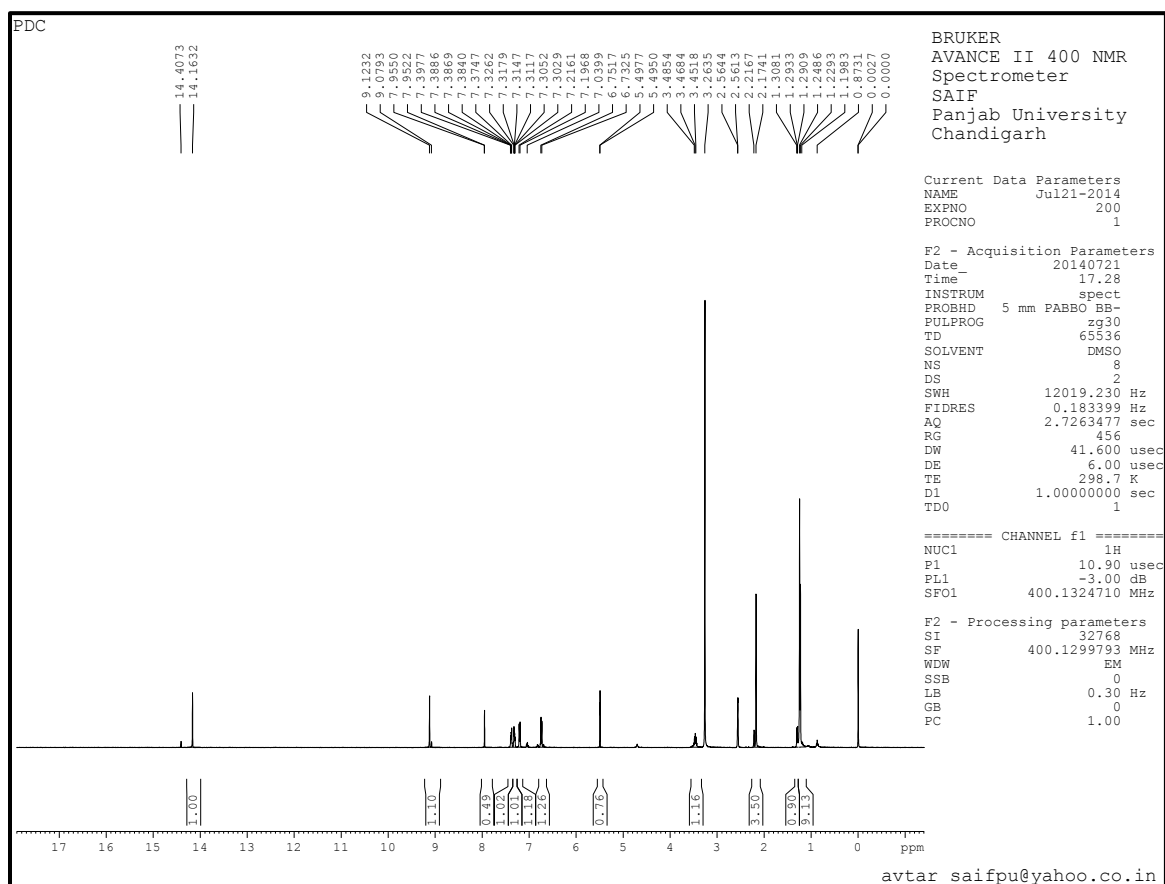
Figure 4.2:. ^{1}H-NMR spectrum of PH ligand
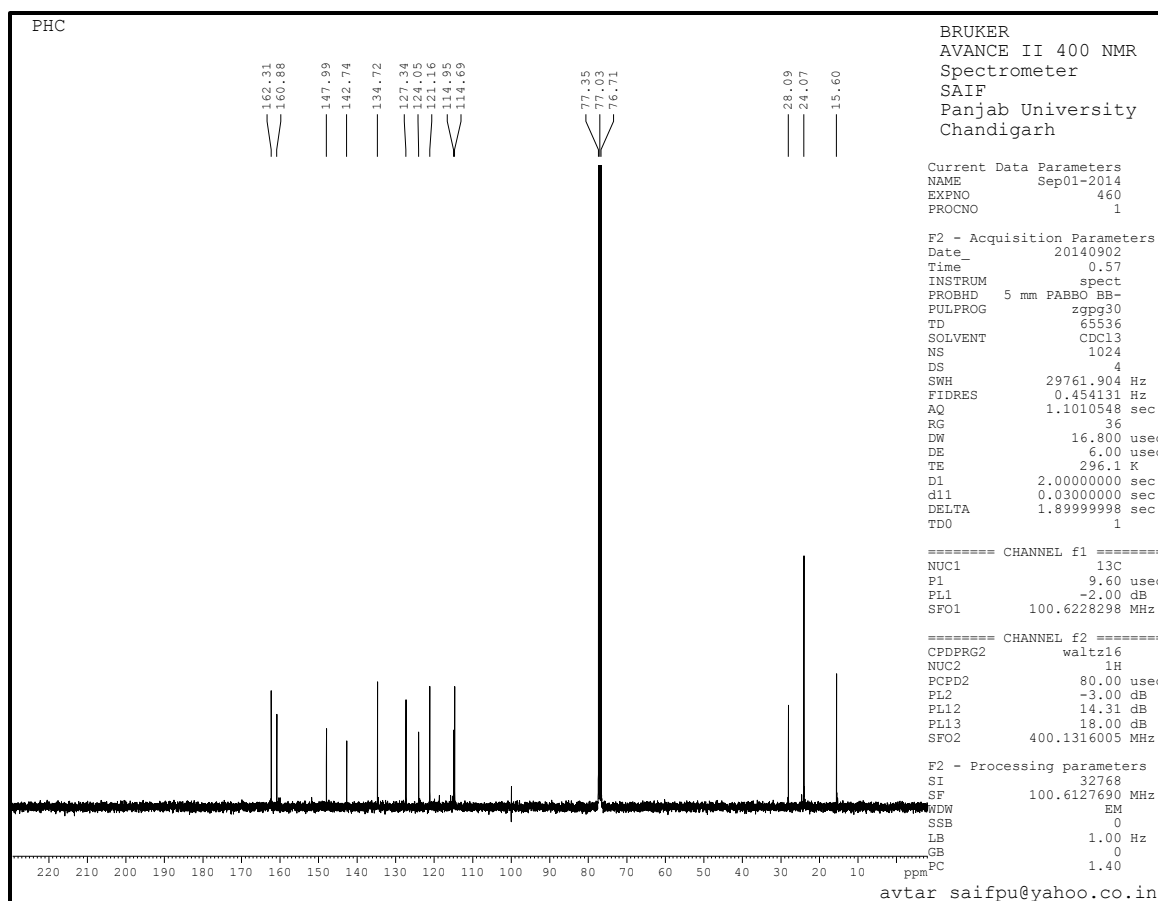
Figure 4.3: ^{13}C-NMR spectrum of PH ligand

4.5.2 UV-Visible spectra

The significant absorptions of PH ligand and its metal complexes are summarized in **Table 4.2**, while, UV-Visible spectra are shown in **Figures 4.4- 4.8**. The absorption value of high energy 265-280 nm and 340- 490 nm are assigned to the intraligand $\pi{\rightarrow}\pi^*$ and n${\rightarrow}\pi^*$ transitions respectively. UV-Visible spectra of PHNi(II) consist of weak d-d transition in the visible region as a broad band at 632 nm attributed to square planar complexes of similar tetradentate schiff base ligands with o-phenylenedimaine, the PHNi(II) complex shows the absorption at 547 nm indicating that the complex is diamagnetic nature and possesses square planar geometry. The absorption at 506 nm and 620 nm shows PHCo(II complex possess the square planar geometry [14].

Table 4.2: UV-Visible spectral data of PH ligand its metal complexes

Compounds	Wavelength (nm)
PH Ligand	282, 341, 347
PHMn(III)	269, 339, 341, 462
PHCo(II)	264, 506, 620
PHNi(II)	267, 307, 386, 490, 547
PHCu(II)	264, 444, 632
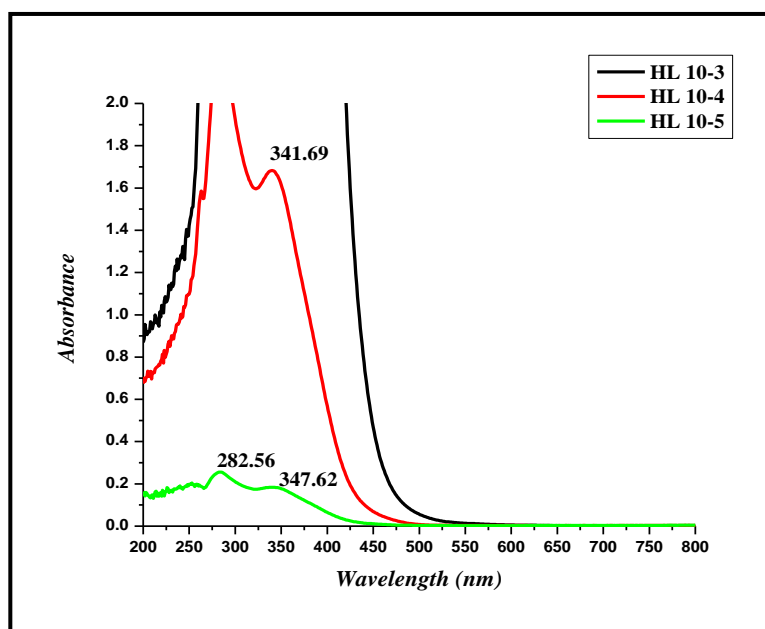
Figure 4.4: UV- Visible spectrum of PH ligand
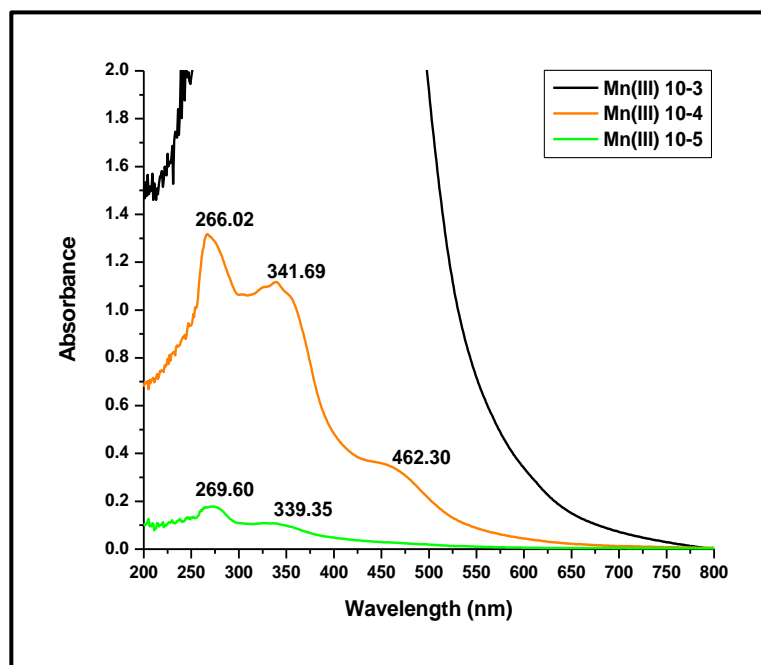
Figure 4.5: UV-Visible spectrum of PHMn(III) complex
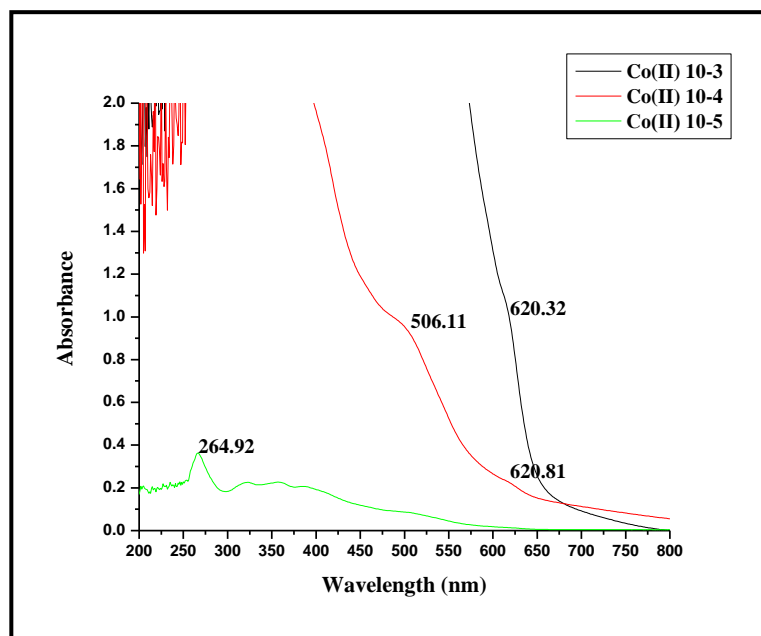
Figure 4.6: UV-Visible spectrum of PHCo(II) complex
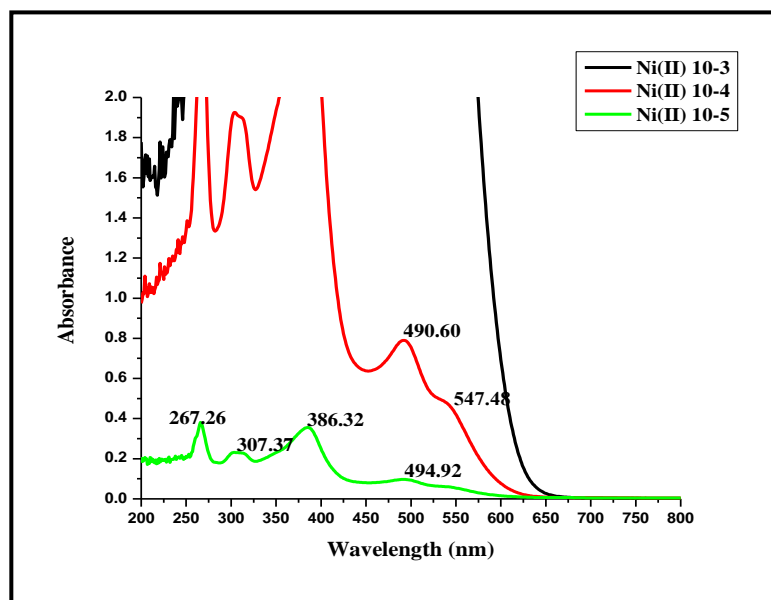
Figure 4.7: UV-Visible spectrum of PHNi(II) complex
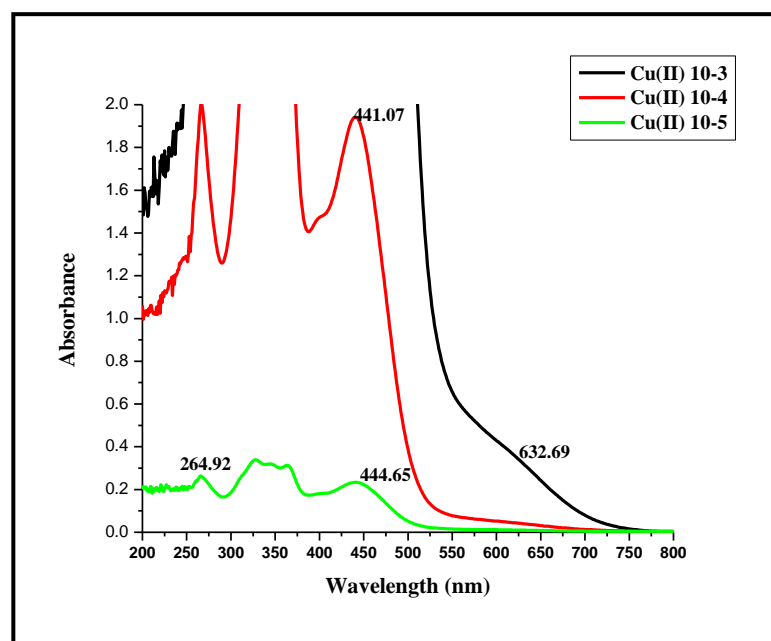
Figure 4.8: UV- Visible spectrum of PHCu(II) complex

4.5.3 FT-IR Spectra

The IR spectroscopy is used to determine the characteristic peaks (OH, C=N, C-O) in ligand before and after complexation The FT-IR spectral data of PH ligand and its metal complexes are mentioned in **Table 4.3**, while the spectra are represented in **Figures 4.9-4.13**. The band at 1601 cm^{-1} is characteristic of the azomethine nitrogen atom present in the schiff base ligand is found to shift to lower frequency region 1546-1556 cm^{-1} in all the complexes and illustrated the involvement of the azomethine nitrogen atom in coordination. The peak at 3412 cm^{-1} appears for the phenolic –OH group of the schiff base, the broad band in the region 3500-3100 cm^{-1} indicated coordination of deprotonated ligand as well as absence of coordinated water molecule in the complexes. The C-O peak appearing in the ligand at 1298 cm^{-1} is shifted to 1340-1388 cm^{-1} in all complexes. The involvement of oxygen and nitrogen atoms in coordination with metal is further definited by the appearance of weak and low frequency bands in the range 400-600 cm^{-1} corresponding to the M-O and M-N respectively [13, 15].

Table 4.3: FT-IR spectral data of PH ligand and its metal complexes

Compounds	Spectral bands cm^{-1}
PH Ligand	2964, 2873, 1600, 1454, 1423, 1298, 1045, 985, 813, 763, 650, 513, 462
PHMn(III)	2958, 1591, 1558, 1382, 1004, 754, 651
PHCo(II)	2956, 1541, 1388, 1205, 1001, 812, 740, 659
PHNi(II)	2958, 1560, 1234, 1452, 474, 432
PHCu(II)	2958, 2357, 1600, 1546, 1404, 1359, 1201, 810, 744, 661
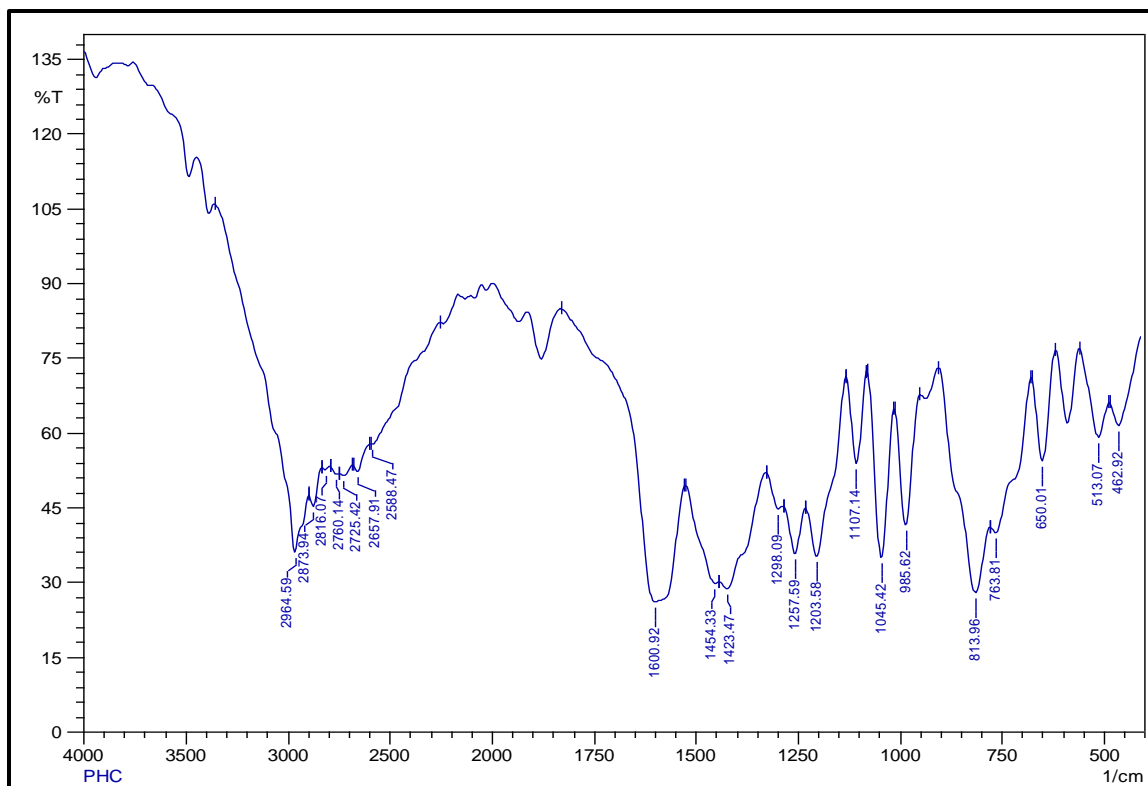
Figure 4.9: FT-IR spectrum of PH ligand
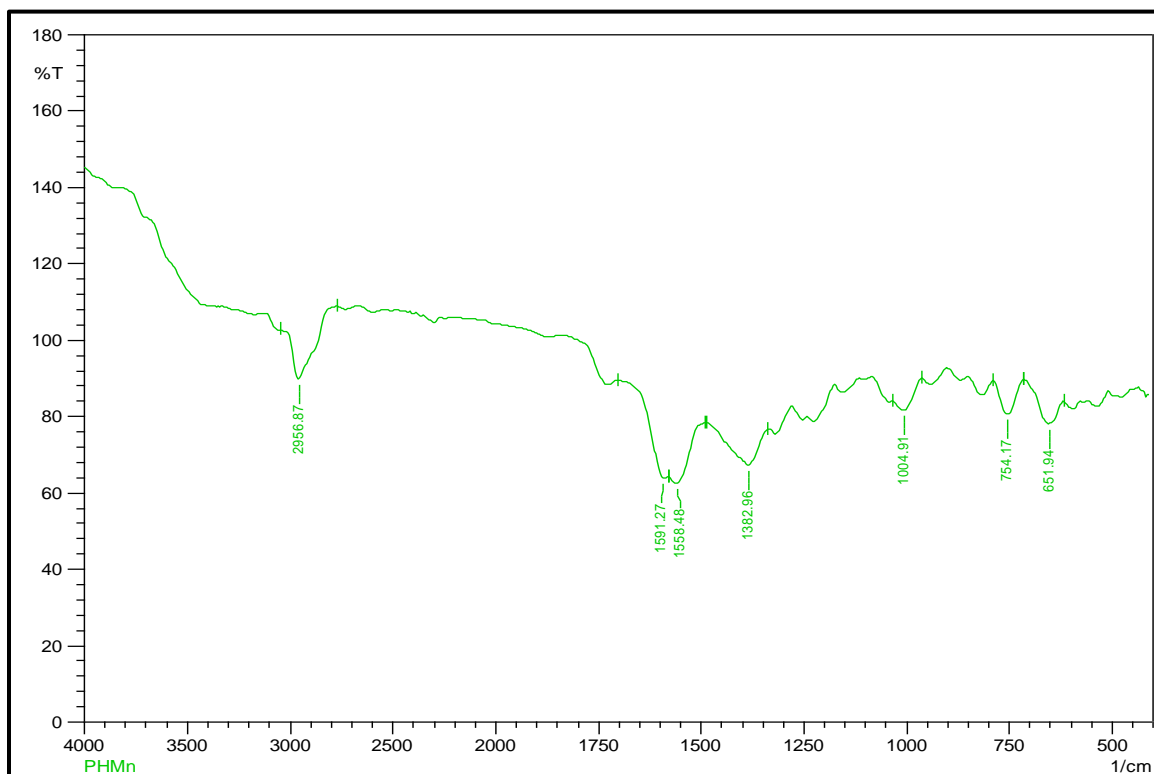
Figure 4.10: FT-IR spectrum of PHMn(III) complex
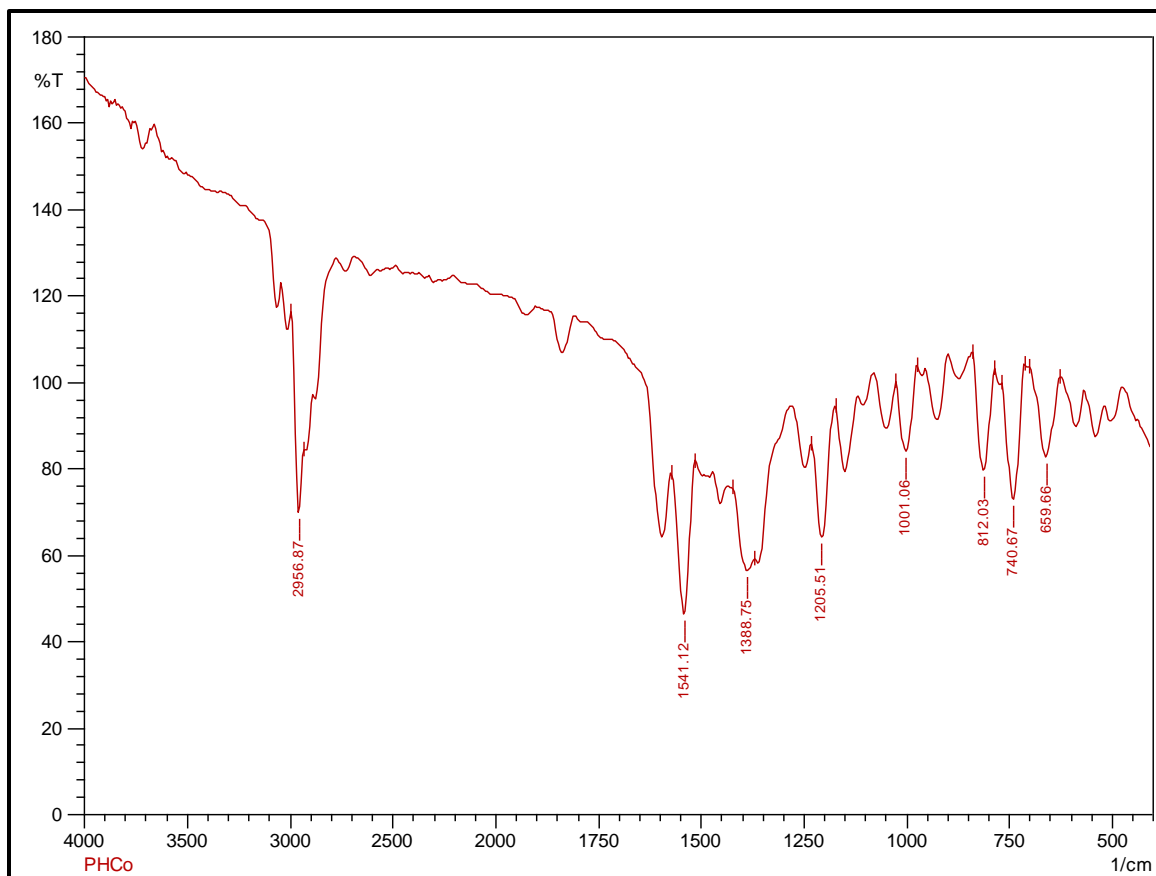
Figure 4.11: FT-IR spectrum of PHCo(II) complex
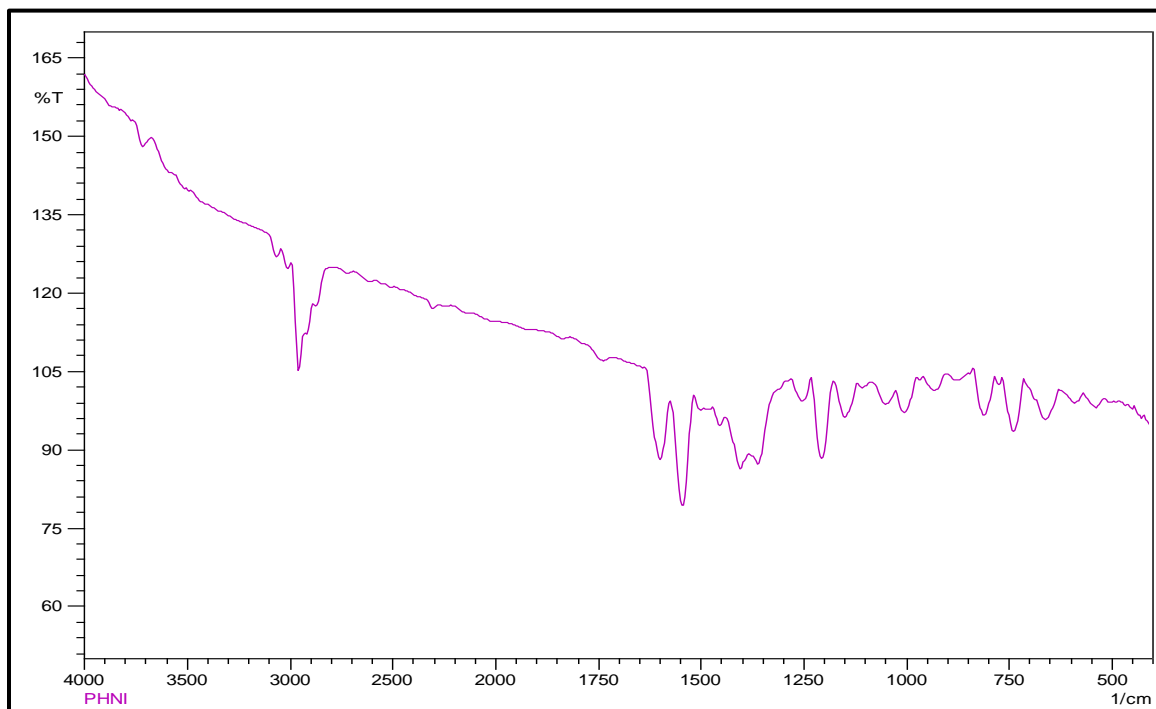
Figure. 4.12: FT-IR spectrum of PHNi(II) complex
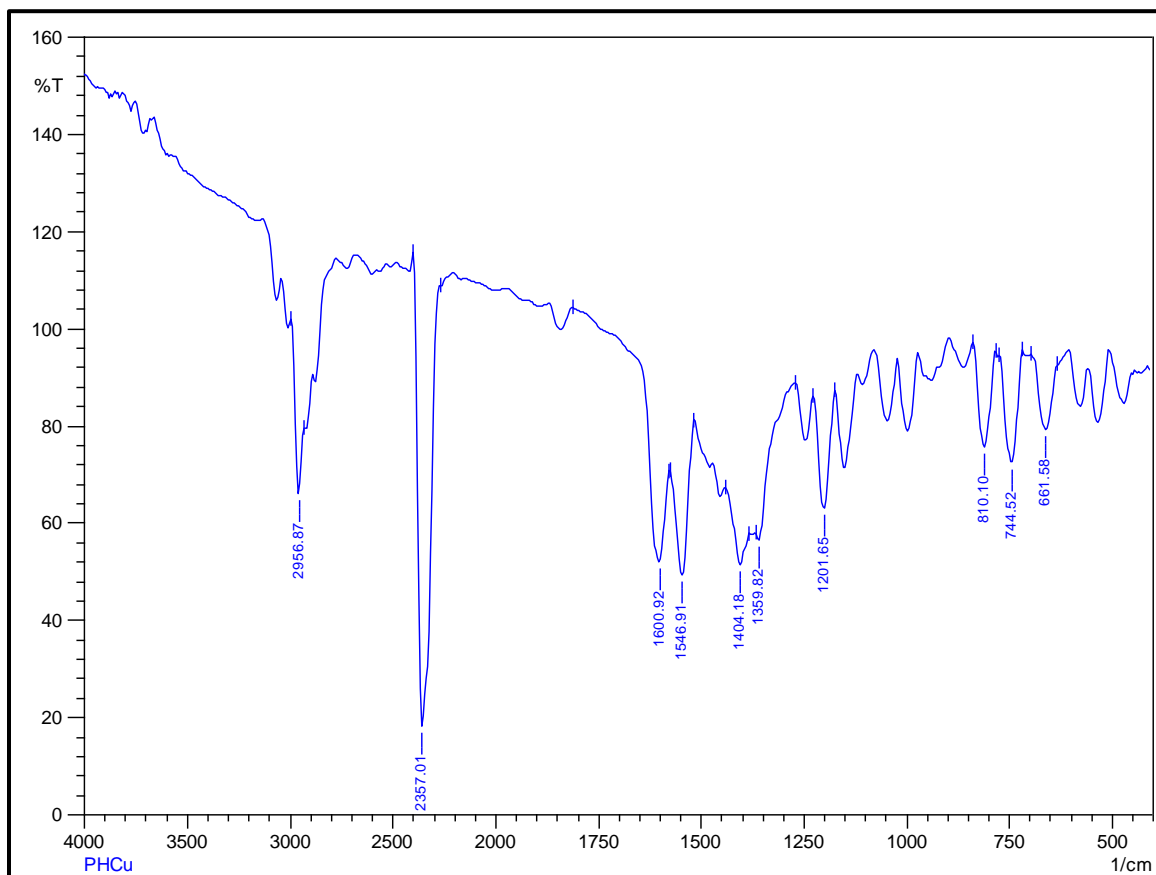
Figure. 4.13: FT-IR spectrum of PHCu(II) complex

4.5.4 Mass spectroscopy

The major LC-MS peaks in the mass spectra of PH ligand and its four metal complexes are summarized in the **Table 4.4**. In the mass spectra of the PH ligand and its metal complexes the molecular ion peak is significantly more abundant than other fragment ions. The proposed fragmentations are equivalent with the empirical formula of proposed structure of the ligand and metal complexes **(Figures 4.14- 4.18).**

Table 4.4: LC-MS Spectral data of PH ligand and its metal complexes

Comp. Name	Mol. Formula	Mol. Wt (Calcd)	Mol. Wt (Found)
PH Ligand	$C_{28}H_{32}N_2O_2$	$M^+ = 428.57$	$M^{+1} = 429.4$
PHMn(III)	$C_{30}H_{33}MnN_2O_4$	$M^+ = 540.53$	$M^{-OAC} = 481.3$
PHCo(II)	$C_{28}H_{30}CoN_2O_2$	$M^+ = 485.48$	$M^+ = 485.3$
PHNi(II)	$C_{28}H_{30}N_2NiO_2$	$M^+ = 485.23$	$M^+ = 485.41$
PHCu(II)	$C_{28}H_{30}CuN_2O_2$	$M^+ = 490.10$	$M^+ = 490.40$
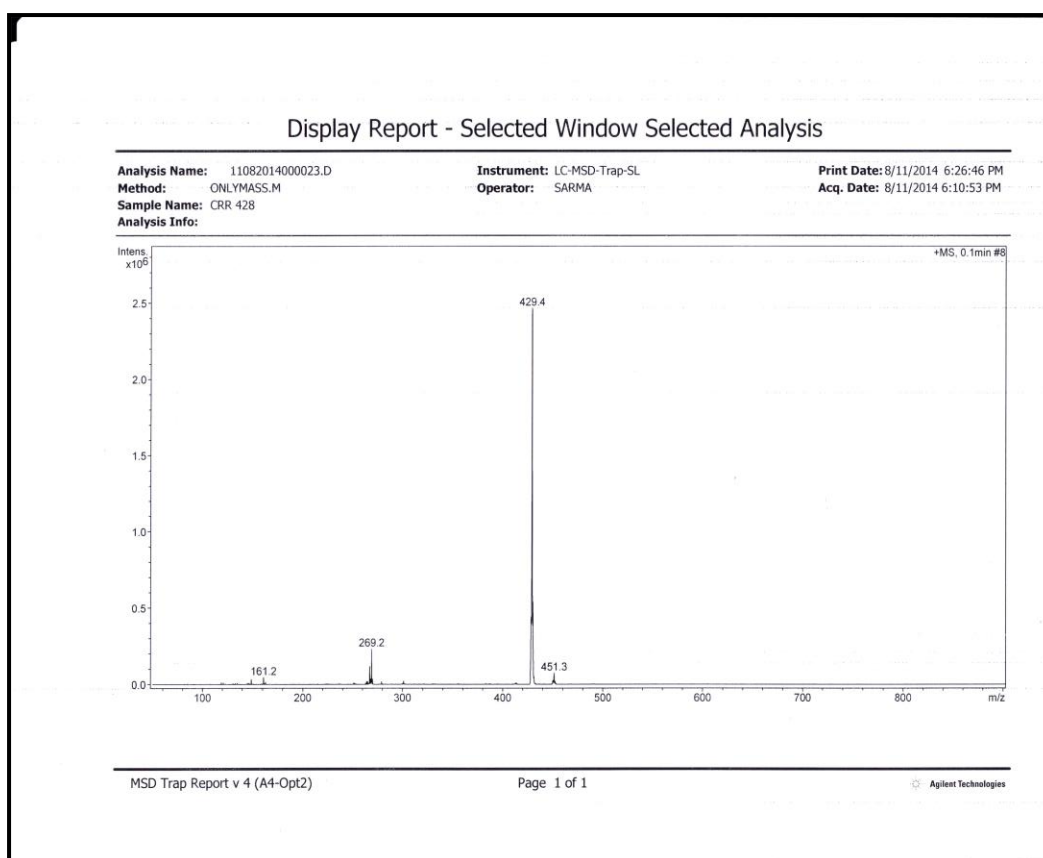
Figure 4.14: LC-MS spectrum of PH ligand
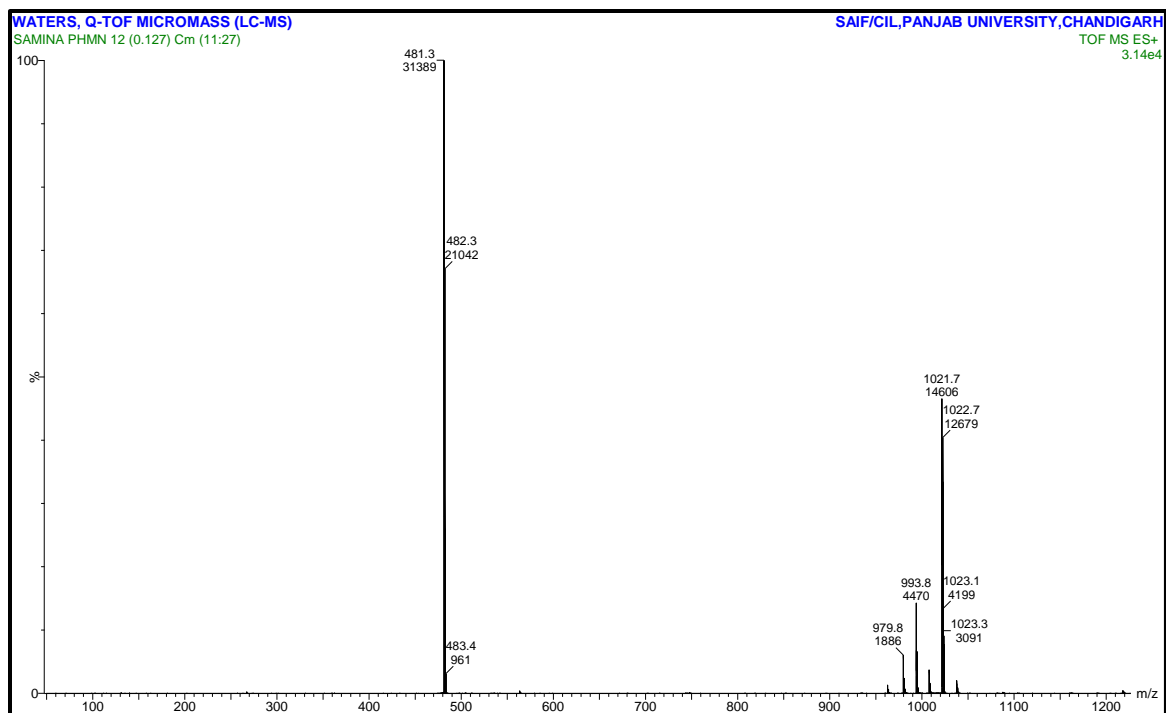
Figure 4.15: LC-MS spectrum of PHMn(III) complex
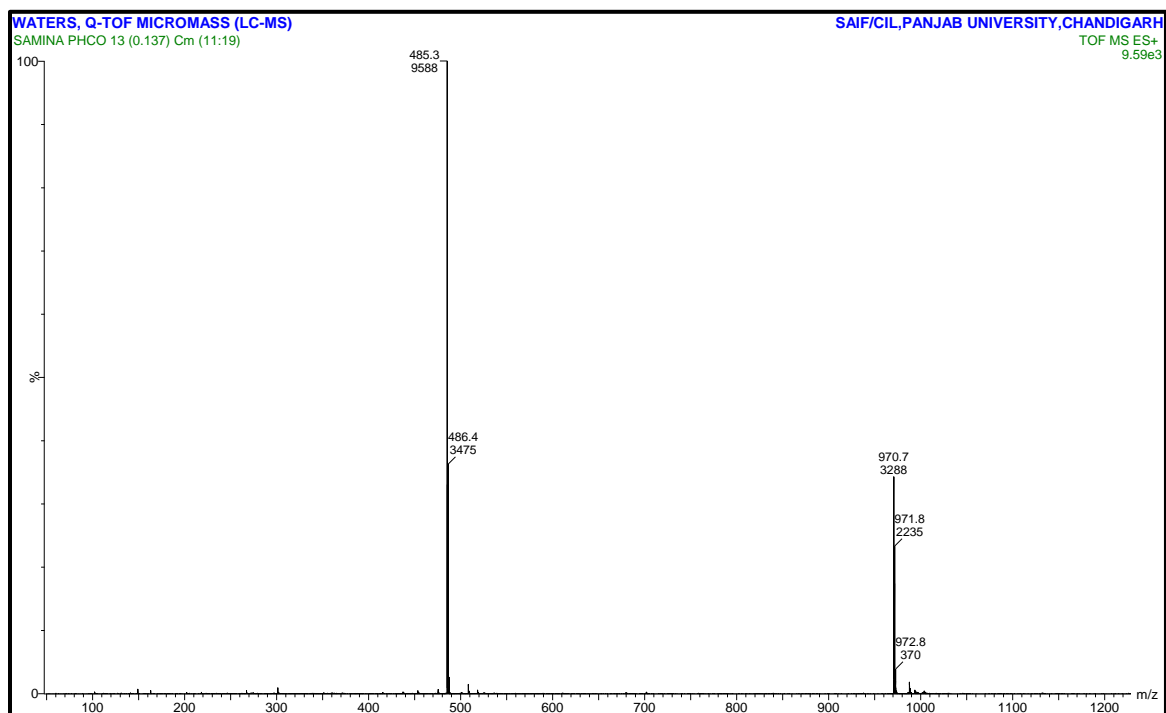
Figure 4.16: LC-MS spectrum of PHCo(II) complex
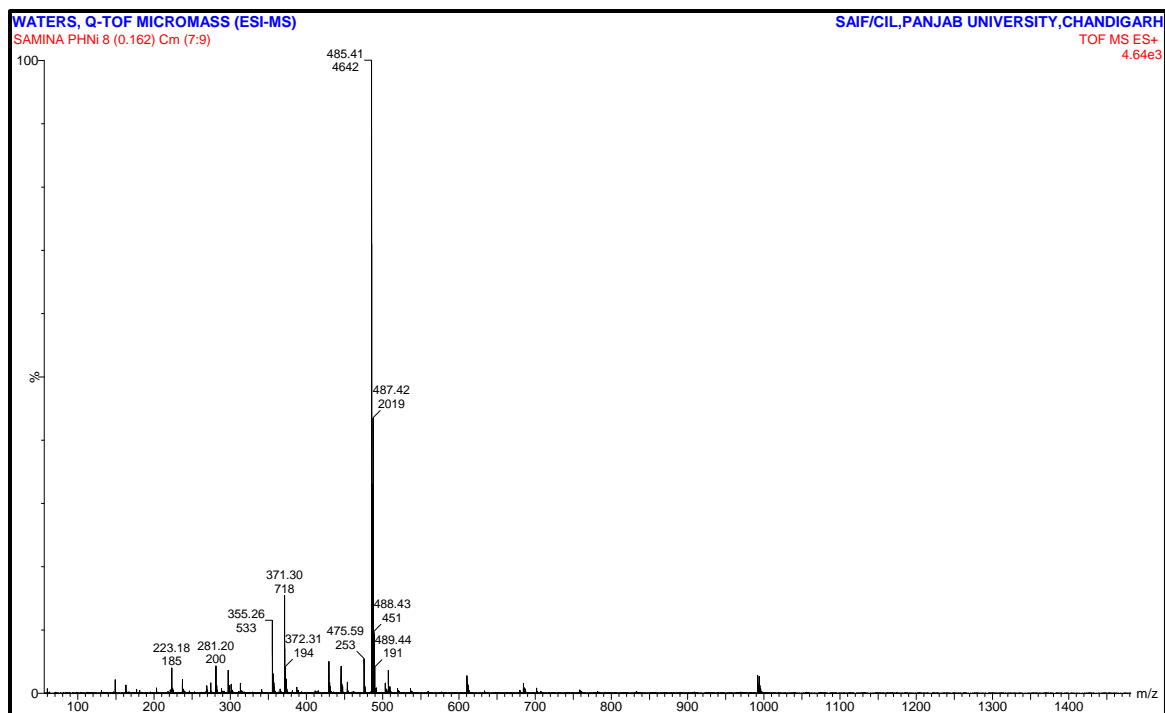
Figure 4.17: LC-MS spectrum of PHNi(II) complex
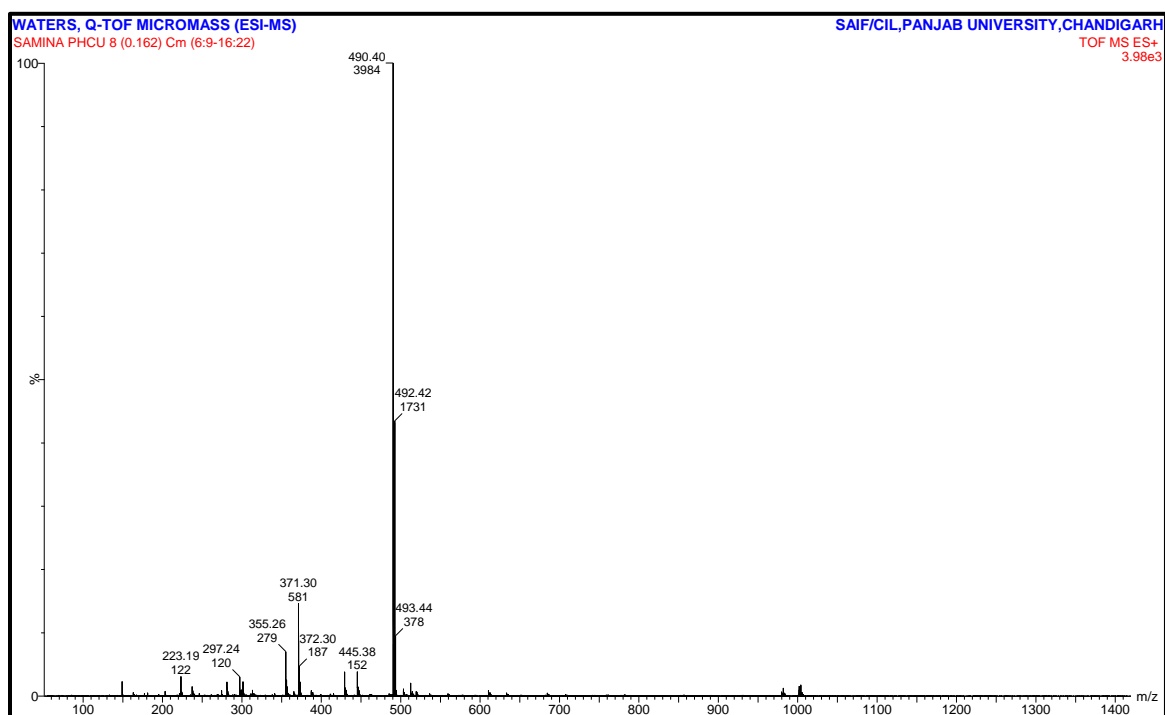
Figure 4.18: LC-MS spectrum of PHCu(II) complex

4.5.5 Elemental analysis

The elemental analysis of the ligand 6,6'-((1E,1'E)-(1,2-phenylenebis(azanylylidene))bis(methanylylidene))bis(5-isopropyl-2-methyl phenol (PH) and its four mononuclear transition metal complexes are listed in **Table. 4.5**. They are in good conformity with molecular formula.

Table 4.5: Elemental analyses data of PH ligand its metal complexes (%):

Compounds. Name	Molecular Formula	C (Cal) Found	H(Cal) Found	N(Cal) Found
PH Ligand	$C_{28}H_{32}N_2O_2$	(78.47) 78.31	(7.53) 8.16	(6.54) 6.61
PHMn(III)	$C_{30}H_{33}MnN_2O_4$	(66.66) 64.93	(6.15) 5.91	(5.18) 5.97
PHCo(II)	$C_{28}H_{30}CoN_2O_2$	(69.27) 68.29	(6.23) 5.14	(5.77) 5.58
PHNi(II)	$C_{28}H_{30}N_2NiO_2$	(69.31) 70.34	(6.23) 6.03	(5.77) 6.35
PHCu(II)	$C_{28}H_{30}CuN_2O_2$	(68.62) 66.79	(6.17) 5.18	(5.72) 5.67

4.5.6 Molar conductivity measurement

The molar conductivity values of the complexes measured in DMF at 10^{-3} concentration were in the range 15-25 Ω^{-1} cm^2 mol^{-1}. The values indicated that the complexes are having non-electrolytic nature **(Table 4.6)** [16].

4.5.7 Magnetic susceptibility measurement

The results regarding magnetic moments are presented in **Table 4.6**. The PHMn(III) complex shows magnetic moment 4.85 B.M which corresponds to the Mn(III) d^4 configuration and square pyramidal geometry of the complex. The magnetic moment of 3.80 B.M. of PHCo(II) complex is consistent with the square planar geometry [17,18]. The PHNi(II) complex is diamagnetic in nature and confirms its square planar geometry [19]. The magnetic moment 1.75 B.M of PHCu(II) complex corresponds to one unpaired electron and represents square planar geometry of the complex [20,21].

Table 4.6: Magnetic susceptibility and molar conductivity measurements of PH ligand and its four mononuclear transition metal complexes

Compounds	Magnetic susceptibility (μeff) (B. M.)	Molar conductivity ($\Omega^{-1} cm^2 mol^{-1}$, RT)
PH Ligand	---	---
PHMn(III)	4.85	9.60
PHCo(II)	3.80	14.35
PHNi(II)	Diamagnetic	15.64
PHCu(II)	1.75	12.67

4.5.8 ESR Spectroscopy

The ESR spectrum of metal chelates provide information about hyperfine and superhyperfine structures which are important in studying the metal ion environment in the complexes i. e. the geometry, nature of the ligating sites from the schiff base of the metal and the degree of covalancy of the metal- ligand bonds. The X- band esr spectrum of PHCu(II) complex in DMF solution at 77 k at liquid nitrogen temperature is shown in **Figure 4.19**, exhibit axial symmetry with well resolved hyperfine in parallel and superhyperfine structures in the perpendicular region of the spectra. In the parallel region, three of four hyperfine features are well resolved while the fourth one is overlapped by $g^{\perp}$ features. The splitting in the perpendicular region of the spectrum can be attributed to interaction of an unpaired electron spin with copper nuclear spin (I^{Cu} = 3/2) [22].

The values of ESR parameters $g\|$, $g\perp$, g_{avg}, G, A$\|$, α^2, f for PHCu(II) complex calculated are 2.22, 2.040, 2.1, 5.75, 186×10^{-4}, 0.79, 118, respectively. From the calculated values it is observed that the copper complex follows the trend $g\| > g\perp > g$ and also provides information about the unpaired electron that it is localized in $d_{X^2-Y^2}$ orbital having $^2B_{1g}$ as ground state, this observation is consistent with the square planar geometry [23]. The extent of geometrical distortion is measured by the $f= g\|/A\|$ ratio [24]. The f values are reported to be in the range of 105- 135 cm^{-1} for square planar complexes and 135- 250 cm-1 for tetragonal distorted complex [25]. The current complex has f = 118 cm^{-1} indicating that copper complex has square planar geometry. The value of the exchange coupling interaction between two Cu(II) ions in terms of G has been explained by the Hathway

expression (g‖-2. 0023) /(g⊥-2. 0023). From the expression, if G > 4·0, the exchange interaction is negligible while when the value of G< 4.0 significant exchange coupling is present in the solid complex [26]. This result indicates that the exchange coupling effects are not effective in the present complex. The value of in plane sigma bonding parameter α^2 was expected from following expression,

$\alpha^2 = -(A_{‖}/0.036) + (g_{‖}-2.0023) +3/7(g_{⊥}-2.0023) + 0.04$

The value of α^2= 0.5, indicates complete covalent bonding, while the value of α^2= 1.0 suggests complete ionic bonding. The observed value of α^2 is less than 1, which indicated that the complex has some covalent character in the ligand environment [27].
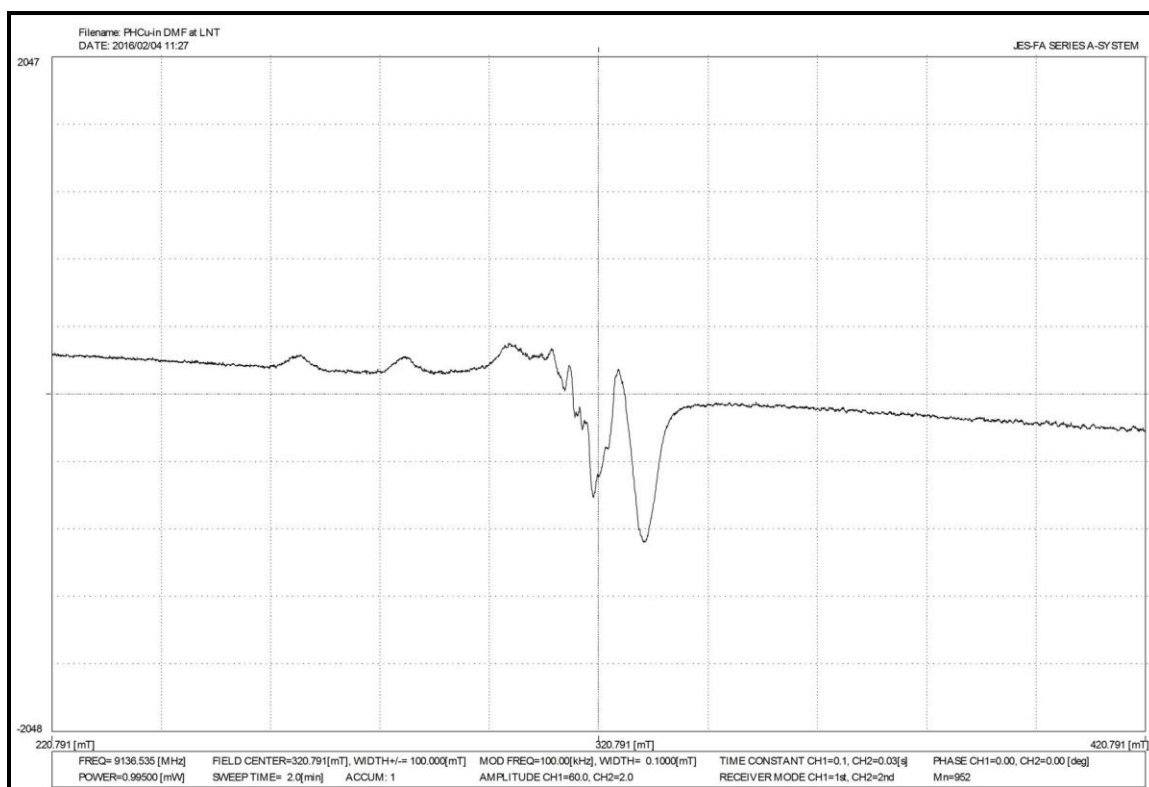
Figure 4.19: X-band ESR spectrum of PHCu(II) complex

4.5.9 SEM analysis

Scanning electron micrograph (SEM) has been currently used to determine the morphology and the particle or grain size of the metal complexes. The SEM images were taken in the different scale range from 1μm to 50 μm and are illustrated in the **Figures 4.20- 4.23** for all the metal complexes. From the SEM photograph it was noted that there is a uniform matrix in all the metal complexes. The photograph of PHMn(III) complex shows flakes

like morphology while PHCo(II) complex exhibits the rod like morphology. The PHNi(II) and PHCu(II) complexes display the fibre like morphology.
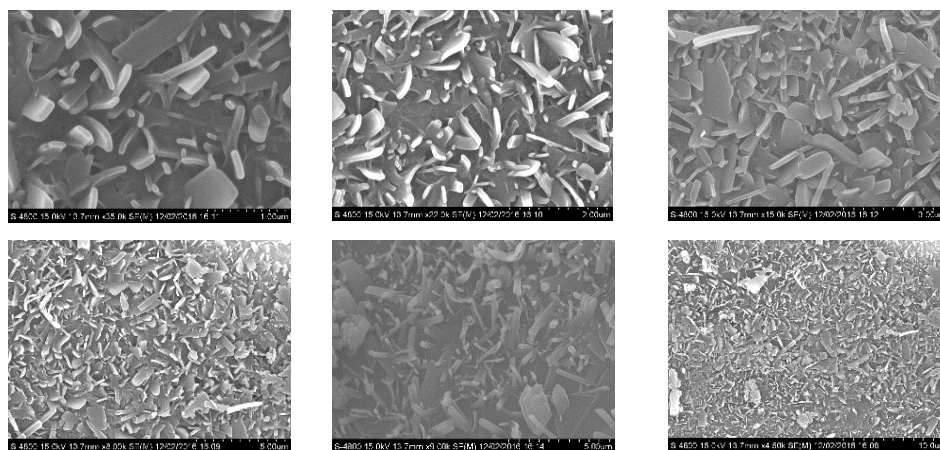
Figure 4.20(a): FE-SEM images of PHMn(III) complex at different magnifications


```
El  AN   Series    unn. C  norm. C  Atom. C  Error (1 Sigma)
                    [wt.%]  [wt.%]   [at.%]           [wt.%]
------------------------------------------------------------
H   1    K-series    0.02    0.02     0.24             0.03
C   6    K-series   62.27   62.27    69.63            10.10
N   7    K-series   13.27   13.27    12.72             5.86
O   8    K-series   19.23   19.23    16.14             5.41
Mn 25    K-series    5.21    5.21     1.27             0.39
------------------------------------------------------------
         Total:    100.00  100.00   100.00
```
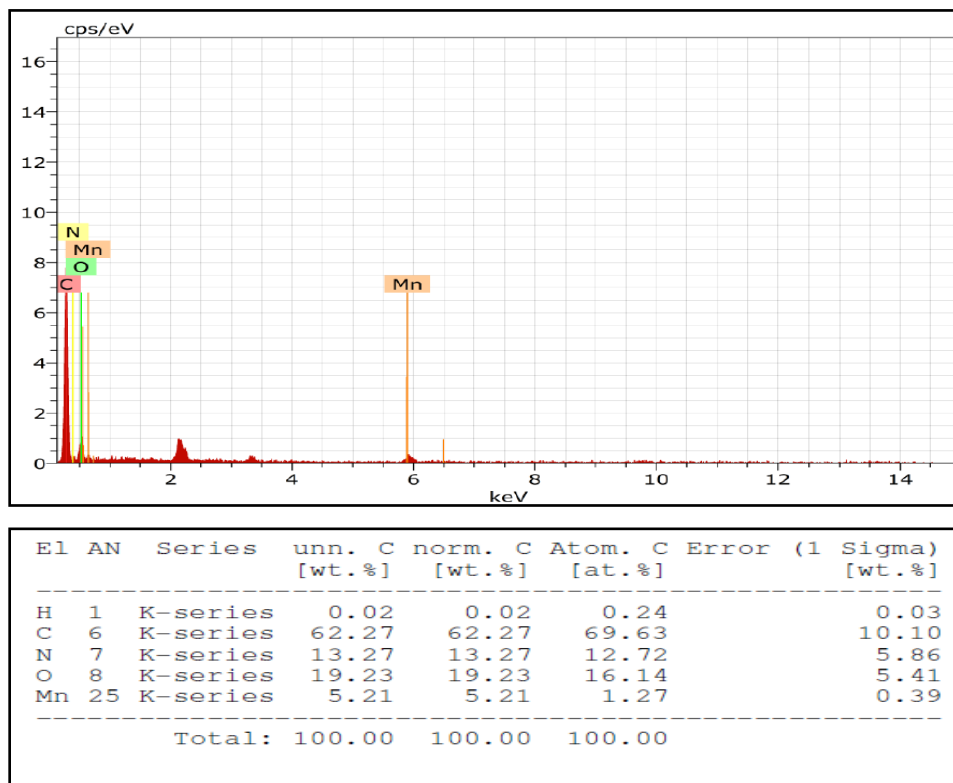
Figure 4.20(b): EDX analysis of PHMn(III) complex
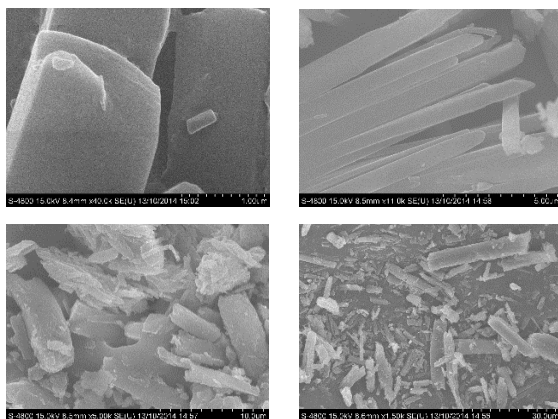
Figure 4.21(a): FE-SEM images of PHCo(II) complex at different magnifications

El	AN	Series	unn. C [wt.%]	norm. C [wt.%]	Atom. C [at.%]	Error (1 Sigma) [wt.%]
C	6	K-series	55.18	70.42	86.11	7.54
O	8	K-series	9.16	11.69	10.74	2.05
Co	27	K-series	8.17	10.43	2.60	0.43
Au	79	M-series	5.85	7.46	0.56	0.31
		Total:	78.36	100.00	100.00	
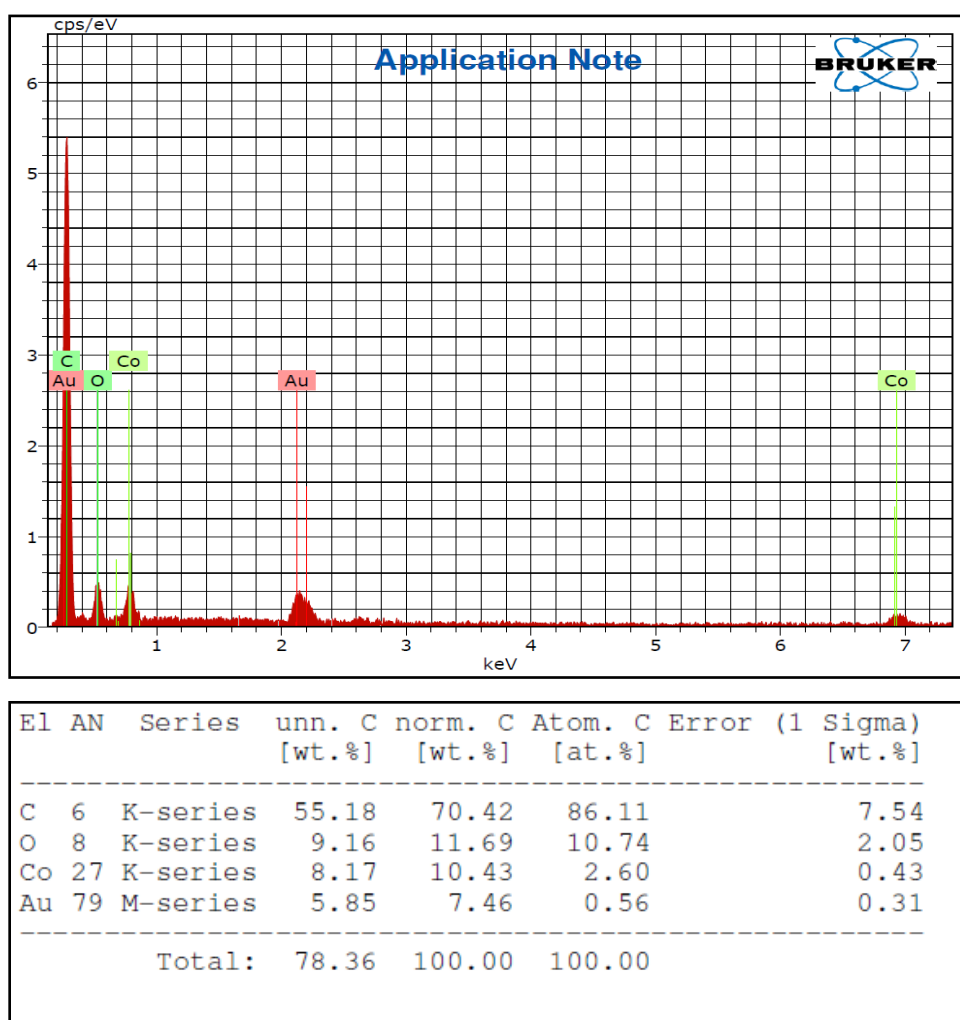
Figure 4.21(b): EDX analysis of PHCo(II) complex
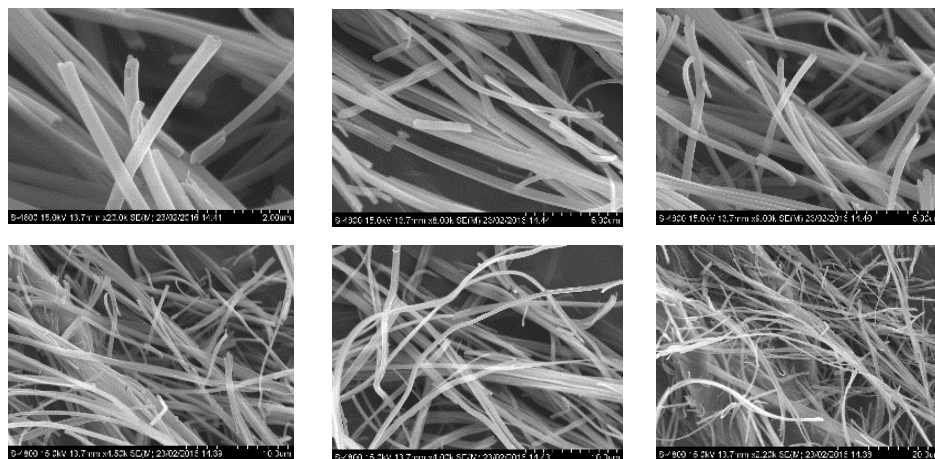
Figure 4.22(a): FE-SEM images of PHNi(II) complex at different magnifications
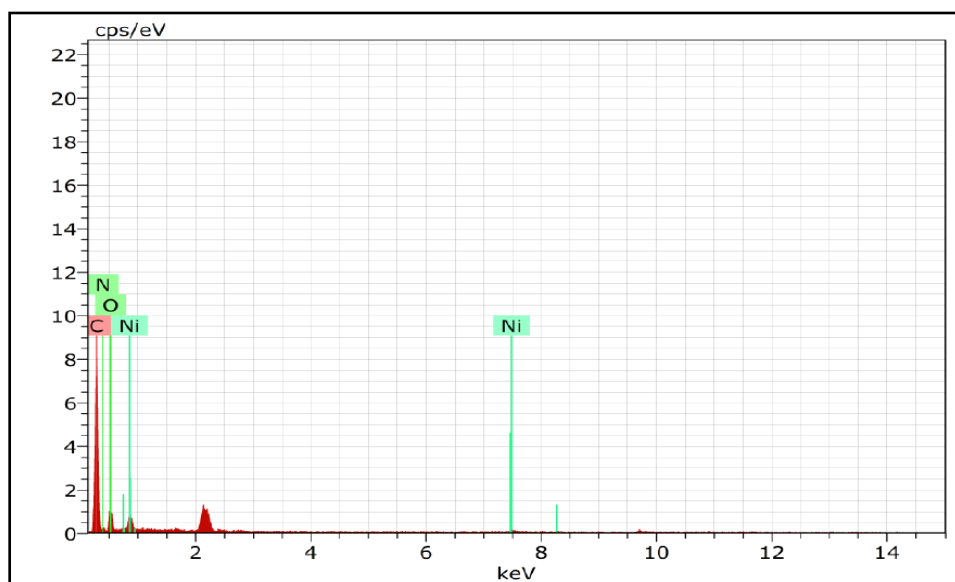

```
El  AN   Series   unn. C norm. C Atom. C Error (1 Sigma)
                  [wt.%]   [wt.%]   [at.%]          [wt.%]
    ------------------------------------------------------
H   1   K-series   0.02     0.02     0.24            0.03
C   6   K-series  61.80    61.80    69.42            9.49
N   7   K-series  12.50    12.50    12.04            4.88
O   8   K-series  20.22    20.22    17.05            4.95
Ni 28   K-series   5.47     5.47     1.26            0.46
    ------------------------------------------------------
        Total: 100.00   100.00   100.00
```

Figure 4.22(b): EDX analysis of PHNi(II) complex
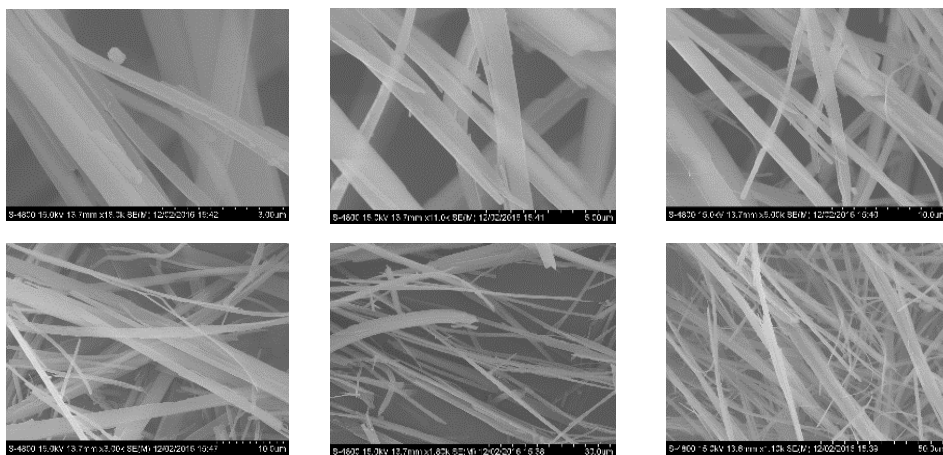
Figure 4.23(a): FE-SEM images of PHCu(II) complex at different magnifications


```
El AN   Series   unn. C norm. C Atom. C Error (1 Sigma)
                 [wt.%]  [wt.%]  [at.%]        [wt.%]
-------------------------------------------------------------
H  1  K-series    0.04    0.04    0.49          0.03
C  6  K-series   65.63   65.63   73.30         10.57
N  7  K-series   13.57   13.57   12.99          5.97
O  8  K-series   14.08   14.08   11.81          4.40
Cu 29 K-series    6.68    6.68    1.41          0.68
-------------------------------------------------------------
      Total: 100.00  100.00  100.00
```
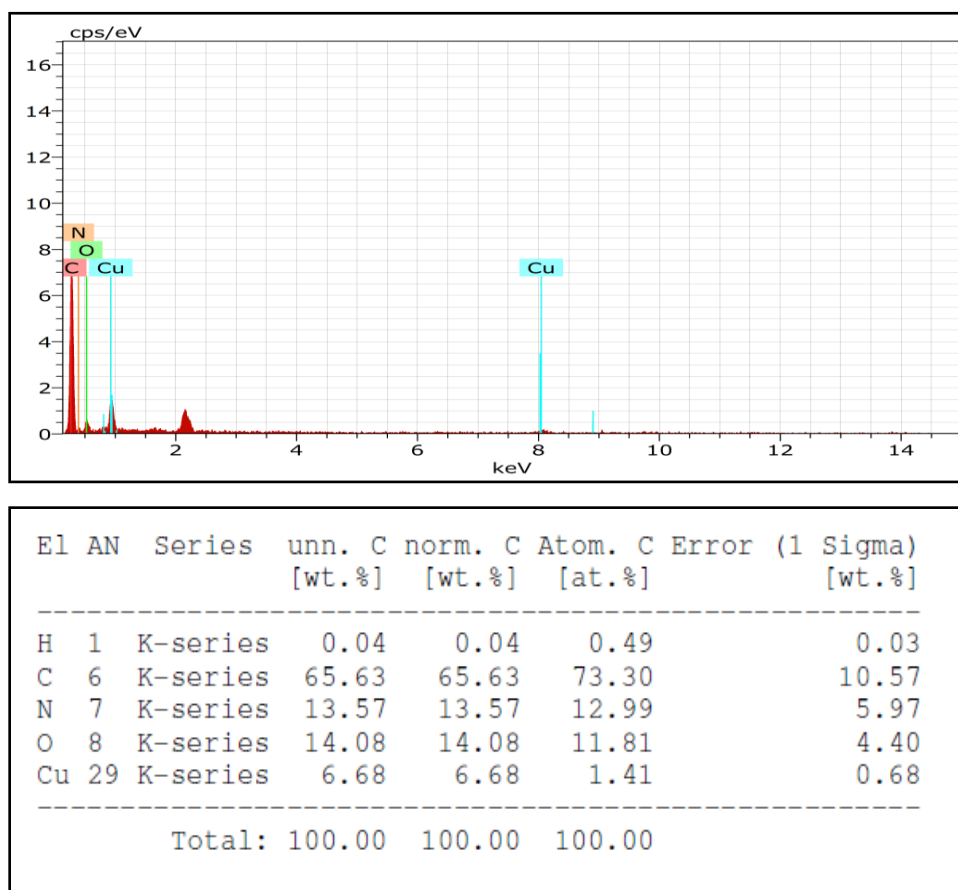
Figure 4.23(b): EDX analysis of PHCu(II) complex

4.5.10 Single crystal X-ray crystallography studies

Yellow colored crystal of PH ligand of suitable size $0.23 \times 0.22 \times 0.21$ mm^3 was mounted on 'Bruker APEX-II CCD' diffractometer equipped with graphite monochromated Mo Kα radiation in the wavelength of 0.71073 Å at room temperature. The summary of crystallographic parameters, data collection and refinement are given in **Table 4.7**. The single crystal of the schiff base demonstrated the monoclinic system having P2$_1$ space group with two molecules in the unit cell. The ORTEP diagram with numbering and crystal packing diagram are shown in the **Figures 4.24 and 4.25** respectively. The selected bond lengths and bond angles are depicted in **Table 4.8,** while, the hydrogen bonding parameters are given in **Table 4.9**. The crystal structure of the symmetric schiff base ligand represented, N1-C15 and C8-N2 distances as 1.286(8) Å and 1.277(8) Å respectively for C=N double bonding. The two C4-O1 and C21-O2 having bond distances 1.339(8) Å and 1.349(8) Å respectively illustrated the C-O phenolic single bond. The intramolecular hydrogen bonding formed by the H1—O1—N2 and H2—O2—N1, has distances 2.617 and 2.579 Å respectively. There is no solvent molecule appearing in the structure. From this crystal structure study, it is confirmed that the symmetric schiff base having two imine nitrogen atoms and two phenolic oxygen as potential donor atoms (N1,N2,O1,O2) has been successfully synthesized and suggests that this ligand can easily act as tetradentate donor to prepare different metal complexes [28-29].
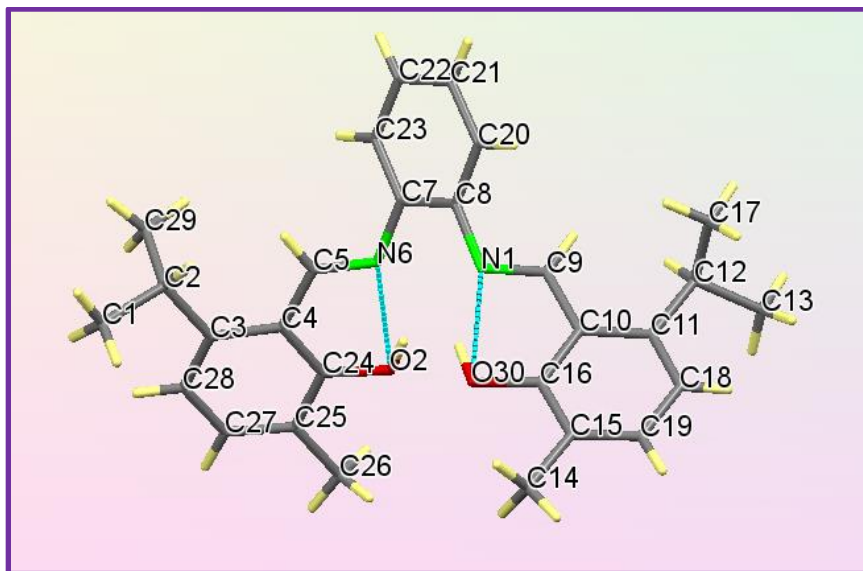
Figure 4.24: ORTEP diagram of PH ligand with atomic labeling

CCDC No. for PH ligand= 1443334
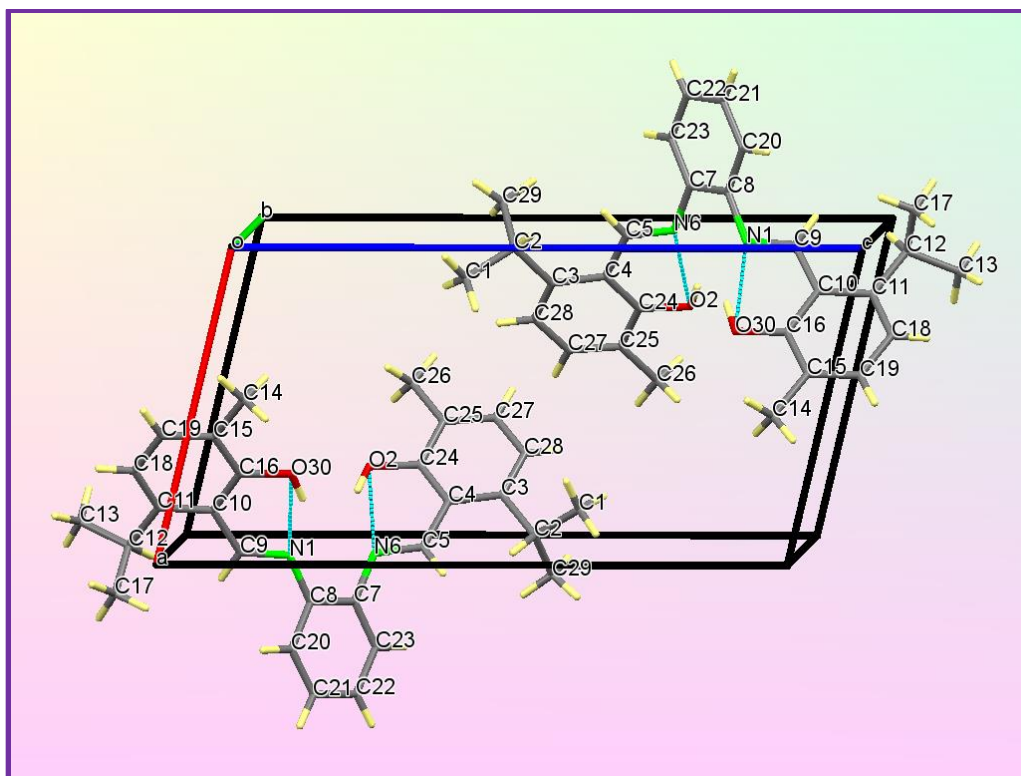
Figure 4.25: Crystal packing diagram viewed along b axis with O—H--N intramolecular hydrogen bonding is shown as a light blue dashed line.

Table 4.7: Crystallographic parameters, data collection and refinement for PH ligand

Empirical formula	$C_{28}H_{32}N_2O_2$
Formula weight	428.55
Temperature/K	296.15
Crystal system	monoclinic
Space group	$P2_1$
a/Å	8.561(2)
b/Å	8.705(2)
c/Å	16.556(4)
α/°	90
β/°	103.736(11)
γ/°	90
Volume/Å^3	1198.6(5)

Z	2
$\rho_{calc}g/cm^3$	1.187
μ/mm^{-1}	0.074
F(000)	460.0
Crystal size/mm^3	$0.23 \times 0.22 \times 0.21$
Radiation	MoKα (λ = 0.71073)
2Θ range for data collection/°	2.532 to 50
Index ranges	-10 ≤ h ≤ 10, -10 ≤ k ≤ 10, -19 ≤ l ≤ 19
Reflections collected	16503
Independent reflections	4178 [R_{int} = 0.0816, R_{sigma} = 0.0720]
Data/restraints/parameters	4178/1/297
Goodness-of-fit on F^2	1.127
Final R indexes [I>=2σ (I)]	R_1 = 0.1051, wR_2 = 0.2745
Final R indexes [all data]	R_1 = 0.1275, wR_2 = 0.2945
Largest diff. peak/hole / e Å^{-3}	0.92/-0.29
Flack parameter	-1.2(10)

Table 4.8: Selected bond lengths/Å and angles/ ° for PH Ligand

Bond Lengths		Bond Angles	
C8-N2	1.277(8)	O1-C4-C3	123.1(6)
N1-C15	1.286(8)	O2-C21-C16	121.5(6)
N2-C9	1.422(8)	N2-C8-C3	124.1(6)
N1-C14	1.422(9)	N1-C15-C16	122.0(6)
O1-C4	1.339(8)	C8-N2-C9	118.6(6)
C21-O2	1.349(8)	C15-N1-C14	115.5(6)

Table 4.9: The intramolecular hydrogen bonds and angles of PH ligand.

D-H…A	d(D-H)	d(H…A)	d(D…A)	<(D-H…A)
O2-H2...N1	0.820	1.847	2.580	148.10
C27-H27B...O1	0.960	2.895	3.819	161.80
C24-H24B...O2	0.960	2.916	3.841	161.93
C12-H12...O2	0.930	2.867	3.717	152.52

Equivalent positions: x,y,z ; -x-2,+y-1/2,-z-1; -x-2,+y+1/2,-z; x-1,+y,+z

4.6 Biological activities

4.6.1 Protocol for antibacterial activity

Protocol for antibacterial activity are same as described in chapter 2 and section 2.5.1

4.6.2 Results of antibacterial activities study

The results of preliminary antibacterial testing of PH ligand and its metal complexes are shown in **Table 4.10**. The MIC values of PH ligand (102 µg/ml), PHMn(III) (111 µg/ml) against *E. Coli* possesses identical to standard drug ampicillin. The MIC values of PHNi(II) (63 µg/ml) and PHCu(II) (74 µg/ml) complexes are slightly more than standard drug ampicillin against *E. coli*.

The MIC value of PH ligand (49 µg/ml) is half in comparison with the standard ampicillin against the *P. aeruginosa*. The MIC value of metal PHMn(III) (101 µg/ml) exhibited equivalent to ampicillin, however PHNi(II) (93 µg/ml) and PHCu(II) (85 µg/ml) were somewhat near about to the standard ampicillin against *P. aeruginosa*.

The MIC values of the PH ligand (63 µg/ml), PHMn(III) (81 µg/ml), PHNi(II) (230 µg/ml) and PHCu(II) (102 µg/ml) against *B. subtilis* exhibited the excellent ant bactericidal activity comparable to ampicillin as standard drug. However, the PH ligand, PHMn(III) and PHNi(II) complex also showed the closely parallel to standard drug ciprofloxacin.

The PH ligand (77 µg/ml), PHMn(III) (115 µg/ml), PHCo(II) (99 µg/ml) PHNi(II) (56 µg/ml) and PHCu(II) (74 µg/ml) showed relatively superb MIC values against the *S. aureus* with the reference ampicillin, meanwhile, PH ligand, PHNi(II) and PHCu(II) complexes also exhibited the nearly similar to Ciprofloxacin standard [30]. The graphical

representation of the results on antibacterial activities of synthesized PH ligand and its metal complexes is shown in **Figure 4.26.**

Table No. 4.10: Representation of antibacterial activity of PH ligand and its metal complexes

Compounds	*E. coli*	*P. aeruginosa*	*B. subtilis*	*S. aureus*
PH Ligand	102	49	63	77
PHMn(III)	111	101	81	115
PHCo(II)	168	170	230	99
PHNi(II)	63	93	74	56
PHCu(II)	74	85	102	74
Ciprofloxacin	25	25	50	50
Ampicillin	100	100	250	250
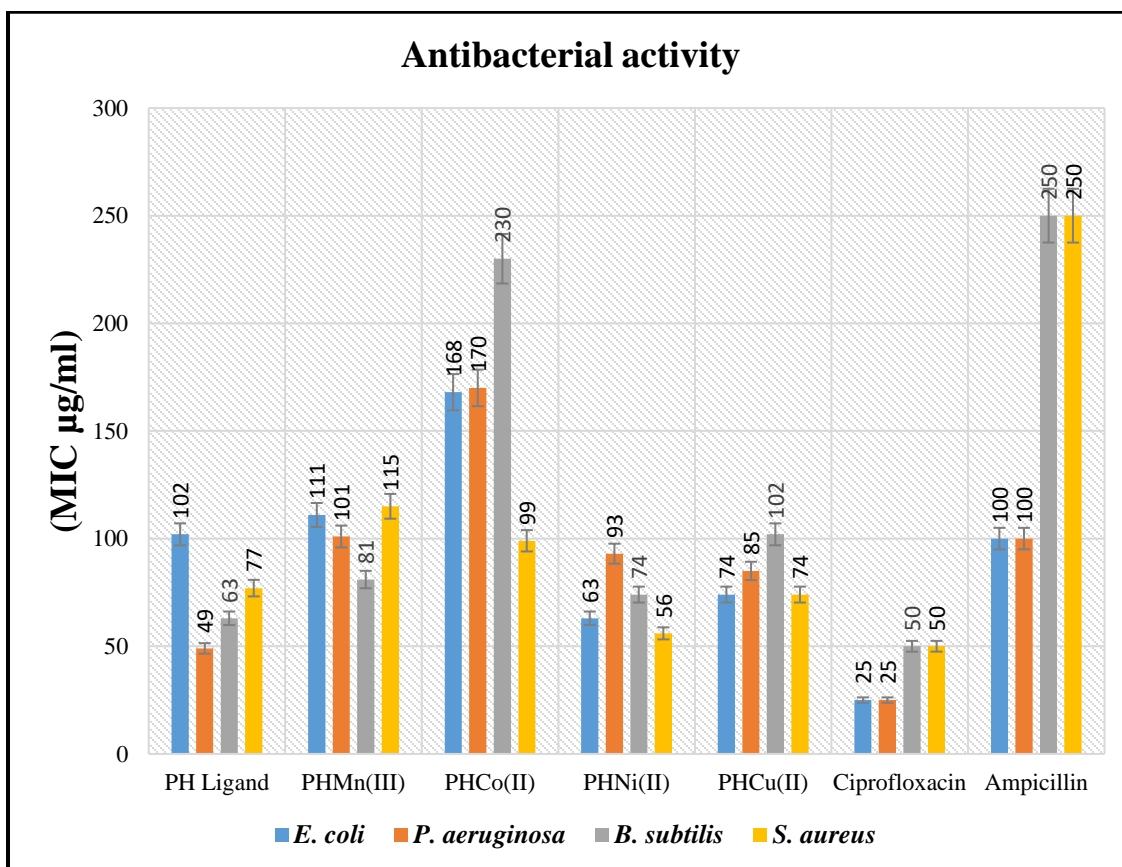
Figure 4.26: Graphical representation of antibacterial activity

4.6.3 Protocol for antifungal activity

Protocol for antifungal activity are same as described in chapter 2 and section 2.5.3

4.6.4 Results of antifungal activity

The antifungal activities results are précised in **Table 4. 11**. The antifungal activity was evaluated against different fungal strains such as C*andida albicans, Aspergillus flavus, Aspergillus niger and C. neoformans.* The PH ligand and its PHMn(III), PHCo(II), PHNi(II) and PHCu(II) complexes showed the negligible antifungal activity against all the mentioned fungal strains. The graphical representation of antifungal activities are shown in **Figures 4.27.**

Table 4.11: Representation of antifungal activity of PH ligand and its metal complexes

Compounds	*C. albicans*	*A. flavus*	*A. niger*	*C. neoformans*
PH Ligand	100	150	150	*
PHMn(III)	125	225	125	*
PHCo(II)	100	100	*	150
PHNi(II)	150	*	100	125
PHCu(II)	150	*	*	*
Fluconazole	25	12.5	25	25
Miconazole	12.5	6.25	12.5	6.25

* No activity reported up to 300 µg/ml
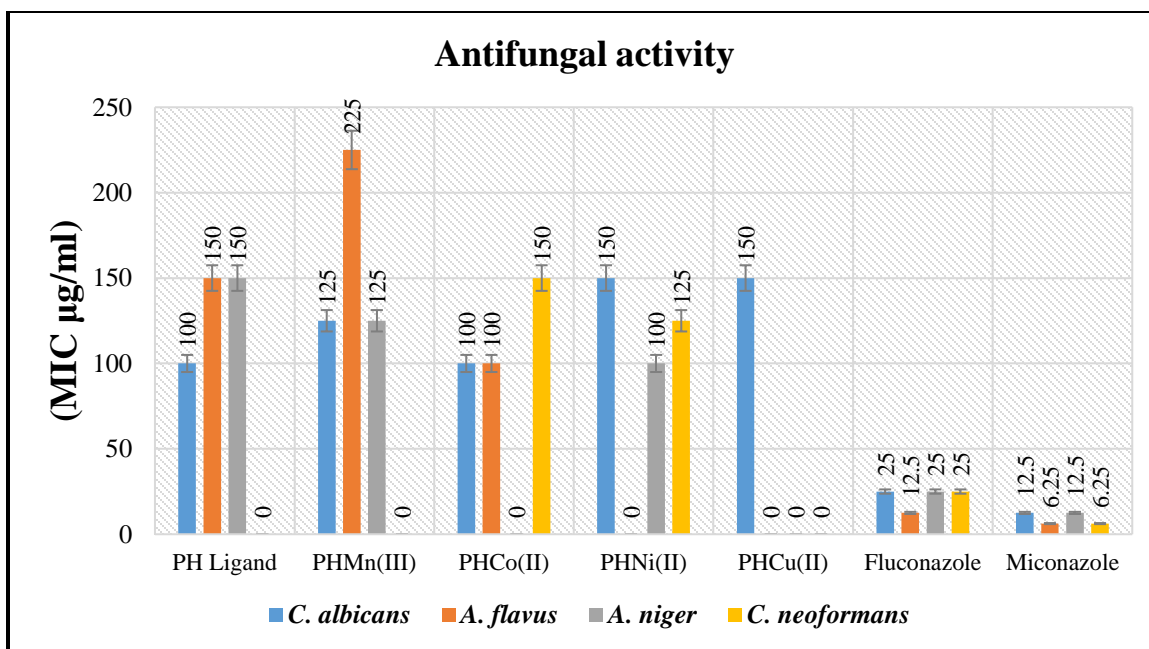
Figure 4.27: Graphical representation of antifungal activity

4.6.5 Protocol for antioxidant activity (DPPH radical scavenging activity)

Procedure: 100 ppm solution of DPPH in methanol was prepared and 1.0 ml of this solution was added to the dilutions of compound solution in water at different concentrations (10 ppm, 20 ppm, 40 ppm, 60 ppm, 80 ppm, 100 ppm). Thirty minutes later, the absorbance at 517 nm was measured. Ascorbic acid was used as standard. Lower absorbance of the reaction mixture indicates higher free radical scavenging activity [31, 32].

4.6.6 Results of antioxidant activity

The process of scavenging DPPH-free radicals has been used to assess the antioxidant activity of specific compounds [33]. DPPH is a stable free radical that can accept an electron or hydrogen radical and get converted to a stable, diamagnetic molecule. DPPH has an odd electron and has strong absorption band at 517 nm. When this electron becomes paired off, the absorption decreases stoichometrically with respect to the number of electrons or hydrogen atoms taken up. Such a change in the absorbance by this reaction has been extensively adopted to test the capacity of several molecules to act as free radical

scavengers. Hence, more rapidly the absorbance decreases, the more potent is the antioxidant activity of the compound [34].

Table 4.12: Representation of antioxidant activity of PH ligand and its metal complexes

Compounds	EC_{50}
PH Ligand	0.1142
PHMn(III)	0.1124
PHCo(II)	0.1172
PHNi(II)	0.1158
PHCu(II)	0.1135
Std (Ascorboc acid)	0.1200
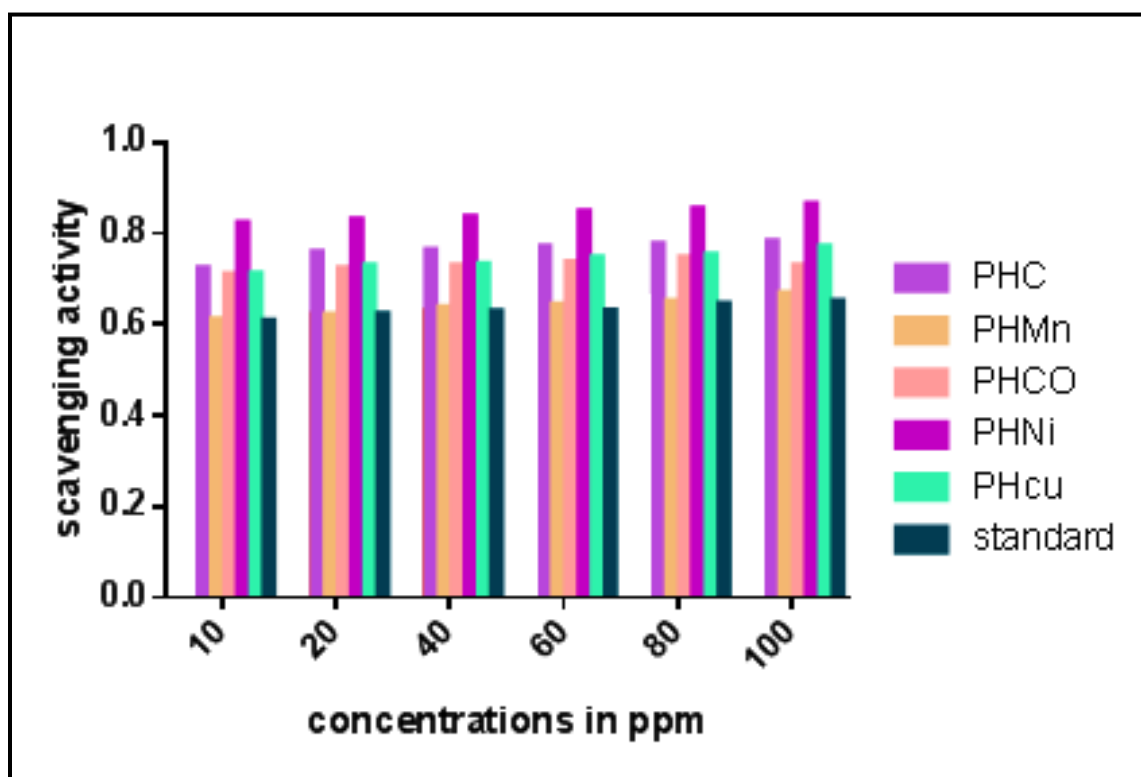
Figure 4.28: Graphical representation of antioxidant activity

The results indicate that all the compounds have comparable or better activity to that of standard ascorbic acid **(Table 4.13).** The PHMn(III) and PHCu(II) complex showed significantly higher antioxidant activity followed by PHNi(II) and PHCo(II) complexes at different concentrations. Graphically representation of antioxidant activitiea are shown in **Figure 4.28**.

4.6.7 DNA cleavage experiment
DNA cleavage experiment are same as described in chapter 2 and section 2.5.7

4.6.8 Results of DNA cleavage activity
The PH ligand and its PHMn(III), PHCo(II), PHNi(II) and PHCu(II) complexes could not show any type of DNA cleavage.

4.7 Conclusion
In this investigation we are reporting the synthesis and characterization of a new symmetrical salen based ligand and its Manganese(III), Cobalt(II), Nickel(II) and Copper(II) complexes. The single crystal structure of schiff base ligand has been solved by single X-ray crystallography which shows two imine nitrogen atoms and two phenolic oxygen as donor atoms and the schiff base act as tetradentate donor. The schiff base ligand and metal complexes were screened for their biological activities such as, in *vitro* antibacterial, antifungal, antioxidant and DNA cleavage activities.

The ligand and its all metal complexes exhibited superior antibacterial activity against all the selected bacterial strains except Cobalt(II) complex which showed the near about comparable activity to ampicillin standard drug against the *E. coli* and *P. aeruginosa*. All the compounds showed inferior antifungal and DNA cleavage activity. The manganese(III) and copper(II) complexes showed good antioxidant activity as compared to the standard drug (ascorbic acid).

4.8 References

1. Whiteoak CJ, Salassa G, Kleij AW, Chemical Society Reviews, 41 (2012) 622-631.

2. Budige G, Puchakayala MR, Kongara SR, Hu A, Vadde R, Chemical and Pharmaceutical Bulletin, 59 (2011) 166-171.

3. Yimer AM, Modern Chemistry & Applications, (2014).

4. Akila EK, Usharani MA, Rajavel RA, International Journal of Pharmacy and Pharmaceutical Sciences, 5 (2013) 573-581.

5. Djebbar-Sid S, Benali-Baitich O, Deloume JP, Transition Metal Chemistry, 23 (1998) 443-447.

6. Klement R, Stock F, Elias H, Paulus H, Pelikan P, Valko M, Mazur M, Polyhedron, 18 (1999) 3617-3628.

7. Niederhoffer EC, Timmons JH, Martell AE, Chemical Reviews, 84 (1984) 137-203.

8. Martell AE, Sawyer DT, Oxygen Complexes and Oxygen Activation by Transition Metals, (1988).

9. Holm RH, Chemical Reviews, 87 (1987) 1401-1449.

10. Dixit PS, Srinivasan K, Inorganic Chemistry, 27 (1988) 4507-4509.

11. Singh P, Goel RL, Singh BP. J. Indian Chem. Soc, 52 (1975) 958-959.

12. Mohindru A, Fisher JM, Rabinovitz M, Nature, 303 (1983) 64-65.

13. Raman N, Raja YP, Kulandaisamy A, Indian Academy of Sciences, 113 (2001) 183-190.

14. Lashanizadegan M, Boghaei DM, Shivapour Z, Seraj S, Synthesis and Reactivity in Inorganic, Metal-Organic, and Nano-Metal Chemistry, 40 (2010) 373-377.

15. Kavitha P, Reddy KL, Arabian Journal of Chemistry, 9 (2016) 596-605.

16. Youssef NS, El-Zahany EA, Barsoum BN, El-Seidy AM, Transition metal chemistry, 34 (2009) 905-914.

17. Temel H, Şekerci M, Synthesis and Reactivity in Inorganic and Metal-Organic Chemistry, 31 (2001) 849-857.

18. Dutta R L, and Syamal A 1992, Elements of Magnetochemistry 2nd edn (New Delhi: Elsvier).

19. Ray A, Banerjee S, Rosair GM, Gramlich V, Mitra S, Structural Chemistry, 19 (2008) 459-465.

20. Rabindra Reddy P, Shilpa A, Chemistry & biodiversity, 8 (2011) 1245-1265.

21. Mohamed GG, Omar MM, Hindy AM, Spectrochimica Acta Part A: Molecular and Biomolecular Spectroscopy, 62 (2005) 1140-1150.

22. Klement R, Stock F, Elias H, Paulus H, Pelikan P, Valko M, Mazur M, Polyhedron, 18 (1999) 3617-3628.

23. Raj BB, Kurup MP, Suresh E, Spectrochimica Acta Part A: Molecular and Biomolecular Spectroscopy, 71 (2008) 1253-1260.

24. El-Boraey HA, Emam SM, Tolan DA, El-Nahas AM, Spectrochimica Acta Part A: Molecular and Biomolecular Spectroscopy, 78 (2011) 360-370.

25. El-Tabl AS, El-Saied FA, Plass W, Al-Hakimi AN, Spectrochimica Acta Part A: Molecular and Biomolecular Spectroscopy, 71 (2008) 90-99.

26. Hathaway B, Billing DE, Coordination Chemistry Reviews, 5 (1970) 143-207.

27. Raman N, Ravichandran S, Synthesis and Reactivity in Inorganic, Metal-Organic, and Nano-Metal Chemistry, 35 (2005) 439-444.

28. Rodríguez-Doutón MJ, Fernández MI, González-Noya AM, Maneiro M, Pedrido R, Romero MJ, Synthesis and Reactivity in Inorganic, Metal-Organic and Nano-Metal Chemistry, 36 (2006) 655-662.

29. Mota VZ, de Carvalho GS, Corbi PP, Bergamini FR, Formiga AL, Diniz R, Freitas MC, da Silva AD, Cuin A, Spectrochimica Acta Part A: Molecular and Biomolecular Spectroscopy, 99 (2012) 110-115.

30. Pandya JH, Jadeja RN, Ganatra KJ, Journal of Saudi Chemical Society, 18 (2014) 190-199.

31. Chandrappa CP, Govindappa M, Kumar AN, Applied Cell Biology, 2 (2013) 52-57.

32. Dery RE, Mathison R, Davison J, Befus AD, International archives of allergy and immunology, 124 (2001) 201-204.

33. Bilgicli AT, Tekin Y, Alici EH, Yaraşir MN, Arabaci G, Kandaz M, Journal of Coordination Chemistry, 68 (2015) 4102-4116.

34. Harinath Y, Reddy DH, Kumar BN, Apparao C, Seshaiah K, Spectrochimica Acta Part A: Molecular and Biomolecular Spectroscopy, 101 (2013) 264-272.

CHAPTER V

Synthesis and characterization of a novel schiff base of 1,2-diaminopropane with substituted salicyaldehyde and its transition metal complexes: single crystal structures and biological activities

5.1 Introduction

Compounds with azomethine functional group (-HC=N), typically known as schiff bases have been synthesized by the condensation of primary amines with active carbonyls (aldehyde or ketone) [1]. The presence of a lone pair of electrons in the sp^2 hybridized orbital of nitrogen atom of the azomethine group presents good chelating ability on schiff bases especially when combined with one or more donor atoms close to the azomethine group. This chelating ability of the schiff base combined with the ease of separation and flexibility in varying the chemical environment about the C=N group, makes schiff base interesting ligands in coordination chemistry [2]. Metal complexes of schiff bases derived from salicylaldehyde and diamine can increase the dimensionality of the system and can form supramolecular architectures through O–H---N and N–H---O type of hydrogen bonds [3]. Moreover, these complexes have remained an important and popular area of research due to their simple synthesis, versatility and diverse range of applications [4-10]. Tetradentate schiff bases with a N_2O_2 donor atom set are well known to coordinate with various metal ions, and have many applications in the organic and inorganic fields [11-16]. Their metal complexes possess effective antibacterial, antifungal [17], antioxidant [18], anticancer [19, 20], anti-inflammatory [21], DNA cleavage [22] and catalytic [23-27] properties, phosphorescence and electroluminescence [28]. Because of their wide applications area, schiff bases have been the focus of attention of scientists and hence the literature relating to schiff bases is extremely rich.

5.2 Experimental section

5.2.1 Chemicals and Solvents

Chemicals and Solvents are same as described in Chapter 2, section 2.2.1

5.2.2 Analytical methods

Analytical methods are same as described in Chapter 2, section 2.2.2

5.3 Synthesis of schiff base ligand 1,2-DP

Systematic route for the the synthesis of 1,2-DP ligand and its 1,2-DPMn(III), 1,2-DPCo(II), 1,2-DPNi(II) and 1,2-DPCu(II) complexes was carried by according to scheme described in **Figure 5.1**.

The 1,2-DP ligand was prepared by dropwise addition of ethanolic solution of propane-1,2-diamine (1 mmol, 0.074 gm,) to a constantly stirring warm solution of 2-hydroxy-6-isopropyl-3-methyl benzaldehyde (2 mmol, 0.356 gm) in ethanol. The resulting solution was refluxed for 2 hrs, the yellow solution, obtained was filtered, and allowed to cool. The yellow crystals formed were collected and washed with water at room temperature.

Analystical and spectral data of 1,2-DP ligand:

Colour: Yellow solid, Yield: 80 %. ^{1}H- NMR (CDCl$_3$, 400 MHz) (δ, ppm): 13.87 (brs, 2H, OH), 8.68 (d, 2H, J= 16 Hz, -HC=N), 7.08 (d, 2H, Ar, J= 8 Hz), 6.60-6.58 (dd, 2H, Ar, J= 4, 8 Hz), 4.01-3.97 (m, 1H, -CH), 4.72-3.68 (m, 1H, -CH), 4.61-3.56 (m, 1H, -CH), 3.25-3.18 (m, 1H, -CH$_2$), 2.18 (d, 6H, J= 8 Hz, 2CH$_3$), 1.45 (d, 3H, J= 8 Hz, CH$_3$), 1.18 (d, 6H, J= 8 Hz, 2CH$_3$), 1.02 (d, 6H, J= 4 Hz, 2CH$_3$). ^{13}C- NMR (CDCl$_3$, 400 MHz) (δ, ppm): 162.53, 160.34, 147.33, 133.74, 123.53, 114.24, 65.92, 65.29, 27.76, 23.52, 20.48, 15.52. UV-vis (DMF) λ_{max} (nm): 269, 333. FT-IR (KBr pellet, cm^{-1}) ν_{max}: 2965 (OH), 1612 (C=N), 1450 (C=C), 1249 (C-O). LC-MS (m/z): calcd 394.26; obsv 395.41. Anal. calcd for C$_{25}$H$_{34}$N$_2$O$_2$ (%): C 76.10, H 8.69, N 7.10; Found: C 77.20, H 8.45, N 7.51.

5.4 General procedure for the synthesis of metal complexes

The complexes were prepared by dropwise addition of ethanolic solution of the corresponding metal salts such as manganese acetate tetrahydrate, cobalt acetate tetrahydrate, nickel chloride hexahydrate and cupric acetate monohydrate (1 mmol) to the ethanolic solution of schiff base ligand (1 mmol) with constant stirring and the product was collected and washed with plenty of water and dried at room temperature.

5.4.1 Analytical and spectral data of 1,2-DPMn(III) complex

Colour: Brown, solid. Yield: 78%. UV-Vis (DMF) λ_{max} (nm): 270, 331, 471. FT-IR (KBr, pellet cm^{-1}) ν_{max}: 1598 (C=N), 1286 (C-O), 1382 (C=C), 524 (M-O), 474 (M-N). LC-MS (m/z): calcd 506.47, obsv 447.47. Anal. calcd for C$_{27}$H$_{35}$MnN$_2$O$_4$ (%): C 64.02, H 6.96, N, 5.53, Found: C 64.08, H 6.49, N 5.80. μ_{eff}: 4.21 B.M. Conductance ($\Lambda_{M,}$ Ω^{-1} cm^2 mol^{-1}) in DMF: 20.0.

5.4.2 Analytical and spectral data of 1,2-DPCo(II) complex

Colour: Shining reddish brown, solid. Yield: 71 %. UV-Vis (DMF) λ_{max} (nm): 264, 357, 420, 507. FT-IR (KBr pellet, cm^{-1}) ν_{max}: 1556 (C=N), 1224 (C-O), 1458 (C=C), 536 (M-O), 450 (M-N). LC-MS (m/z): calcd 451.47, obsv 451.1. Anal. calcd for $C_{25}H_{32}CoN_2O_2$ (%): C 66.51, H 7.14, N 6.20, Found: C 66.38, H 7.33, N 6.06. μ_{eff}: 1.33 B.M. Conductance (Λ_M, Ω^{-1} cm^2 mol^{-1}) in DMF: 5.5.

5.4.3 Analytical and spectral data of 1,2-DPNi(II) complex

Colour: Orange, solid. Yield: 79 %. UV-Vis (DMF) λ_{max} (nm): 264, 354, 426, 549. FT-IR (KBr pellet, cm^{-1}) ν_{max}: 1558 (C=N), 1226 (C-O), 1456 (C=C), 523 (M-O), 433 (M-N). LC-MS (m/z): calcd 451.23; obsv 451.28. Anal. calcd for $C_{50}H_{64}N_4Ni_2O_4$(%): C 66.54, H 7.14, N 6.20; Found: C 66.20, H 7.56, N 6.35. Conductance (Λ_M, Ω^{-1} cm^2 mol^{-1}) in DMF: 12.0.

5.4.4 Analytical and spectral data of 1,2-DPCu(II) complex

Colour: dark green, solid. Yield: 72 %. UV-Vis: (DMF) λ_{max} (nm): 287, 377, 561. FT-IR (KBr pellet, cm^{-1}) ν_{max}: 1566 (C=N), 1240 (C-O), 1454 (C=C), 613 (M-O), 487 (M-N). LC-MS (m/z): calcd 456.08, obsv 456.25. Anal. calcd for $C_{25}H_{32}CuN_2O_2$(%): C 65.84, H 7.07, N 6.14, Found: C 65.82, H 7.01, N 5.98. μ_{eff}: Diamagnetic, Conductance (Λ_M Ω^{-1} cm^2 mol^{-1}): 17.8.
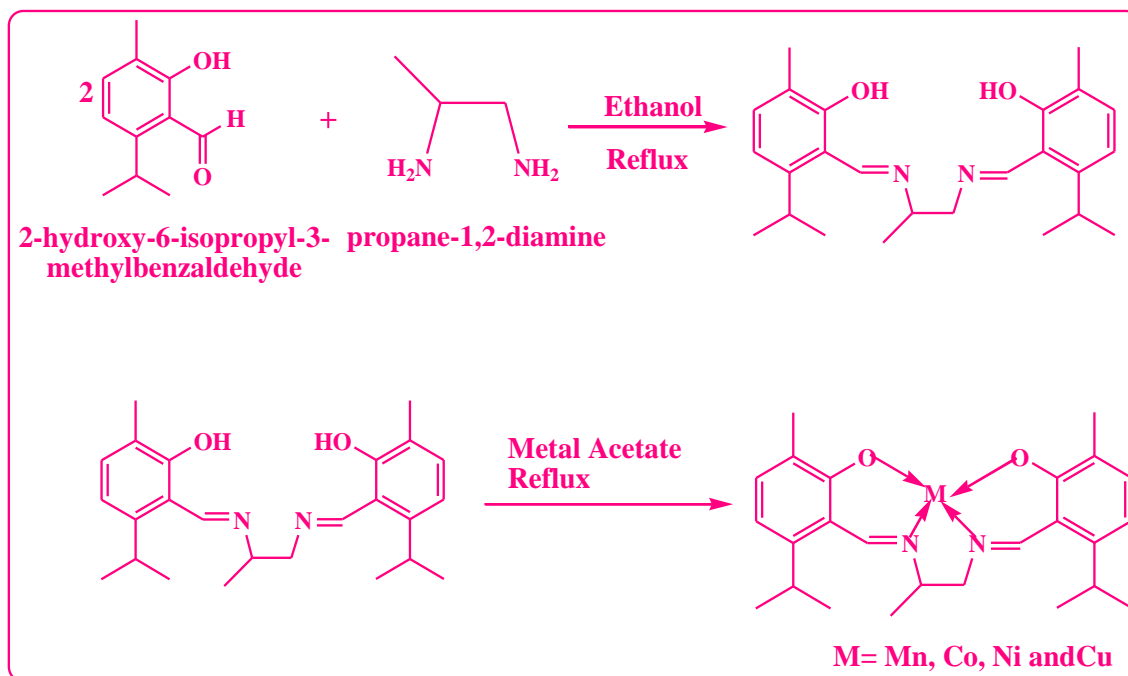
Figure 5.1: Synthesis of 1,2-DP ligand and its metal complexes.

5.5 Characterization of 1,2-DP ligand and its DPMn(III), DPCo(II), DPNi(II) and DPCu(II) metal complexes

All the synthesized compounds have been characterized through sophisticated techniques such as, UV-visible, FT-IR, NMR, LC-MS, elemental analysis ESR. Magenetic susceptibility, conductivity measurements, SEM analysis and finally the single crystal X-ray diffraction techniques and the results are discussed below.

5.5.1 NMR Spectra

The ^{1}H & ^{13}C NMR spectra of 1,2-DP schiff base ligand are shown in Figure 5.2 and Figure 5.3 respectively. Their δ values are represented in Table 5.1.

In the ^{1}H-NMR spectra, the broad peak at δ 13.87 corresponds to phenolic -OH group. The doublet peak appearing at δ 8.68 are assigned to 2H for (-HC=N). The peak values in the range δ 6.58- 6.60 refer to the aromatic region. The multiplet signals appearing at δ 4.01-3.97 are due to 1H, (-CH isopropyl's group) and another multiplet signal appearing at δ 4.72- 3.68 are of 1H, (-CH isopropyl's group). The multiplet exhibited at δ 4.61- 3.56 for (-CH$_2$). The signal appear for the methyl protons at δ 2.18 (6H, 2(CH$_3$)). The doublet peak

appear for 3H(CH$_3$) at δ 1.45. The doublet peak δ 1.18 appearing for 6H (2-CH$_3$) and another doublet peak appearing at 6H (2-CH$_3$).

Table 5.1: NMR spectral data of 1,2-DP ligand

Compounds	Assignments of peaks δ ppm
^{1}H-NMR (400 MHz, CDCl$_3$) (δ, ppm):	13.87 (brs, 2H, OH), 8.68 (d, 2H, J= 16 Hz, HC=N), 7.08 (d, 2H, Ar-CH, J= 8Hz), 6.60- 6.58 (dd, 2H, Ar-CH, J=8 Hz), 4.01-3.97 (m, 1H, -CH), 4.72- 3.68 (m, 1H, -CH), 4.61-3.56 (m, 1H, -CH$_2$), 2.18 (d, 6H, J= 8 Hz, 2 CH$_3$), 1.45 (d, 3H, J= 8 Hz, CH$_3$), 1.18 (d, 6H, J= 8Hz, 2 (CH$_3$)), 1.02(d, 6H, J= 4Hz, 2(CH$_3$)).
^{13}C-NMR (400 MHz, CDCl$_3$) (δ, ppm):	162.53, 160.34, 147.33, 133.74, 123.53, 114.24, 65.92, 65.29, 27.76, 23.52, 20.48, 15.52.
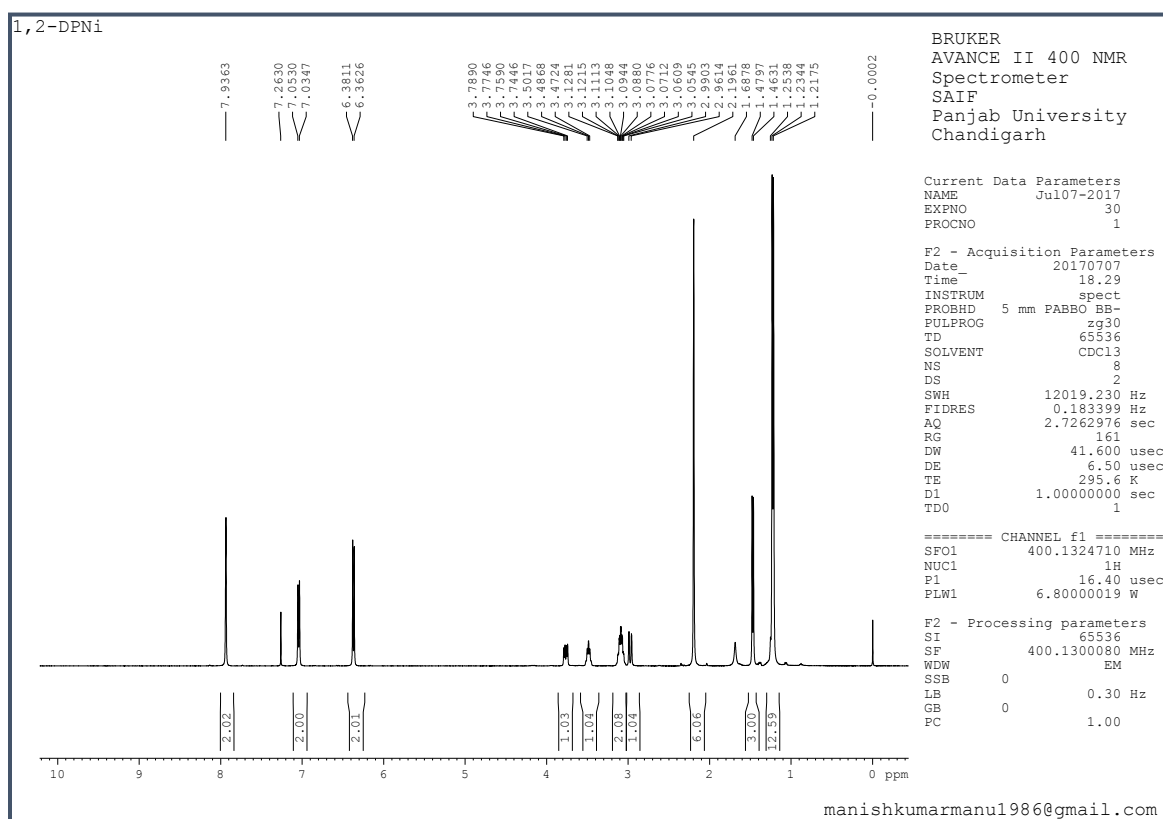
Figure 5.2:. ^{1}H-NMR spectrum of 1,2-DP ligand
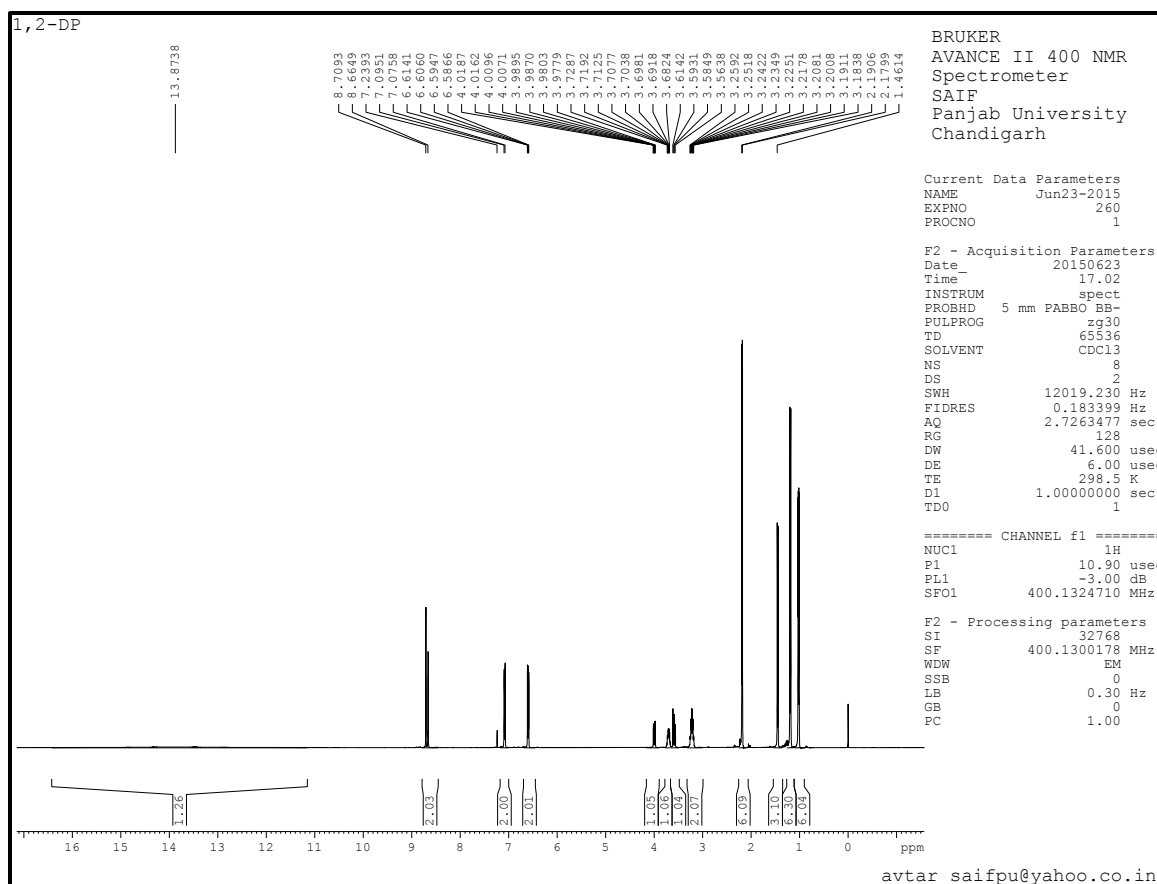
Figure 5.3:. ^{13}C-NMR spectrum of 1,2-DP ligand

5.5.2 UV-Visible spectra

The UV-Visible spectra of the 1,2-DP ligand and its metal complexes are listed in **Figures 5.4-5.8** and the spectral data are represented in **Table 5.2**. The UV-Visible spectra in DMF solution showing absorption of high energy 265-280 nm and 340- 490 nm are assigned to the intraligand π→π* and n→π* transitions respectively [29]. For cobalt(II) and nickel(II) complexes, d-d transition appeared below 600 nm, which is the characteristic feature of square planar structure [30]. A well-defined absorption in the region 561 nm corresponding to a d–d transition is assigned to a square planar copper(II) complex [31].

Table 5.2: UV-Visible spectral data of 1,2DP ligand its metal complexes

Compounds	Wavelength (nm)
1,2-DP Ligand	269, 333
1,2-DPMn(III)	270, 331, 471
1,2-DPCo(II)	264, 357, 420, 507
1,2-DPNi(II)	264, 354, 426, 549
1,2-DPCu(II)	287, 377, 561
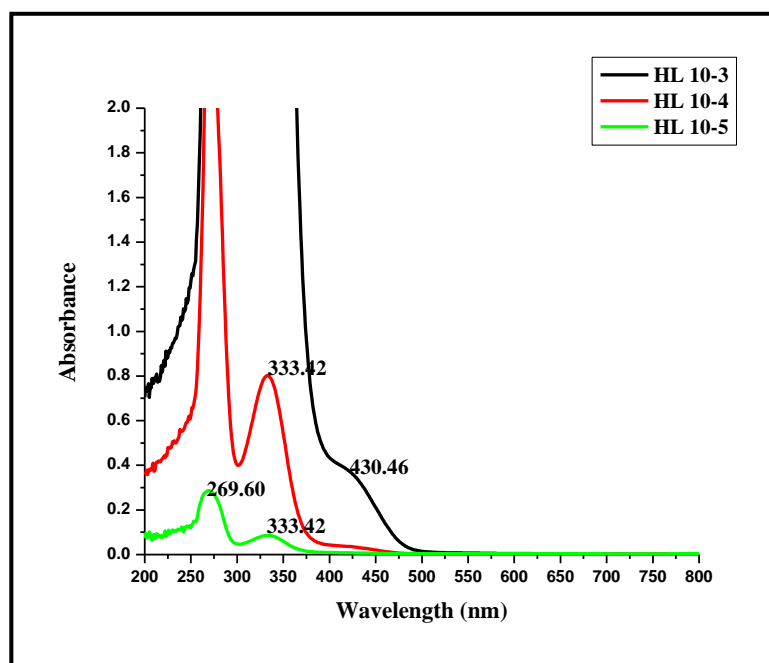
Figure 5.4: UV- Visible spectrum of 1,2-DP ligand
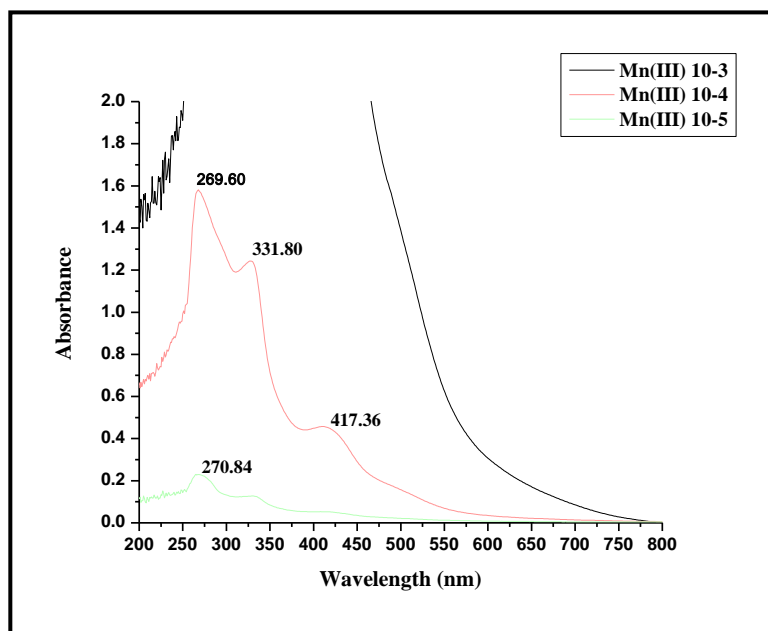
Figure 5.5: UV-Visible spectrum of 1,2- DPMn(III) complex
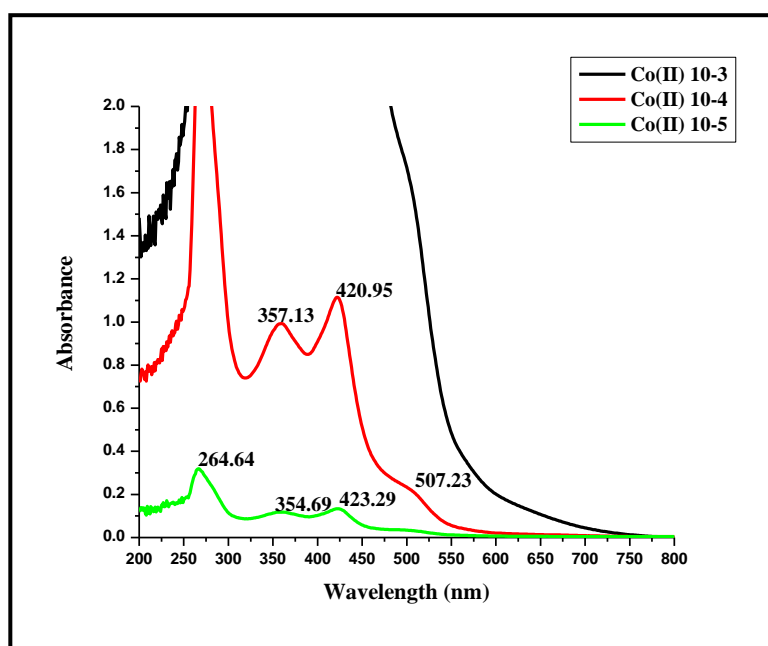
Figure 5.6: UV-Visible spectrum of 1,2-Co(II) complex
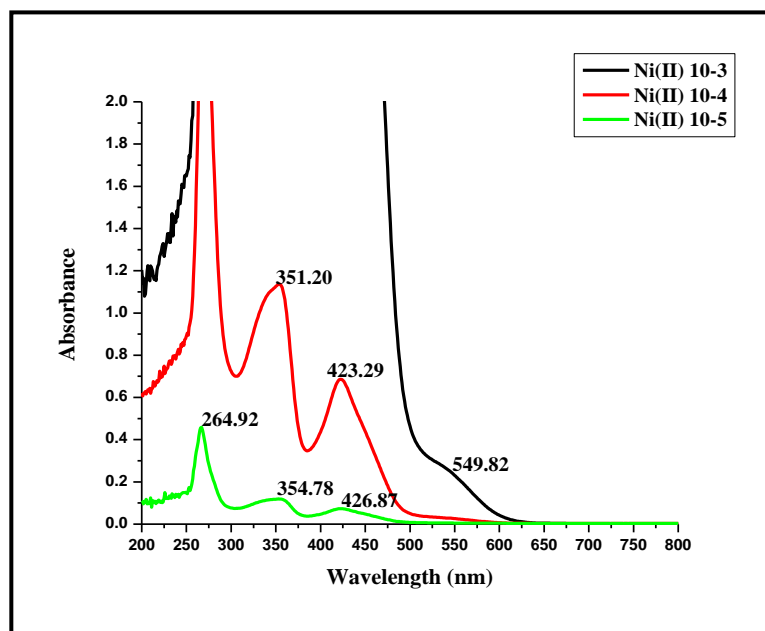
Figure 5.7: UV-Visible spectrum of 1,2-DPNi(II) complex
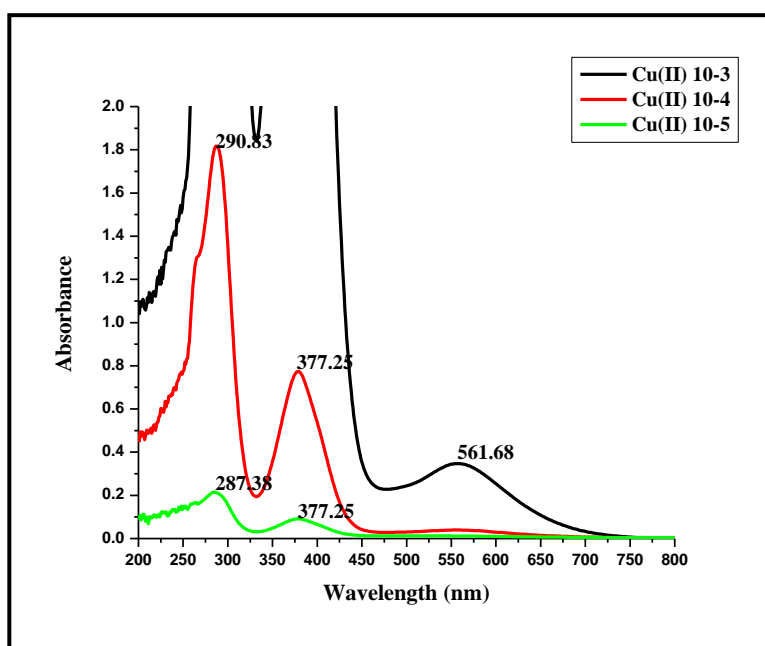
Figure 5.8: UV-Visible spectrum of 1,2-Cu(II) complex

5.5.3 FT-IR Spectra

Table 5.3 summarizes the absorption bands in IR spectra of 1,2-DP ligand and ita metal complexes and the spectra for 1,2-DP, 1,2-DPMn(III), 1,2-DPCo(II), 1,2-DPNi(II) and 1,2-DPCu(II) complexes are shown in **Figures 5.9-5.13**.

The FT-IR spectrum of the 1,2-DP ligand shows a band at 3417 cm^{-1} which is assigned to the phenolic OH group and its frequency was found to disappear in the complexes. A band at 1612 cm^{-1} region is assigned to C=N absorption, this band of ligand undergoes small shifts to lower frequencies and fall in the range 1598-1566 cm^{-1} in the spectra of the complexes indicating coordination of the imine nitrogen [32, 33]. Additional evidence for coordination of oxygen (M-O) and nitrogen (M-N) is the presence of the bands in the range 523- 673 and 433- 487 cm^{-1} respectively which is in agreement with the literature [34].

Table 5.3: FT-IR sprectral data of 1,2-DP ligand and its metal complexes

Compounds	Spectral bands cm^{-1}
1,2-DP Ligand	2956, 2594, 1612, 1512, 1390, 1249, 1043
1,2-DPMn(III)	2964, 2694, 2509, 1880, 1680, 1598, 1564, 1406, 1323, 1228, 1047, 875, 817, 740, 626, 524, 474
1,2-DPCo(II)	2960, 1614, 1566, 1458, 1396, 1327, 1224, 1047, 969, 810, 666, 536
1,2-DPNi(II)	2958, 2877, 1604, 1560, 1452, 1425, 1348, 1296, 1234, 1114, 1020, 806, 659, 634, 557, 474, 432
1,2-DPCu(II)	1618, 1558, 1456, 1344, 1226, 1112, 1069, 933, 962, 806, 646, 532, 443
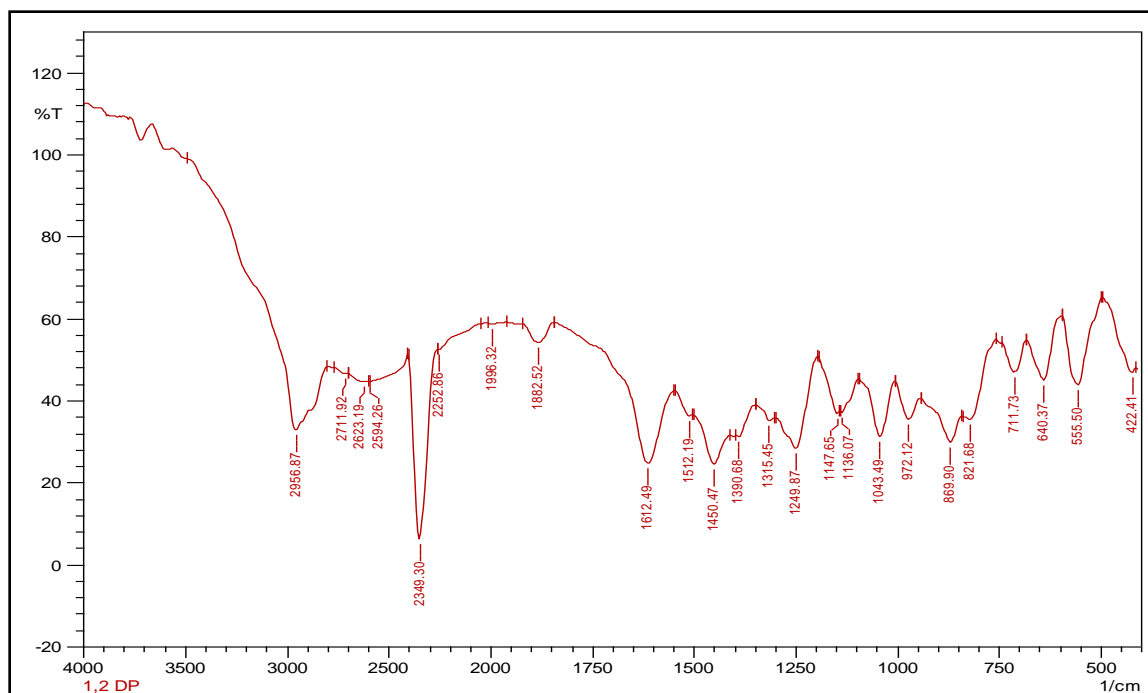
Figure 5.9: FT-IR spectrum of 1,2-DP ligand
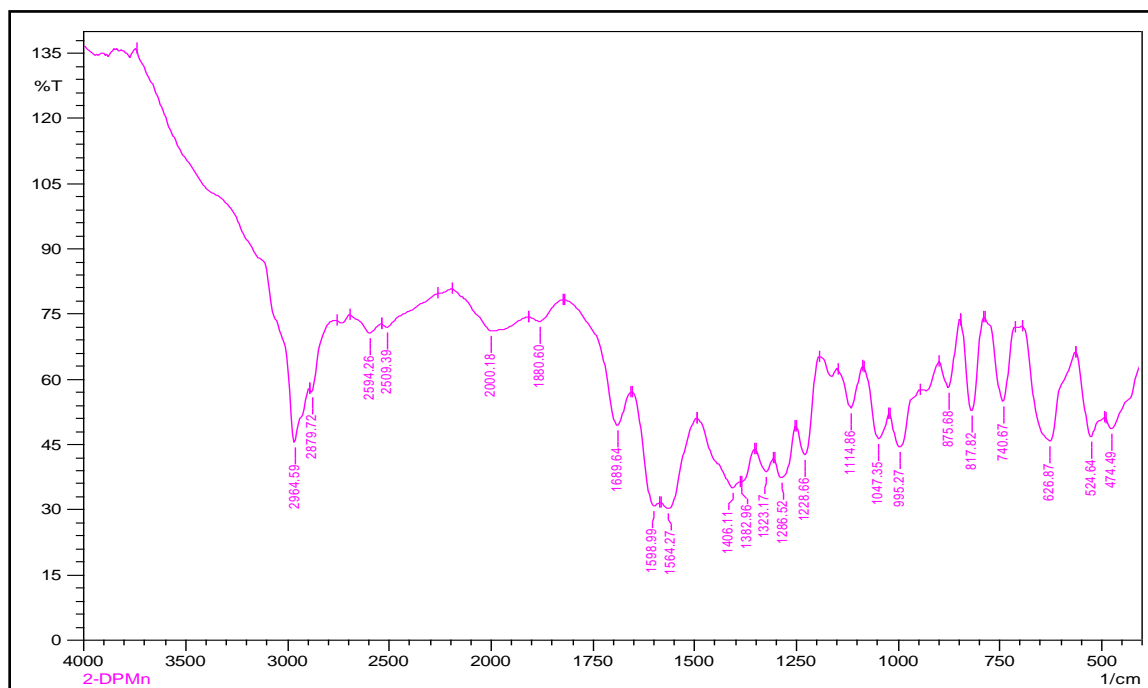
Figure 5.10: FT-IR spectrum of 1,2-DPMn(III) complex
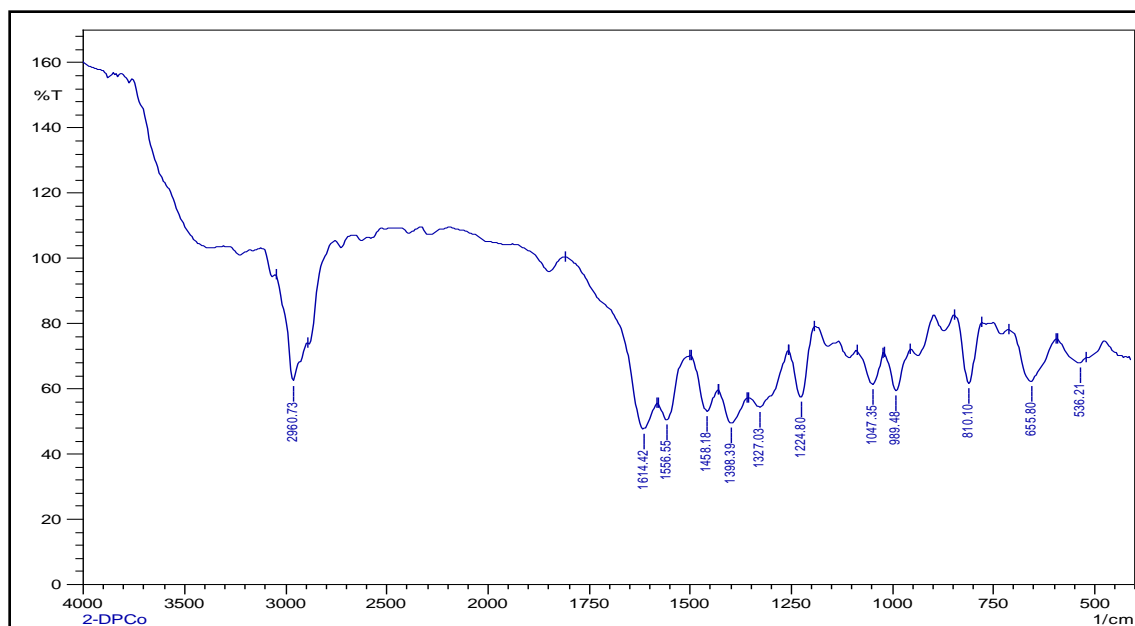
Figure 5.11: FT-IR spectrum of 1,2-DPCo(II) complex
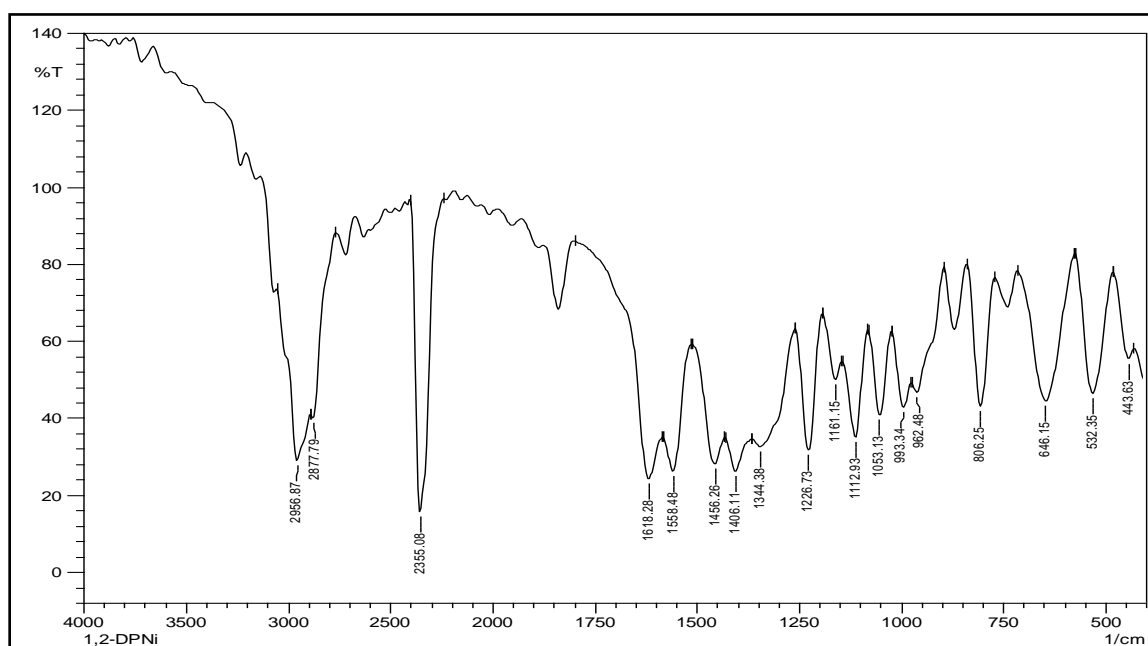
Figure 5.12: FT-IR spectrum of 1,2-DPNi(II) complex
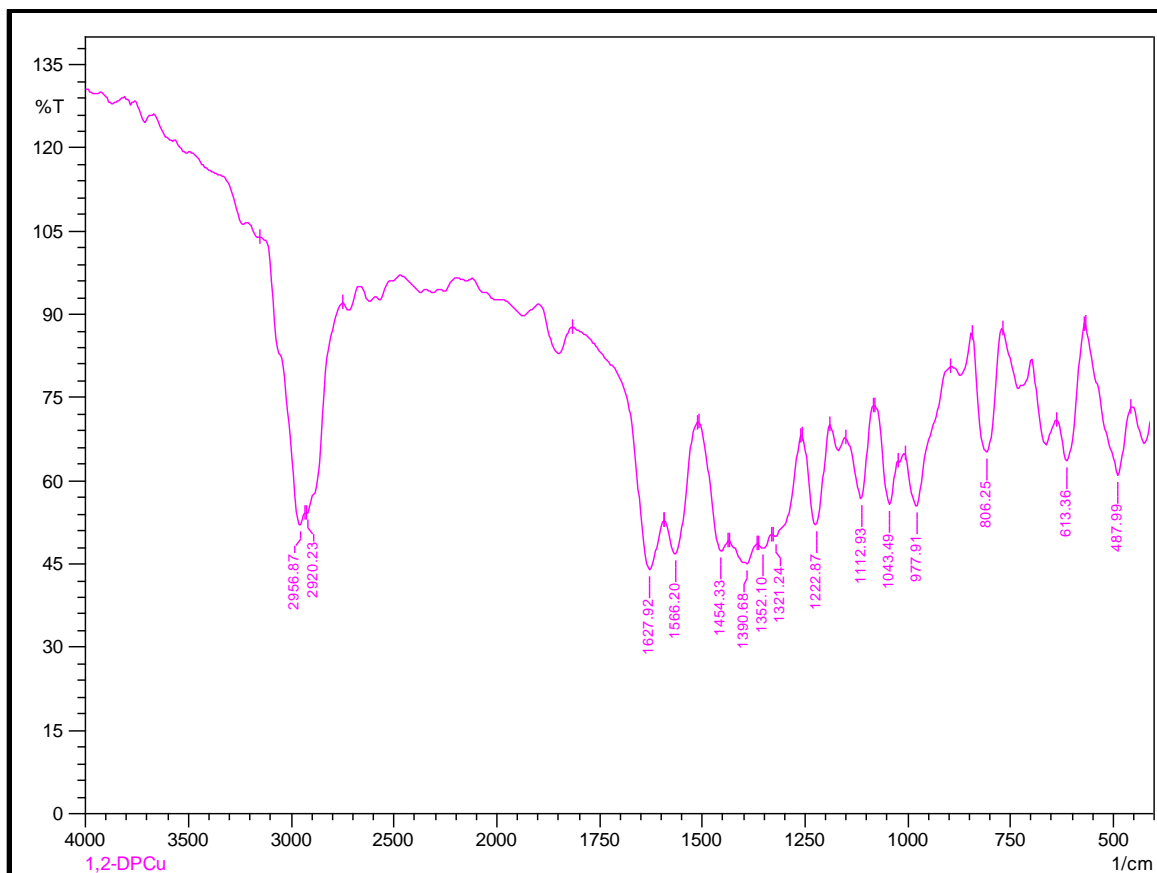
Figure 5.13: FT-IR spectrum of 1,2-DPCu(II) complex

5.5.4 Mass spectroscopy

The mass spectra of the 1,2-DP ligand and its four transition metal complexes are shown as **Figures. 5.14-5.18** and the data is gathered in the **Table 5.4**. The In the present investigation, the mass spectrum of 1,2-DP ligand shows molecular ion peak at m/z = 395 [M^{+1}] corresponding to [$C_{25}H_{34}N_2O_2$] ion. The spectrum also exhibits peaks for the fragment at m/z 235 corresponding to [$C_{14}H_{22}N_2O$]$^{+1}$. The spectra of 1,2-DP Mn(III), 1,2-DPCo(II), 1,2-DPNi(II) and 1,2-DPCu(II) complexes show molecular ion peaks at m/z 447 [M^{-OAC}], 451 [M^+], 451 [M^+] and 456 [M^+] respectively and these are equivalent to their molecular weights. The Mn(III) complex gives a fragment ion peak at m/z 287 [M^{-1}] corresponding to $C_{14}H_{21}MnN_2O$ and Ni(II) complex shows molecular ion peak at m/z 453 [M^{+2}]. The m/z of all the fragments of metal complexes of schiff base ligand 1,2-DP confirm the [ML] stoichiometry of the complexes.

Table 5.4: LC-MS Spectral data of 1,2-DP ligand and its metal complexes

Comp. Name	Mol. Formula	Mol. Wt (Calcd)	Mol. Wt (Found)
1,2-DP Ligand	$C_{25}H_{34}N_2O_2$	$M^+ = 394.26$	$M^{+1} = 395.41$
1,2-DPMn(III)	$C_{27}H_{35}MnN_2O_4$	$M^+ = 506.47$	$M^+ = 447.2$
1,2-DPCo(II)	$C_{25}H_{32}CoN_2O_2$	$M^+ = 451.47$	$M^+ = 451.1$
1,2-DPNi(II)	$C_{25}H_{32}N_2NiO_2$	$M^+ = 451.23$	$M^+ = 451.28$
1,2-DPCu(II)	$C_{25}H_{32}CuN_2O_2$	$M^+ = 456.08$	$M^+ = 456.25$
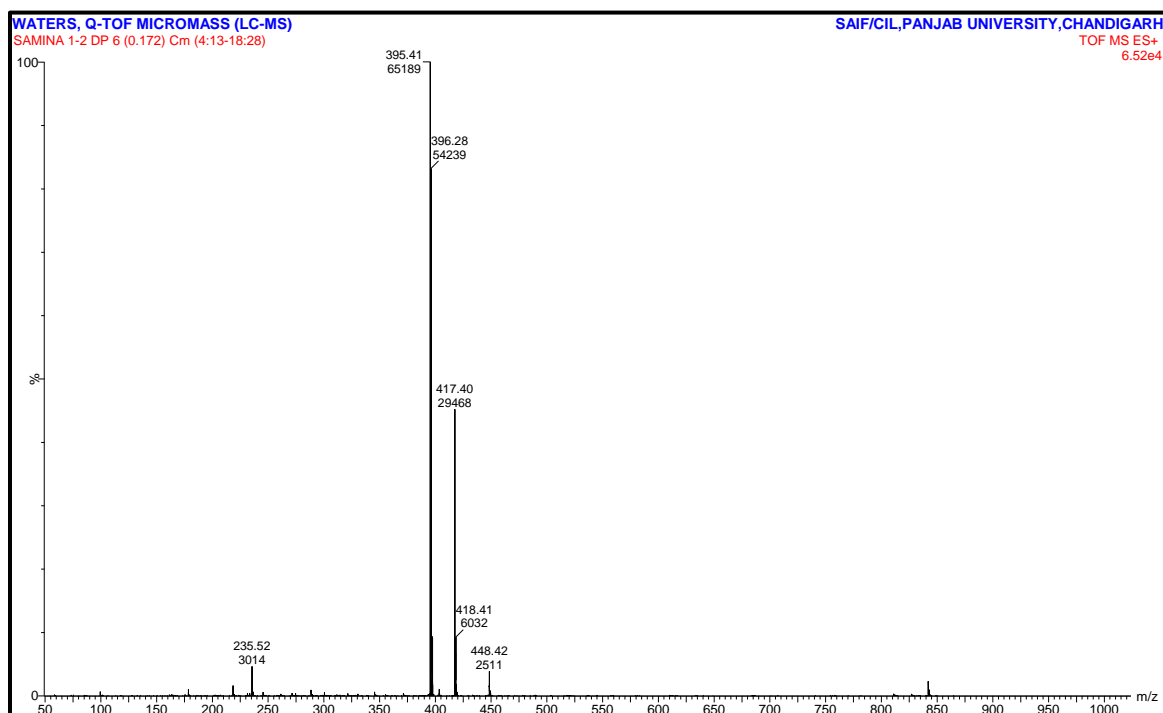
Figure 5.14: LC-MS spectrum of 1,2-DP ligand

Spectrum Plot - 11/17/2015 10:20 AM

1 A Scan 39 from ...ternal-2015-2016\lcms-38\1,2-dp-mn-447-msms.xms

Spectrum 1A
BP: 432.0 (6.746e+6=100%), 1,2-dp-mn-447-msms.xms   0.387 min, Scan: 39, 447.0>132:457 [2.20V], Ion: 158 us, RIC: 6.735e+7
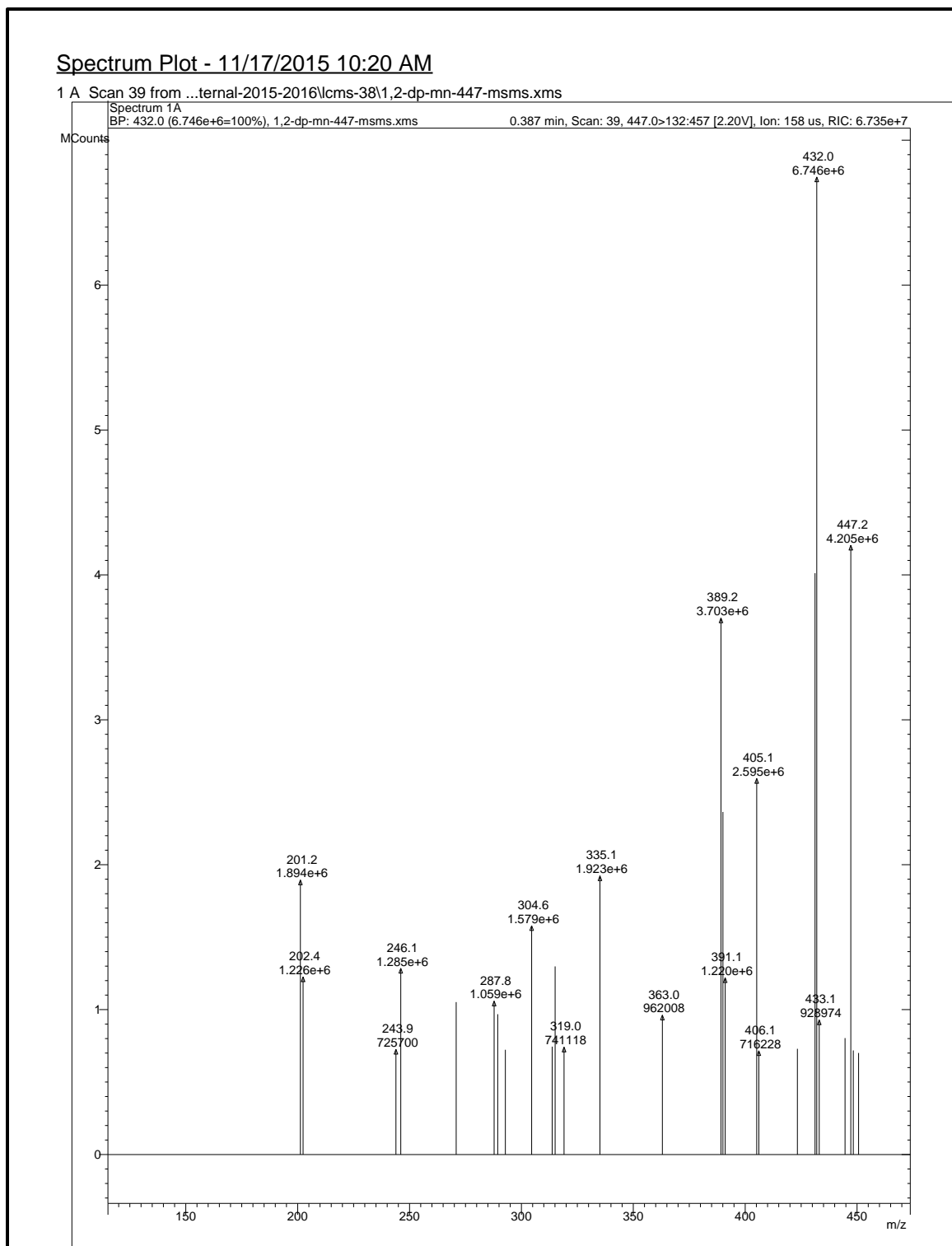
Figure 5.15: LC-MS spectrum of 1,2-DPMn(III) complex
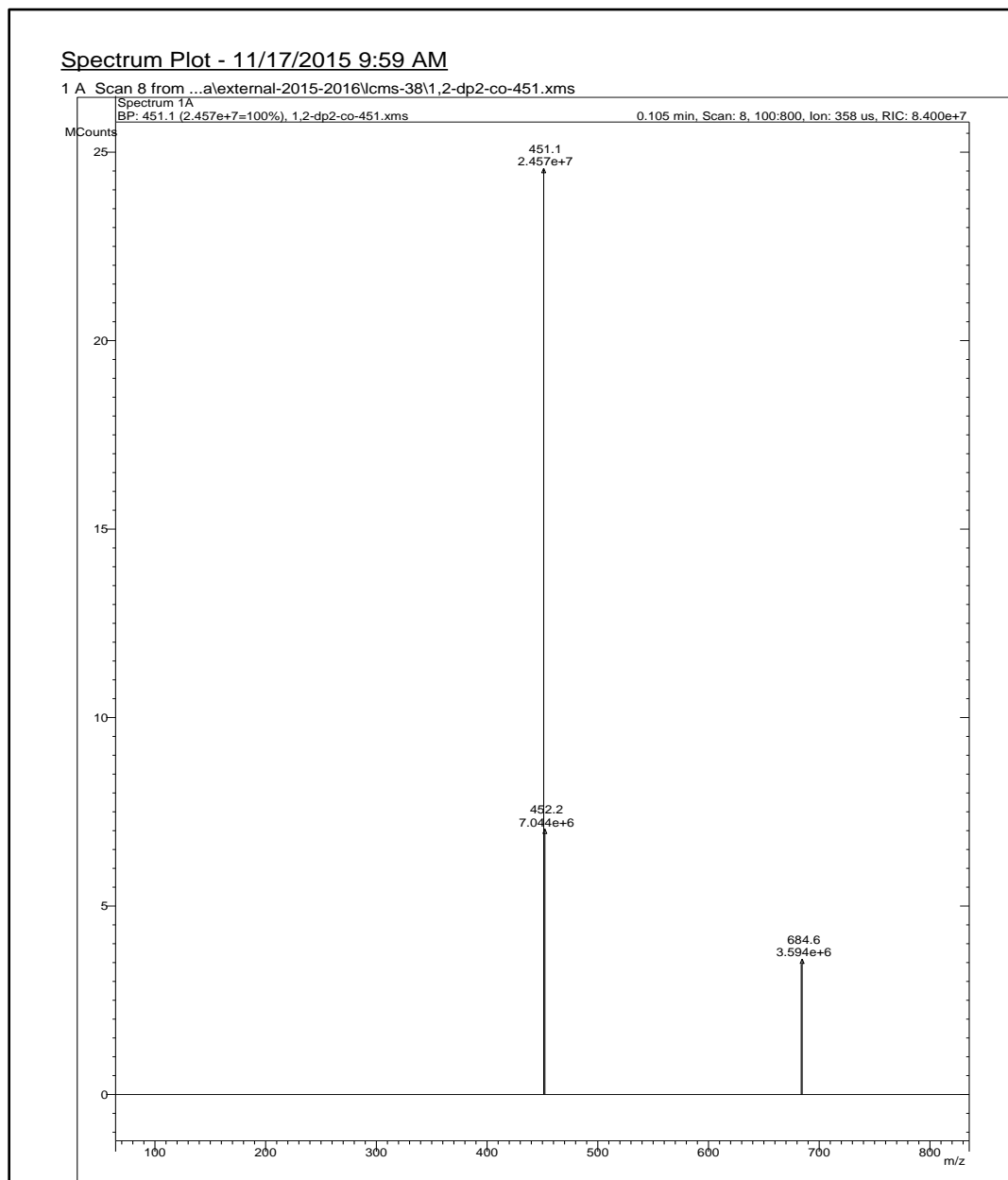
Figure 5.16: LC-MS spectrum of 1,2-DPCo(II) complex
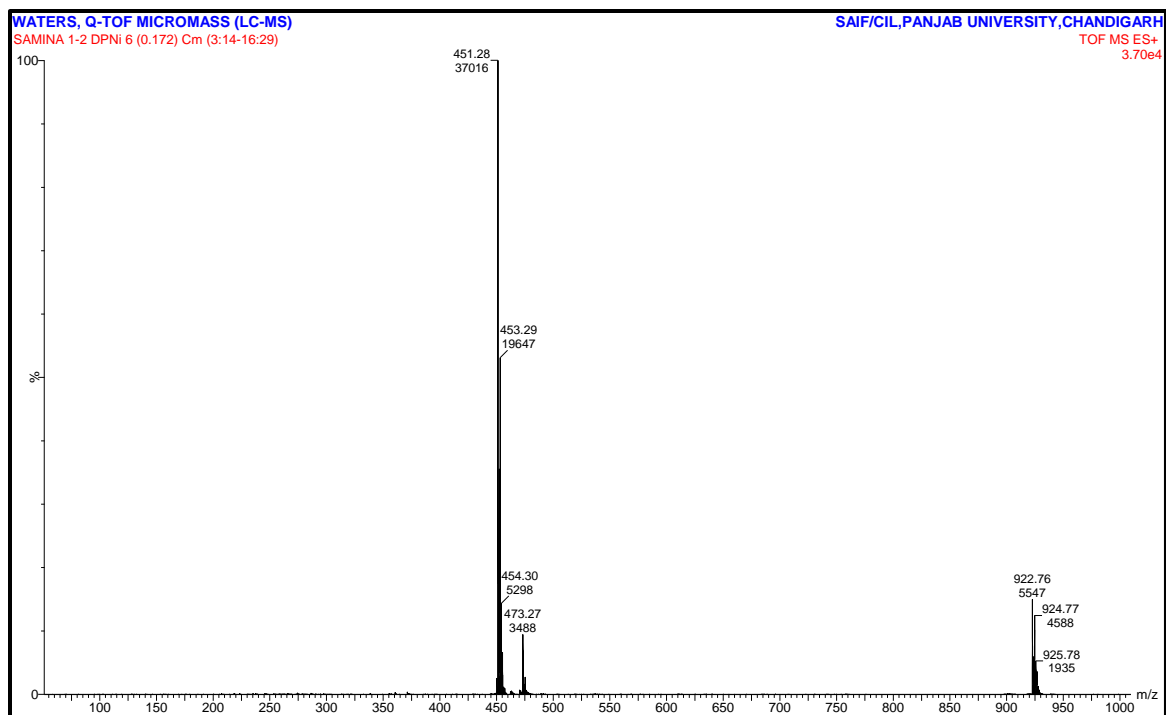
**Figure 5.17: LC-MS spectrum of 1,2-DPNi(II) complex**
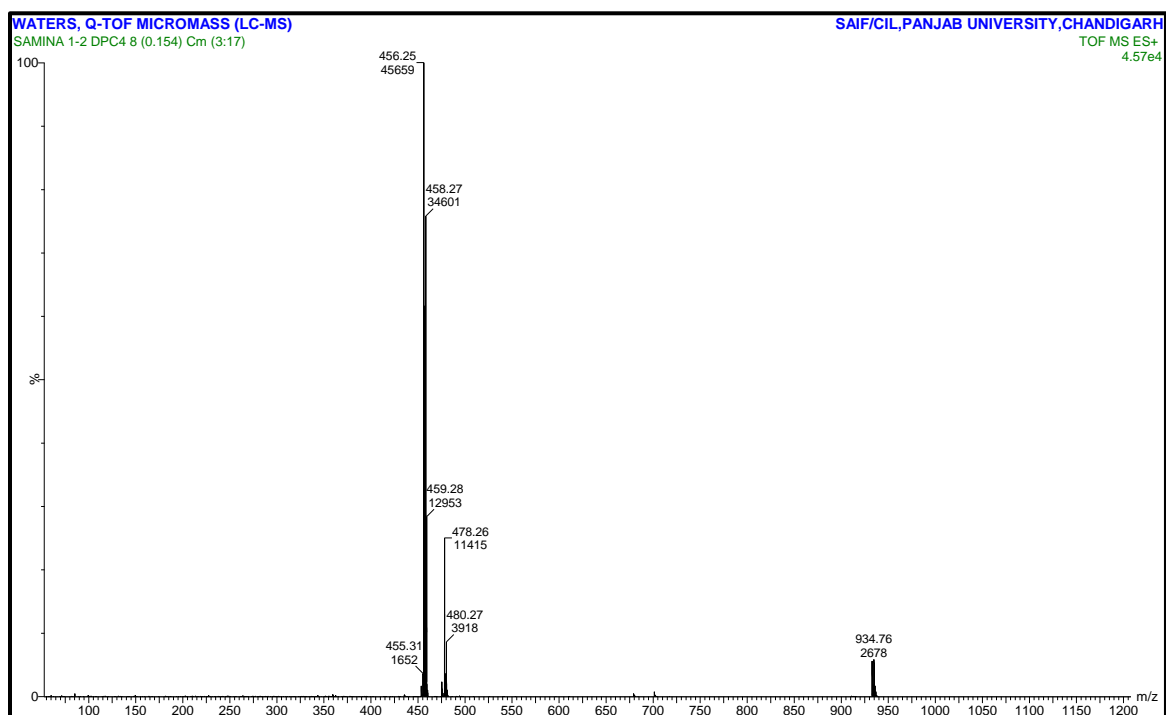
Figure 5.18: LC-MS spectrum of 1,2-DPCu(II)

5.5.5 Elemental analysis

The elemental analyses of 1,2-DP ligand and its four mononuclear transition metal complexes are given in the **Table 5.5**. They are in good conformity with molecular formula.

Table 5.5: Elemental analyses data of 1,2-DP ligand its metal complexes (%):

Comp. Name	C (Cal) Found	H(Cal) Found	N(Cal) Found
1,2-DP Ligand	76.10 (77.20)	8.69 (8.45)	7.10 (7.51)
1,2-DPMn(III)	(64.02) 64.08	(6.96) 6.49	(5.53) 5.80
1,2-DPCo(II)	(66.51) 66.38	(7.14) 7.33	(6.20) 6.06
1,2-DPNi(II)	(66.54) 66.20	(7.14) 7.56	(6.20) 6.35
1,2-DPCu(II)	(65.84) 65.82	(7.07) 7.01	(6.14) 5.98

5.5.6 Molar conductivity measurement

The complexes were dissolved in DMF and the molar conductivities of their 10^{-3} M solutions were measured at room temperature. The molar conductivity values of the complexes were in the range 4 to 28 Ω^{-1} cm^{-1} mol^{-1}. These values indicated that the complexes have non-electrolytic in nature (refer **Table 5.6**) [35].

5.5.7 Magnetic susceptibility measurement

The magnetic moments of 1,2-DPMn(III), 1,2-DPCo(II), 1,2-DPNi(II) and 1,2-DPCu(II) complexes are mentioned in **Table 5.6.**

The 1,2-DPMn(III) complex shows the magnetic moment 4.85 B.M. which corresponds for Mn(III) d^4 configuration [36]. The magnetic moment 1.33 B. M. of the 1,2-DPCo(II) complex is consistent with square-planar geometry [37]. The 1,2-DPNi(II) and 1,2-DPCu(II) complexes are square planar and diamagnetic in nature.

Table 5.6: Magnetic susceptibility and molar conductivity measurements

Compunds	Magnetic susceptibility (μeff) (B. M.)	Molar conductivity (Ω-1 cm2 mol, RT)
1,2-DPMn(III)	4.21	20
1,2-DPCo(II)	1.33	5.5
1,2-DPNi(II)	Diamagnetic	12
1,2-DPCu(II)	Diamagnetic	17.8

5.5.8 ESR Spectroscopy

ESR studies of copper complexes give information about the distribution of the unpaired electrons and the nature of the bonding between the metal ion and its ligands. The ESR spectrum of 1,2-DPCu(II) complex, recorded in DMF at LNT (77 k) (**Figure 5.19**) three of four hyperfine features are well resolved while the fourth one is overlapped by g features [38] and is having g|| = 2.34 and g⊥ = 2.04 consistent with the square-planar geometry predicted from the trend followed by g tensor value i.e. g|| > g⊥ > ge (2.0023) and this trend also shows that the unpaired electron occupies the d_{x2-y2} orbital with ^{2}B1g ground state [39]. The present results show that $g||$ is 2.34 which is in conformity with the presence of mixed copper-nitrogen and copper–oxygen bonds in these chelates and molecular orbital coeffficient α^2 value found as 0.90 suggested the covalent character in the ligand environment [40, 41]. The value is G > 4; according to Hathaway and Billing [42], if the G value is greater than 4, the exchange interaction is negligible, while a value of less than 4 indicates a considerable exchange interaction in the complex.
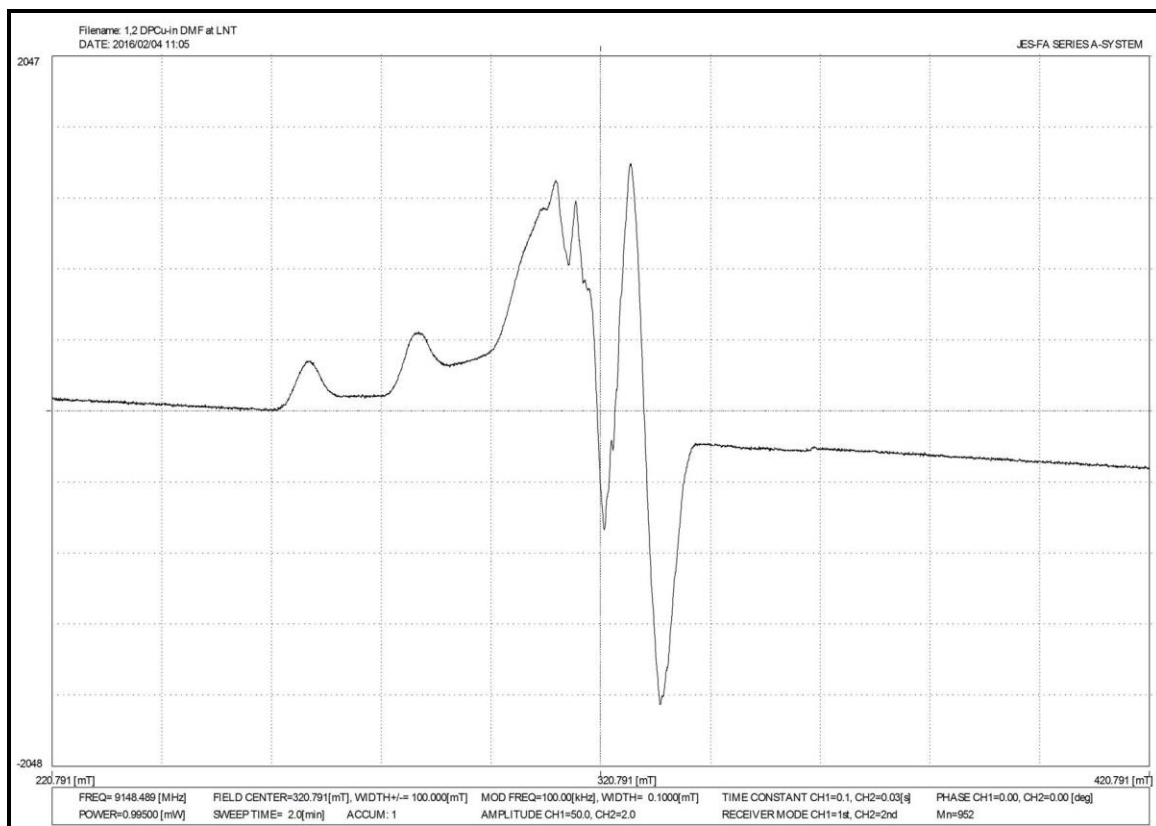
Figure 5.19: X-band ESR spectrum of 1,2-DPCu(II) complex

5.5.9 SEM analysis

Scanning electron micrograph (SEM) determines the morphology and the particle or grain size of the metal complexes. The SEM photographs of all the metal complexes are illustrated in the **Figures 5.20- 5.23**. The SEM photographs were taken in the different scale range from 2 μm to 20 μm. From the SEM photograph it was noted that there is a uniform matrix in all the metal complexes with homogeneous phase material. The photograph of 1,2-DPCu(II) complex shows the layer type morphology while single phase formation in 1,2-DPMn(III), 1,2-DPCo(II), and 1,2-DPCu(II) complexes having morphologies with particle size 1 μm to 10 μm.
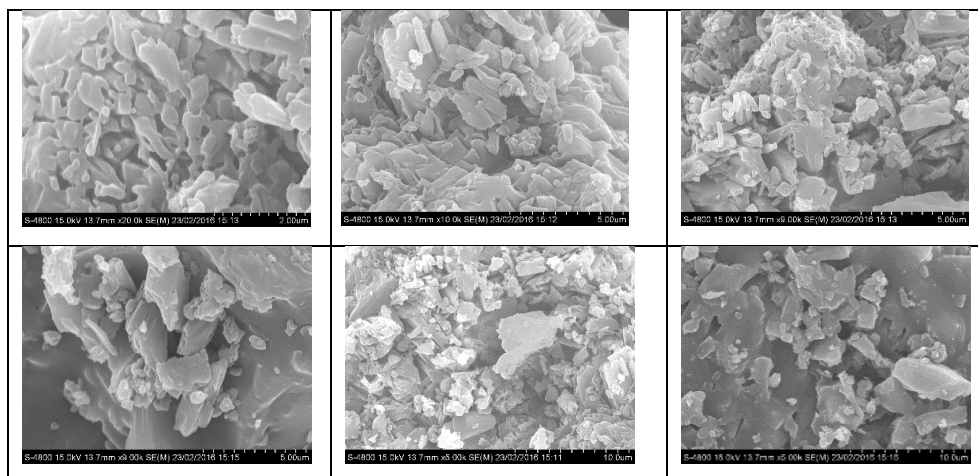
Figure 5.20(a): FE-SEM images of 1,2-DPMn(III) complex at different magnifications

Figure 5.20(b): EDX analysis of 1,2-DPMn(III) complex
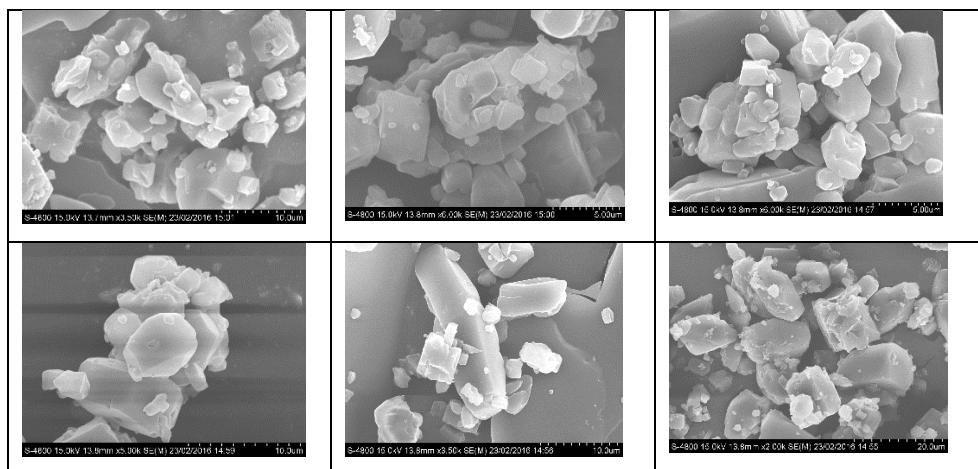
Figure 5.21(a): FE-SEM images of 1,2-DPCo(II) complex at different magnifications


```
El AN   Series   unn. C norm. C Atom. C Error (1 Sigma)
                 [wt.%]   [wt.%]   [at.%]          [wt.%]
-------------------------------------------------------
H   1  K-series   0.04     0.04     0.50            0.03
C   6  K-series  68.14    68.14    76.85           11.90
N   7  K-series  10.49    10.49    10.15            6.21
O   8  K-series  12.33    12.33    10.44            4.70
Co 27  K-series   9.00     9.00     2.07            0.76
-------------------------------------------------------
       Total: 100.00   100.00   100.00
```

Figure 5.21 (a): EDX analysis of 1,2-DPCo(II) complex
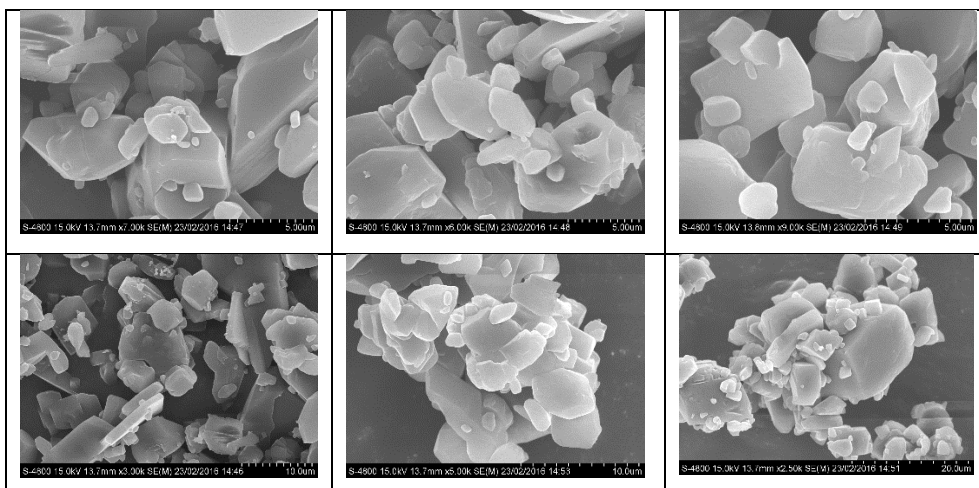
Figure 5.22(a): FE-SEM images of 1,2-DPNi(II) complex at different magnifications
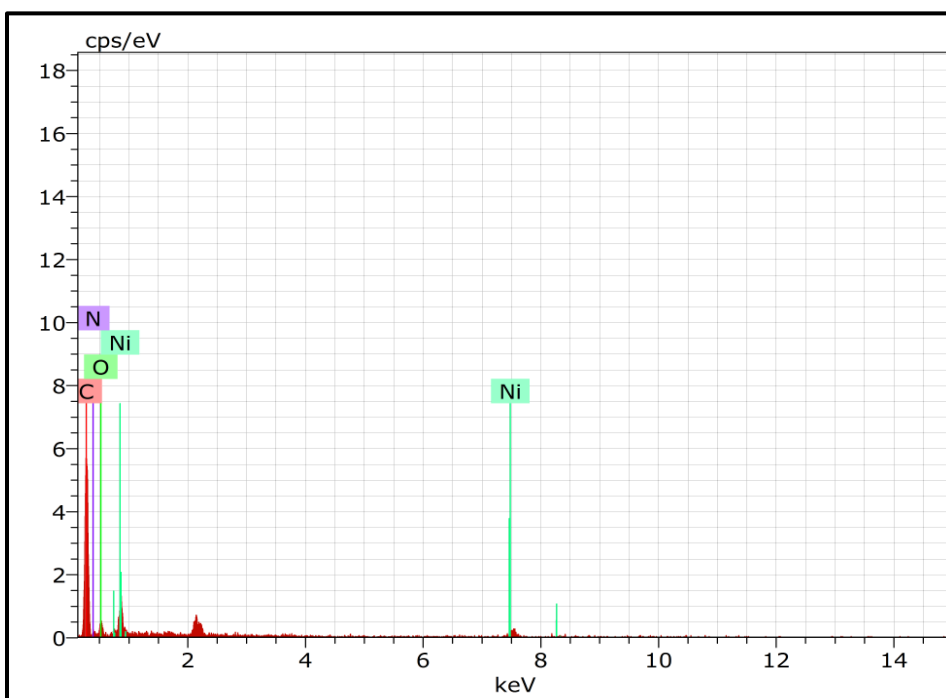
El	AN	Series	unn. C [wt.%]	norm. C [wt.%]	Atom. C [at.%]	Error (1 Sigma) [wt.%]
H	1	K-series	0.07	0.08	1.11	0.03
C	6	K-series	53.65	65.56	74.68	9.33
N	7	K-series	9.36	11.44	11.17	4.95
O	8	K-series	10.13	12.38	10.59	3.63
Ni	28	K-series	8.62	10.54	2.46	0.71
		Total:	81.83	100.00	100.00	

Figure 5.22 (b): EDX analysis of 1,2-DPNi(II) complex
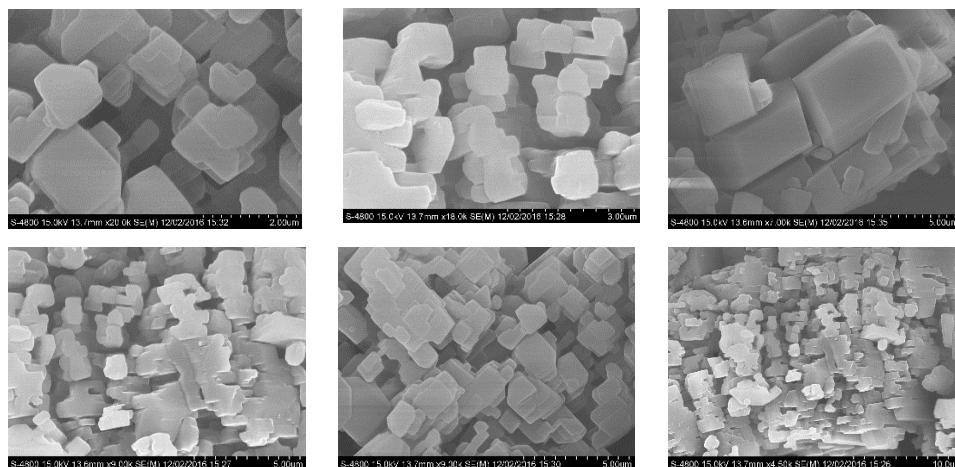
Figure 5.23(a): FE-SEM images of 1,2-DPCu(II) complex at different magnifications


```
El AN  Series   unn. C norm. C Atom. C Error (1 Sigma)
                [wt.%]   [wt.%]  [at.%]        [wt.%]
       --------------------------------------------------
H  1   K-series   1.68     2.68   28.24          0.19
C  6   K-series  39.73    63.48   56.16          7.25
N  7   K-series   6.21     9.93    7.53          3.59
O  8   K-series   5.14     8.21    5.45          2.20
Cu 29  K-series   9.83    15.70    2.63          0.84
       --------------------------------------------------
       Total:    62.58   100.00  100.00
```
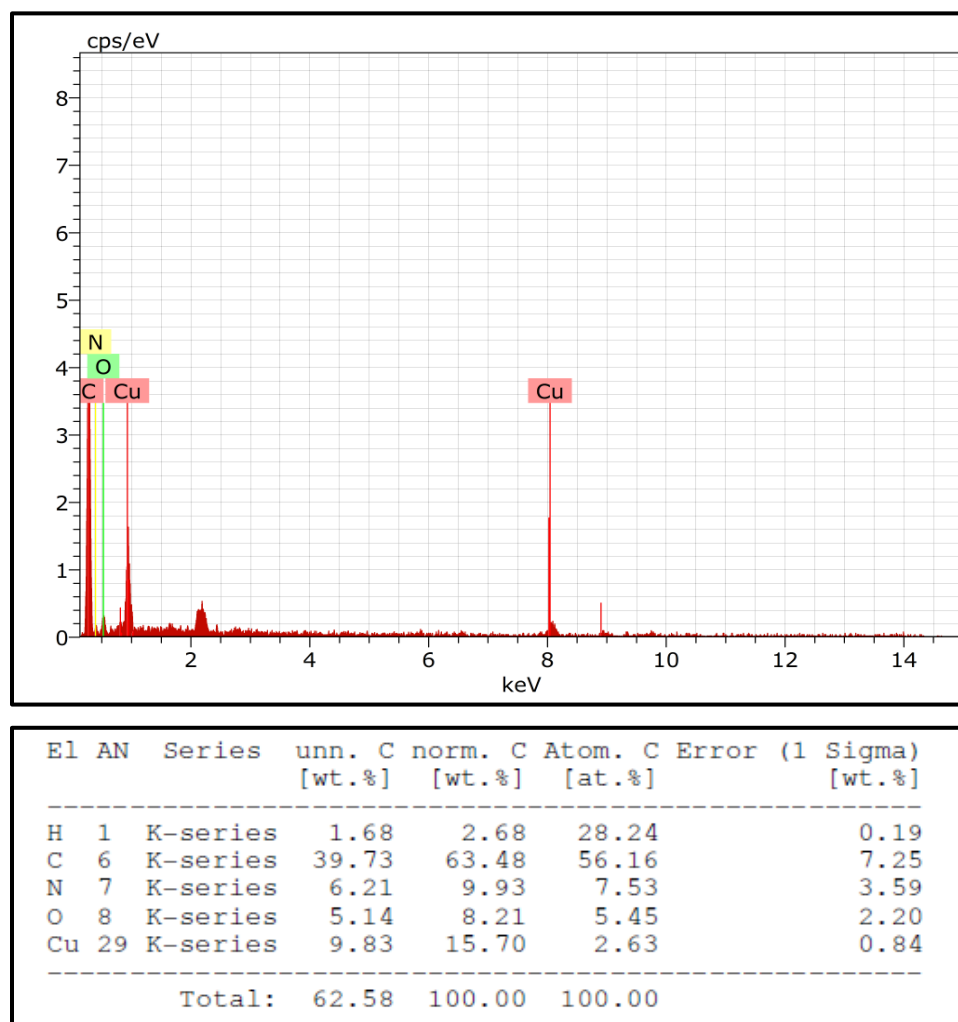
Figure 5.23(b): EDX analysis of 1,2-DPCu(II) complex

5.5.10 Cyclic voltammetry

The electrochemical behavior of 1,2-DP schiff base ligand and its metal complexes was examined in DMF and TBAP as supporting electrolyte. **Figure 5.24** shows the electrochemical cyclic voltammograms of curves of ligand, 1,2-DPMn(III), 1,2-DPCo(II), 1,2-DPNi(II) and 1,2-DPCu(II) complexes in DMF at 10^{-3} M concentration of compounds containing 0.1 M tetrabutyl ammonium perchlorate (TBAP) as electrolyte with Ag/AgCl as reference electrode at scan rate 100 mVs^{-1}.

Table 5.7: Electrochemical cyclic voltammetry data of metal complexes in DMF solution containing 0.1 M TBAP as electrolyte at scan rate of 100 mVs^{-1}.

Compounds	Epa (II→I) (V)	Epc (I→II) (V)	ΔE (V)
1,2-DP Ligand	-1.141	-0.999	0.142
1,2-DPMn(III)	-1.138	-0.242	0.896
1,2-DPCo(II)	-1.123	-0.935	0.188
1,2-DPNi(II)	-1.129	-0.98	0.149
1,2-DPCu(II)	-0.751	-1.184	-0.433

For the 1,2-DP schiff base ligand, a cyclic sweep in the -1.5 to +0.50 V range shows a cathodic peak at -0.999 V and an anodic peak at -1.141 V. The electrochemical properties of manganese complex show the one-electron reduction peak (Epc), corresponding to the Mn(III/II) which occurs at -0.242 V and during the reverse scan the oxidation peak (Epa) is observed at -1.138 V. During the forward scan the Mn(III) gets reduced as:

$$\text{Mn (III)} + e^- \xrightarrow{reduction} \text{Mn (II)}$$
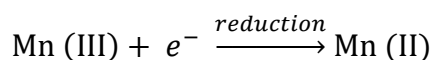
Similarly during the reverse potential the oxidation of the Mn(II) takes place to Mn(III) which can be shown as:

$$\text{Mn (II)} + \xrightarrow{oxidation} \text{Mn (III)} + e^-$$
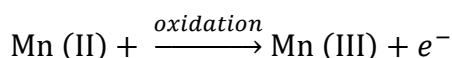
The redox reaction therefore, can be used as an indication of major analytical tool for the determination of the trace elements which are electroactive in nature.

The electrochemical data of cobalt and nickel complexes have similar reduction peaks (Epc) in the potential range given in **Table 5.7**, attributed to the Co (II/I) and Ni (II/I), the sweep potential shows the oxidation peak (Epa) for both the complexes at the potential value -1.123 V and -1.129 V respectively, while the copper complex shows the one-electron reduction peak (Epc) corresponding to the Cu (II/I), at -1.184 V and the reverse scan reoxidation peak (Epa) is at -0.751 V [43].

(a)

(b)

(c)

(d)

(e)
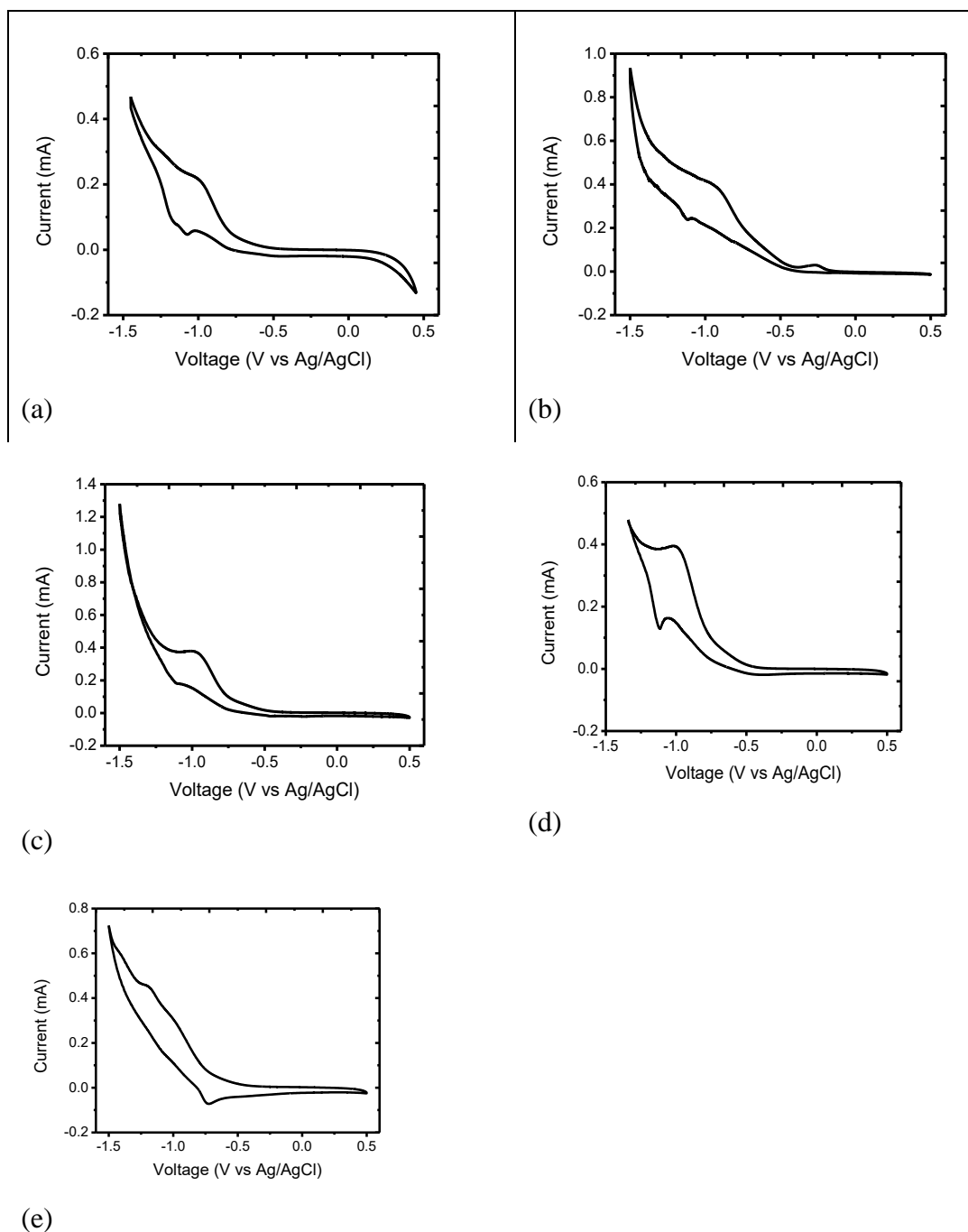
Figure 5.24: Cyclic voltammograms of (a) schiff base ligand L; (b) Mn(III)L; (c) Co(II)L; (d) Ni(II)L; and (e) Cu(II)L complexes respectively at room temperature in DMF solution containing 0.1 M TBAP as electrolyte at scan rate of 100 mVs⁻¹.

5.5.11 Single crystal X-ray crystallography studies

The ORTEP diagrams and packing diagrams of 1,2-DP ligand and its nickel's dimeric complex are shown in the **Figures 5.24-5.27**. The crystallographic parameters, data collection and refinement for the 1,2-DP schiff base ligand and its dimeric [1,2-DPNi]2 complex are as shown in the **Table 5.8**. The selected bond lengths and bond angles are given in **Tables 5.9 & 5.10** While, the hydrogen bonding parameters are given in **Tables 5.11 & 5. 12.** The crystal structure of the 1,2-DP schiff base ligand represented, the N1-C8 distance as 1.271(6) for C=N double bond. The molecule adopts E- configuration in connection with C = N bond with C9i-C9-N1-C8 and C22i-C22-N2-C21 torsion angle found as 151(5)°, -150.7(18)°. The bond distance 1.350 (5) for C7-O1 illustrated the C-O phenolic single bond. In the ligand structure, molecule is associated with intramolecular hydrogen bonding, where the H atom of phenolic hydroxyl group forms a strong O-H….N intramolecular hydrogen bond with O….N distance 2.53 Å [44-46].
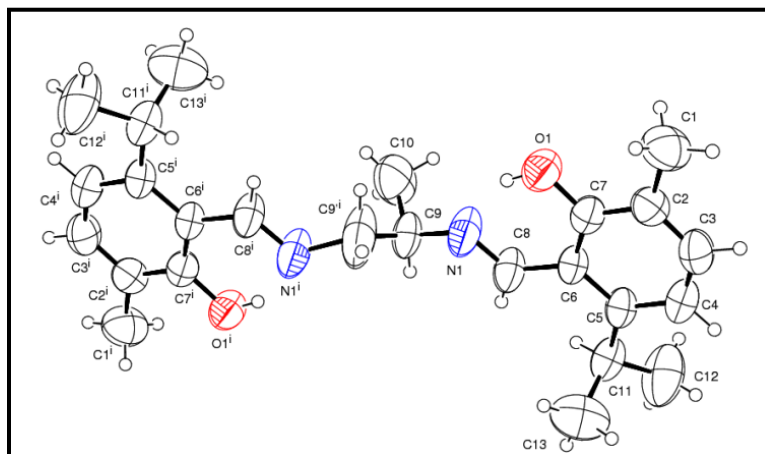
Figure 5. 25: ORTEP diagram of 1,2-DP schiff base ligand

CCDC No. for 1,2-DP ligand= 1525072
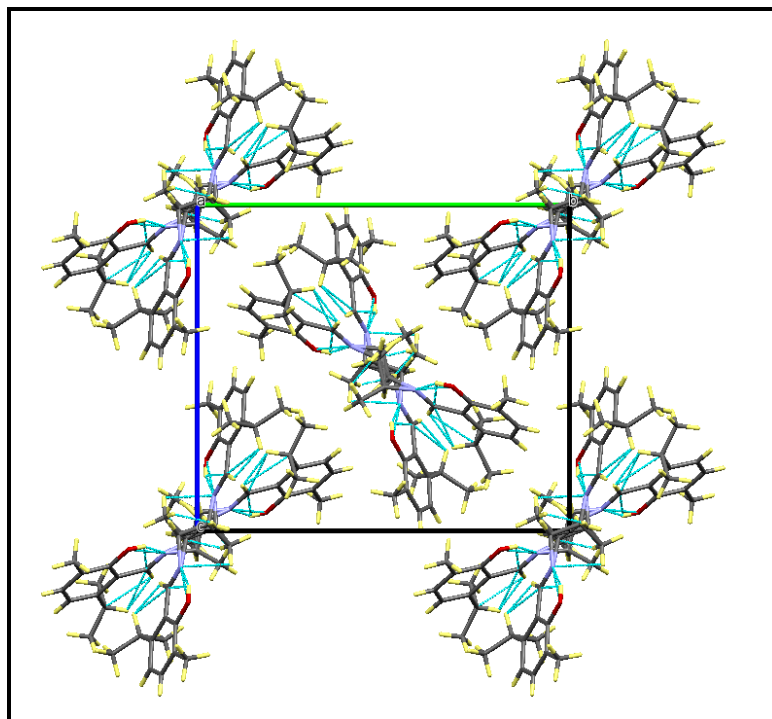
Figure 5. 26: The crystal packing of the 1,2-DP schiff base ligand viewed along a axis. The intramolecular C-H--O and C-H--N hydrogen bonds are shown as a light blue dashed line, and all atomic labels have been omitted for clarity.
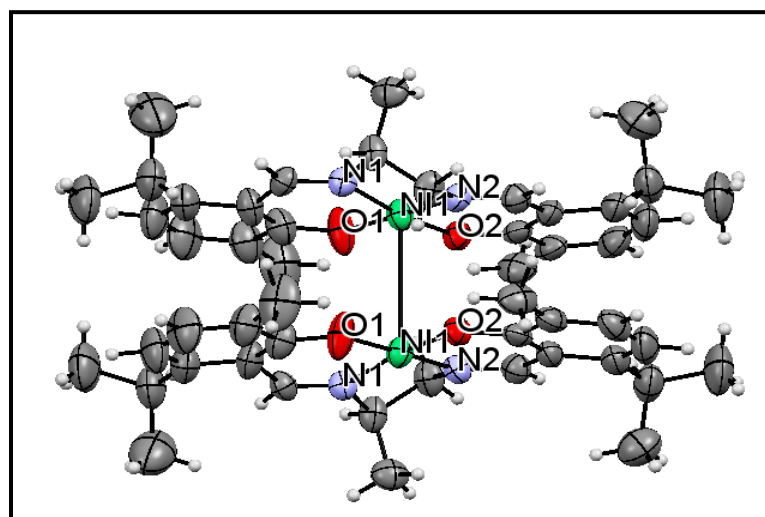
Figure 5. 27: ORTEP diagram of dimeric [1,2-DPNi]2 complex

CCDC No. for 1,2-DPNi ligand= 1523079
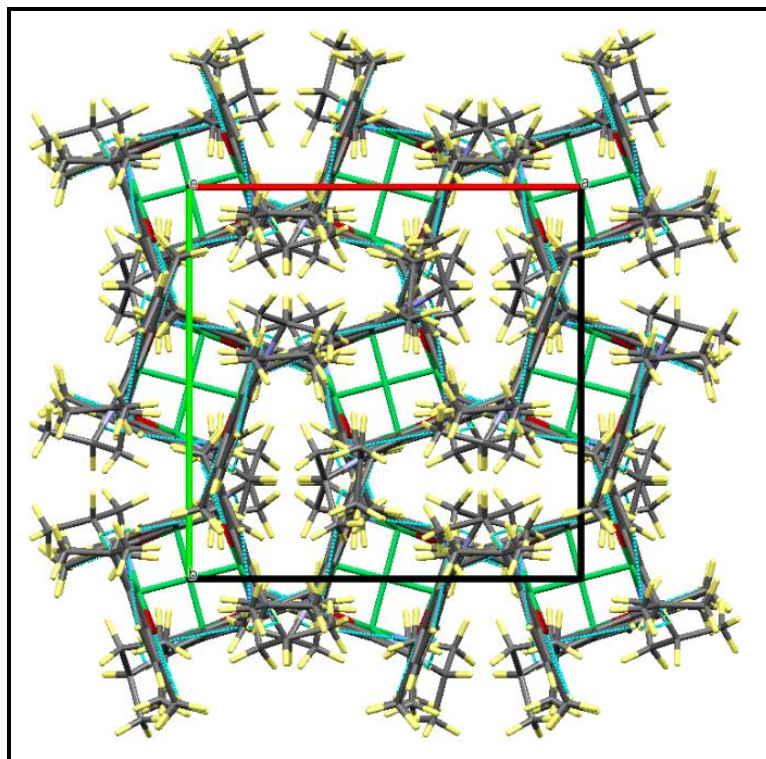
Figure 5. 28: The crystal packing of the dimeric nickel [1,2-DPNi]2 complex viewed along the c axis with 101 plane. The intramolecular C-H--O and C-H--N hydrogen bond is shown as a light blue dashed line, and all atomic labels have been omitted for clarity.

In the present nickel's dimeric crystal structure the bond lengths of Ni-O and Ni-N are in the range of 1.824-1.832 Å and 1.820-1.877 Å respectively. The N2-Ni-O1 and O2-Ni-O1 bond angles have been found to be 178.51 (16)° and 170.9 (3)° respectively; and from these trans values of each metal ions, it can be concluded that complex has distorted square planar geometry. The bond angles around the metal ion N2-Ni-O2, O1-Ni-O2, N2-Ni-N1, and O1-Ni-N1 exhibit the values viz. 93.95 (15)°, 87.47 (12)°, 85.7 (3)° and 92.8 (3)° respectively. All these mentioned values are nearly same as related reported nickel complexes [31, 43, 47]. In addition the packing diagram shows intramolecular C-H--O interaction between one methyl H atoms of benzene ring and neighboring oxygen atoms. Another intramolecular C-H--N interaction is observed in diamine bridge where methyl's one H atom is in vicinity of one imine nitrogen.

Table 5.8: Crystallographic parameters, data collection and refinement for ligand 1,2-DP and its dimeric [1,2-DPNi]2 complex

Compounds	1,2-DP ligand	[1,2-DPNi]2 complex
Empirical formula	C25 H34 N2 O2	C25 H32 N2 Ni O2
Formula weight	394.54	451.23
Temperature	296(2) K	296(2) K
Wavelength	0.71073 Å	0.71073 Å
Crystal system	Monoclinic	Tetragonal
Space group	$P2_1/n$	I-42d
Unit cell dimensions	a = 10.2052(7) Å b = 16.5306(11) Å c = 14.7520(8) Å α= 90º β= 100.699(2)º γ= 90º	a = 12.3870(3) Å b = 12.3870(3) Å c = 60.928(2) Å α= 90º β= 90º γ= 90º
Volume	2445.4(3) Å^3	9348.7(6) Å^3
Z	4	16
Density (calculated)	1.072 Mg/m^3	1.282 Mg/m^3
Absorption coefficient	0.068 mm^{-1}	0.853 mm^{-1}
F(000)	856	3840
Crystal size	0.350 x 0.300 x 0.250 mm^3	0.300 x 0.250 x 0.200 mm^3
Theta range for data collection	2.245 to 25.000°	1.678 to 24.996°
Index ranges	-12<=h<=12, -19<=k<=19, -17<=l<=14	-14<=h<=14, -14<=k<=14, -72<=l<=72
Reflections collected	33069	106989
Independent	4307 [R(int) = 0.0505]	4120 [R(int) = 0.0635]

reflections		
Completeness to theta = 25.000°	99.9 %	99.9 %
Absorption correction	Semi-empirical from Equivalents	Semi-empirical from equivalents
Max. and min. transmission	0.995 and 0.967	0.85 and 0.71
Refinement method	Full-matrix least-squares on F^2	Full-matrix least-squares on F^2
Data / restraints / parameters	4307 / 64 / 300	4120 / 111 / 317
Goodness-of-fit on F^2	1.081	1.154
Final R indices [I>2sigma(I)]	R1 = 0.0819, wR2 = 0.1996	R1 = 0.0311, wR2 = 0.0795
R indices (all data)	R1 = 0.1667, wR2 = 0.2912	R1 = 0.0401, wR2 = 0.0848
Largest diff. peak and hole	0.247 and -0.167 e.Å^{-3}	0.254 and -0.179 e.Å^{-3}

Table 5.9: Selected bond lengths (A°) and bond angles (°) for 1,2-DP schiff base ligand

Bond Lengths		Bond Angles	
C(6)-C(8)	1.457(6)	C(7)-C(6)-C(8)	120.1(4)
C(7)-O(1)	1.350(5)	C(5)-C(6)-C(8)	120.3(4)
C(8)-N(1)	1.271(6)	O(1)-C(7)-C(6)	121.0(4)
C(9)-N(1)	1.474(10)	N(1)-C(9)-C(10)	114.8(10)
C(9)-C(10)	1.481(13)	N(1)-C(8)-H(8)	119.2
C(9)-H(9)	0.9800	C(10)-C(9)-H(9)	108.7

Table 5.10: Selected bond lengths (A⁰) and bond angles (⁰) for dimeric [1,2-DPNi]2 complex

Bond Lengths		Bond angles	
C(13)-N(2)	1.487(12)	N(2)- Ni(1)-O(2)	93.95(15)
C(10)-N(1)	1.288(11)	O(1)- Ni(1)-O(2)	87.47(12)
N(1)-Ni(1)	1.877(9)	N(2)- Ni(1)-N(1)	85.7(3)
N(2)-Ni(1)	1.820(3)	O(1)- Ni(1)-N(1)	92.8(3)
O(1)-Ni(1)	1.824(3)	O(2)- Ni(1)-N(1)	170.9(3)
O(2)-Ni(1)	1.832(3)	N(2)- Ni(1)-O(1)	178.51(16)

Table 5.11: Hydrogen bonding for schiff base ligand H2L

D-H…A	d(D-H)	d(H…A)	d(D…A)	<(DHA)
C(8)-H(8)...O(2)#3	0.93	2.66	3.520(6)	154.7
C(9)-H(9)...O(2)#3	0.98	2.65	3.580(19)	157.4
C(21)-H(21)...O(1)	0.93	2.63	3.467(6)	149.4
C(22')-H(22B)...O(1)	0.97	2.60	3.51(3)	155.8
O(1)-H(1)...N(1)	0.82	1.79	2.530(5)	148.7
O(2)-H(2)...N(2)	0.82	1.78	2.519(5)	148.7

Symmetry transformations used to generate equivalent atoms:

#1 -x+1,-y+2,-z   #2 -x,-y+2,-z   #3 x+1,y,z

Table 5.12: Hydrogen bonding for dimeric [NiL]2 complex

D-H…A	d(D-H)	d(H…A)	d(D…A)	<(DHA)
C(13')-H(13C)...O(1)#1	0.97	2.64	3.260(14)	122.0
C(13')-H(13C)...O(1)#1	0.97	2.64	3.260(14)	122.0

Symmetry transformations used to generate equivalent atoms: #1 -x+2,-y,z

5.6 Biological activities

5.6.1 Protocol for antibacterial activity

Protocol for antibacterial activity are same as described in chapter 2 and section 2.5.1

5.6.2 . Results of antibacterial activity

The results of the antibacterial activity are presented in **Table 5.13** and graphically representation are shown in **Figure 5.28.** The Minimal Inhibitory Concentration (MIC) of schiff base ligand and their metal complexes against bacteria were compared with the MIC values of standard drugs ciprofloxacin and ampicillin. The MIC values of the 1,2-DP schiff base ligand was observed to be 91 μg/ml, 91 μg/mL and 111 μg/mL against *E. coli*, *B. subtilis* and *S. aureus* respectively, the values exhibit better activities as compared to the standard drug ampicillin and lower activities than ciprofloxacin. In case of the MIC values of metal complex, 1,2-DPMn(III) complex possesses MIC values (90 μg/mL) and (65 μg/mL) which are better than the MIC value of ampicillin against *E. coli* and *B. subtilis*. The 1,2-DPCo complex exhibited super MIC values as (165 μg/mL) and (176 μg/mL) against *B. subtilis* and *S. aureus* respectively, while the MIC values against *P. aeruginosa* was very high (209 μg/mL) as compared to standards. The [1,2-DPNi]2 complex acquired excellent MIC values as (49 μg/mL), (55 μg/mL) and (42 μg/mL) against *P. aeruginosa*, *B. subtilis* and *S. aureus* respectively as compared to standard drugs ampicillin and ciprofloxacin, while its MIC (125 μg/mL) value against *E. coli* shows negligible activity. The 1,2-DPCu(II) complex exhibited very good MIC values (168 μg/mL) and (226 μg/mL) against *E. coli* and *P. aeruginosa* and very high MIC value for *B. subtilis* and *S. aureus* as compared to the standards ciprofloxacin and ampicillin drugs.

Table 5.13: Representation of antibacterial activity of 1,2-DP ligand and its metal complexes

Compounds	(MIC μg/ml)			
	E. coli	*P. aeruginosa*	*B. subtilis*	*S. aureus*
1,2- DP Ligand	91	154.5	91	111.5
1,2- DPMn(III)	90	110	65.5	*

1,2- DPCo(II)	*	209	165	176
1,2- DPNi(II)	125	49	55	42
1,2- DPCu(II)	168	226	*	*
Ciprofloxacin	25	25	50	50
Ampicillin	100	100	250	250

* No activity reported up to 500 µg/ml
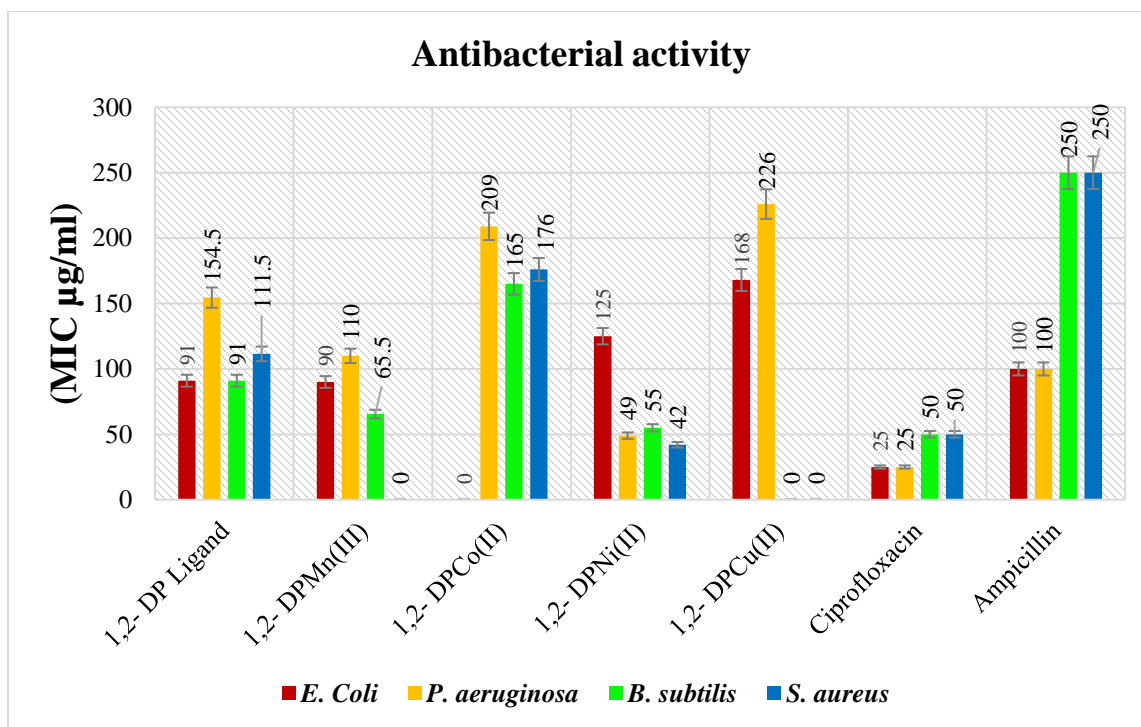
Figure 5.29: Graphical representation of antibacterial activity

The enhanced activity of the complexes can be explained on the basis of Overtone's concept and Tweedy's Chelation theory [48, 49]. The Chelation considerably decreases the polarity of the metal ion because of partial sharing of its positive charge with donor groups and possible pi-electron delocalization over the whole chelate ring. Such a chelation could enhance the lipophilic character of the central metal atom, which subsequently favors its permeation through the lipid layer of the cell membrane.

5.6.3 Protocol for antifungal activity

Protocol for antifungal activity are same as described in chapter 2 and section 2.5.3

5.6.4 Results of antifungal activity:

The graphical representation of antifungal activities results are shown in **Figure 5.29**. The MIC values of the 1,2-DP schiff base ligand and its four metal complexes 1,2-DPMn(III), 1,2-DPCo(II), [1,2-DPNi]2 and 1,2-DPCu(II) show very poor activity as compared to standard drugs miconazole and fluconazole (**Table 5.14**) except 1,2-DPCo(II) complex which possesses equal antifungal activity against the fungi *C. neoformans* as compared to the standard drug miconazole. The low activity of the compounds might be visualized because low cell permeability, fitness of the particles size of the metal ion and the presence of the bulkier organic moieties [50].

Table 5.14: Representation of antifungal activity of 1,2-DP ligand and its metal complexes

Compounds	(MIC µg/ml)			
	C. albicans	*A. flavus*	*A. niger*	*C. neoformans*
1,2- DP	137.5	187.5	50	150
1,2- DPMn(III)	150	125	*	137.5
1,2- DPCo(II)	*	*	125	25
1,2- DPNi(II)	100	100	*	*
1,2- DPCu(II)	137.5	150	150	137.5
Miconazole	25	12.5	25	25
Fluconazole	12.5	6.25	12.5	6.25

*** No activity reported up to 500 µg/ml**
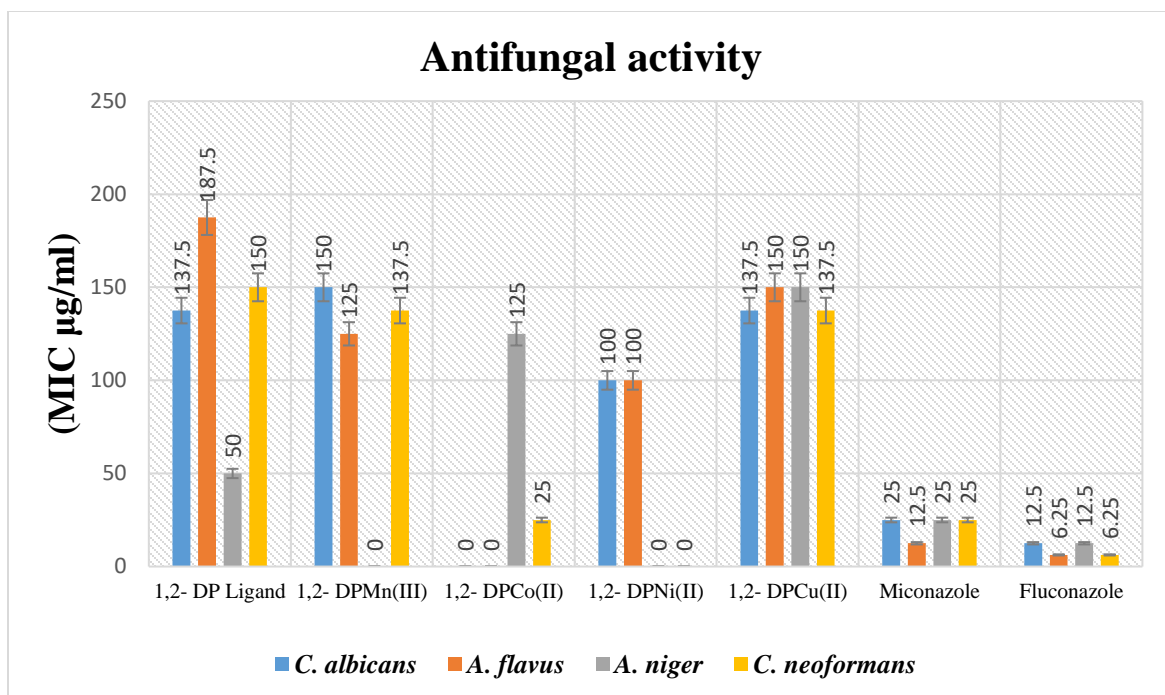
Figure 5.30: Graphical representation of antifungal activity

5.6.5 Protocol for antioxidant activity (DPPH radical scavenging activity)

Protocol for antioxidant activity are same as described in chapter 4 and section 4.5.5

5.6.6 Results of antioxidant activity

DPPH radical form absorbs at 517 nm. When a hydrogen atom or electron is transferred to the odd electron in DPPH radical, the absorbance at 517 nm decreases proportionally to the increase of nonradical forms of DPPH. As a consequence, DPPH radical is usually used as a substrate to estimate the anti-oxidative activity of antioxidants. Hence, if the absorbance decreases more rapidly, the more potent is the antioxidant activity of the compound. It is also visually noticeable as a change in color from purple to yellow [51, 52].

Table 5.15: Representation of antioxidant activity of 1,2-DP ligand and its metal complexes

| Compounds	EC$_{50}$
1,2-DP Ligand	0.1157
1,2-DPMn(III)	0.1138
1,2-DPCo(II)	0.1140
1,2-DPNi(II)	0.1136
1,2-DPCu(II)	0.1117
Standard (Ascorbic acid)	0.120
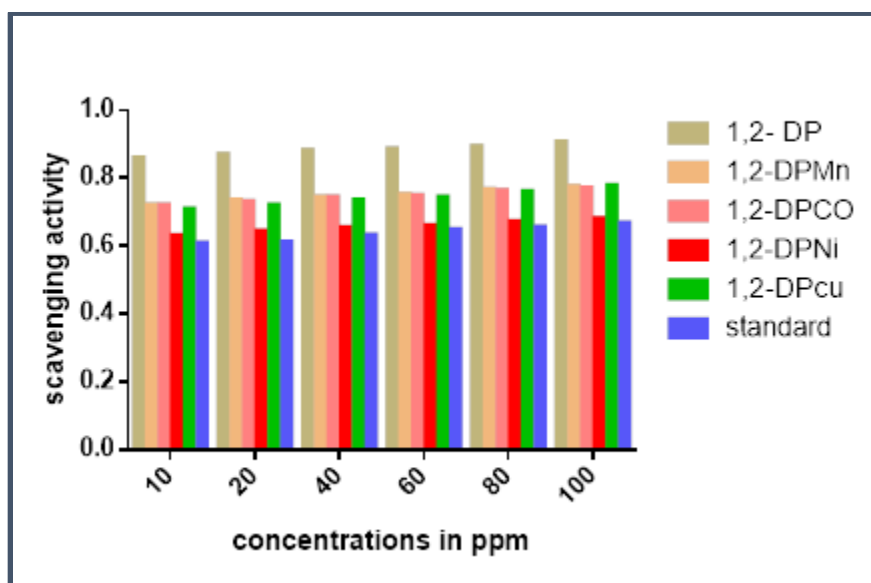
Figure 5.31: Graphical representation of antioxidant acivity

The synthesized 1,2-DP ligand possesses better antioxidant property with (EC$_{50}$= 0.1157) as compared to ascorbic acid as a standard. The ligand upon complexation with the metals 1,2-DPMn(III), 1,2-DPCo(II), [1,2-DPNi]2 and 1,2-DPCu(II) demonstrated a broad spectrum of results. The 1,2-DPCu(II) complex have exhibited an excellent scavenging activity. Whereas, [1,2-DPNi]2, 1,2-DPMn(III) and 1,2-DPCo(II) complexes showed a super activity. In general, all other complexes exhibited higher scavenging activity than the 1,2-DP schiff base ligand. These results clarify that, the synthesized compounds scavenged the DPPH radical in a concentration dependent approach.

5.6.7 DNA cleavage experiment

DNA cleavage experiment are same as described in chapter 2 and section 2.5.7

5.6.8 Results DNA cleavage activity

The chemical nuclease activity of all the compounds has been investigated by agarose gel electrophoresis using pBR322 DNA as a substrate **(Figures 5.27- 5.31)**. When circular plasmid DNA is subjected to electrophoresis, relatively fast migration is observed for the supercoiled form (SC form I). If scission occurs on one strand (nicking), the supercoil will relax to generate a slower moving open circular form (NC form II). If both strands are cleaved, a linear form (form III) that migrates between form I and form II is generated. The plasmid pBR322 DNA (200 ng) were mixed with different concentrations of compounds in the presence of oxidant H_2O_2. In presence of H_2O_2, pBR322 DNA was converted from SC (form I) to NC (form II). The 1,2-DP ligand and 1,2-DPMn(III) and [1,2-DPNi]2 complexes showed the cleavage of the SC form (form I) to NC (form II), while, the 1,2-DPCo complex showed the complete conversion of SC form I to nicked DNA form (II) as the concentration increases from 20 µM to 200 µM [53, 54].
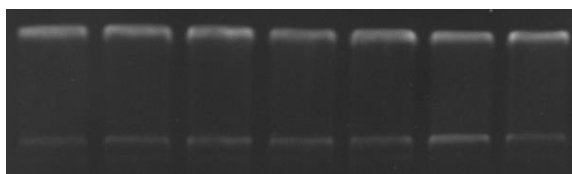
Figure 5.32: Agarose gel electrophoretic pattern of pBR322 DNA by H_2O_2 and 1,2-DP ligand : **(From left to right)** Lane 1-DNA+ H_2O_2 alone; Lane 2- DNA + 10 µM sample + H_2O_2; Lane 3-DNA + 20 µM sample + H_2O_2; Lane 4-DNA + 50 µM sample + H_2O_2; Lane 5-DNA + 100 µM sample + H_2O_2; Lane 6-DNA+ 150 µM sample + H_2O_2; Lane 7-DNA + 200 µM sample + H_2O_2.
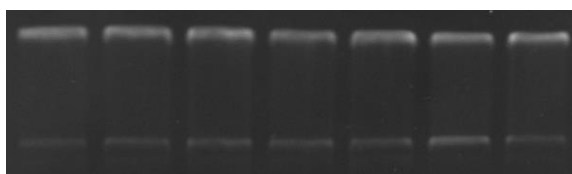
Figure 5.33 : Agarose gel electrophoretic pattern of pBR322 DNA by H_2O_2 and 1,2-DPMn(III) **(From left to right)** Lane 1-DNA+ H_2O_2 alone; Lane 2- DNA + 10 µM sample + H_2O_2; Lane 3-DNA + 20 µM sample + H_2O_2; Lane 4-DNA + 50 µM sample + H_2O_2; Lane 5-DNA + 100 µM sample + H_2O_2; Lane 6-DNA+ 150 µM sample + H_2O_2; Lane 7-DNA + 200 µM sample + H_2O_2.


Figure 5.34: Agarose gel electrophoretic pattern of pBR322 DNA by H_2O_2 and 1,2-DPCo **(From left to right)** Lane 1-DNA+ H_2O_2 alone; Lane 2- DNA + 10 µM sample + H_2O_2; Lane 3-DNA + 20 µM sample + H_2O_2; Lane 4-DNA + 50 µM sample + H_2O_2; Lane 5-DNA + 100 µM sample + H_2O_2; Lane 6-DNA+ 150 µM sample + H_2O_2; Lane 7-DNA + 200 µM sample + H_2O_2.
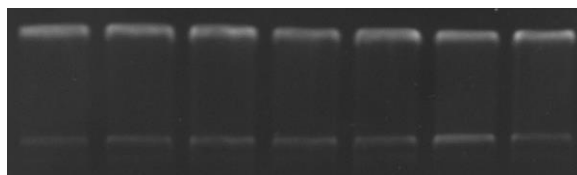

Figure 5.35: Agarose gel electrophoretic pattern of pBR322 DNA by H_2O_2 and [1,2-DPNi]2 **(From left to right)** Lane 1-DNA+ H_2O_2 alone; Lane 2- DNA + 10 µM sample + H_2O_2; Lane 3-DNA + 20 µM sample + H_2O_2; Lane 4-DNA + 50 µM sample + H_2O_2; Lane 5-DNA + 100 µM sample + H_2O_2; Lane 6-DNA+ 150 µM sample + H_2O_2; Lane 7-DNA + 200 µM sample + H_2O_2.
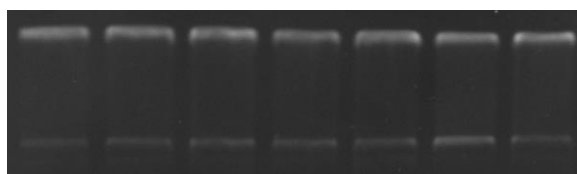
Figure 5.36: Agarose gel electrophoretic pattern of pBR322 DNA by H_2O_2 and (1,2-DPCu) **(From left to right)** Lane 1-DNA+ H_2O_2 alone; Lane 2- DNA + 10 µM sample + H_2O_2; Lane 3-DNA + 20 µM sample + H_2O_2; Lane 4-DNA + 50 µM sample + H_2O_2; Lane 5-DNA + 100 µM sample + H_2O_2; Lane 6-DNA+ 150 µM sample + H_2O_2; Lane 7-DNA + 200 µM sample + H_2O_2.

5.7 Conclusion

In this study, the transition metal complexes of Mn(III), Co(II) and Ni(II) and Cu(II) have been prepared from a new salen type ligand (1,2-DP) and characterized through elemental, spectral, magnetic measurements, molar conductivity, electrochemical measurements and single crystal structures, from this data structures of the ligand and complexes have been confirmed. The antibacterial activity of the compounds was performed against *E.coli*, *P. aeruginosa*, *B. subtilis*, and *S. aureus* and compared with standard drugs ciprofloxacin and ampicillin, the result indicated that the activity increased upon complexation of the ligand. Simultaneously, antifungal activity was estimated on selected fungal strains *C. albicans*, *A. flavus*, *A.niger, C. neoformans* using standard drugs miconazole and fluconazole. Some of the metal complexes showed good antibacterial activity, however, all the compounds exhibited very poor antifungal activity as compared to standards drugs. All the compounds also exhibited better antioxidant activity as compared to ascorbic acid as standard and the 1,2-DPCo(II) complex showed pBR322 DNA cleavage in the presence of H_2O_2.

5.8 References

1. Cozzi PG, Chemical Society Reviews, 33 (2004) 410-421.

2. Obasi LN, Kaior GU, Rhyman L, Alswaidan IA, Fun HK, Ramasami P, Journal of Molecular Structure, 1120 (2016) 180-186.

3. Ray A, Banerjee S, Rosair GM, Gramlich V, Mitra S, Structural Chemistry, 19 (2008) 459-65.

4. Kelode SR, Mandlik PR, Asian Journal of Research in Chemistry, 5 (2012).

5. Kervinen K, Korpi H, Gerbrand Mesu J, Soulimani F, Repo T, Rieger B, Leskelä M, Weckhuysen BM, European journal of inorganic chemistry, 2005 (2005) 2591-2599.

6. Pan ZH, Zhao GQ, Xue LW, Yang WC, Synthesis and Reactivity in Inorganic, Metal-Organic, and Nano-Metal Chemistry, 46 (2016) 1759-1764.

7. Aziz AA, Synthesis and Reactivity in Inorganic, Metal-Organic, and Nano-Metal Chemistry, 41 (2011) 384-393.

8. Mohie EM, El-Shishtawy RM, Asian Journal of Chemistry, 25 (2013) 2719.

9. Ding CX, He CH, Xie YS, Chinese Chemical Letters, 24 (2013) 463-466.

10. Zwettler N, Schachner JA, Belaj F, Mosch-Zanetti NC, Inorganic chemistry, 55 (2016) 5973-5982.

11. Deligonul N, Tumer M, Serin S, Transition metal chemistry, 31 (2006) 920-929.

12. Budige G, Puchakayala MR, Kongara SR, Hu A, Vadde R, Chemical and Pharmaceutical Bulletin, 59 (2011) 166-171.

13. Leung AC, MacLachlan MJ, Journal of Inorganic and Organometallic Polymers and Materials, 17 (2007) 57-89.

14. Metcalfe C, Thomas JA, Chemical Society Reviews, 32 (2003) 215-224.

15. Haak RM, Wezenberg SJ, Kleij AW, Chemical Communications, 46 (2010) 2713-2723.

16. Rajput JD, Bagul SD, Hosamani AA, Patil MM, Bendre RS, Research on Chemical Intermediates, 43 (2017) 5377-5393.

17. Bartyzel A, Journal of Coordination Chemistry, 66 (2013) 4292-4303.

18. Liu ZC, Wang BD, Yang ZY, Li Y, Qin DD, Li TR, European journal of medicinal chemistry, 44 (2009) 4477-4484.

19. Wang M, Wang LF, Li YZ, Li QX, Xu ZD, Qu DM, Transition Metal Chemistry, 26 (2001) 307-310.

20. Rajput JD, Bagul SD, Tadavi S, Bendre RS, Med. Aromat. Plants (Los Angel), 5 (2016).

21. Bekhit AA, Ashour HM, Ghany YS, Bekhit AE, Baraka A, European journal of medicinal chemistry, 43 (2008) 456-463.

22. Neelakantan MA, Rusalraj F, Dharmaraja J, Johnsonraja S, Jeyakumar T, Pillai MS, Spectrochimica Acta Part A: Molecular and Biomolecular Spectroscopy, 71 (2008) 1599-1609.

23. Zanello P, Tamburini S, Vigato PA, Mazzocchin GA, Coordination chemistry reviews, 77 (1987) 165-273.

24. Vigato PA, Tamburini S, Fenton DE, Coordination Chemistry Reviews, 106 (1990) 25-170.

25. Niederhoffer EC, Timmons JH, Martell AE, Chemical Reviews, 84 (1984) 137-203.

26. Olive GH, Olivé S, The chemistry of the catalyzed hydrogenation of carbon monoxide. Berlin: Springer; 1984.

27. Djebbar-Sid S, Benali-Baitich O, Deloume JP, Transition Metal Chemistry, 23 (1998) 443-447.

28. Ahmadi M, Mague JT, Akbari A, Takjoo R, Polyhedron, 42 (2012) 128-134.

29. Kavitha P, Reddy KL, Arabian Journal of Chemistry, 9 (2016) 596-605.

30. Lashanizadegan M, Journal of Sciences, Islamic Republic of Iran, 22 (2011) 121-121.

31. Selvarani V, Annaraj B, Neelakantan MA, Sundaramoorthy S, Velmurugan D, Polyhedron, 54 (2013) 74-83.

32. Losada J, Del Peso I, Beyer L, Inorganica Chimica Acta. 321 (2001) 107-115.

33. Sobha S, Mahalakshmi R, Raman N, Spectrochimica Acta Part A: Molecular and Biomolecular Spectroscopy, 92 (2012) 175-183.

34. Uçan SY, Mercimek B, Synthesis and Reactivity in Inorganic, Metal-Organic and Nano-Metal Chemistry, 35 (2005) 197-201.

35. Prakash A, Gangwar MP, Singh KK, Journal of Developmental Biology and Tissue Engineering, 3 (2011) 13-19.

36. Temel H, Şekerci M, Synthesis and Reactivity in Inorganic and Metal-Organic Chemistry, 31 (2001) 849-857.

37. R. L. Dutta, A. Syamal, Elements of Magnetochemistry, 2nd edn. (Elsevier, New Delhi, 1992)

38. Klement R, Stock F, Elias H, Paulus H, Pelikan P, Valko M, Mazur M, Polyhedron, 18 (1999) 3617-3628.

39. Neelakantan MA, Rusalraj F, Dharmaraja J, Johnsonraja S, Jeyakumar T, Pillai MS, Spectrochimica Acta Part A: Molecular and Biomolecular Spectroscopy, 71 (2008) 1599-1609.

40. Raman N, Raja YP, Kulandaisamy A, Indian Academy of Sciences, 113 (2001) 183-190.

41. Aziz AA, Salem AN, Sayed MA, Aboaly MM, Journal of Molecular Structure, 1010 (2012) 130-138.

42. Hathaway B, Billing DE, Coordination Chemistry Reviews, 5 (1970) 143-207.

43. Tadavi SK, Rajput JD, Bagul SD, Hosamani AA, Sangshetti JN, Bendre RS, Research on Chemical Intermediates, 43 (2017) 4863-4879.

44. Samina KT, Jamatsingh DR, Suresh DR, Jaiprakash NS, Amar AH, Mod Chem Appl, 5 (2017).

45. Alaşalvar C, Güder A, Gökçe H, Kaştaş ÇA, Çelik RÇ, Journal of Molecular Structure, 1133 (2017) 37-48.

46. Kuwar AS, Fegade UA, Tayade KC, Patil UD, Puschmann H, Gite VV, Dalal DS, Bendre RS, Journal of fluorescence, 23 (2013) 859-864.

47. Yadav S, Ahmad M, Siddiqi KS, Spectrochimica Acta Part A: Molecular and Biomolecular Spectroscopy, 98 (2012) 240-246.

48. Tweedy BG. Plant extracts with metal ions as potential antimicrobial agents. Phytopathology. 1964;55:910-4.

49. Belaid S, Landreau A, Djebbar S, Benali-Baitich O, Bouet G, Bouchara JP, Journal of inorganic biochemistry, 102 (2008) 63-69.

50. Dharmaraj N, Viswanathamurthi P, Transition Metal Chemistry, 26 (2001) 105-109.

51. Nair R, Shah A, Baluja S, Chanda S, Journal of the Serbian Chemical Society, 71 (2006) 733-44.

52. Güder A, Korkmaz H, Iranian journal of pharmaceutical research IJPR, 11 (2012) 913.

53. Arjmand F, Aziz M, European journal of medicinal chemistry, 44 (2009) 834-844.

54. Halli MB, Sumathi RB, Arabian Journal of Chemistry, 10 (2017) 1748-1759.

RESEARCH

PUBLICATIONS

CrossMark

Synthesis, crystal structures and biological activities of transition metal complexes of a salen-type ligand

Ratnamala S. Bendre[1] · Samina K. Tadavi[1] · Manohar M. Patil[1]

Abstract

Manganese(III), cobalt(II), nickel(II) and copper(II) complexes of a salen-type ligand, namely 6,6′-((1E,1′E)-(ethane-1,2-diylbis(azanylylidene))bis(methanylylidene))bis(5-isopropyl-2-methylphenol) (H_2L), have been synthesized and characterized by physicochemical and spectroscopic methods. In addition, single-crystal X-ray analysis confirmed the formulae of the manganese and nickel complexes as [Mn(OAc)(L)] and [Ni(L)], respectively. The free Schiff base and its complexes have been screened for in vitro antibacterial activity by colony count methods, and the antioxidant activity was assayed by DPPH radical scavenging. The ability of free H_2L and its complexes to mediate DNA cleavage was studied by agarose gel electrophoresis.

Introduction

DNA remains a long-term target for the diagnosis and treatment of human diseases [1]. DNA plays an essential role in the life process since it encodes all the genetic information required for the cellular functions [2]. Metal complexes of Schiff bases derived from salicyaldehyde have been found to be effective in DNA cleavage and can also possess anticancer and antibacterial activities [3–6]. DNA cleavage may lead to various pathological changes in living organisms and is also relevant to the synthetic restriction enzymes, chemotherapeutic drugs and DNA footprinting agents [7]. Recently, the ability of transition metal complexes to mediate DNA cleavage in the presence of oxidants such as O_2, H_2O_2 or peracids has been extensively studied. Efforts have been made to design transition metal complexes as chemical nucleases suitable for nicking or direct DNA strand scission [8, 9]. Cobalt complexes with different oxidation states have been found to possess DNA cleavage activity [10]. In this context, we report here the

synthesis of an N_2O_2 donor tetradentate Schiff base ligand H_2L-6,6′-((1E,1′E)-(ethane-1,2-diylbis(azanylylidene))bis(methanylylidene))bis(5-isopropyl-2-methylphenol), prepared by the condensation of ethane-1,2-diamine with 2-hydroxy-6-isopropyl-3-methyl benzaldehyde, together with its manganese(III), cobalt(II), nickel(II) and copper(II) complexes. All the compounds were characterized by physicochemical and spectroscopic methods and further screened for antibacterial, antioxidant and DNA cleavage activities.

Experimental

Materials and methods

Carvacrol, ethane-1,2-diamine, ethidium bromide, tris-boric acid-EDTA buffer (10X TBE buffer), loading dye mix, agarose gel, L-histidine, DABCO, D-mannitol and H_2O_2 30% were purchased from Sigma-Aldrich. Sodium hydroxide, triethylamine, chloroform, ethanol, methanol, hexane, ethyl acetate, acetonitrile, DMF, DMSO, EDTA, manganese acetate tetrahydrate, cobalt acetate tetrahydrate, nickel chloride hexahydrate and copper(II) acetate monohydrate were Loba Chemie products. All the chemicals and solvents were used without further purification. The DNA pBR322 and DNA loading dye were purchased from Bangalore Genei. The electronic spectra were recorded as DMSO solutions on a Shimadzu UV 2450 series spectrophotometer in the range 200–800 nm. FTIR

✉ Ratnamala S. Bendre
   bendrers@gmail.com

1   School of Chemical Sciences, North Maharashtra University, Jalgaon, Maharashtra 425 001, India

✐ Springer
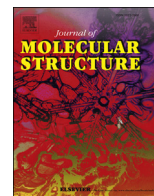
Synthesis and characterization of a novel schiff base of 1,2-diaminopropane with substituted salicyaldehyde and its transition metal complexes: Single crystal structures and biological activities

Samina K. Tadavi [a], Abhijit A. Yadav [b], Ratnamala S. Bendre [a, *]

[a] School of Chemical Sciences, North Maharashtra University, Jalgaon 425 001, Maharashtra, India
[b] Thin Film Physics Laboratory, Department of Physics, Electronics and Photonics, Rajarshi Shahu Mahavidyalaya, (Autonomous), Latur 413512, Maharashtra, India

ABSTRACT

A novel schiff base H2L derived from simple condensation of 2-hydroxy-6-isopropyl-3-methyl benzaldehyde and 1,2-diaminopropane in 2:1 M ratio and its [MnL], [CoL] and [NiL]2 complexes have been prepared and characterized by spectroscopic technique, elemental analysis, SEM-EDX analysis, and cyclic voltammetry. Additionally, single crystal X-ray diffraction technique has been applied to the schiff base ligand H2L and its nickel complex. The structure of nickel complex exhibited dimeric form with formula [NiL]2 with distorted square planar geometry around each nickel center. Furthermore, all the synthesized compounds were screened for their antimicrobial and antioxidant and DNA cleavage activities.

© 2017 Published by Elsevier B.V.

1. Introduction

Compounds with azomethine functional group (−HC=N), typically known as schiff bases have been synthesized by the condensation of primary amines with active carbonyls (aldehyde or ketone) [1]. The presence of a lone pair of electrons in the sp² hybridized orbital of nitrogen atom of the azomethine group presents good chelating ability on schiff bases especially when combined with one or more donor atoms close to the azomethine group. This chelating ability of the Schiff base combined with the ease of separation and flexibility in varying the chemical environment about the C=N group, makes Schiff base interesting ligands in coordination chemistry [2]. Metal complexes of schiff bases derived from salicylaldehyde and diamine can increase the dimensionality of the system and can form supramolecular architectures through O−H−−N and N−H−−O type of hydrogen bonds [3]. Moreover, these complexes have remained an important and popular area of research due to their simple synthesis, versatility and diverse range of applications [4−10]. Tetradentate schiff bases with a N_2O_2 donor

atom set are well known to coordinate with various metal ions, and have many applications in the organic and inorganic fields [11−16]. Their metal complexes possess effective antibacterial, antifungal [17], antioxidant [18], anticancer [19,20], anti-inflammatory [21], DNA cleavage [22] and catalytic [23−27] properties, phosphorescence and electroluminescence [28]. Because of their wide applications area, schiff bases have been the focus of attention of scientists and hence the literature relating to schiff bases is extremely rich [16−28]. To contribute to search area of schiff base we report synthesis of a new type of tetradentate schiff base ligand formed by the simple condensation of 1,2-diamino propane with 2-hydroxy-6-isopropyl-3-methyl benzaldehyde and its Mn(III), Co(II), and Ni(II) complexes. The synthesized ligand and its complexes were characterized using elemental analysis, FT-IR, UV−visible, NMR, LC-MS and single crystal X-ray crystallography, magnetic susceptibility, cyclic voltammetry and further screened for antimicrobial and antioxidant activities.

2. Experimental

All the solvents and chemicals were of commercial reagent grade and used as received without further purification. FT-IR spectra were recorded as KBr pellets on a SHIMADZU FT-IR-8400

* Corresponding author.
  E-mail address: bendrers@gmail.com (R.S. Bendre).

CrossMark

Synthesis, crystal structures, biological screening and electrochemical analysis of some salen-based transition metal complexes

Samina K. Tadavi[1] · Jamatsing D. Rajput[1] ·
Suresh D. Bagul[1] · Amar A. Hosamani[2] ·
Jaiprakash N. Sangshetti[3] · Ratnamala S. Bendre[1]

Abstract A new series of transition metal complexes with (1) Mn(III), (2) Co(II), (3) Ni(II) and (4) Cu(II) have been synthesized by the reaction of [6,6′-((1E,1′E)-(propane-1,3-diylbis(azanylylidene))bis(methanylylidene))bis(5-isopropyl-2-methyl-phenol)] with suitable metal salts. The synthesized complexes have been characterized by elemental analysis and spectroscopic techniques. The results of single crystal structures show that the metal is bonded to the ligand through the phenolic oxygens and imino nitrogens. Synthesized complexes have been evaluated for antibacterial activity and antioxidant activity, which shows considerable results.

Keywords N_2O_2 donor · Transition metal complexes · Cyclic voltammetry · ESR

Introduction

During the past few decades, considerable attention has been paid to the chemistry of metal complexes of Schiff bases containing nitrogen and oxygen as donor atoms, which have been found to occupy an important role in the development of the chemistry of chelate systems [1, 2]. Schiff bases have been reported to possess

✉ Ratnamala S. Bendre
   bendrers@gmail.com

1   School of Chemical Sciences, North Maharashtra University, Jalgaon, Maharashtra 425 001, India

2   Solid State and Structural Chemistry Unit, Indian Institute of Science, Bangalore 560 012, India

3   Y. B. Chavan College of Pharmacy, Dr. Rafiq Zakaria Campus, Aurangabad, Maharashtra 431 001, India

🙂 Springer

Modern Chemistry & Applications

Crystal Structure, Spectral Characterization and Biologically Studies of Mononuclear Transition Metal Complexes Derived from New N$_2$O$_2$ Type Ligand

Samina K Tadavi[1], Jamatsing D Rajput[1], Suresh D Bagul[1], Jaiprakash N Sangshetti[3], Amar A Hosamani[2] and Ratnamala S Bendre[1]*

[1]*School of Chemical Sciences, North Maharashtra Jalgaon, Maharashtra, India*
[2]*Solid State and Structural Chemistry Unit, Indian Institute of Science, Bangalore, Karnataka, India*
[3]*YB Chavan College of Pharmacy, Dr. Rafiq Zakaria Campus, Aurangabad, Maharashtra, India*

Abstract

The new mononuclear metal complexes viz Mn(III), Co(II), Ni(II) and Cu(II) have been synthesized by using tetradentate N2O2 donor symmetric schiff base 6,6'-((1E,1'E)-(1,2-phenylenebis(azanylylidene))bis(methanylylidene)) bis(5-isopropyl-2-methylphenol) HL and employing with corresponding metal chloride or acetate salts. After successful synthesis of compounds were thoroughly characterized by Elemental analysis, FT-IR, Uv-visible, NMR spectroscopy, LC-MS spectrometry, SEM analysis, Magnetic susceptibility measurement, Molar conductance, ESR spectroscopy. X-ray single crystal structure of HL schiff base has been determined. The synthesized compounds have been screened for their antimicrobial and antioxidant activities, which show significant results.
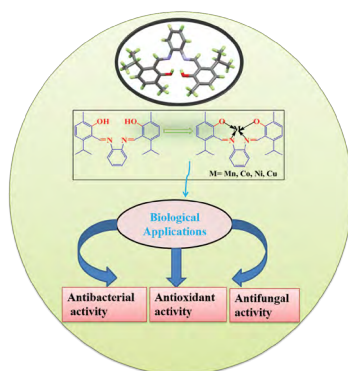
Keywords: Schiff base; Mononuclear transition metal complexes; ESR; Antimicrobial activity; Antioxidant activity

Introduction

Schiff bases (RHC=NR) are a class of organic compounds typically formed by condensation of a primary amine and an aldehyde and they are considered as privilege ligand [1,2]. Schiff base ligands with N$_2$O$_2$ donor atoms are well known to coordinate with a variety of metal ions. They have attracted much interest in recent years, due to ease of synthesis, their stability under a variety of oxidative and reductive conditions and their structural versatility associated with various applications. These compounds have various applications in industries as dyes, drug synthesis [3] bioinorganic chemistry [4] electrochemistry [5] dioxygen uptake and catalysis [6-10]. Tetra-dentate N$_2$O$_2$ donors schiff bases derived from o-phenylenediamine and salicyaldehyde have been widely studied in solid state. They have been studied for a variety of applications including biological, clinical and analytical. The previous work has shown that some drugs showed increased activity when administered as metal chelates rather than as organic compounds [11-13]. A search through literature reveals that no work has been done on the transition metal complexes of the symmetrical schiff base derived from o-phenylenediamine and 2-hydroxy-6-isopropyl-3-methyl benzaldehyde. In this paper, we report synthesis of a new type of tetradentate Schiff base ligand formed by the simple condensation of o-phenylenediamine with 2-hydroxy-6-isopropyl-3-methyl benzaldehyde and its Mn(III), Co(II), Ni(II) and Cu(II) mononuclear complexes. The prepared ligand and complexes were characterized using Elemental analysis, FT-IR, UV-visible, NMR, LC-MS, ESR and crystal structure and further screened for antimicrobial and antioxidant activity.

Experimental

All the solvents and chemicals were of commercial reagent grade and used as received without further purification. FT-IR spectra were recorded as KBr pellets on a SHIMADZU FT-IR- 8400 spectrometer from range 4000 to 400 cm^{-1}. The electronic spectra were recorded in DMF solutions on the UV 2400 series spectrophotometer. ^{1}H and ^{13}C-NMR spectra were precise with a BRUKER AVANCE III (400 MHz) spectrometer and proton chemical shifts are recorded in ppm relative to tetramethylsilane as an internal standard using CDCl$_3$ as solvent and the LC-MS spectra have been carried out with Waters Micromass Q-Tof Micro instrument. The elemental analyses were carried out with a Thermo Finnigan elemental analyzer. The X-band ESR spectra of

Design, synthesis and biological activities of novel 5-isopropyl-2-methylphenolhydrazide-based sulfonamide derivatives

Suresh D. Bagul[1] · **Jamatsing D. Rajput**[1] ·
Samina K. Tadavi[1] · **Ratnamala S. Bendre**[1]

Abstract Sulfonamides have enormous importance in biological sciences. In the present investigation, the fundamental energetic group, hydrazide-based sulfonamide, has been incorporated into a naturally occurring phenolic monoterpenoid, carvacrol (5-isopropyl-2-methylphenol) moiety, with the aim of combining the active groups in order to generate more potent antimicrobial and anti-oxidant agents. Series of hydrazide-based sulfonamide derivatives (**IV a–g**) have been synthesized and characterized by modern sophisticated techniques such as ^{1}H NMR, ^{13}C NMR and LC–MS. The newly synthesized derivatives were screened for their antimicrobial activities against three fungal (*Aspergillus niger*, *A. flavus* and *A. fumigatus*) and three bacterial (*Escherichia coli*, *Staphylococcus aureus* and *Bacillus subtilis*) species, of which compounds **IVc** and **IVd** were found to have good antifungal activity and compounds **IVd** and **IVg** exhibited decent antibacterial activities. antioxidant activity was performed by DPPH radical scavenging assay. Compound **IVd** has been found to be more active in comparison to standard ascorbic acid and compounds **IVa**, **IVb**, and **IVc** demonstrated excellent antioxidant activity.

✉ Ratnamala S. Bendre
  bendrers@gmail.com; bendrers@rediffmail.com

1   Department of Pesticides and Agrochemicals, School of Chemical Sciences, North Maharashtra University, Jalgaon, Maharashtra 425 001, India

Medicinal & Aromatic Plants

Commentary　　　　　　　　　　　　　　　　　　　　　　　　　　　　**Open Access**

Comparative Anti-Proliferative Studies of Natural Phenolic Monoterpenoids on Human Malignant Tumour Cells

Jamatsing D Rajput, Suresh D Bagul, Samina Tadavi and Ratnamala S Bendre*

School of Chemical Sciences, North Maharashtra University, Jalgaon, Maharashtra, India

Abstract

In present study we report prominent effect of carvacrol (5-isopropyl-2-methyl phenol), thymol (2-isopropyl-5-methyl phenol) and eugenol (4 allyl-2-methoxyphenol) on Human melanoma cells. These three compounds were screened for Anti-proliferative test by using Sulforhodamine B (SRB) assay. For this investigation we used human breast melanoma cell line MCF-7, human skin melanoma cell line SK-MEL-2, human colon melanoma cell line HCT-15 and human pancreatic melanoma cell line MIAPaCa-2. Carvacrol was identified as most potent molecule with low GI_{50} value as 0.1 µL for selected human cancer cell lines; which is comparatively equal to standard drug 14 Adriamycin (ADR). Thymol and Eugenol also exhibited remarkable GI_{50} for human cancer cell 15 lines.
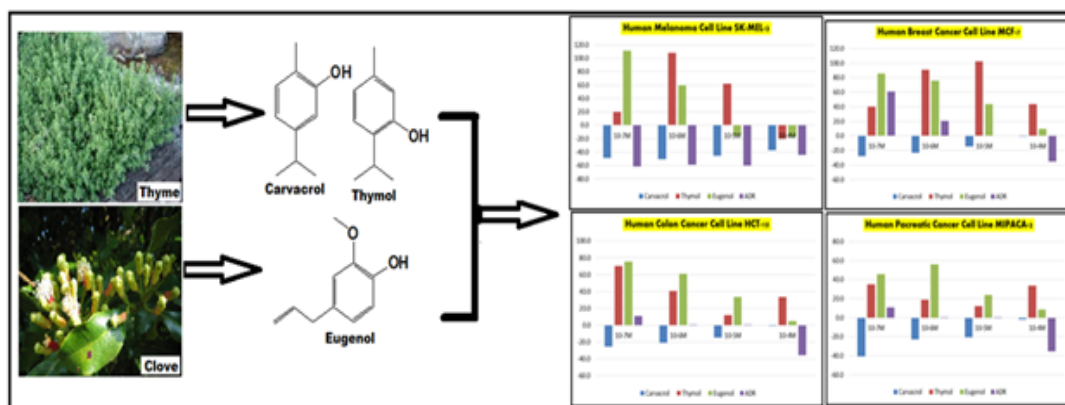
Keywords: SRB; Carvacrol thymol; Eugenol; MCF-7: SK-MEL-2; HCT-15; MIAPaCa-2

Introduction

Cancer is a serious chronic disease that arises due to changes in many physiological processes in body [1,2]. In general, symbols of cancer were found to be sustaining proliferative signalling, avoiding growth suppressors, control cell death, enabling replicative immortality, inducing angiogenesis, and activating incursion and metastasis, along with two emerging symbols including reprogramming energy metabolism and absconding immune damage [3-5]. The search for novel small molecules as drugs is still a priority goal for cancer therapy, due to the rapid development of resistance to chemotherapeutic drugs [6]. In addition, the high toxicity usually associated with some bulky anticancer drugs and their undesirable side-effects increase the demand for novel anti-tumour drugs active towards untreatable tumours [7,8] Natural products have long been a substantial source of treatment for melanoma, which is projected to become the main causes of death in this century [9,10]. The research of last 40 years demonstrated that more than one thousand plants possess significant anticancer properties [11]. while many molecules obtained from these plants have shown wonderful anticancer properties [12,13]. Some of them showed effective delivery in biological system to reduce the action of cancer disease, without toxic and other side effects against healthy cells and tissues [14].

Carvacrol (1), thymol (2) and eugenol (3) are part of a naturally occurring class of compounds known as phenols [15]. They are well-known naturally occurring phenolic monoterpenoids found primarily in oils of oregano, thyme, and marjoram, and are recognized as traditional therapeutic agents [16,17]. All the major groups of angiosperms biosynthesize these biocides [18]. Currently, these biocides are used in food flavouring ingredients and preservatives, as well as a fragrance ingredients in cosmetic formulations [19]. In recent years, significant research has been undertaken as an effort to establish the biological actions of these phenolic monoterpenoids for their potential use in pharmaceutical and agricultural applications [20]. Some results from *in-vitro* and *in-vivo* studies showed that carvacrol,

Medicinal chemistry

Research Article   **Open Access**

Design, Synthesis and Biological Evaluation of Novel Class Diindolyl Methanes (DIMs) Derived from Naturally Occurring Phenolic Monoterpenoids

Jamatsing D Rajput, Suresh D Bagul, Samina K Tadavi, Pravin S Karandikar and Ratnamala S Bendre*

School of Chemical Sciences, North Maharashtra University, Jalgaon, Maharashtra, India

Abstract

Several Diindolyl alkanes and their derivatives have been isolated from plant and marine sources. Among the various derivatives of indoles, Diindolyl methanes have wide medicinal applications such as to induce apoptosis in human cancer cells, antibacterial, Anti-inflammatory, antiviral and hormonal control activities. Therefore, they play essential role in marine as well as terrestrial living systems. In present studies we report novel class of Diindolyl methanes prepared from natural phenolic monoterpenoids, via ortho formylation of phenolic monoterpenoids (Carvacrol, Thymol and Eugenol), followed by synthesis, characterization, anticancer, antioxidant and α-amylase inhibitory activities. All the synthesized derivatives show moderate anticancer activities against human breast cell line MCF$_7$, good antioxidant and α-amylase inhibitory activities using DPPH and α-amylase assay respectively.

Introduction

The Diindolyl methanes (DIMs) are a class of alkaloids that includes fundamental framework of two indol-3-yl groups bridged by single methyl group and they are differentiated by the substituents attached to the bridging methyl carbon [1]. Commonly most DIMs are found in both marine and terrestrial organisms; a few of them are reported exclusively from either terrestrial or marine organisms. First DIMs derivatives were isolated from genotoxic metabolite of human intestinal bacteria *Streptococcus faecium,* [2] (Streptindol; Figure 1). Later on number of naturally occurring analogs of DIMs were isolated and reported Some of the naturally occurring Di(Diindolyl)methane derivatives [3] are depicted in Figure 1. Moreover, there are number of reports on synthetic derivatives of DIMs [4,5]. Due to excellent bio-efficacy of Diindolyl methanes, large number of reports are available in literature, [6-9] on their synthesis; most of these methods involve treatment of indoles with aldehydes in presence of homogeneous acid catalysts or lewis acids and only few reports are based on the use of heterogeneous catalysts [10-12]. Recently some organic chemists have made an effort for development of a hazard-free, waste-free and energy-efficient synthetic route and it may be of great use for economical synthesis of this class of compounds [13]. In persistence to our efforts towards development of efficient synthetic methodologies for preparation of biologically significant scaffolds; herein we have developed an efficient procedure for preparation of new class of Diindolyl methanes and performed their biological activities.

Carvacrol, Thymol, and Eugenol are found in essential oils of many plants [14,15]. These three naturally occurring phenolic monoterpenoids are outstanding resourceful molecules incorporated as useful ingredients in various products and have found applications in pharmaceutical, agricultural, fragrance, flavour, cosmetic and various other industries [16,17]. There huge range of pharmacological activities including antimicrobial, anti-inflammatory, analgesic, anti-oxidant and anticancer activities have been well-researched [18,19]. We synthesized ortho formyl phenolic monoterpenoids using Reimer-Tiemann Reaction [20] and constructed a new series of Diindolyl methanes using ortho formyl derivatives carvacrol, thymol and eugenol.

In the present work, we report a simple synthetic method for the synthesis of new class of Diindolyl methane derivatives in the presence of SnCl$_4$, AlCl$_3$ and citric acid as catalysts in ethanol as solvent at ambient temperature and investigated the biological activities of these synthesized derivatives.

## Results and Bioassay

Reaction scheme
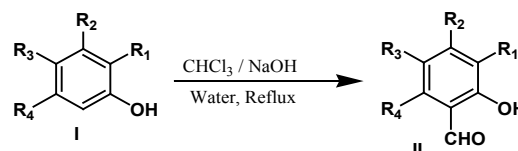
R$_1$=CH$_3$, R$_2$=H, R$_3$=H and R$_4$=CH(CH$_3$)$_2$ then Carvacrol.

R$_1$=CH(CH$_3$)$_2$, R$_2$=H, R$_3$=H and R$_4$=CH$_3$ then Thymol.

R$_1$=OCH$_3$, R$_2$=H, R$_3$=allyl and R$_4$=H then Eugenol.

Scheme 1: Reaction protocol for the synthesis of ortho formylation of phenolic monoterpenoids.

X= SnCl4, AlCl3 and citric acid

R$_1$=CH$_3$, R$_2$=H, R$_3$=H and R$_4$=CH(CH$_3$)$_2$ then Carvacryl Diindolyl methane (CDI).

CONFERENCES ATTENDED

CONFERENCES /WORKSHOPS ATTENDED

International Conference

❖ "Studies on synthesis, characterization and SOD activities of copper and zinc complexes bearing Tetradentate Schiff base ligand" International Conference on **Global Opportunities for Latest Developments in Chemistry and Technology (GOLD-CT-2014)** 6-8 February 2014, School of Chemical Sciences, North Maharashtra University Jalgaon (Participated in Poster presentation).

National/ State level Conferences

❖ "Cobalt ONNO complexes as oxidation catalysts" **University Level Aviskhar**, 5th October 2013. North Maharashtra University, Jalgaon (Participated in Poster presentation).

❖ "Cobalt ONNO complexes as oxidation catalysts" **District Level Aviskhar**, 17-18th October 2013. North Maharashtra University, Jalgaon (Participated in Poster presentation).

❖ "Synthesis, characterization and Applications of Transition Metal Complexes of Symmetric N_2O_2 Donor Schiffs Bases Derived from 2-hydroxy-6-isopropyl methyl benzaldehyde." **University Level Avishkar 2015**, North Maharashtra University, Jalgaon (Participated in Poster presentation).

❖ "Synthesis, characterization and Applications of Transition Metal Complexes of Symmetric N_2O_2 Donor Schiffs Bases Derived from 2-hydroxy-6-isopropyl methyl benzaldehyde." **District Level Avishkar 2015**, North Maharashtra University, Jalgaon (Participated in Poster presentation).

❖ "Synthesis and Characterization of Transition Metal Complexes derived from N_2O_2 donor Schiff's Base Ligands". National Conference on **Frontiers in Chemical & Material Sciences (FCMS- 2015)**, 16-17th January 2015, Department of Chemistry, Shivaji University, Kolhapur (Participated in Poster presentation).

❖ "Synthesis, Characterization and Biological Activities of Transition Metal Complexes of Symmetric N_2O_2 Donor Schiff Base Derived from 2-hydroxy-6-isopropyl-3-methyl benzaldehyde" **RSC Symposium on Frontiers of Advances in Chemistry and Technology (FACT- 2015)**, 11-12th December 2015, School of Chemical Sciences, NMU, Jalgaon (Participated in Poster presentation).

❖ "Synthesis, characterization and Biological Applications of Transition Metal Complexes of Symmetric N_2O_2 Donor Schiff Bases Derived from 2-hydroxy-6-isopropyl-3-methyl benzaldehyde." **Advances in Chemical Sciences (ACS-2017)**, 4th March 2017, School of Chemical Sciences, North Maharashtra University, Jalgaon (Participated in Poster presentation).